Optimization and Application of Boron-Doped Diamond Electrooxidation for Landfill Leachate Treatment and Mixed Antibiotic Removal from Wastewater

By

MD Tanvir Hasnine

A Thesis submitted to the Faculty of Graduate and Postdoctoral Studies of

The University of Manitoba

In partial fulfillment of the requirements of the degree of

DOCTOR OF PHILOSOPHY

Department of Civil Engineering

University of Manitoba

Winnipeg, MB R3T 2N2, Canada

ABSTRACT

This thesis investigated boron-doped diamond (BDD) electrooxidation as an advanced treatment option for mature landfill leachate and antibiotic-contaminated wastewater. The first phase examined real mature landfill leachate collected from the Brady Road Resource Management Facility in Winnipeg, Canada. Niobium (Nb) based BDD electrooxidation was conducted in a batch reactor, and response surface methodology was applied to optimize current density and pH for the simultaneous removal of COD, color, ammonium, and phosphate. Current density, treatment time, and pH strongly influenced treatment performance. The optimum condition was obtained at 125 mA/cm^2 and pH 8, achieving removal efficiencies of 95.47%, 80.27%, 71.15%, and 47.15% for color, NH_4^+, COD, and PO_4^{3-}, respectively.

The second phase evaluated Nb/BDD electrooxidation for removing a ternary antibiotic mixture containing sulfanilamide (SN), tetracycline hydrochloride (TC-HCl) and sulfamethazine (SMZ). Acidic conditions and higher current density improved parent-compound removal and mineralization. At pH 3.5, 35 mA/cm^2, 4000 µg/L, and 60 min, the removals reached approximately 77%, 77–80%, and 79% for sulfanilamide, tetracycline hydrochloride, and sulfamethazine, respectively. TOC decreased from 160 to 75 mg/L, corresponding to 53.13% mineralization.

The final phase optimized H_2O_2-supplemented Nb/BDD electrooxidation using central composite design-based response surface methodology. The optimum condition was 30 mA/cm^2, pH 4.95, 2.5 mM H_2O_2, and 6000 µg/L at 90 min. Experimental validation confirmed removals of 97%, 95.50%, and 88% for sulfanilamide, tetracycline hydrochloride, and sulfamethazine, respectively. TOC decreased from 85 to 20 mg/L, indicating 76.47% mineralization. The process required 66 kWh/m^3, with an estimated electrical cost of 6.51 CAD/m^3. Overall, BDD electrooxidation showed strong potential as a targeted polishing process for refractory leachate contaminants and mixed antibiotics.

Keywords: Boron-doped diamond anode; electrochemical advanced oxidation; mature landfill leachate; pharmaceutical-contaminated wastewater; mixed antibiotic degradation; response surface methodology; desirability optimization; hydroxyl radicals; mineralization; specific energy consumption.

Acknowledgements

I would like to express my heartfelt gratitude to my supervisor, Dr. Qiuyan Yuan, for her mentorship, unwavering support, and invaluable guidance throughout my doctoral journey. I would not have reached this point and shaped my academic journey without her advice, guidance, and encouragement. My heartfelt appreciation goes to my supervisor for providing resources and financial support throughout my academic journey. I would also like to extend my gratitude to my other committee members, Dr. Gregg Thomas Tomy and Dr. Chengjin Wang, for their insightful feedback, constructive criticism, and scholarly guidance. Their expertise and encouragement have played a vital role in shaping the route of my research and academic activities.

My heartfelt appreciation goes to the University of Manitoba Graduate Fellowship (UMGF) for providing me with funding and financial support during my doctoral journey. I would also like to thank the Department of Civil Engineering, Price Faculty of Engineering, for their scholarship, Faculty of Graduate and Postdoctoral Studies research completion scholarships, engineering awards and scholarships such as Petro Canada resource graduate fellowship, Edward R. Toporeck Graduate Fellowship, Emil and Lynette Hain scholarships, travel grant, bursary, and so forth, to pursue my academic goals.

I sincerely thank all my colleagues in the lab, and I would also like to express my special gratitude to our lab manager, Dr. Victor Wei from our Environmental Engineering program, who helped me in every possible way in the lab for my research experiments. A special mention goes to my friend Dr. Ali Zoungrana and Dr. Mahmudul Hasan who I have shared my challenging projects and always supported me mentally.

Finally, I extend my heartfelt thanks to my wife, whose unwavering love and support have been my constant source of strength throughout my academic journey.

DEDICATION

I would like to dedicate this thesis to my parents, my deceased grandmother, my elder brother, my wonderful wife, and my loving son, to believe in and support in every possible way.

CONTRIBUTIONS OF AUTHORS

The contributions of authors in different manuscripts included in the thesis are shown below:

Manuscript No. 1: Optimisation of electrochemical oxidation process with boron-doped diamond (BDD) for removing COD, colour, ammonium, and phosphate in landfill leachate. This work has been published in ***Environmental Technology*** (T. Hasnine et al., 2023)**.**

Author's contribution: ***MD Tanvir Hasnine*** -Conceptualization, Literature review, Investigation, Methodology, Visualization, Formal analysis, Writing - original draft, revisions, and editing; *Elisabeth Cuervo Lumbaque* – Visualization and data analysis, Writing – review and editing; *Qiuyan Yuan* –Conceptualization, project administration, resources, supervision, investigation, Writing – review and editing.

Manuscript No. 2: Influence of operational parameters on mixed pharmaceutical antibiotics removal from wastewater using Boron-doped diamond (BDD) electrooxidation. This work has been submitted and is now under revision in ***Electrochimica Acta*****,** (Hasnine and Yuan, 2026).

Author's contribution: ***MD Tanvir Hasnine*** -Conceptualization, Literature review, Investigation, Methodology, Visualization, Formal analysis, Writing - original draft, revisions, and editing; *Qiuyan Yuan* –conceptualization, project administration, resources, supervision, investigation, Writing – review and editing.

Manuscript No. 3: Application of response surface methodology for optimization and electrochemical oxidation of three mixed antibiotics at boron-doped diamond electrodes. This work has been published in ***Desalination and water treatment*** journal (Hasnine and Yuan, 2026).

Author's contribution: ***MD Tanvir Hasnine*** -Conceptualization, Literature review, Investigation, Methodology, Visualization, Formal analysis, Writing - original draft, revisions, and editing;

Qiuyan Yuan –conceptualization, project administration, resources, supervision, investigation, Writing – review and editing.

Other contributions as a primary and secondary author

Other manuscripts and book chapters as a primary and secondary author, but not included in the thesis, are shown below:

1. **Tanvir Hasnine,** Prangya Ranjan Rout & Qiuyan Yuan (2025). "Forever chemicals (PFAS) in landfill leachate: Insights into fate, transport, and treatment strategies" *Desalination and Water Treatment*, https://doi.org/10.1016/j.dwt.2025.101565
2. **Hasnine, M.D.T.,** Anik, A.H., Alam, M., Yuan, Q. (2024). "Navigating Microplastic Challenges: Separation and Detection Strategies in Wastewater Treatment". In: Kumar, A., Singh, V. (eds) Microplastics Pollution and its Remediation. Springer, Singapore. https://doi.org/10.1007/978-981-97-4068-0_1
3. Alam, M., Sultan M.B., Anik A.H., Hossain S., **Hasnine M.T**., Yuan Q., (2024). "Microplastics in Landfill and Leachate". In: Kumar, A., Singh, V. (eds) Microplastics Pollution and its Remediation. Springer, Singapore. https://doi.org/10.1007/978-981-97-4068-0_13
4. **Hasnine, M.T.,** Anand, N., Zoungrana, A., Palani, S.G., Yuan, Q. (2022). An Overview of Physicochemical and Biological Treatment of Landfill Leachate. In: Pathak, P., Palani, S.G. (eds) Circular Economy in Municipal Solid Waste Landfilling: Biomining & Leachate Treatment. Radionuclides and Heavy Metals in the Environment. Springer, Cham. https://doi.org/10.1007/978-3-031-07785-2_6
5. Zoungrana, A., **Hasnine, M.T.,** Yuan, Q. (2022). Landfill Mining: Significance, Operation, and Global Perspectives. In: Pathak, P., Palani, S.G. (eds) Circular Economy in Municipal Solid

Waste. Landfilling: Biomining & Leachate Treatment. Radionuclides and Heavy Metals in the Environment. Springer, Cham. https://doi.org/10.1007/978-3-031-07785-2_2

6. Thapa, Pradeep**, MD Tanvir Hasnine**, Ali Zoungrana, Sandeep Thakur, and Qiuyan Yuan. (2022). "Food Waste Treatments and the Impact of Composting on Carbon Footprint in Canada" Fermentation 8, no. 10: 566. https://doi.org/10.3390/fermentation8100566
7. Vanja Karpisek, **MD Tanvir Hasnine**, Nazim Cicek, & Qiuyan Yuan (2021): Natural wetlands contribution to phosphorus removal in small northern communities in Canada, Environmental Technology, DOI: 10.1080/09593330.2021.196522
8. Amit Hasan Anik, Shabiha Hossain, Mahbub Alam, Maisha Binte Sultan, **MD. Tanvir Hasnine**, Md. Mostafizur Rahman (2021), "Microplastics pollution: A comprehensive review on the sources, fates, effects, and potential remediation". Environmental Nanotechnology, Monitoring & Management, Volume 16, 2021. https://doi.org/10.1016/j.enmm.2021.100530.

COPYRIGHTS FOR MANUSCRIPT NO. 1 and 3

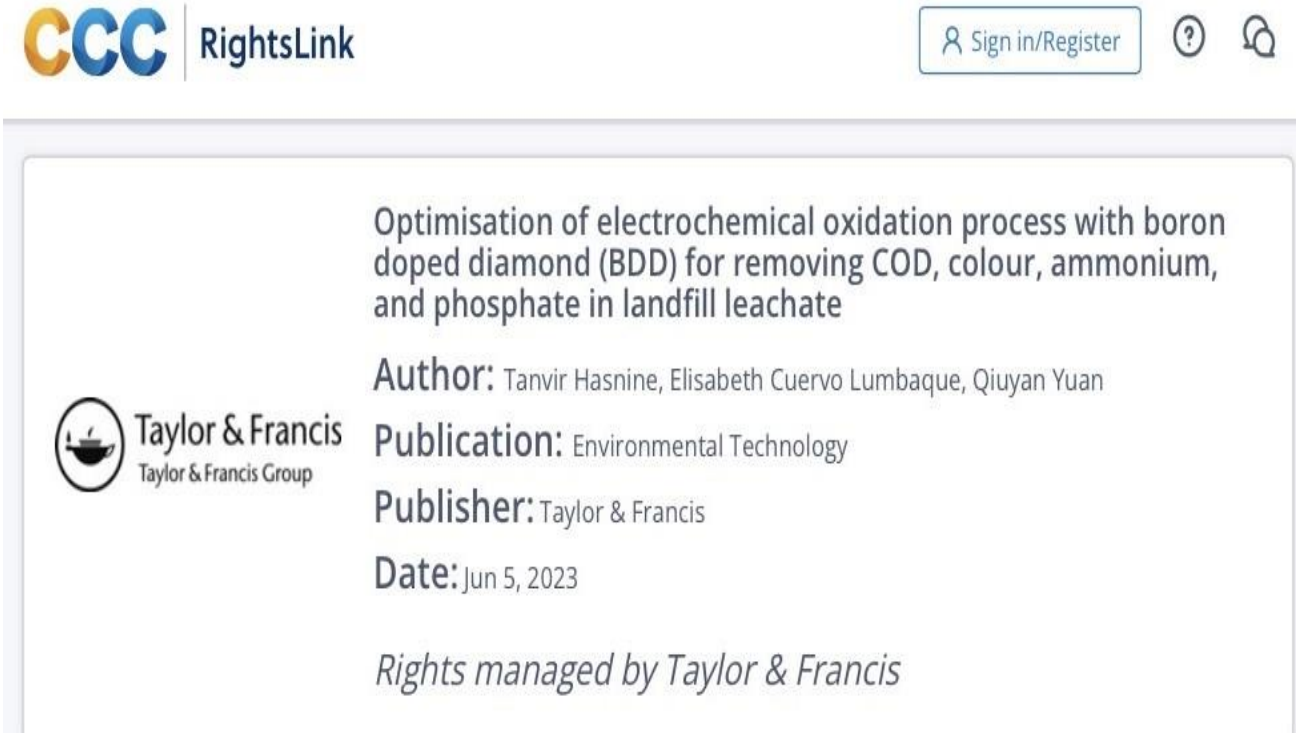

TABLE OF CONTENTS

Contents

LIST OF FIGURES

LIST OF TABLES

ABBREVIATIONS

AEO	Advanced Electrochemical Oxidation
ANOVA	Analysis of Variance
AO	Anodic Oxidation
AOPs	Advanced Oxidation Processes
BDD	Boron-Doped Diamond
BOD	Biochemical Oxygen Demand
CCD	Central Composite Design
COD	Chemical Oxygen Demand
DoE	Design of Experiments
EAOPs	Electrochemical Advanced Oxidation Processes
ECs	Emerging Contaminants
EO	Electrooxidation
Fe^{2+}/H_2O_2	Ferrous Ion / Hydrogen Peroxide (Fenton Reagent)
H_2O_2	Hydrogen Peroxide
HPLC	High-Performance Liquid Chromatography
HPLC-PDA	High-Performance Liquid Chromatography - Photodiode Array Detector
J	Current Density (mA/cm^2)
Nb/BDD	Niobium-based Boron-Doped Diamond
NH_4^+	Ammonium
NH_4^+-N	Ammonium Nitrogen
OER	Oxygen Evolution Reaction

PFAS	Per- and Polyfluoroalkyl Substances
PFOA	Perfluorooctanoic Acid
PFOS	Perfluorooctane Sulfonate
PO_4^{3-}	Phosphate
PO_4^{3-}-P	Phosphate Phosphorus
RO	Reverse Osmosis
RSM	Response Surface Methodology
SD	Standard Deviation
SEC	Specific Energy Consumption
SHE	Standard Hydrogen Electrode
SMZ	Sulfamethazine
SN	Sulfanilamide
TC-HCl	Tetracycline Hydrochloride
TOC	Total Organic Carbon
UV	Ultraviolet

Chapter 1: Introduction

1.1 General Introduction

Landfill leachate and antibiotic wastewater represent two important classes of complex wastewater that remain difficult to treat using conventional biological processes alone. Landfill leachate contains a variable mixture of refractory organic matter, ammonium, color-causing humic substances, inorganic ions, and nutrients, while pharmaceutical wastewaters may contain biologically active micropollutants that persist after secondary treatment (Abdel-Shafy et al., 2024; Q. Yuan et al., 2023). These contaminants are environmentally significant because residual organic matter, nitrogen species, phosphorus, color, and antibiotics can affect aquatic systems and complicate downstream discharge and reuse requirements (Abdel-Shafy et al., 2024; Fabiańska et al., 2014; T. Hasnine et al., 2023; Q. Yuan et al., 2023).

Landfill leachate treatment is particularly challenging because its composition changes with landfill age, waste characteristics, climate, and site operation (Abdel-Shafy et al., 2024; C. Teng et al., 2021). Mature leachate often contains poorly biodegradable organic matter and elevated ammonium, which can limit the effectiveness of biological treatment. Therefore, advanced treatment or polishing technologies are often required to improve the removal of COD, color, ammonium, and phosphate (M. D. T. Hasnine et al., 2022; Jiachen Wang & Qiao, 2024). Electrochemical oxidation has been widely investigated for these types of applications because oxidants are generated in situ at the electrode surface and can degrade refractory organic compounds without requiring large chemical addition (Abdel-Shafy et al., 2024; Gaetan et al., 2025; Urtiaga et al., 2022). Previous studies have shown that electrochemical advanced oxidation processes can improve treatment of complex landfill leachate and nanofiltration concentrates,

although performance is strongly controlled by current density, pH, wastewater matrix, and energy demand (Urtiaga et al., 2022).

Pharmaceutical residues, especially antibiotics, present an additional concern because they are frequently detected in municipal, hospital, livestock, and pharmaceutical wastewaters (Fabiańska et al., 2014; Nishmitha et al., 2025; Song et al., 2022). Antibiotics may be only partially removed in conventional wastewater treatment plants and can contribute to antimicrobial resistance, ecological toxicity, and formation of transformation products (Brouwir et al., 2025; Sambaza & Naicker, 2023). Recent reviews have identified electrochemical advanced oxidation processes as promising treatment options for antibiotic-contaminated wastewater because they generate reactive oxygen species such as hydroxyl radicals, sulfate radicals, hydrogen peroxide, and active chlorine species depending on electrode material and electrolyte composition (Brillas & Garcia-Segura, 2025; Q. Yuan et al., 2023). Key factors influencing antibiotic degradation include electrode type, initial antibiotic concentration, operating conditions, electrolyte composition, and wastewater matrix (Song et al., 2022; Q. Yuan et al., 2023).

Boron-doped diamond (BDD) electrodes are among the most effective anodes for electrochemical oxidation because they perform as non-active electrodes with high oxygen evolution overpotential, chemical stability, and strong capacity to generate weakly adsorbed hydroxyl radicals (Agustina et al., 2019; Calzadilla et al., 2021; de Souza et al., 2024). These radicals can non-selectively oxidize refractory organic compounds, including humic-like leachate organics and pharmaceutical molecules, toward smaller intermediates and mineralization products (Agustina et al., 2019; Ivantsova et al., 2025; Karim et al., 2021). In antibiotic treatment, BDD-based electrooxidation has been shown to degrade sulfonamides and tetracycline-type compounds through hydroxylation, bond cleavage, ring opening, and further oxidation of intermediates (Abdelhameed & El-Shahat,

2024; S. Hu et al., 2025a; Vasilie et al., 2018). For example, BDD electrooxidation has been reported for tetracycline degradation, sulfonamide oxidation, and secondary wastewater treatment containing sulfamethazine, supporting its relevance for mixed pharmaceutical systems (T. S. Chen et al., 2014; S. Hu et al., 2025a).

Even with these advantages, BDD electrooxidation is highly dependent on operating conditions (Agustina et al., 2019; Anglada et al., 2011; Brinzila et al., 2014). Higher current density can increase hydroxyl radical generation, but excessive current may reduce current efficiency through oxygen evolution, radical recombination, and increased energy consumption. Solution pH affects the speciation of contaminants, the stability of oxidants, and the oxidation potential of reactive species. Initial contaminant concentration determines the oxidant-to-pollutant ratio, while auxiliary oxidants such as H_2O_2 may enhance degradation at moderate doses but may also scavenge hydroxyl radicals at excessive levels (Xuechun Wang et al., 2023). Therefore, systematic optimization is necessary to identify operating conditions that provide high treatment efficiency while maintaining practical energy demand.

Response surface methodology (RSM) provides a statistically efficient approach for evaluating the effects of multiple operating variables and their interactions (J. Hu et al., 2020; Leili et al., 2020; Nashat et al., 2022). Compared with one-factor-at-a-time experimentation, RSM can quantify linear, quadratic, and interaction effects using fewer experimental runs (Gaetan et al., 2025). In electrochemical wastewater treatment, this is useful because pH, current density, oxidant dose, treatment time, and pollutant loading are interdependent. In this thesis, RSM and desirability-based optimization were used in two related contexts. First, a factorial design with a central point, in association with RSM and desirability profiling, was applied to optimize current density and pH for the removal of COD, color, NH_4^+, and PO_4^{3-} from raw landfill leachate using STATISTICA®.

Analysis of variance was used to evaluate the explanatory strength of the fitted model and select the best model form. Second, central composite design-based RSM was used using design expert software to optimize H_2O_2-supplemented Nb/BDD electrooxidation for simultaneous removal of sulfanilamide, tetracycline hydrochloride, and sulfamethazine from biologically treated synthetic wastewater.

1.2 Knowledge gaps

The research gap addressed in this thesis is the limited integration of Nb/BDD electrooxidation across both landfill leachate treatment and mixed pharmaceutical compounds removal in wastewater. Many studies focus either on conventional leachate parameters such as COD and ammonium or on individual pharmaceutical compounds in simplified aqueous matrices. Fewer studies connect these two treatment challenges under a unified electrochemical framework, and fewer studies evaluate mixed antibiotics removal together with model optimization, mineralization, energy consumption, and cost indicators. This thesis, therefore, examines BDD electrooxidation from both an applied real leachate treatment perspective and a targeted micropollutant degradation perspective in wastewater. The landfill leachate and antibiotic studies represent sequential applications of the same Nb/BDD electrooxidation platform. The leachate study established the feasibility of treating a complex real wastewater matrix and identified current density and pH as key operational parameters. It also demonstrated the energy penalty associated with high-current operation. These findings informed the selection of current density and pH as major factors in the subsequent antibiotic studies. The antibiotic work extended the investigation from bulk water-quality indicators to compound-specific removal of SN, TC-HCl, and SMZ. Thus, the leachate study provided the process-level basis, while the antibiotic studies refined the

treatment approach for structurally distinct emerging contaminants and supported optimization under different wastewater conditions.

1.3 Hypothesis

The central hypothesis of this thesis is that BDD electrooxidation can effectively remove refractory organic matter, nutrients, color, and selected antibiotics from complex wastewater matrices, and that treatment performance could be improved by optimizing operating variables that control oxidant generation, contaminant speciation, and oxidant-to-pollutant ratio. A related hypothesis is that RSM-based optimization could identify balanced operating conditions that maximize treatment performance while providing a statistically reliable prediction of process behavior.

1.4 Goals and Objectives

The overall objective of this thesis is to evaluate and optimize BDD electrooxidation for the treatment of landfill leachate and mixed pharmaceutical antibiotics. The specific objectives are:

1. to optimize electrochemical oxidation using Nb/BDD electrodes for the removal of COD, color, ammonium, and phosphate from landfill leachate;
2. to investigate the influence of operational parameters on the removal of mixed pharmaceutical antibiotics (SN, TC-HCL, SMZ) from wastewater using Nb/BDD electrooxidation;
3. to apply RSM for optimization of H_2O_2-supplemented Nb/BDD electrooxidation for the removal of SN, TC-HCl, and SMZ from wastewater; and
4. to assess optimized treatment performance using parent-compound removal, TOC mineralization, energy consumption, and electrical cost analysis.

1.5 Novelty of the thesis

The novelty of this thesis lies in its combined evaluation of Nb/BDD electrooxidation for two connected environmental engineering problems, which are a complex landfill leachate treatment and mixed pharmaceutical antibiotic removal. Chapter 3 addresses high-strength wastewater-quality improvement by optimizing COD, color, ammonium, and phosphate removal from landfill leachate. Chapter 4 extends the work to mixed antibiotic degradation by examining how operating conditions influence simultaneous removal of SN, TC-HCl, and SMZ. Chapter 5 advances the thesis by applying RSM to optimize H_2O_2-assisted Nb/BDD electrooxidation and by linking parent-compound removal with TOC mineralization, energy demand, and cost estimation.

1.6 Thesis organization

This thesis is a grouped manuscript (sandwich) thesis and comprises six chapters, where chapters 3 to 5 were each formatted as a research manuscript.

Chapter 1 presents the general introduction, research gaps, objectives, hypotheses, novelty, and thesis structure.

Chapter 2 reviews the literature on landfill leachate treatment, pharmaceutical contaminants, BDD electrooxidation, hydroxyl-radical-mediated degradation, and RSM-based optimization.

Chapter 3, "Optimization of Electrochemical Oxidation Process with Boron Doped Diamond (BDD) for Removing COD, Color, Ammonium, and Phosphate in Landfill Leachate," evaluates the application of Nb/BDD electrooxidation for landfill leachate treatment.

Chapter 4, "Influence of Operational Parameters on Mixed Pharmaceutical Antibiotics Removal from Wastewater Using Boron-Doped Diamond (BDD) Electrooxidation," investigates the effects of operating variables on ternary antibiotic degradation.

Chapter 5, "Application of Response Surface Methodology for Optimization and Electrochemical Oxidation of Three Mixed Antibiotics at Boron-Doped Diamond Electrodes," develops and validates the RSM-based optimization of H_2O_2 -assisted Nb/BDD electrooxidation.

The final **Chapter 6** summarizes the major findings, engineering significance of the overall thesis, and provides recommendations for future research and scale-up.

Chapter 2: Literature Review

2.1. Introduction to Wastewater Treatment Challenges

Recent studies have highlighted that wastewater treatment systems are currently facing the challenge of a wide variety of persistent contaminants, particularly landfill leachate constituents and pharmaceutical residues (Canabarro et al., 2026; Gaetan et al., 2025). Landfill leachates are generated through precipitation infiltration and waste decomposition, and often contain high concentrations of organic and inorganic pollutants, ammonia, heavy metals, color-causing substances, and xenobiotic compounds, including pharmaceuticals and industrial chemicals (Canabarro et al., 2026; Jiachen Wang & Qiao, 2024). Leachate treatment is important because of its potential risks to groundwater quality and aquatic ecosystems. However, effective management remains challenging because leachate volume and contaminant composition can vary significantly with landfill age, waste characteristics, precipitation, and site operating conditions (Canabarro et al., 2026). Pharmaceutical pollutants, such as antibiotics, hormones, and analgesics, usually go around both municipal and industrial wastewater facilities with little to no elimination, and are found in detectable amounts in surface waters of the global environment (Mariano et al., 2023; Wada & Olawade, 2025). These compounds are of concern because they have the potential to cause chronic toxicity, bioaccumulation, and increase antimicrobial resistance; also, their concentration increases more by traditional treatment technologies, which focus on bulk removal of organic content instead of trace micropollutant removal (Singh et al., 2024; Wada & Olawade, 2025). In recent times, there has been an increased focus on per- and polyfluoroalkyl substances (PFAS), commonly known as forever chemicals, which are strongly persistent synthetic organic pollutants that can be found in large amounts in landfill leachate (Goukeh et al., 2025; Lu et al., 2023; Xia Yu et al., 2025). According to recent studies, both conventional and advanced treatment

methods, such as membrane filtration, adsorption, and advanced oxidation, cannot completely remove PFAS; in fact, leachate treatment in some situations has even converted PFAS precursors into even more inert and harmful forms of PFOS and PFOA, increasing environmental hazards (Gokgoz et al., 2023; Lu et al., 2023; Sabba et al., 2025). To resolve these complex issues, the current literature supports the application of advanced solutions and the necessity to conduct more research and develop new monitoring and treatment systems to reduce the risks of emerging contaminants in wastewater and improve the leachate treatment system (Yexiang Chen et al., 2025; Nishmitha et al., 2025; Jiachen Wang & Qiao, 2024; Haiya Zhang et al., 2025).

2.1.1 Global Wastewater Pollution and Emerging Contaminants

The growing environmental and public health impacts of wastewater pollution have become a major concern due to the increasing occurrence of emerging contaminants. These contaminants include pharmaceuticals, personal care products, microplastics, endocrine disruptors, nanomaterials, PFAS, and persistent industrial chemicals (Yexiang Chen et al., 2025; M. T. Hasnine et al., 2025; Meena et al., 2025). According to recent research, in most developing economies, these contaminants are frequently found at trace levels, and they have been reported to cause endocrine, reproductive, and developmental effects in aquatic organisms with potential bioaccumulation through the food chain and long-term risks to human health (Bayabil et al., 2022; Das et al., 2024; Puri et al., 2023). The increased industrialization, urbanization, and the use of chemicals and pharmaceuticals by consumers in developing and developed countries increase the spread of these contaminants (Bayabil et al., 2022; Das et al., 2024; Puri et al., 2023). Investigation shows that they are persistent even in different environmental matrices like surface water, groundwater, soil, and even some drinking water sources because conventional and even advanced treatment technologies are unable to achieve sufficient removal (T. Jiang et al., 2024; Jones et al.,

2022; Tisler et al., 2025). As a result, wastewater treatment facilities have become a major and continued source of emerging pollutants in the globe (T. Jiang et al., 2024). The existing scientific opinion is that there is a need to adopt integrated management approaches and investment in modern and hybrid treatment methods, including membrane filtration and advanced oxidation (Senthil Rathi et al., 2024; Simonetti et al., 2025). However, such solutions are not feasible in practice due to financial and technological disparities, especially in the Global South, and are worsened by inconsistent enforcement of regulations. Unless significant efforts are undertaken on various fronts, the emerging contaminants will keep eroding water security. Thus, it will negatively affect the achievement of Sustainable Development Goals regarding clean water, the well-being of ecosystems, and human health, as highlighted in the recent studies (Jones et al., 2022; Puri et al., 2023).

2.1.2 Challenges of Landfill Leachate Treatment

Landfill leachate is generated by the percolation of water through waste deposits, which mobilizes dissolved and suspended solids, including high concentrations of organic matter, ammoniacal nitrogen, heavy metals, and emerging pollutants such as PFAS, pharmaceutical antibiotics, and microplastics (Gaur et al., 2024; M. T. Hasnine et al., 2025; Jiachen Wang & Qiao, 2024). However, leachate composition changes with landfill age, waste type, and hydrological conditions (Canabarro et al., 2026), and the major challenge here is the presence of recalcitrant organics that resist biodegradation and usually persist in conventional treatment (C. Teng et al., 2021). Previous studies mentioned that stabilized leachate often contains humic and fulvic-like substances, aromatic compounds, and nitrogen-rich organics that reduce biodegradability and increase treatment cost (Monje-Ramirez & Velásquez, 2004). Though coagulation or biological pretreatment removes a large fraction of COD, a significant residual fraction often remains because

these compounds are poorly reactive and can accumulate in concentrates generated by membrane systems (Q. Li et al., 2023). In addition, different membrane-based technologies, especially reverse osmosis (RO) and nanofiltration, are characterized by high removal efficiencies but are not effective due to membrane fouling, high cost of operation, and the most significant challenge of handling contaminated concentrate byproducts, which require additional treatment or safe disposal (Jiachen Wang & Qiao, 2024). For this reason, landfill leachate management is very important, and if it is reinjected or poorly managed, it can overload upstream processes and create secondary environmental risks (Q. Li et al., 2023).

Another problem in landfill leachate is the presence of high concentrations of ammonia, which can inhibit biological treatment, especially when combined with salinity and toxic trace organics (C. Teng et al., 2021). In the coagulation process, it can reduce color and lower the amount of COD removal, and the treatment process is not effective for the complete removal of refractory dissolved organics (H. Chen et al., 2024). However, advanced oxidation processes can degrade persistent compounds and improve biodegradability, although their efficiency depends on oxidant generation, reaction kinetics, wastewater matrix composition, and the inhibitory effects of salts and competing organics (Kumari & Kumar, 2023).

From an engineering perspective, the main challenge is the economic and sustainability aspect because the leachate treatment is one of the most expensive factors in landfill management (Q. Li et al., 2023). High energy requirements, substantial chemical consumption, and the environmental impact of treatment by-products usually limit the feasibility of the process, particularly in regions with limited resources and developing countries (Igwegbe et al., 2024; Xiang et al., 2025). Recent studies focus on artificial intelligence with machine learning for waste characterization and process optimization for treatment purposes, but these are in the initial steps of implementation (Gaur et

al., 2024). Finally, the landfill leachate treatment process demands persistence of technological development, multi-faceted and location-specific management approaches, and intensifies the environmental requirements all over the world (Gaur et al., 2024; Igwegbe et al., 2024; Jiachen Wang & Qiao, 2024).

2.1.3 Pharmaceutical Compounds as Emerging Environmental Contaminants

The presence of pharmaceutical compounds in the environment has emerged as one of the major concerns of the world and has been named as a category of emerging contaminants (ECs). The sources of these pollutants are mainly human and veterinary medicine, improper disposal, excretion, industrial discharge, and agricultural runoff, and their routes are the effluents of wastewater treatment plants, and runoff of areas with insufficient sanitation infrastructure (Xingyu Li et al., 2024; Wada & Olawade, 2025). Research indicates that pharmaceutical substances like antibiotics (e.g., amoxicillin, ciprofloxacin), analgesics (acetaminophen, ibuprofen), antiepileptics (carbamazepine), hormones, and other personal care products are widely distributed in surface water, groundwater, and, in some cases, even in drinking water, and their concentrations are often much higher in areas with no centralized sewage treatment, e.g., parts of Africa and Latin America (Eapen et al., 2024; Wada & Olawade, 2025). These compounds have a variety of physicochemical characteristics, resulting in different behaviors and recalcitrance in aquatic systems; some of them are biologically active at trace levels, resist biodegradation, and may bioaccumulate or undergo transformation into equally concerning intermediates (Das et al., 2024). Their ecological effects are disrupting the reproductive and behavioral systems of aquatic organisms, causing antibiotic resistance vertically and horizontally through gene transfer. They also change the structures of microbial and macroinvertebrate communities, and the human health risks are related to chronic exposure at low doses and transmission of antibiotic resistance genes (Das et al., 2024; Eapen et

al., 2024; Wada & Olawade, 2025). Traditional methods of wastewater treatment are usually not sufficient to eliminate these micropollutants, particularly those that are persistent, such as carbamazepine, and lead to their extensive spread into the environment (Sundararaman et al., 2022; Wada & Olawade, 2025). Recent studies aim at implementing advanced oxidation processes (AOPs) that use BDD electrodes, which are especially effective at generating powerful oxidizing radicals capable of mineralizing various pharmaceuticals and reducing toxicity (Ahmed et al., 2025). In addition, other treatment processes such as membrane filtration, biochar-based systems, and decentralized point-of-use systems are useful in resource-restricted environments (Eapen et al., 2024; Wada & Olawade, 2025). For this reason, adaptation of sustainable treatment strategies and implementation of regulations for pharmaceutical sources are outlined as the key measures to reduce this issue worldwide (Das et al., 2024; Eapen et al., 2024; Wada & Olawade, 2025).

2.2 Advanced Oxidation Processes (AOPs) for Wastewater Treatment

Advanced oxidation processes (AOPs) are widely recognized as efficient treatment methods for both leachate and pharmaceutical wastewater because they produce highly reactive species, such as hydroxyl and sulfate radicals, that can non-selectively degrade persistent organic pollutants (Hama Aziz et al., 2025). Recent work highlights the effectiveness of Fenton-based reactions, ozonation, photocatalysis, and electrochemical oxidation for removing refractory compounds from this type of wastewater (Całus-Makowska et al., 2025; Morker & Saini, 2024). Studies indicate that the combination of AOPs with physical, chemical, or biological methods increases the efficiency of removal and mineralization compared to conventional treatments that are used separately (Adeoye et al., 2024). In the case of landfill leachate, the ultrasound-assisted AOPs have been shown to enhance the rate of hydroxyl radical production, which enhances the degradation rates (Jiachen Wang & Qiao, 2024). In a similar way, the photo-assisted TiO_2/ZnO oxidation

provides high efficacy in the degradation of recalcitrant leachate pollutants, especially when operating under the optimal pH and temperature conditions (Jiachen Wang & Qiao, 2024). AOPs have been used in the treatment of pharmaceutical wastewater with almost complete mineralization of the hazardous residues, reducing the environmental and public health hazards and producing minimal secondary sludge (Hama Aziz et al., 2025). These treatments are especially beneficial to contaminants that are toxic, carcinogenic, and bioaccumulative, which are the properties that are often difficult to treat with biological treatment methods (Kanakaraju et al., 2025). However, there are still issues, such as energy consumption, operational, and in some cases, sludge formation of reagents used in Fenton processes (Adeoye et al., 2024). Overall, current literature describes AOPs as a sustainable treatment system for complex wastewater matrices, especially in combination with other technologies (Jiachen Wang & Qiao, 2024).

2.2.1 Principles of AOPs

In advanced oxidation processes, highly reactive radical species such as hydroxyl and sulfate radicals are predominantly generated. These radicals are directly able to degrade persistent organic pollutants and are increasingly regarded as a cutting-edge technology for treating leachate and removing pharmaceutical contaminants from wastewater (Hama Aziz et al., 2025; Jiachen Wang & Qiao, 2024). The basic concept of AOPs is the generation of these radicals by a variety of methods including photocatalysis, Fenton reactions, and Fenton-like reactions, electrochemical oxidation, ozonation, non-thermal plasma and combinations of these, which combinedly provide a strong, non-selective oxidation environment that can mineralize complex and recalcitrant contaminants to CO_2, H_2O and mineral acids (Hama Aziz et al., 2025; Vinayagam et al., 2024). When advanced oxidation processes, particularly Fenton-based treatments and ozone-driven oxidation, are applied to landfill leachate, they are especially effective for organic-rich matter and

refractory compounds removal. These methods achieve chemical oxygen demand (COD) reductions exceeding 75 %, under optimized key operational conditions such as Fe^{2+}/H_2O_2 ratios, pH, reaction time, and iron sludge formation (Jiachen Wang & Qiao, 2024). Photocatalysis using UV-activated TiO_2 or composite catalysts also takes an essential stage in leachate and provides a significant amount of mineralization of the pharmaceuticals and other xenobiotics in the presence of controlled light, pH, and dosage conditions (Hama Aziz et al., 2025; Morker & Saini, 2024). In the case of pharmaceutical wastewater, the AOPs offer high removal efficiencies of toxic and bioaccumulative compounds like antibiotics, anti-inflammatories, and chemotherapy remnants, in which other physical or biological treatment methods fail because of the non-biodegradability nature of such micropollutants (Hama Aziz et al., 2025; Morker & Saini, 2024). The main advantages of these processes include a high reaction rate, the ability to control the operation, and complete mineralization without the presence of a secondary waste and sludge, especially in hybrid AOPs, which involve oxidative, photochemical, and catalytic routes (Hama Aziz et al., 2025; Morker & Saini, 2024). Ozone-based AOPs and non-thermal plasma have additional benefits since they can be used to oxidize in mild conditions, but are limited by transfer and energy input, and previous research aims to solve this issue with new catalysts and process integration (Hama Aziz et al., 2025; Vinayagam et al., 2024). However, the main weaknesses of AOPs include energy usage, cost, scalability, and, in some cases, secondary pollution or catalysts recovery; but because of the recent advances in green materials, hybridization, and optimized combinatory approaches are proving to increase sustainability and large-scale viability to leachate and pharmaceutical wastewater treatment {Formatting Citation}. In general, the latest scientific literature has strong arguments in favor of AOPs as a strong, versatile, and sustainable strategy for the combined reduction of leachate-based contaminants and pharmaceutical compounds, thus contributing to the

environmental protection and water safety goals (Vinayagam et al., 2024; Jiachen Wang & Qiao, 2024).

2.2.2 Overview of Electrochemical Advanced Oxidation Processes (EAOPs)

In Electrochemical Advanced Oxidation Processes (EAOPs), the main principle is the electrochemical production of highly oxidative species in situ, which is mostly the hydroxyl radical (•OH), with a strong oxidizing potential (E^o = 2.80 V vs. SHE) (Brillas et al., 2009; P. V. Nidheesh et al., 2023). The hydroxyl radical has strong characteristics of reactivity, such as indiscriminate oxidation and a fast reaction rate with the majority of organic substances. This allows the process of mineralization of organic pollutants by a series of oxidative degradation reactions, which eventually produce environmentally harmless final products, such as carbon dioxide, water, and inorganic salts (Brillas et al., 2009; Juan Li et al., 2016). The performance of conventional biological treatment systems is often poor in the treatment of mature leachate due to the presence of bio-refractory compounds and the possible cytotoxic impact of these compounds on the population of microorganisms (Sirés et al., 2014a). EAOPs have shown an effective performance in the degradation of various antibiotics, such as β-lactams, tetracyclines, sulfonamides, and fluoroquinolones (Ivantsova et al., 2025) and have reported more than 95% removal for parent compounds with almost complete mineralization (Ivantsova et al., 2025).

The performance of EAOP also depends on the choice of electrode materials, which determine the efficiency and selectivity of the oxidation process. Current density has an impact on the rate of oxidant production and the overall kinetics of the treatment, but excessive current densities can cause parasitic reactions and decreased current efficiency (Sopaj et al., 2015). The pH of the solution determines the speciation of target compounds and the stability of formed oxidants,

whereas the ionic strength and the composition of supporting electrolytes determine the mass transfer properties and conductivity (Sirés et al., 2014b; Vinayagam et al., 2024).

Although the effectiveness of EAOPs is proven, several technical and economic issues need to be improved for their adoption. The consumption of energy is an issue of concern, especially when it comes to large-scale usage, where electrochemical processes generally consume a lot of electricity. The processes of electrode fouling and deactivation, such as polymeric film formation and catalyst reactions, may have a serious effect on the long-term stability of operation and treatment. Also, the risk of the formation of potentially harmful oxidation by-products needs to be monitored and evaluated (Sirés et al., 2014b). To overcome these shortcomings, new strategies that include the design of new electrode materials with increased catalytic efficiency and stability, the combination of EAOPs with other treatment technologies in hybrid systems, and optimization of operational conditions are very important for improving overall treatment performance (P. V. Nidheesh et al., 2023).

2.3 Boron-Doped Diamond (BDD) Electrodes in Electrochemical Oxidation

2.3.1 Properties and Advantages of BDD Electrodes

BDD electrodes are steadily considered to be one of the most promising anode materials in AEO due to their exceptional physicochemical and electrochemical characteristics (Castillo-Cabrera et al., 2023; Carlos A. Martínez-Huitle et al., 2015). The principle of AEO consists of polarising a conductive substrate with a polarisation potential to produce highly oxidising reactive species (HORS), which are mostly hydroxyl radicals (•OH), at the electrode-solution interface (Ganiyu et al., 2019; Xinmin Yu et al., 2014). Among different electrode materials, Nb/BDD electrodes are particularly promising due to the unique set of characteristics that enable the most efficient degradation of pollutants (Castillo-Cabrera et al., 2023).

The main advantage of BDD electrodes is that they have an extremely high overpotential of the oxygen evolution reaction (OER) such that hydroxyl radicals can be produced over a wide range of potential before oxygen evolution takes over (McBeath et al., 2019). It has been confirmed that IrO_2, which is an active anode, has a low oxygen evolution potential of about 1.48 V vs SHE as compared to non-active anodes like Ebonex®, which has an overpotential of about 2.6 V versus SHE (G. Liu et al., 2021). The non-active anode category of BDD electrodes, which is also referred to as a high overpotential anode, is an ineffective catalyst in the production of O_2 but an excellent catalyst in the production of hydroxyl radicals (Comninellis, 1994; Panizza & Cerisola, 2009).

The chemical structure of BDD electrodes, especially the sp^3 /sp^2 carbon ratio, significantly affects the electrochemical performance of the electrodes. As much evidence shows, the BDD electrodes with increased sp^3 /sp^2 ratios generate a larger number of •OH and move the OER to more positive potentials (Espinoza et al., 2018). The potential of onset that can be reached by oxygen evolution is linear with the sp^3 /sp^2 ratio; the examples of onset potentials observed include about 2.16 V up to more sp^2 impurity content, depending on the quality of the diamond (Espinoza et al., 2018). This structure-performance relationship is important to explaining the high oxidation performance of high-quality BDD electrodes.

The process that supports the production of •OH on the BDD electrode has been widely investigated. The latest studies show that the generation of the •OH is not strongly dependent on surface functionalization and pH (pH 7.4 vs 9.2), which highlights that the •OH is produced by the outer-sphere electron-transfer reaction of H_2O (Henke et al., 2019). This is in contrast to oxygen evolution, which occurs through an inner-sphere mechanism that is highly sensitive to surface characteristics. The external-sphere character of the generation of the radicals suggests that radical

generation is highly reliant on the applied potential instead of intricate surface correlations, which makes BDD electrodes more predictable and resistant to changes in how they operate (G. Liu et al., 2021).

State-of-the-art detection methods, including scanning electrochemical microscopy (SECM) using spin trap reagents, including 5,5-dimethyl-1-pyrroline-N-oxide (DMPO), have provided quantitative information on the formation of •OH at BDD surfaces. According to research reports, the efficiencies of •OH generation at BDD electrodes are about 1-2 % at the potentials between 1.3 and 1.4 V vs. Ag/AgCl, and increase to a maximum of about 5% at the potentials between 1.8 and 2.2 V vs. Ag/AgCl (Barroso-Martínez et al., 2022). Its maximum efficiency is recorded in an acidic medium, which is consistent with the findings that the generation of •OH is maintained at low pH values (Barroso-Martínez et al., 2022). The collection of DMPO-OH begins at approximately 1.4 V vs. Ag^+ and continues until approximately 2.4–2.5 V, at which point the collection slows, likely because of DMPO decomposition or termination of •OH generation (Barroso-Martínez et al., 2022). In addition, BDD electrodes are highly chemically stable and resistant to corrosion, and maintain their structural integrity and electrochemical characteristics even in extreme environments, including pH levels and applied potentials (Castillo-Cabrera et al., 2023). The wide electrochemical potential window of BDD can reach well over 3V in aqueous solutions, which enables far more powerful oxidative conditions compared with conventional electrode materials (Panizza & Cerisola, 2009). Both the low value of double-layer capacitance and low adsorption strength are important because they help reduce the performance of BDD surfaces by strong adsorption of organic intermediates and facilitating the formation of weakly physisorbed •OH with a high oxidation potential ($E° = 2.80$ V vs SHE) (Comninellis, 1994).

Diamond material has a high thermal conductivity, which can be as high as 2000 W/m.K, and this allows the efficient heat removal during electrochemical processes, and thus localized overheating and electrode degradation are avoided (Panizza & Cerisola, 2009). This feature is essential, especially when operating continuously at high current densities where Joule heating is a major concern. Additionally, BDD electrodes have better mechanical strength and fouling resistance, which is vital in the treatment of complex matrices like landfill leachate and wastewaters with recalcitrant organic compounds and suspended solids (Castillo-Cabrera et al., 2023). Hydroxyl radicals are regarded as the major contributors to the superior oxidation ability of BDD electrodes, and they are considered some of the strongest oxidants known besides fluorine and exhibit an extremely high standard reduction potential (Qiao et al., 2024). This allows organic matter and toxic pollutants to be degraded quickly and with high efficiency and comparatively benign reaction pathways (Qiao et al., 2024). The •OH, with its short-lived and highly reactive nature, is able to oxidize a large range of organic compounds by a wide variety of different reactions, including hydrogen abstraction, electron transfer, and addition reactions (Enache et al., 2009).

2.3.2 Comparison with Other Electrode Materials

There have been many comparative studies comparing BDD electrodes with more traditional anode materials, including dimensionally stable anodes (DSA) of mixed-metalloy oxides, platinum, graphite, lead dioxide (PbO_2), and antimony-doped tin oxide (SnO_2 -Sb). It has been proven that these studies have shown significant variations in oxidation efficiency, mineralization capacity, and electrode stability (Panizza & Cerisola, 2009; Radjenovic & Sedlak, 2015). In addition, these comparisons are necessary to explain the advantages and limitations of BDD technology and inform about the choice of appropriate electrode materials during wastewater treatment.

Dimensionally Stable Anodes (DSA)

In industrial electrochemical processes, the most popular electrode materials are dimensionally stable anodes (DSA), which are typically titanium-based substrates coated with mixed metal oxides; ruthenium(IV) oxide (RuO_2) and iridium oxide (IrO_2) alone or in combination, because they are inexpensive and have satisfactory electrocatalytic properties (Comninellis, 1994). However, systematic comparisons have always indicated that BDD electrodes were significantly better than DSA materials in terms of organic pollutant mineralization and overall treatment efficiency. As an example, a BDD electrode was used to remove 96% of total organic carbon (TOC) at the same experimental conditions, whereas Ti/PbO_2 -IrO_2 -RuO_2, Ti/IrO_2 -RuO_2 -TiO_2, Ti/IrO_2 -RuO_2-SnO_2 and Ti/RuO_2-SnO_2 electrodes achieved 57, 35, 31, and 30% removal, respectively (Yaşar Çırak et al., 2025).

Performance difference is based on different electrochemical properties. DSA electrodes can be regarded as active anodes, with low OEP typically ranging between 1.484 V and 1.8 V against the standard hydrogen electrode (SHE), and which facilitates preferential oxygen evolution over •OH generation (Comninellis, 1994; G. Liu et al., 2021). Compared to this, BDD electrodes, which are considered non-active anodes, have significantly higher OEPs (>2.2 V vs SHE), and thus have a larger potential window in which •OH can be generated before oxygen evolution starts (Qiao et al., 2024). This relationship is confirmed in the studies of linear sweep voltammetry (LSV) with OEP values rising in the sequence Ti/RuO_2 -IrO_2 < Ti/Ta_2O_5 -SnO_2 -IrO_2 < Ti/Ta_2O_5 -IrO_2; electrodes with better OEP values demonstrate high-quality degradation behavior and lower power consumption during the electrochemical treatment (Zhao et al., 2019).

These results are supported by comparative degradation tests on the antibiotic amoxicillin. BDD electrodes depleted the target compound before 100 minutes, and DSA (Ti/RuO_2 -IrO_2) electrodes

oxidized less than half of the initial antibiotic concentration in the same period (Sopaj et al., 2015). The high performance of BDD is explained by the fact that weakly physisorbed •OH are formed on the BDD surfaces, and •OH on DSA electrodes are chemisorbed, which results in reduced oxidation potential and lower reactivity with organic contaminants (Sopaj et al., 2015). Moreover, BDD electrodes were also highly efficient in electrolysis at a wide range of current densities, suggesting that the mediated oxidation through the •OH still occurs as the most significant mechanism under a wide operating system (Sopaj et al., 2015).

A study on the degradation of Reactive Red 120, which is an azo dye, showed significant dissimilarities between the DSA and BDD performance (Panakoulias et al., 2010). In comparison, whereas both types of electrodes gave almost complete decolorization, BDD was able to do so in a significantly shorter period, and only 2 Ah/L of electrical charge was required as compared to 25 Ah/L with DSA. More importantly, Ti/IrO_2 -RuO_2 DSA electrodes exhibited low oxidation capacity and high selectivity of intermediate organic compounds, with only 10 -40% removal of TOC at 25ºC and 80ºC, respectively; BDD electrodes were capable of mineralizing the organic load to CO_2 completely (Panakoulias et al., 2010).

This difference was also demonstrated by instantaneous current efficiency (ICE) values with BDD reaching up to 0.45 and Ti/IrO_2 -RuO_2 electrodes reaching only 0.13 (Panakoulias et al., 2010). The quantification of •OH studies has been used to shed light on the mechanistic differences with the use of the DMPO spin-trap agents. The •OH concentration of DSA electrodes amounted to about 6.6×10^{-15} M, as opposed to 3.8×10^{-15} M with BDD electrodes (Sirés et al., 2014b). However, BDD electrodes had higher total oxidation efficiency, indicating that the nature-physiosorbed and chemisorbed-hydroxyl radicals are more significant than their absolute concentrations (Sirés et al., 2014b).

Platinum Electrodes

Although platinum electrodes possess very high electrical conductivity and have clear electrochemical characteristics, they have a number of major limitations that limit their use in wastewater treatment (Panizza & Cerisola, 2009). According to comparative works, platinum achieves a significantly lower TOC removal efficiency (24%) compared to BDD (96%) in the same conditions when paracetamol is degraded (Yaşar Çırak et al., 2025). The main disadvantages of platinum electrodes are their vulnerability to organic compounds and the generation of chloride ions, a limited electrochemical window, and the fact that it becomes deactivated when exposed to oxidative stress (Radjenovic & Sedlak, 2015). Platinum is an active anode, and in this case, intense reactions between •OH and the electrode surface result in chemisorbed M(•OH) species, which do not participate in the oxidation of organic substances but instead in the production of oxygen (Comninellis, 1994). The oxidation process on platinum surfaces is through the formation of higher platinum oxide species (PtO, PtO_2), which mediate selective oxidation reaction instead of total mineralization (Panizza & Cerisola, 2009). Moreover, the platinum is very expensive and, therefore, is not economically feasible to use in large-scale wastewater treatment, despite having excellent conductivity and electrochemical reversibility (Sopaj et al., 2015).

Lead Dioxide (PbO_2) Electrodes

Another unique category of non-active anodes is lead dioxide electrodes, which possess a high oxygen evolution overpotential, which makes them potentially useful in the oxidation of organic pollutants (Panizza & Cerisola, 2009). PbO_2 electrodes demonstrate good electrical conductivity and mediocre oxidation capacity, and comparative analysis shows intermediate results compared to DSA and BDD electrodes (Radjenovic & Sedlak, 2015). However, PbO_2 electrodes have major limitations that limit their practical use, the most notable of which is the danger of lead leaching

during the treatment process, which creates serious environmental and health concerns (Qiao et al., 2024).

Gradual corrosion and dissolution of the active layer of the PbO_2 electrode, in general, reduces the life span and, especially under acidic conditions or high current densities, limits the service lifespan of PbO_2 electrodes compared to BDD electrodes (Panizza & Cerisola, 2009). Even though there are studies that have claimed improved performance by the addition of IrO_2 and RuO_2 to the PbO_2 coatings, which achieved a TOC removal efficiency of (52-57 %), these are still significantly lower compared to the results with BDD electrodes (58-96 %) (Yaşar Çırak et al., 2025). The ecological issues related to the possible lead pollution of treated water have significantly constrained the usage of PbO_2 electrodes, particularly in situations where treated effluent is released into the natural water systems or reused (Radjenovic & Sedlak, 2015).

Tin Oxide (SnO_2-Sb) Electrodes

Electrodes made of antimony-doped tin oxide (SnO_2-Sb) have been proposed as inexpensive alternatives to BDD, with a fairly high oxygen evolution capacity and excellent oxidation of a variety of organic substances (Qiao et al., 2024). SnO_2-Sb anodes prefer total oxidation of pollutants to CO_2 and H_2O, and are especially effective in the degradation of phenol and phenolic compounds (Qiao et al., 2024). The cost-benefit of SnO_2-Sb electrodes over BDD makes them appealing to electrochemical oxidation processes, especially in such applications where moderate treatment efficiency serves (Radjenovic & Sedlak, 2015). Nevertheless, the major deficiency of SnO_2-Sb electrodes is the short lifespan of the materials, which is caused by the lack of strong adhesion between the titanium substrate and the coating of SnO_2, which causes the premature removal of the coating and subsequent breakdown of the electrodes (Qiao et al., 2024; Ren et al., 2025). This instability in operation significantly increases the cost of operation since electrode

replacement is a frequent requirement. Comparative analysis of thiocyanate removal of coke oven wastewater shows that BDD electrodes have 96.51% removal efficiency, which is significantly higher than Ti/IrO_2, Ti/IrO_2 -RuO_2, and Ti/IrO_2 -RuO_2 -TiO_2 DSA electrodes (Turan et al., 2020). The mechanical weakness and erosive nature of SnO_2-Sb at high current densities continue to be significant challenges to the large-scale use of SnO_2- Sb electrodes in continuous industrial processes (Ren et al., 2025).

Graphite Electrodes

Graphite electrodes are economically viable, common, and easy to find, but do not show good dimensional stability and corrode heavily during anodic polarization (Sopaj et al., 2015). The oxidation of graphite anodes by electricity causes the carbon particles to be released into the treated solution, thus leading to turbidity, which will require further filtration measures (Panizza & Cerisola, 2009). Comparative analysis reveals that graphite electrodes have significantly lower oxidation and current efficiencies than boron-doped diamond (BDD) electrodes, and their performance decreases very quickly, which requires a lot of replacement (Sopaj et al., 2015). The overpotential of the low oxygen evolution of graphite electrodes restricts the generation of •OH, hence oxidation instead of total mineralization of organic compounds is selective (Comninellis, 1994). Besides, graphite surfaces are easily contaminated by organic intermediates and humic compounds, especially in the treatment of complex wastewater matrices, including landfill leachate, thus reducing the treatment efficiency of the system over time (Radjenovic & Sedlak, 2015). Graphite electrodes are therefore usually used in low-cost, low-efficiency treatment situations where an intermediate level of pollutant removal is required (Panizza & Cerisola, 2009).

Summary of Comparative Performance

Extensive comparative studies have been made to determine that BDD electrodes are always better than the conventional electrode materials in terms of mineralization efficacy, treatment time, and electrode stability (Radjenovic & Sedlak, 2015). Although DSA electrodes have the cost benefit of being used in the selective oxidation or chlorine evolution process, BDD electrodes are the best option in total mineralization of recalcitrant organic pollutants (Panizza & Cerisola, 2009). The high initial price of BDD electrodes can be compensated by their longer service life (thousand hours of operation), lower energy usage per unit of pollutant treated, and high treatment efficiency, making them economically demanding in wastewater treatment processes (Carlos A. Martínez-Huitle et al., 2015). The benefits of BDD in the mechanistic viewpoint, such as high oxygen evolution overpotential, weak adsorption characteristics, and effective •OH generation, employ these electrodes as the standard of electrochemical advanced oxidation processes (Castillo-Cabrera et al., 2023).

2.3.3. Mechanisms of Oxidation on BDD Surfaces

The electrochemical oxidation process of BDD electrodes includes both direct electron transfer on the electrode surface and indirect oxidation through electrogenerated oxidants, for most organic pollutants removal (Panizza & Cerisola, 2009; Qiao et al., 2024). Direct anodic oxidation involves the adsorption of pollutants on the anode surface, and the electron transfer reaction, or highly reactive •OH are generated to degrade it (Sánchez-Sánchez et al., 2007). The indirect oxidation happens mainly due to the production of •OH by oxidizing water on the anode surface, described by the following reaction **(2-1)**, (Panizza & Cerisola, 2009).

$$BDD + H_2O \rightarrow BDD(\bullet OH) + H^+ + e^- \quad \textbf{(2-1)}$$

However, the production of •OH is largely determined by the applied potential and not the intricate surface interactions (Henke et al., 2019; G. Liu et al., 2021). It has been proven that indirect oxidation with the use of •OH is the dominant mode of pollutant degradation, and the direct oxidation at the electrode surface is a minor process (Qiao et al., 2024). The •OH formed on BDD surfaces are not chemisorbed, but loosely physisorbed, and hence, they retain an oxidation potential near to that of free •OH (Comninellis, 1994; Sopaj et al., 2015). However, BDD electrodes are able to produce active chlorine species Cl_2, HOCl, and ClO^- in the presence of chloride ions, by a series of electrochemical reactions (Castillo-Cabrera et al., 2023). At the electrode surface, the oxidation of Cl^- occurs through the adsorbed •OH by the following reaction **(2-2)**; (Mostafa et al., 2018).

$$BDD(\bullet OH) + Cl^- \rightarrow BDD + HOCl + e^- \quad \textbf{(2-2)}$$

Chlorine-based oxidants, primarily hypochlorous acid (HOCl), participate in radical-driven oxidation pathways in advanced oxidation processes. HOCl has a standard reduction potential of approximately 1.49 V vs. NHE, making it a sufficiently strong oxidant to degrade many recalcitrant organic compounds (Castillo-Cabrera et al., 2023). It has also been observed that additional reactive oxygen species (ROS), such as peroxydisulfate ($S_2O_8^{2-}$), can form when sulfate ions are present in the electrolyte (Khamis et al., 2010). The generation of peroxydisulfate is achieved by reacting the •OH with sulfate ions, which produces more oxidizing species, which enhance COD degradation by direct oxidation in the anode and indirect oxidation via the electrogenerated species (Khamis et al., 2010). The ability of several oxidants to be produced at once, such as •OH, active chlorine species, and peroxydisulfate, also leads to the higher degradation and mineralization rates of BDD electrodes compared to other electrode materials (Carlos A. Martínez-Huitle et al., 2015; Panizza & Cerisola, 2009).

2.4 Landfill Leachate Treatment by Electrooxidation

2.4.1 Characteristics of Landfill Leachate

Landfill leachate represents a major problem in wastewater treatment due to its highly variable and complex composition, which is determined by various factors, such as the age, waste composition, the pattern of precipitation, and seasonal change (Abbas et al., 2009; Renou et al., 2008).

Landfill leachate is commonly classified according to landfill age into three stages, which are young leachate (<5 years), intermediate leachate (5-10 years), and mature or stabilised leachate (>10 years) (Dereli et al., 2014; Renou et al., 2008). Biodegradable organic matter is often high in young landfill leachate, where biochemical oxygen demand (BOD_5) would range between 4000 and 15000 mg O_2/L and COD between 25000 and 60000mg O_2/L (Amor et al., 2015). As a result, the ratio of BOD_5/COD in young leachate is rather high, typically 0.15-0.25, which is a sign of a high percentage of readily biodegradable organics (Amor et al., 2015; Bikash Adhikari & Sanjay Nath Khanal, 2015). Young leachate is usually acidic with a pH of about 4 and 6.5 due to accumulated volatile fatty acids formed in the active process of anaerobic decomposition (Bikash Adhikari & Sanjay Nath Khanal, 2015).On the other hand, mature landfill leachate has very distinct characteristics, thus making the treatment process difficult. The ratio between the BOD_5 and COD in mature leachate is minimal (less than 0.1), which indicates that the organic fraction consists of recalcitrant substances, including humic and fulvic compounds that cannot be broken down by biological processes (Amor et al., 2015; Kulikowska & Klimiuk, 2008). The levels of COD are also high, but tend to be lower than in young leachate, ranging between 10000 and 70000 mg/L and more often between 2000 and 8000 mg/L based on the landfill nature (Kulikowska & Klimiuk, 2008; Wainaina et al., 2020). The pH of mature leachate increases to higher than 7,

usually 7.5 to 9, due to the consumption of volatile fatty acids and the creation of methanogenic conditions (Amor et al., 2015).

Ammonium nitrogen is also a major pollutant in landfill leachate, and concentrations are often in the range of 1500 mg /L and up to 2500 to 3000 mg/L in mature leachate (Kulikowska and Klimiuk, 2008). An increasing trend in the ammonium concentration with landfill age has already been observed in other research; a study has reported the increase between 98 mg/L, $N\text{-}NH_4$, and 364 mg/L, $N\text{-}NH_4$ (Kulikowska & Klimiuk, 2008). Ammonium at high concentrations is harmful to the environment, such as eutrophication of the receiving waters and toxicity to aquatic life, when released without proper treatment (Kulikowska & Klimiuk, 2008).

In landfill leachate, the total phosphorus concentrations are in the range of 5 to 500 mg/L, but the concentration may differ depending on the waste composition (Renou et al., 2008). Landfill leachate colour, which can mainly be explained by the high molecular-weight humic compounds, is also an important aesthetic parameter that increases with the age of the landfill, giving the mature leachate a typical colour of dark brown to black (Kulikowska & Klimiuk, 2008). Mature leachate treatment studies have also reported the significant colour removal achieved by approximately 74% in coagulation/flocculation processes (Amor et al., 2015).

Heavy metals, such as iron, manganese, zinc, lead, cadmium, chromium, and nickel, further complicate the treatment of leachates, but the amount of heavy metals in leachate tends to decrease as the pH increases in mature leachates as a result of precipitation (Kulikowska & Klimiuk, 2008). Trace element concentrations that have been reported in landfill leachate include manganese (1.7 mg/L) and cadmium (0.05 mg/L), iron (14 mg/L), nickel (1.6 mg/L), and zinc (6.7 mg/L) (Abbas et al., 2009). The electrical conductivity of leachate is high, which is usually between 10 and 25

mS/cm, and it indicates the high concentration of dissolved salts and ions (Kulikowska & Klimiuk, 2008).

Poor performance of conventional biological treatment systems due to the recalcitrant nature of mature leachate organics and inhibitory impact of high ammonium concentrations on nitrifying bacteria has led to low levels of effective biological treatment of mature leachate in some European countries; less than 21% effective biological treatment of mature leachate is obtained by conventional biological treatment systems (Renou et al., 2008). This has led to the need to develop and implement better physicochemical treatment technologies, including chemical oxidation, coagulation-flocculation, membrane processes, and electrochemical oxidation, in order to satisfy discharges (Amor et al., 2015; Renou et al., 2008).

2.4.2 Previous studies on BDD-Based leachate treatment

The performance of Ti-Ru-Sn ternary oxide, PbO_2, and BDD anodes was evaluated in a closed municipal solid waste landfill site and compared their performance (initial COD: 780 mg/L; NH_4+ -N: 266 mg/L) (Sirés et al., 2014b). Electrolysis of Ti-Ru-Sn anode after 8 hours at a current of 2A gave only 35% COD, 52% colour, and 65% ammonium removal (Panizza & Martinez-Huitle, 2013). Comparatively, the use of BDD anodes in post-treatment of biologically pre-treated landfill leachate has produced remarkably high removals of leachate (Panizza & Martinez-Huitle, 2013). At a current density of 83 mA/cm^2, Ti/BDD electrodes achieved removal efficiencies of 95.17% for COD, 91.89% for TOC, 81.18% for NH_4^+-N, and 63.54% for total nitrogen (TN) after eight hours of electrolysis. In comparison, Ti/RuO_2 anodes exhibited excellent ammonium removal (97.85%), whereas the BDD electrodes delivered higher COD and TOC removal and used less energy (Luu, 2020). The research determined that low pH is favourable in removing organic substances and inhibits the effectiveness of removing ammonium, and high current density

enhances overall pollutant removal (Luu, 2020). An electrochemical system with a corroding iron electrode between the BDD anode and a carbon felt cathode was investigated to treat the biologically pre-treated landfill leachate through the response surface methodology (Tang et al., 2022). The system recorded COD and NH_3-N removal efficiencies of 81.3 % and 99.8 % under optimised conditions (current density: 25 mA/cm^2, electrolytic time: 9 h, pH:11), respectively (Tang et al., 2022). Electrolytic time became the most dominant parameter that influenced COD and NH_3 -N degradation, followed by current density and pH (Tang et al., 2022). A study on the role of current density, pH, and ionic composition (Cl^-:SO_4^{2-} ratios) proved that current density has a significant impact on COD and colour removal of landfill leachate (Agustina et al., 2019). The highest COD removal efficiency 49% was obtained at current densities of 50, 75, and 100 mA/cm^2, with the maximum removal occurring at the highest current density (Agustina et al., 2019). The highest colour removal was observed at 36% of the same conditions. The experiment has found that pH had a considerable impact upon COD removal at high (Cl^-:SO_4^{2-} ratios), at lower ratios (18:1), pH had a little effect, and about 40% of the COD removal was obtained at all pH values (Agustina et al., 2019). Removal of ammonium was higher at alkaline pH because of NH_3 volatilisation, and the original leachate pH (about 8.5) produced the best ammonium removal in contrast to acidic conditions (Agustina et al., 2019). Ammonium removal of landfill leachate using anodic oxidation in the presence of BDD electrodes has been investigated with exceptionally high efficiencies with values of less than the disposal limit of 15 mg/L of NH_4^+-N in the treated leachate (Cabeza, Urtiaga, Rivero, et al., 2007). Two categories of leachates were compared; untreated leachate with an initial NH_4^+-N concentration of 1900 mg/L and biologically pre-treated leachate; both of them displayed good ammonium removal by indirect oxidation using electrogenerated active chlorine species (Cabeza, Urtiaga, Rivero, et al., 2007). The working principle is the

chlorine formation on the anode and then the homogeneous reaction with the ammonium ions, which is indicated by the following **Eq. (2-3);** (Cabeza, Urtiaga, Rivero, et al., 2007).

$$2NH_4^+ + 3\,HOCl \rightarrow N_2 + 3H_2O + 5H^+ + 3Cl^- \quad \textbf{(2-3)}$$

The kinetic modelling studies have explained the electrochemical removal mechanisms of ammonium and COD on landfill leachates (Urtiaga et al., 2012). The study identified two COD oxidation regimes; direct oxidation controlled by mass transfer, and oxidation that was indirect and took place in the bulk solution through the oxidants produced by the electrode (Urtiaga et al., 2012). The oxidation of ammonium was mainly carried out using electrogenerated chlorine species, and the kinetic parameters were related to the initial COD concentration and the applied current density (Urtiaga et al., 2012). The model was able to describe experimental data and predict the process optimisation (Urtiaga et al., 2012). A study that used the factorial design approach to test the effect of the operating variables, including treatment time, initial pH, current intensity, and chloride concentration, revealed that the interaction of pH and chloride concentration had a significant impact on COD and NH_4^+-N removal (Jiale Li et al., 2019). The outcomes showed that nitrogen gas (N_2) was the major transformation product of NH_4^+-N, and its percentage declined with the increase in current density (50 to 100 mA/cm^2) during the electrolysis (4 hours) (Jiale Li et al., 2019). With the addition of chloride, the formation of NO_3^--N is suppressed, while the accumulation of intermediate nitrogen species such as NO_2^--N is enhanced (Jiale Li et al., 2019). The analysis of the energy consumption plays a crucial role in practice. Research has demonstrated that an increase in the density of current enhances the efficacy of pollutant removal but also increases specific energy consumption (Agustina et al., 2019). The best energy consumption was found at pH 3 in all the tested Cl^-:SO_4^{2-} ratios, and the best energy consumption was found at the initial leachate pH with high chloride concentration (Agustina et al., 2019). Average removal

efficiencies of 63 % COD, 35 % TOC, 98 % NH_4^+ , and 52 % phosphorus were obtained with sequential treatment using a membrane bioreactor (MBR) and BDD-based electrooxidation with optimal conditions of 3A current density over 120 min (Zolfaghari et al., 2016). However, the effluent was more toxic because of the radicals and organochlorinated products that were generated during the electrooxidation. This underscores the importance of optimizing treatment parameters to achieve an effective balance between pollutant removal and the minimization of undesirable by-products (Zolfaghari et al., 2016).

2.5 Removal of Pharmaceutical Compounds

2.5.1 Environmental Significance of Sulfamethazine (SMZ), Sulfanilamide (SN), and Tetracycline Hydrochloride (TC-HCl)

Sulfonamide antibiotics (SAs), such as sulfamethazine and sulfanilamide, are widely used in human and veterinary practice and have been continuously detected in municipal effluents, surface waters, and other environmental matrices found in previous research (Chang et al., 2008; Kokoszka et al., 2021). These antimicrobial compounds are not generated naturally or released through biological treatment processes; therefore, their presence in aquatic systems reflects contamination originating from human activities (Ou et al., 2015). Sulfamethazine has been observed in diverse water bodies, where the concentrations prove to be considerably different depending on the sources and geographical location. In Northwestern Spain, sulfonamides most often detected in the surface waters were sulfamethazine, reaching its highest concentration of 63.6 ng/L (Iglesias et al., 2013). Whereas these values are numerically small, they are sufficient to selectively pressurize the environmental bacterial communities. The major environmental impact issue associated with sulfamethazine relates to its role in the development of antimicrobial resistance. It is proven that the concentration of sulfamethazine has a positive relationship with the

abundance of sulfamethazine-resistant bacteria (SRB) in aquatic habitats and that the densities of SRBs range between (2.17×10^3) to (3.69×10^4) colony-forming units per millilitre (CFUs/ml) (Ou et al., 2015). Moreover, the 16S rRNA gene sequencing of 121 SRB isolates showed that they were highly diverse, and 48.7% of them were multidrug-resistant to at least three antibiotics (Ou et al., 2015). Their persistent occurrence of highly heterogeneous SRB and their multidrug resistance characteristics are likely to be the relatable selective pressures applied by aquatic systems to human health (Ou et al., 2015). The comparatively limited focus on Sulfanilamide as the prototype sulfonamide and a metabolite of various sulfa drugs in environmental impact studies has been less popular than other sulfonamides; nevertheless, it has been reported in hospital wastewater and municipal WWTP effluents (Kokoszka et al., 2021). Although few specific quantitative data are available, the research on the transformation products of sulfonamides reveals that the resulting metabolites can reach the same concentration as their corresponding compounds; for this, the use of sulfanilamide as a degradation product should be included in environmental risk assessment (Kokoszka et al., 2021). The medium hydrophilicity and pH-variable ionisation affect the sorption properties of the compound and its movement in the water body. TC-HCl, a member of the tetracycline class of antibiotics, is one of the most prescribed antibiotics in the world and has been broadly found in wastewater, as well as in water (W. Xu et al., 2007). Concentration in effluents in hospitals and pharmaceutical manufacturing discharges may be significantly greater, reaching the micro to milligram per litre interval, which is greater than the common municipal wastewater discharges. In addition to the implication of antimicrobial resistance, TCs are phototoxic, chelate vital divalent metal ions such as (Ca^{2+}, Mg^{2+}, Fe^{3+}), and show ecotoxic effects on non-target organisms such as algae, daphnids, and fish (Carvalho & Santos, 2016). The traditional WWTPs show non-uniform and, in most cases, sub-optimal

efficiency in removing the pharmaceutical compounds. Municipal WWTPs have been reported to remove sulfonamides with percentages ranging between (23.5 to 27 %) to excellent percentages (72.7 to 96%) depending upon the individual antibiotic, configuration of the plant, and the conditions (L. Gao et al., 2012; L. J. Zhou et al., 2011). The concentration of antibiotics in secondary treated effluents commonly falls between 10 and 1000 ng/L, including sulfonamides and tetracyclines (W. Xu et al., 2007). The mechanisms of sulfonamide removal include sorption onto activated sludge and biodegradation; however, the formation of transformation products, such as acetylated metabolites, makes it difficult to measure the actual removal efficiency (S. fen Yuan et al., 2019). Their difficult behavior to biological treatment, combined with the constant loading of aquatic ecosystems through wastewater release, highlights the urgency of the need to implement modern treatment methods that would allow complete degradation and not only metabolic conversion to possibly toxic products (X. Gao et al., 2019; Kokoszka et al., 2021).

2.5.2 Electrochemical Degradation of Sulfamethazine

Electrochemical oxidation using BDD electrodes has also been found to be very useful in the degradation of sulfamethazine (SMZ) in aqueous conditions. The SMZ and five other sulfonamides that underwent BDD oxidation exhibited pseudo-first-order kinetic behavior, and the effect of the byproducts did not affect the rate constants at all (Fabiańska et al., 2014). It was noted that enhanced degradation efficiencies at higher temperatures and acidic conditions of the reaction and SMZ oxidation through municipal wastewater treatment plant (WWTP) effluents were more effective than SMZ oxidation through a sodium sulfate (Na_2SO_4) supporting electrolyte, which was likely a result of chloride and nitrate ions being present (Fabiańska et al., 2014). The latest studies utilise the use of pulsed alternating electrochemical oxidation (PAEO) with the use of BDD electrodes to examine SMZ removal in antibiotic-contaminated wastewater (S. Hu et al., 2025a).

At various current densities (20, 25, 30, 35, 40 mA/cm²), COD removal efficiencies after 90 minutes were 80.3%, 82.5%, 94.2%, 88.1%, and 85.6%, respectively, with the optimal current density identified at 30 mA/cm² (S. Hu et al., 2025a). The degradation process conformed to a pseudo-first-order kinetic model with rate constants (k_1) of 0.0189, 0.0208, 0.0344, 0.0253, and 0.0229 per min corresponding to increasing current densities (S. Hu et al., 2025a). The experiment showed that polarization of concentration and the passivation of electrodes could be reduced by the alternating current waveform and, consequently, the efficiency of current could be improved (S. Hu et al., 2025a). Under optimised conditions (persulfate loading =0.40 g/L, pH = 4, current density =21 mA/cm^2), SMZ removal (50mg/L) was achieved with BDD electrodes (EO/BDD -PS) in 15min (Nashat et al., 2022). An RSM design was applied to the central-composite design aimed at optimising the amount of persulfate, solution pH, and current density (Nashat et al., 2022). BDD-PS showed significantly better degradation of the SMZ as compared to electro-Fenton and standard anodic oxidation that was conducted in the same BDD reactors (Nashat et al., 2022). The cost analysis revealed that complete implementation of the BDD-PS system in similar contaminated waters would cost about \$2.23/m^3 (Nashat et al., 2022). The hydroxyl radical attacks the sulfonamide (S–N) bond, and the aromatic rings (the aniline and the pyrimidine ring) are attacked, as well, and are considered the SMZ degradation pathway (Fabiańska et al., 2014). A set of intermediates formed during the process of oxidation was determined by liquid chromatography-mass spectrometry (LC-MS) and gas chromatography-mass spectrometry (GC-MS). Aromatic intermediates observed in SMZ electrooxidation were 1,2-benzenediol, 1,4-benzenediol, p-benzoquinone, and 4, 6-dimethyl-2-pyrimidinamine (García-Montoya et al., 2015). The carboxylic acids (maleic, fumaric, acetic, formic, oxalic, and oxamic acids) were determined; ion chromatography was used to determine the transformation of the original organic nitrogen

content to ammonium and nitrate ions (García-Montoya et al., 2015). Through competition kinetics, the rate constant of SMZ oxidation by •OH was 1.87×10^9 M·/S, which highlights the speed of the reaction mediated by the use of •OH (Barhoumi et al., 2016). The use of pyrite as the source of iron in heterogeneous electrofenton (EF) processes had better SMZ oxidation and mineralisation. Using BDD and Pt anodes, pyrite-EF obtained 95 and 87% total organic carbon (TOC) removal, respectively, which is comparable to 90 and 83 % with conventional EF with BDD and Pt reactors (Barhoumi et al., 2016). The ecotoxicological analysis on Lemna minor indicated that transformation products have variable acute toxicity when produced by the use of electrooxidation; the eliminated by-products emphasize the importance of monitoring the reaction to reduce the toxicity of the products (Fabiańska et al., 2014).

2.5.3 Electrochemical Degradation of Sulfanilamide

The mechanism of sulfanilamide degradation includes both the anodic oxidation and •OH mediated degradation. The direct oxidation and •OH were proven to be the main mechanisms after scavenger experiments and electrode characterisation (Kim et al., 2024). The production of •OH was best at higher currents, suggesting that CF anodes play a role in degradation via surface oxidation and radical generation (Kim et al., 2024). The paper highlights the environmental and economic advantages of an anode made of carbon compared to metal-based electrodes and does not produce the possible toxic metal like lead (Kim et al., 2024). Sulfanilamide degradation has a systematic effect on electrolyte composition. It has been shown that the chloride Cl^- and SO_4^{2-} ions are electrochemically transformed into active species such as active chlorine and persulfate, and increase the efficiency of degradation (Kim et al., 2024). On the other hand, natural groundwater electrolytes and bicarbonate inhibit the oxidation performance because they scavenge hydroxyl radicals, thus lowering the overall performance of the treatment (Kim et al., 2024). These results

highlight the importance of electrolytes, such as the composition of the water matrix, in determining the effectiveness of an electrochemical treatment.

The systematic study of electrolyte composition on sulfanilamide degradation showed that chloride and sulfate ions are electrochemically changed into the active species chlorine and persulfate, and consequently enhance degradation efficacy (Kim et al., 2024). On the other hand, bicarbonate and groundwater electrolytes reduce oxidative performance by eliminating hydroxyl radicals that eventually reduce the overall effect of treatment (Kim et al., 2024).

Recent pilot-scale tests investigated the possibility of removing multiple contaminants at once, such as Cr(VI), As(III), and sulfanilamide, with an electrochemical barrier (e-barrier) system (Kim et al., 2024). The e-barrier system was proven to be able to treat contaminated groundwater in realistic flow-through systems, indicating a possibility of application on a field scale (Kim et al., 2025). Although there are operational parameters that determine specific efficiencies of sulfanilamide in mixed-contaminant systems, the study confirmed that electrochemical systems have the ability to treat multiple pollutants at the same time (Kim et al., 2025). The investigation of similar sulfonamide analogs gives information about the sulfonamide breakdown mechanisms. Studies on sulfonamide analogue SMT (structurally similar to sulfamethylthiadiazole) used three-dimensional electrocatalytic technology using GAC by Ni/Fe particle electrodes, and under optimal conditions (nickel-iron loading ratio 1:1), they found 90.89% removal in 30 min (S. Li et al., 2022). Degradation-pathway analysis that is founded on intermediates found by ultra-high-performance liquid chromatography and bond-energy calculations using Gaussian software showed that the sulfonamide degradation is associated with the S-N bond cleavage and hydroxylation of aromatic rings (S. Li et al., 2022).

Comparative analysis of the electrochemical processes of pharmaceutical degradation has revealed that the degradation can be improved by the oxygenated electrochemical oxidation (García-Espinoza & Nacheva, 2019). The study of mixed pharmaceutical compounds, such as sulfamethoxazole, with Nb/BDD anodes showed that oxygen injection had a strong effect on the degradation kinetics and the first-order rate constants (García-Espinoza & Nacheva, 2019). Even though there is a lack of specific data specifically regarding sulfanilamide, the fact that it has a simpler molecular structure compared to the more complex sulfonamides implies that it can have a similar or even faster degradation rate under similar conditions.

Considerations of energy consumption are important for practical implementation. It has been noted that moderate current densities give the best balance between degradation performance and electrode life because extreme current densities may cause parasitic reactions and decreased current efficiency (Kim et al., 2024). The creation of affordable carbon-based electrodes also has the potential for mass-scale treatment of sulfanilamide, especially in the case of groundwater remediation, which requires continuous flow-through treatment (Kim et al., 2024).

2.5.4 Electrochemical Degradation of Tetracycline Hydrochloride

The degradation of TC-HCl through electrochemical oxidation with BDD and other anodes has received much attention due to the complex structure of the molecule, which consists of multiple functional groups and is widespread in the environment. A study using $Ti/Ta_2O_5\text{-}IrO_2$ as anode showed that pseudo-first-order rate constants lowered to 0.02009 per minute when initial TC concentrations rose to 80 mg/L, compared to 0.08656 per min when initial TC concentrations rose to 20 mg/L (D. Li et al., 2024). The HPLC-MS analysis led to the identification of nine main intermediates, and the presence of degradation pathways was suggested according to the results of the UV-vis analysis and TOC analysis (D. Li et al., 2024).

Research on BDD electrode systems to degrade TC-HCl used a new mode of electrifying power-on and power-off to activate sulfate, hence producing sulfate radicals SO_4•$^-$ and •OH (Xiaobao Li et al., 2022). The system was able to remove TC-HCl effectively, and SO_4•$^-$ dimerized to produce peroxydisulfate ($S_2O_8^{2-}$), which in turn was activated by heat and quinones to be dissolved continuously during power-off phases (Xiaobao Li et al., 2022). The analysis of a full-factorial design showed that the persulfate concentration could achieve 16.2mM within 120min, and the discontinuous electrifying mode used less energy than the continuous mode (Xiaobao Li et al., 2022).

The degradation of TC involves hydroxylation, demethylation, and a ring-opening reaction. Using Ti/Ti_4O_7 anodes, HPLC-QTOF-MS identified several transformation intermediates, while bioluminescence inhibition tests showed peak toxicity at 10 min (55.41%) due to highly toxic species with m/z 461, 432, and 477. As these intermediates continued to degrade, toxicity declined to 16.78% after 40 min. Among them, the most frequently reported intermediate was m/z= 461 ($C_{22}H_{25}N_2O_9$), typically formed through hydroxylation reactions (Jianbing Wang et al., 2018b).

A three-dimensional electrode reactor with IrO_2-RuO_2-Ti anodes and granular activated carbon was used in advanced oxidation studies, which showed a TC degradation of ≥96 % within two hours at a current density of 12.5 mA/cm^2, with •OH and superoxide radicals as the dominant reactive oxygen species found through optimization of response surface methods (Yufan Chen et al., 2024). The detailed degradation pathway study using LC-MS and density functional theory (DFT) showed that TC primarily degraded to decarboxylation, deamidation, and ring-opening reactions under the attack of •OH, producing intermediates with m/z values of 427, 433, 350, 246, 461, 424, 330, 352, 309, 263, and 233 (D. Li et al., 2024). Electrodes based on Pt/Ti recorded TC oxidation efficiencies of 97 ± 2% in 0.64 wt% HCl and 85 ± 3% in 0.64 wt% NaCl within 15

minutes of electrolysis (Ivantsova et al., 2025). The π-conjugated electron system of the antibiotic was found to be degraded according to UV-visible spectroscopy, and the appearance of oxidation intermediates with a molecular weight greater than 70 was not detected by HPLC-MS experiments, which indicated extensive mineralization (Ivantsova et al., 2025).

2.6 Treatment of Mixed Pharmaceutical Compounds

Recent research investigated the electrochemical removal of a multicomponent pharmaceutical mixture containing atenolol, ibuprofen, and norfloxacin using boron-doped diamond (BDD) electrodes and concluded that all three analytes could be effectively removed, with atenolol being the most recalcitrant to the electrochemical removal process (Balseviciute et al., 2025). The efficiency of mineralization was found to be maximum at applied currents of more than 200 mA/cm^2 (Balseviciute et al., 2025). Total organic carbon (TOC) showed a linear decrease at the beginning of the treatment, and an exponential increase as the mineralization approached the final stages (Balseviciute et al., 2025). The highest levels of intermediate byproducts were found at intermediate operating times, including ammonia and nitrite ions, which were then oxidized and diminished at the end of the process, but the fluoride and nitrate ions were near table concentrations (Balseviciute et al., 2025).

The kinetics of mixed pharmaceutical degradation are highly dependent on operational parameters. (García-Espinoza & Nacheva, 2019), First-order kinetic constants were on the rise when Na_2SO_4 and NaBr were used as the electrolyte, but they were on the decline when NaCl was added. In spiked secondary effluent, SMX and PRO were completely degraded in 30 min in an oxygen-rich system with an applied current of 2.5 A without any electrolyte, which is longer than CBZ (García-Espinoza & Nacheva, 2019). The presence of oxygen resulted in better decontamination of TOC and COD, with a 67% and 89% decrease, respectively (García-Espinoza & Nacheva, 2019).

Matrix effects within real wastewater constituents significantly influence treatment performance. The study by (Bosio et al., 2021) involved the electrochemical degradation of psychotropic drugs, namely alprazolam, clonazepam, diazepam, lorazepam, and carbamazepine, with the help of municipal wastewater (MWW). Ti/Pt anodes reached 40 % degradation of the target compounds after 120 min, and BDD anodes reached a removal efficiency between 33% and 52% (Bosio et al., 2021) . A similar degradation in synthetic solutions was attained in 5 min at a current density of 75 A/m² (Bosio et al., 2021). Neurotoxicity tests with Wistar rat hippocampal slices showed that MWW treated with BDD-coated electrodes did not cause any significant changes in the production of reactive oxygen species (ROS), which is a marker of successful toxicity inhibition, and Ti/Pt-treated samples showed fluctuations in ROS signaling (Bosio et al., 2021). Other studies (de Souza et al., 2024) utilized the method of suspect screening using ultra-high-performance liquid chromatography and quadrupole time-of-flight mass spectrometry on the effluents of municipal wastewater treatment facilities and detected 24 organic micropollutants. Ten of them were verified with reference standards and quantified at relevant concentrations (~25 μg/L) of quaternary anodic oxidation, highlighting that quaternary anodic oxidation can be used to concurrently degrade in synthetic solutions and real wastewater matrices (de Souza et al., 2024). As the authors emphasized, it was important to define the products of degradation and the toxicity levels of mixed pharmaceutical remediation (de Souza et al., 2024).

The efficiency of the electricity used and the efficiency of the current are very important in the electrochemical remediation of mixed pharmaceuticals. According to (Balseviciute et al., 2025), high operational currents decrease mineralization efficiency and increase specific energy consumption, though faster kinetics are observed at higher currents. At a constant current, the degradation curve was essentially linear regardless of the changes in organic load or supporting

electrolyte concentration, indicating that when the solution is more concentrated, the utilization of •OH is more efficient (Balseviciute et al., 2025). (Wakejo et al., 2024) showed that hybrid systems that combine electrochemical oxidation with adsorption can simultaneously eliminate acetaminophen and ciprofloxacin, thus eliminating the weaknesses of each of the two methods.

2.6.1. Effect of Initial pH

Solution pH represents a critical operational parameter that greatly influences electrochemical oxidation efficiency through multiple mechanisms, including the ionization state of target pollutants, the stability and reactivity of electro-generated oxidants, electrode surface properties, and reaction kinetics (Moreira et al., 2017; Tang et al., 2022). In the case of pharmaceuticals containing ionizable functional groups, molecular speciation is determined by pH and, consequently, directly by reactivity to hydroxyl radicals and other oxidative species. In their study, (Xiaobao Li et al., 2022) investigated the degradation of TC on Ti/Ta_2O_5-IrO_2 anodes and revealed that the pseudo-first-order rate constants were highly dependent on pH; degradation rates were usually higher in acidic conditions (pH 3.5) than in neutral or alkaline conditions. (Fabiańska et al., 2014) described that the degradation rate of sulfamethazine was enhanced significantly at a low pH, and sulfonamides were oxidized more efficiently in effluents of the municipal wastewater treatment plants than in a pure solution of Na_2SO_4 to support electrolyte, which can be explained by the existence of chloride and nitrate ions. The pKa value, which is the pH-dependent speciation of the sulfamethazine compound are approximately 2.3 and 7.5, representing its reactivity where at pH below 2 the compound is largely cationic, at pH between 2 and 7 the molecule is in a zwitterionic form, and at pH above 7 the compound is anionic. The best electrochemical degradation is usually in the range of acidic to neutral pH, where the reaction of •OH is enhanced (García-Montoya et al., 2015).

Effects of pH in the context of landfill leachate remediation are complex in nature due to the buffering capacity of leachate and the simultaneous multiplicity of reactions. Using response-surface methodology, investigated a BDD-Fe-CF system and concluded that response-surface methodology has been applied to COD and ammonium nitrogen NH_3-N removal, with electrolytic duration having a more pronounced effect than pH, although pH is equally important. COD and NH_3-N removal efficiencies of 81.3% and 99.8% were attained under ideal conditions (pH = 11) (Tang et al., 2022). The degradation mechanism includes the formation of •OH at the anode surface of BDD and Fenton-type reaction under acidic environment, and under alkaline pH, the contribution of $Fe(OH)_3$ coagulation and Fe(VI) oxidation reaction to organic compound degradation is significant (Tang et al., 2022). Extensive research on the electrochemical advanced oxidation processes for sanitary landfill leachate treatment has shown that the most desirable results were obtained by the PEF-BDD-UVA process, in which no external addition of oxalic acid was used, with the pH maintained at 2.8. Conversely, a starting amount of a 1:3 ratio of Fe(III)-to-oxalate allowed it to work at a pH of 3.5 with even higher efficiency and at 4.0 with a minor performance loss (Moreira et al., 2017). The study found that the BDD anode showed better performance in electro-Fenton, photoelectro-Fenton under UVA light, and solar photoelectro-Fenton systems because physisorbed hydroxyl radicals at the anode surface are important in the oxidation of landfill leachate (Moreira et al., 2017). The pH also has a great impact on the production and stability of electro-generated oxidants. Active chlorine is very pH-dependent in chloride-containing systems. Below pH 3, chlorine is the dominant species, between 3 and 8, HOCl is the dominant species, and above 8, OCl^- is the dominant species (Castillo-Cabrera et al., 2023). Studies of electrooxidation of landfill leachate showed that the removal of ammonium was more effective in alkaline conditions due to the volatilization of NH_3, and in the initial conditions of the

leachate (about 8.5), ammonium removal was best compared to acidic environments (Agustina et al., 2019). The study of the degradation of psychotropic drugs in the municipal wastewater investigated the pH values of 3 to 10 and discovered that the targeted compounds were effectively degraded in five minutes when the current density was 75 mA/m^2, but the pH significantly influenced the character and toxicity of the transformation products (Bosio et al., 2021).

2.6.2 Effect of Applied Current Density

The most important operational parameter of the electrochemical oxidation process is the applied current density, which directly controls the rate of the generation of oxidants, mass transfer constraints, current efficiency, and energy consumption (García-Espinoza & Nacheva, 2019; S. Hu et al., 2025b). The rate of electrochemical reactions, according to the Butler -Volmer equation, can be controlled by changing the density of current, which determines the flux of electrons at which a reaction can occur and, therefore, the rate at which •OH and other active species can be produced (S. Hu et al., 2025a). Studies of sulfamethazine degradation by using BDD electrodes under pulsed alternating electrochemical oxidation reported COD removal efficiencies of 80.3%, 82.5%, 94.2%, 88.1%, and 85.6%, respectively at current densities of 20, 25, 30, 35, and 40 mA/cm^2, respectively, after 90 minutes and optimum performance was achieved at 30 mA/cm^2 (S. Hu et al., 2025a). These degradations took a pseudo-first-order kinetic model with rate constants (k_1) of 0.0189, 0.0208, 0.0344, 0.0253, and 0.0229 per minute corresponding to increasing current densities, and the relationship between the current density and the degradation efficiency was nonlinear (S. Hu et al., 2025a). It was also found in the study that current densities that were higher than optimal resulted in lower efficiency because of parasitic oxygen evolution reactions and low current efficiency (S. Hu et al., 2025a). A relative comparison of the sulfamethazine degradation at current densities of (5, 10, and 15 mA/cm^2) with an initial COD of 50 mg/L showed that the

removal efficiency rose to 68.40 %, 94.28 %, and 99.25 %, respectively, with a current density, showing a proportional increase in the degradation rates with current density under moderate conditions (Najafinejad et al., 2023). However, studies with higher current densities (50, 80, 120, 150, and 230 mA/cm^2) of contaminant removal using BDD anodes achieved the highest level of contaminant removal of around 96% at 230 mA/cm^2, but optimum current density was found at 120 mA/cm^2, where an excellent contaminant removal efficiency was obtained and low energy consumption was achieved (Najafinejad et al., 2023). The power consumption change was drastically great, between 85 kWh/m^3 and 785 kWh/m^3 with the change of current density between 50 mA/cm^2 and 230 mA/cm^2, demonstrating the importance of the equilibrium between removal efficiency and energy expenses (Najafinejad et al., 2023). In the case of tetracycline degradation, the optimization of response surface methodology with Graphite/β-PbO_2 anodes found an optimal current density of 1.98 mA/cm^2 at a test range of 0.5-4.5 mA/cm^2 and maximized the removal efficiency with minimum energy consumption (Dargahi et al., 2023). A study using Ti/Ta_2O_5-IrO_2 as anode showed that pseudo first-order rate constants were dependent on current density, with a higher current density speeding up the rate of degradation but also increasing the likelihood of electrode passivation and lack of current efficiency at such high current densities (Dong et al., 2021). Oxytetracycline degradation using Ti/TiO_2-RuO_2 electrodes was studied in a factorial design with current densities of 6.0, 10, and 20 A/m^2, demonstrating that current density had a significant impact on removal efficiency and formation of transformation products (Sanchez-Castrillon et al., 2024). Regarding the use of the BDD-Fe-CF system in the landfill leachate treatment framework, the research that utilizes the response surface methodology and the BDD-Fe-CF system to identify the key variables in the system revealed that current density was one of the most important variables; however, the electrolytic time was identified as the most important

variable (Tang et al., 2022). COD and NH_3-N removal efficiencies of 81.3 % and 99.8 %, respectively, were achieved after nine hours at an optimized condition of 25 mA/cm^2 current density (Tang et al., 2022). In a study on landfill leachate electrooxidation, the current densities of 50, 75, and 100 mA/cm^2 were investigated, and the results showed that the higher the current density, the greater the removal of COD at the cost of specific energy consumption (Agustina et al., 2019). The best performance of advanced electrooxidation reactors with gas recycling and nanofiltration concentrates of landfill leachates was recorded at 33.3 mA/cm^2, with COD, TOC, TKN, and NH_3-N removal efficiency of 77.8%, 70.6%, 95.5%, and 94.0%, respectively (Akhtar et al., 2025a). The current density-treatment performance relationship needs to consider the efficiency of the treatment as well as the cost of operation. Although an increase in current densities minimizes the treatment time and the reactor volume requirements (capital costs), it increases energy consumption (operational costs), which requires optimization to find the most favorable compromise (Balseviciute et al., 2025; S. Hu et al., 2025a). Research has found that the moderate current densities (20-40 mA/cm^2) for BDD electrodes generally give the best balance between the degradation efficiency, treatment time, and energy use in pharmaceutical and leachate treatment applications (S. Hu et al., 2025a; Tang et al., 2022).

2.6.3 Effect of Initial Pollutant Concentration

The initial level of pollutant concentration has a significant effect on the kinetics of the electrochemical oxidation process, the efficiency of treatment, energy consumption, and the economic feasibility of the process in general (Dong et al., 2021; Jianbing Wang et al., 2018b). When using tetracycline to degrade Ti/Ta_2O_5-IrO_2 anodes, the concentration of tetracycline used in the initial experiments was between 20 and 80 mg/L, and the pseudo-first-order rate constant decreased to 0.08656 per min at 20 mg/L and 0.02009 per min as the amount of tetracycline

increased to 20 and 80 mg/L, respectively (Dong et al., 2021). This decrease in the apparent rate constants with initial concentration is due to a constant rate of oxidant-generation under constant current density and a compromise between effective interaction with hydroxyl radicals by coverage of the electrode-surface by target molecules and intermediates (Dong et al., 2021; Jianbing Wang et al., 2018b). The Beer-Lambert law and competitive adsorption theory could explain the phenomenon as the initial concentrations increase, target molecules and their intermediates gradually cover the active sites on the electrode surface and neutralize the available hydroxyl radicals, reducing the active concentration of oxidants to be used in degradation reactions (Dong et al., 2021). Studies that utilised Ti/Ti_4O_7 anodes established that the initial TC level is a crucial variable in the rate of decay, with the electrode recording 95.8 % removal in 40 minutes at reduced initial concentrations (Jianbing Wang et al., 2018b). In the case of pharmaceutical compounds, optimization studies with response-surface methodology used Graphite/β-PbO_2 anodes at the start of the process to determine the initial tetracycline concentrations ranging from 20 to 100 mg/L, with an optimal concentration of 25.6 mg/L identified to maximize removal efficiency with minimum consumption of energy (Dargahi et al., 2023). The Sono-electro-Fenton process has reached a removal efficiency of 98.8 % under these optimized conditions (pH -3.5, electrolysis duration 42.6 minutes, and current density 1.98 mA/cm^2 (Dargahi et al., 2023). Similarly, research on the degradation of sulfamethazine showed that initial COD levels of 50, 100, and 150 mg/L produced removal efficiencies of 99.25%, 94.28%, and 68.40%, respectively, at a fixed current density of 15 mA/cm^2, which also indicated that initial concentration and percentage removal were negatively correlated (Najafinejad et al., 2023). However, the absolute rate of removal of pollutants per unit time increases with the initial concentration because of the increased driving forces of mass transfer and better use of the generated oxidants, leading to high

current efficiency and reduced specific energy consumption at high initial concentrations (Balseviciute et al., 2025; S. Hu et al., 2025a). Studies with multicomponent pharmaceutical mixtures showed that, at constant current, the reaction rate is constant with organic concentration, implying greater use of hydroxyl radical at the higher concentration of the solution (Balseviciute et al., 2025). This has significant consequences because longer treatment times are necessary to achieve the target removal efficiency in dilute pharmaceutical wastewater; higher absolute removal rates can be reached using concentrated streams with reduced energy efficiency per unit mass removed. The initial concentration and treatment performance relationship should take both into consideration, removal efficiency and the cost of operation, because a high initial concentration increases the total amount of energy used per unit mass treated and decreases the specific energy used per unit mass removed (S. Hu et al., 2025a). It has been observed that the specific energy consumption declines as the initial concentration of pollutants rises since better current efficiency and the enhanced use of electro-generated oxidants are achieved (Balseviciute et al., 2025). Putting it in practice, pre-dilution of highly concentrated pharmaceutical or leachate streams might not be economically beneficial, since it increases treatment volume and reduces energy efficiency, though the accumulation of transformation products at high initial concentrations becomes even more critical (García-Espinoza & Nacheva, 2019).

2.6.4 Effect of Reaction Time

Reaction time defines the level of pollutant degradation, level of mineralization, and general costs of the treatment in the process of electrochemical oxidation (El Kateb et al., 2019; Jianbing Wang et al., 2018b). The time-dependent dynamics of pollutant removal are typically divided into several periods, such as a high-rate degradation phase when the parent compounds react with the large numbers of oxidants, an intermediate phase when the primary transformation products are

further oxidized, and a final phase when the recalcitrant intermediates are slowly mineralized (Dong et al., 2021; Sanchez-Castrillon et al., 2024). The TC degradation study using Ti/Ti_4O_7 anodes showed that the electrochemical oxidation of TC was 95.8 % in 40 minutes, and the electrochemical process was governed by pseudo-first-order kinetics (Jianbing Wang et al., 2018b). The experiment found that the elimination of the contaminants occurred very fast within the initial 30 minutes and then slowed down, which was the disappearance of easily oxidizing substances and the formation of more recalcitrant intermediates (Jianbing Wang et al., 2018b). The same trend in time was detected in experiments on the degradation of oxytetracycline under Ti/TiO_2-RuO_2 electrodes, where it was found that about 97% of the degradation was accomplished after 20 minutes of electrolysis under favorable conditions (20 A/m^2, pH 6.5), and the reaction followed pseudo-first-order kinetics (Sanchez-Castrillon et al., 2024). Further studies utilizing BDD-Fe-CF systems found that electrolysis time was the key factor affecting COD and ammonia-based nitrogen (NH_3-N) degradation, and an optimized nine-hour run time achieved COD and ammonia-based nitrogen NH_3-N removal efficiencies of 81.3% and 99.8%, respectively (Tang et al., 2022). Heterogeneous electro-Fenton oxidation with carbon-felt cathodes modified with catalytic additives yielded the best mineralization, which was 96% of removed dissolved organic carbon (DOC) after 8 hours of electrolysis of nanofiltration concentrate from landfill leachate. This experiment had a circumneutral starting pH ($pH_0 = 7.9$) and a current density of 8.3 mA/cm^2 (El Kateb et al., 2019). More energy-efficient protocol, on the other hand, consisted of operating heterogeneous electro-Fenton at 4.2 mA/cm^2 accompanied by anodic oxidation using a Ti_4O_7 anode, where similar mineralization was achieved using a much lower consumption of 0.11 kWh/g DOC removed (El Kateb et al., 2019). The correlation between the duration of treatment and energy usage is approximately linear, which makes long-term electrolysis more and more

expensive (Akhtar et al., 2025b). Electrochemical oxidation experiments of graphite PVC electrodes of landfill leachate showed that the removal of COD increased with the current density within a fixed electrolysis time of three hours and then decreased between 2.5 and 3 hours (El Kateb et al., 2019).

2.6.5 Role of Hydrogen Peroxide (H_2O_2) in Enhanced Electrooxidation

One of the promising approaches to increase the treatment efficacy by producing more reactive oxygen species and facilitating electro-Fenton or peroxide-assisted reaction is the dosing of H_2O_2 to the electrooxidation process (El Kateb et al., 2019). The H_2O_2 may be added or produced in situ through the two-electron reduction of oxygen at the cathode or the two-electron oxidation of water at the anode, but external dosing provides a better control over the H_2O_2 levels (Ma et al., 2024; Yin et al., 2025). Comparative analysis of electro-catalytic oxidation systems using peroxymonosulfate (PMS), peroxydisulfate (PDS), and hydrogen peroxide showed that the EO-Fe(III)-H_2O_2 system is mainly based on •OH, with the highest degradation efficiency of sulfamethoxazole, carbamazepine, and bisphenol A (Long et al., 2024). Response-surface methodology suggested that despite the EO-Fe(III)-PMS route being less sensitive to complex aqueous media, biotoxicity measurements showed the EO-Fe(III)- H_2O_2 system to be the most appropriate in the removal of sulfamethoxazole, which proved to be advantageous in terms of environmental performance (Long et al., 2024). The basic process of H_2O_2 to enhance electrochemical oxidation is complex; electrochemical activation of H_2O_2 on the anode surface to produce more •OH; cathodic reduction of H_2O_2 to hydroxyl radicals by Fenton-like reactions in the presence of electrogenerated Fe^{2+}, and the reaction of H_2O_2 with the electrogenerated active species to highly reactive oxidants (Castillo-Cabrera et al., 2023). Research on in situ H_2O_2 generation has demonstrated significant enhancement in the degradation of pharmaceutical

compounds. In-situ generation of H_2O_2 with carbon black modified reticulated vitreous carbon cathodes and BDD anodes was demonstrated with a current efficiency of up to 93%. The resultant H_2O_2 was able to drastically increase the rate of electrooxidation of losartan and irbesartan, with nearly six times as much of each compound being removed and eliminated within ten minutes using the resultant H_2O_2 (Pérez et al., 2023). Developed electro oxidation studies on nanofiltration concentrate of landfill leachate using heterogeneous electro-Fenton with modified carbon-felt cathodes to generate in-situ H_2O_2, which resulted in a 96% mineralization rate of DOC in eight hours of electrolysis at an initial pH (pH = 7.9) and 8.3 mA/cm² (El Kateb et al., 2019). The most effective treatment plan was a combination of heterogeneous electrooxidation at 4.2 mA/cm² and anodic oxidation with a Ti_4O_7 anode, which had similar mineralization but used only 0.11 kWh/g DOC removed (El Kateb et al., 2019). This shows the high-energy saving capacity of the H_2O_2-enhanced systems that can be optimised well. Studies on BDD electrodes from water oxidation to generate H_2O_2 indicated that modulated BDD films have a maximum faradaic efficiency of 87 % and can generate H_2O_2 at a rate of 76.4 μmol/cm^2/min combined with a 10-hour electrochemical stability in carbonate-based solutions with 200 mA/cm² (Mavrikis et al., 2021). The experiment determined that the best H_2/Ar ratios in BDD synthesis selectively outline sp² impurities and maintain conductive networks in a synergistic interaction between defect-mediated electron transfer and chemically robust sp^3 structures (Ma et al., 2024). A nanostructured BDD with a ratio of sp^3/sp^2 of 0.46 had a maximum faradaic efficiency of 82.3 % at 1.9 V versus RHE, and a ratio of 1.14 had a faradaic efficiency of 65.2% but a longer half-life with a steady output over 50 hours of operation (Ma et al., 2024).

The most efficient amount of H_2O_2 is a vital factor that requires careful optimization. Sono-electro-Fenton studies have used external addition of H_2O_2, where it has been shown that the presence of

H_2O_2 increases the degradation of tetracycline, with response surface methodology (RSM) determining the best H_2O_2 concentrations, which balance between increasing the effect and the possibility of scavenging the •OH at too high levels (Dargahi et al., 2023). The economic evaluation of H_2O_2 dosing should consider the price of H_2O_2 and the possible decrease in energy usage or treatment period. There is sufficient evidence that H_2O_2-enhanced systems have the potential to cut certain energy consumption by 20-40% and obtain the same pollutant removal as the traditional electrooxidation (El Kateb et al., 2019).

2.7 Optimization Strategies in Electrochemical Processes

2.7.1 Limitations of Traditional Optimization Methods

Conventional optimization methods in the electrochemical processes have mainly been based on the one factor at a time (OFAT) approach, where the parameters are manipulated one at a time, with all other factors remaining constant (Podder & Mukherjee, 2024). This conventional method has a number of shortcomings that can limit its ability to detect real optimal conditions and explain the complicated interactions that determine electrochemical oxidation processes (Deshpande et al., 2012). The major weakness of OFAT is that it cannot identify parameter interactions, which are dominant in electrochemical systems where current density, pH, and initial concentration can interact with one another and affect the oxidant generation, mass transfer, and reaction kinetics in equal ways (Saleh et al., 2021). Several research has also shown that the best conditions found with the help of the OFAT procedures can be local optima instead of global ones because the best value of one variable is usually determined by the values of other variables, a dependence which the OFAT fails to consider (Deshpande et al., 2012). The experiments necessary to properly explore at least a small number of parameters are large in the OFAT approach, making the method practically infeasible when four or more factors must be optimized. Additionally, the techniques

of OFAT do not offer any statistical structure to evaluate the error of the experiment, the reliability of the results, and the relevance of the observed effects, which makes it hard to differentiate between the actual parameter effects and the experimental noise (Leili et al., 2018). The lack of mathematical models between the parameters and responses does not give the possibility to predict the behavior of the system under conditions not tested and does not provide any information about the relative significance of various factors or their interactions (Podder & Mukherjee, 2024).

2.8 Design of Experiments (DoE) and Response Surface Methodology (RSM)

2.8.1 Principles of DoE and RSM

Design of Experiments (DoE) is a methodical, statistically intensive technique of planning, implementing, and conducting experiments with the goal of determining associations between various input parameters and output reactions and reducing the work of experiments (Ferreira et al., 2007). RSM builds based on the DoE principles by modeling experimental data in the form of a mathematical model, usually a second-order polynomial equation, and thus establishing continuous response surfaces that characterize the system behavior over the experimental domain, and this is how they facilitate the optimization (Ferreira et al., 2007; Podder & Mukherjee, 2024). As part of electrochemical oxidation research, central composite designs (CCD) and Box-Behnken designs (BBD) are the most frequently used types of experimental designs that can be used to fit second-order polynomials (Deshpande et al., 2012). The central composite designs are combinations of factorial or fractional factorial points with axial (star) points and center points; they are the most popular designs in electrochemical process optimization (Nashat et al., 2022; Tang et al., 2022). Box-Behnken designs are a third type of design, which uses fewer experimental runs than CCD and does not allow extreme combinations of factors, which makes them especially appealing when extreme values may cause experimental challenges (Dargahi et al., 2023; Wu et

al., 2025). The RSM mathematical background is expressed as the model of the second-order polynomials that allow predicting the responses, determining the most appropriate conditions, and understanding the interactions between the parameters through the statistical analysis, such as analysis of variance (ANOVA). ANOVA measures adequacy of models in terms of F-values, *p*-values, R^2, adjusted R^2, and predicted R^2 (Deshpande et al., 2012).

2.8.2 Electrochemical Optimization Using Design Expert Software

Design Expert software has become a standard tool for deploying DoE and RSM to the research of electrochemical wastewater treatment that has full capabilities of generating experimental designs, data analysis, model fitting, statistical validation, and optimization (Bello et al., 2017; Bezerra et al., 2008). The software simplifies the optimization process by creating coded and actual experimental design matrices with randomization to minimize systematic errors, and by calculating the number of required runs, with replicated center points to estimate errors (Podder & Mukherjee, 2024). Experiments that use Design Expert to optimize pharmaceutical degradation have shown its efficiency in determining synergistic relations among parameters that would not be possible to identify by using the OFAT techniques (S. Hu et al., 2025a; Nashat et al., 2022).

The use of Design Expert in electrochemical pharmaceutical degradation has utilized central composite designs (CCD) with 4 to 5 influencing variables, which require 30 to 50 experimental runs to develop validated predictive models with $R^2 > 0.95$ for removal efficiency and energy consumption responses (Dargahi et al., 2023; Nashat et al., 2022). Research examining the breakdown of sulfamethazine using BDD electrodes with persulfate activation utilized response surface methodology coupled with central composite design (RSM-CCD) to optimize three important factors, including persulfate dose (0.2-0.6 g/L), pH (3-7), and current density (17-25 mA/cm^2). The full degradation was obtained in 15 minutes under the optimized operating

conditions (persulfate = 0.40 g/L, pH = 4, current density = 21 mA/cm^2) with a cost estimation of \$2.23/m^3 (Nashat et al., 2022). Design Expert was also used to optimize the elimination of COD and NH_3-N by a BDD-Fe-CF electrochemical system in the same context of landfill leachate treatment. The RSM methodology indicated that the most significant factor was the electrolytic time, and then the current density and pH, respectively, achieving 81.3% COD and 99.8% NH_3-N removal under optimized conditions (Tang et al., 2022). The software's numerical optimization module employs desirability function methodology to simultaneously optimize multiple responses with different objectives (maximize removal efficiency, minimize energy consumption) and varying importance weights (S. Hu et al., 2025a; Wu et al., 2025). In a study of tetracycline degradation, in which sono-electro-Fenton technology was employed, Design Expert was applied to explore the optimal conditions of pH, electrolysis time, current density, and initial concentration (pH 3.5, electrolysis time 42.6 minutes, current density 1.98 mA/cm^2, initial concentration 25.6 mg/L), achieving 98.8% removal efficiency with model validation confirming R^2=0.98. Comparative studies show that optimisation based on RSM usually cuts the experimental load by 50-70 % compared to traditional, sequential exploration methods, and at the same time increases the accuracy of optimisation by considering factorial interactions explicitly and correctly validating the results statistically (Ferreira et al., 2007; Podder & Mukherjee, 2024).

2.9 Optimization of Pharmaceutical Degradation (with and without H_2O_2)

The influence of H_2O_2 addition has been used to understand the benefits of the addition of peroxide, as well as the optimal working conditions of each treatment configuration (El Kateb et al., 2019; Nashat et al., 2022). When using sulfamethazine, electrochemical activation of persulfate with the help of BDD electrodes was used, which resulted in complete degradation at a significantly faster rate compared to the standard anodic oxidation; response surface methodology

was able to properly capture the complicated nature of the interactions between persulfate concentration, pH, and current density (Nashat et al., 2022). In addition, quadratic models of both the un-augmented system and the system with H_2O_2 enhancement have been created and tested, and the R^2 values of the models are R^2 values > 0.92 for removal efficiency, > 0.88 for energy consumption, and > 0.85 for mineralization efficiency, which confirms the good predictive ability of such models (Dargahi et al., 2023; Tang et al., 2022). The desirability framework of multi-objective optimisation that can be enabled by the desirability function has been particularly useful in identifying operating regimes that balance mutually exclusive objectives, including operating with removal efficiency of (>95%), maximizing TOC removal (>75%), and minimizing energy consumption (<50 kWh/m^3) (S. Hu et al., 2025a; Nashat et al., 2022). Experiential comparisons show that H_2O_2-assisted processes tend to reduce treatment time by 30 to 40 % and also cut energy consumption by 20 to 35 %, but also increase the removal of TOC by 10 to 20 %; however, this benefit has to be offset by the increase in chemical cost of H_2O_2 (Ali et al., 2023; El Kateb et al., 2019). The RSM predictions were repeatedly verified by experimental validation at the software-predicted optimum conditions with a mean deviation of 5-10 % of all response variables, thus highlighting the strength of the optimisation methodology (Dargahi et al., 2023; Wu et al., 2025).

Chapter 3: Manuscript no. 1

Optimization of Electrochemical Oxidation Process with Boron-doped diamond (BDD) for removing COD, Color, Ammonium, and Phosphate in Landfill Leachate

Abstract

This study investigated the electrooxidation (EO) of mature landfill leachate from the Brady Road Resource Management Facility, Winnipeg (Canada). EO using boron-doped diamond (BDD) electrodes was applied to treat real landfill leachate using a batch reactor. Response surface methodology (RSM) was used to determine the optimum process parameter levels. This research mainly focused on how different current densities (64, 95, and 125 mA/cm^2) and operational time (30 minutes, 1 hr, 1.5 hr, 2 hr, 2.5 hr, and 3 hr.) influenced the optimization of parameters such as chemical oxygen demand (COD), color, ammonium, and phosphate removal in mature landfill leachate at varied pH. To attain a high percentage of removal for the parameters mentioned above, the optimal conditions were found to be a current density (J) of 125 mA/cm^2 and a pH of 8. The optimum conditions resulted in removal percentages of 95.47%, 80.27%, 71.15%, and 47.15% for color, NH_4^+, COD, and $PO_4^{3-,}$ respectively, with an energy consumption of 50 kWh/m^3. The removal is related to a mechanism of the decomposition of water molecules to hydroxyl radicals and by direct anodic oxidation, where the pollutants are transformed to CO_2 and H_2O. The novelty of this research lies in the optimization of BDD electrode-based treatment for the simultaneous removal of COD, ammonium, phosphate, and color from mature leachate collected from a severely cold climatic region of Canada. The BDD electrode showed excellent removal efficiencies for the targeted contaminants with lower energy consumption, making it a feasible method for on-site landfill leachate treatment.

3.1 Introduction

The expansion of industrial operations, population growth, and changes in lifestyle have mostly contributed to the overall rise of municipal solid waste (MSW) throughout the years (A. M. Costa et al., 2019). Based on the Global Waste Statistics - 2022, the world generates 2.01 billion metric tons of municipal solid waste annually, and this is projected to increase by more than 70% to reach 3.4 billion metric tons by 2050 (Kaza et al., 2018). Among the different MSW management approaches, landfilling is the widely used technique for solid waste management and disposal, but the major drawback associated with landfilling is the generation of leachate that is difficult to manage and a source of environmental threats (Bashir et al., 2009; Zambrano & Min, 2020). Landfill leachate can be defined as a type of complex wastewater derived from municipal solid waste landfills that contain organic compounds, heavy metals, ammonium, and various unidentified xenobiotic organic compounds (XOCs) such as volatile, hydrophobic, aromatic, and aliphatic organic compounds (M. D. T. Hasnine et al., 2022; Zoungrana et al., 2022). Contaminants of Emerging Concern (CECs) are a potentially serious issue among those refractory OCs in terms of the suspected threat to both the environment and human well-being. CECs found in landfill leachate include pharmaceutical and personal care products (PPCPs), perfluorinated compounds (PFCs) like PFAS, persistent organic pollutants (POPs), microplastics, and nanomaterials (Hasan Anik et al., 2021; C. Qi et al., 2018). Furthermore, landfill age, precipitation, weather variations, waste type, and composition all have an impact on the amount and quality of leachate. Landfilling methods (waterproof coverings, required liners, for instance clay and geotextiles) also play a role in changing the composition of landfill leachate (Agustina et al., 2019). Stabilized leachates from aging landfill sites have a long-term harmful influence on the environment (Pérez et al., 2012). The impacts of leachate discharged into surface water involve eutrophication, ammonia toxicity,

and harm to human health (Kjeldsen et al., 2002). When toxic substances in leachate are assimilated by aquatic organisms, they enter into the food chain and bioaccumulate, causing health concerns (Matejczyk et al., 2011; Zambrano & Min, 2020). Therefore, landfill leachate should be collected and adequately treated to prevent its unfortunate fate in human health and the environment.

The contamination level in mature landfill leachate determines the choice of biological and/or physicochemical leachate treatment (Postacchini et al., 2018). Since the biological treatment procedure is temperature-dependent, it is unsuited for growing microorganisms in cold regions, ineffective for mature sanitary landfills, and generates undesired sludge that requires additional treatment and costs (Jagaba et al., 2021; C. Qi et al., 2014, 2017). Another challenge in the biological treatment of landfill leachate is its poor biodegradability and low BOD/COD ratio caused by the refractory organics (Renou et al., 2008). However, when we employ a membrane bioreactor (MBR) to treat wastewater or leachate, both biological treatment and membrane separation are required. MBR has some drawbacks, particularly in high operating costs due to the issue of membrane fouling and a reduction in both water quantity and quality (M. Liu et al., 2011). In contrast, Physical-chemical treatments are more effective with mature landfill leachate. (A. M. Costa et al., 2019; M. D. T. Hasnine et al., 2022). Electrochemical oxidation is a physicochemical approach that uses an advanced oxidation process to remove refractory compounds, including organic compounds, heavy metals, and nitrogen compounds from stabilized leachate (Jagaba et al., 2021; Kurniawan et al., 2006; Renou et al., 2008). Electrochemical oxidation works by generating highly reactive hydroxyl radicals that can break down the chemical bonds of refractory compounds, resulting in their conversion into less harmful by-products. Other advantages of electrochemical oxidation include its simplicity of use and environmental compatibility, as well as

its effectiveness in dissolving non-biodegradable pollutants, high organics removal effectiveness, including no sludge generation, and improved biodegradability index (BOD/COD) (Jagaba et al., 2021; Mandal et al., 2017). Other AOPs, such as the Fenton process, are based on hydrogen peroxide catalyzed by ferrous ions to produce hydroxyl radicals, which result in organic oxidation (Ting et al., 2008). Sono-Fenton, a Fenton process combined with sonolysis, has been shown to be useful for decreasing chemical dose and enhancing organic removal efficiency in leachate treatment (Zha et al., 2015). Furthermore, ultraviolet light/hydrogen peroxide (UV/H_2O_2) treatment is a type of advanced oxidation process that involves the use of ultraviolet light and hydrogen peroxide to generate hydroxyl radicals that react with organic contaminants in the leachate, breaking them down into simpler, less harmful compounds (Córdova et al., 2019). Compared to other advanced oxidation techniques, such as ozonation and Fenton's reagent, UV/H_2O_2 treatment has certain benefits over other advanced oxidation techniques in terms of organic matter and ammoniacal nitrogen removal, leachate biodegradability enhancement, and color reduction (Brito et al., 2010; Córdova et al., 2019). Other benefits include its simplicity, which requires only UV lamps, hydrogen peroxide, and a reaction vessel, also produces fewer harmful by-products, such as chlorinated compounds, which can be a problem with other oxidation methods.

In Winnipeg, Manitoba, the wastewater treatment plant (WWTP) treats municipal sewage and landfill leachate simultaneously (Islam et al., 2020), which is not suitable for removing refractory compounds. This is because wastewater treatment plants are not mainly designed for the treatment of leachate, which comprises a range of complex organics. Electrochemical oxidation, which is not temperature-dependent like the biological treatment, could be a better alternative for landfill leachate treatment in Winnipeg and other colder places across the world. As shown in research,

under optimal conditions of 200 mA applied current, pH 6.8, and reaction period of 1 hour 20 minutes, EAOP removed 64.3 %, 79 %, and 83.6 % ammonia, color, and COD, respectively, from landfill leachate (Ghanbari et al., 2021). In our present study, the electrooxidation (EO) technique was applied for mature landfill leachate treatment to remove dissolved organic pollutants such as COD, Color, and inorganic nutrients, e.g., NH_4^+- N, PO_4^{3-}. Electrooxidation (EO), one of the most popular EAOPs, includes both direct electron transfer (DET) and indirect oxidation. In terms of indirect oxidation, the oxidation of the pollutant is achieved over the generation of oxidizing species, for example, ozone, chlorinated compounds, hydroxyl radicals, sulfate or persulphate radicals, etc., generated from water ions (Moreira et al., 2013). In recent studies, BDD electrodes are highly efficient in generating ozone at temperatures above zero (Rahmani, Azarian, et al., 2018). This process can assist in the oxidation of pollutants present in wastewater.

The efficiency, selectivity, and energy usage of the oxidative degradation process are all influenced by the electrode material selected, making it vital for the EO process (Gonzaga et al., 2020; He et al., 2019). In this study, the BDD electrode was used for the electrooxidation process. BDD electrodes have been an innovative solution for the treatment of leachate because of their unique properties like corrosion resistivity, chemical inertness, permanence, high overpotential, and superior current effectiveness, which make the electrode versatile for electrochemical mineralization of organic compounds (Divyapriya & Nidheesh, 2021; P. V. Nidheesh et al., 2019). Also, BDD electrodes can withstand harsh chemical and electrochemical environments, which makes them suitable for long-term use in leachate treatment. This durability reduces the need for frequent replacement of electrodes, thereby reducing maintenance costs. In addition to its effectiveness in treating leachate, the use of BDD electrodes has also been found to produce fewer toxic by-products compared to other treatment methods (P. V. Nidheesh et al., 2019). Furthermore,

the energy consumption of the electrodes drops, and degradation efficiency improves when the O_2 evolution potential of the electrodes increases (X. Gao et al., 2019). BDD electrodes can also provide more reactive oxygen species to the system (Carlos Alberto Martínez-Huitle & Panizza, 2018; M. A. Oturan, 2021), and are useful to produce more •OH physically adsorbed on the surface (BDD [·OH]) (Karim et al., 2021), which is responsible for organic materials removal. Thus, the BDD electrode reduces the environmental impact of the treatment process and provides a safer option for treating leachate.

However, BDD electrodes can be expensive because of their synthesis and associated fabrication, but recent advances in BDD electrode manufacturing, including the use of cost-effective deposition methods and alternative boron sources, have significantly reduced the cost of BDD electrodes, making them more economically viable for large-scale applications. Additionally, the high efficiency of BDD electrodes in treating wastewater can result in cost savings in the long run, as less energy and chemicals are required for the same level of treatment compared to other technologies, making it a viable and sustainable option for industrial-scale purifications.

In this study, we aimed to evaluate the effect of various operational factors, such as current density, pH, and time, in the electrooxidation process of landfill leachate for removing soluble COD (sCOD), color, and nutrients (phosphate), which have not been well studied in research using BDD electrodes. Phosphate is simultaneously present with ammonia nitrogen in wastewater. The presence of phosphate has a negative effect on ammonia removal due to oxygen evolution (Mahvi et al., 2011), thus phosphate removal is urgent along with other recalcitrant contaminants by the EO process. EO using a BDD electrode can remove phosphate over the generation of oxidizing species generated from water ions. Also, phosphate transfers more electric current than Cl^- due to its higher electric charge, thus increasing the efficiency of ammonium removal. Because of this, it

is crucial to remove phosphate along with other contaminants from wastewater. Furthermore, energy consumption was determined to evaluate the system performance, which is better compared to other studies.

3.2 Materials and Methods

3.2.1 Sample Collection and Characterization of the Landfill Leachate

The landfill leachate was collected from the Brady Road Resource Management Facility (BRRMF), Winnipeg, Canada (well identification number # 13). BRRMF is the City of Winnipeg's only active municipal solid waste landfill located in Manitoba, Canada. The landfill, which has been in operation since 1973 for the disposal of waste from both commercial and household sources, is anticipated to serve another 100 years. The physicochemical properties of the leachate were assessed immediately as they arrived at the laboratory. For soluble COD (sCOD), samples were filtered through cellulose-based fiber paper to remove all suspended solids. Before proceeding with the tests, the samples were kept at 4 °C.

However, substantial levels of COD, pH, ammonia nitrogen, and heavy metals, as well as strong color and terrible odor, can be found in landfill leachate. The composition and volume of the leachate, as well as the number of biodegradable materials contained in the leachate, change with time. The leachate category is considered completely mature when the landfill's underground waste cell is older than 10 years (Islam et al., 2020; J. Zhang et al., 2015). Leachate treatment is challenging and complex due to all these reasons. The characteristics of the leachate are summarized in **Table 3-1.**

Table 3-1. Characteristics of the mature raw landfill leachate used in this study

Parameters	Units	Mature raw leachate
pH		7.4 ± 0.21
sCOD	mg/L	900 ± 11.32
BOD_5	mg/L	222 ± 26.32
Color	Pt-Co	1.14 ± 0.023
Ammonia Nitrogen (NH_4^+-N)	mg/L	590 ± 22.63
Phosphate (PO_4^{3-})	mg/L	4.9 ± 0.19
Chloride (Cl^-)	mg/L	1248 ± 21.51
Conductivity	mS/cm	15.22 ± 3.16
Resistivity	ohm	668 ± 12.46
BOD_5/sCOD		0.24

Parameters are represented as average values with the corresponding standard deviation of the mean.

3.2.2 Experimental setup

The CONDIAPURE® test system (CONDIAS GmbH, Itzehoe, Germany) was used in experiments with a DIACHEM® electrode stack (CONDIAS). Four boron-doped diamond electrodes were used as anode/ cathode with an active electrode area of (2 x 26 x 205) mm per anode. An inter-electrode gap of 3 mm separated the electrodes, which were arranged vertically, parallel to one another. The reactor was run in a batch mode with a sample volume of 3 L in a single-cell acrylic-made reactor. The length of the reactor was 23 cm, and the diameter of the reactor was 19.51 cm. The reactor was placed on a magnetic stirrer (Fisher Scientific, model 11-

100-49S) to keep the leachate well mixed. Power was provided by (B&K Precision 1901-B) DC Switching Power Supply with current-voltage monitoring and a maximum output of 30 A -32 V. **Figure 3-1** represents the experimental setup for electro-oxidation of landfill leachate.

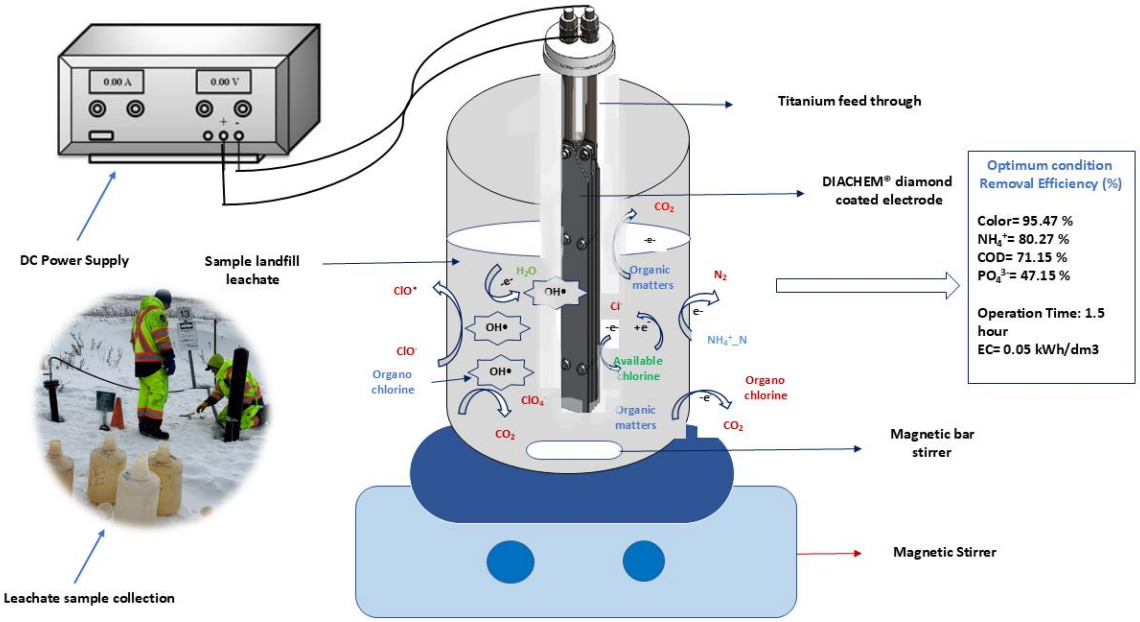

Figure 3- 5. Experimental set-up for Electro-oxidation of mature landfill leachate

3.2.3 Analytical method

Deionized (DI) water was used as the analytical blank or control for COD, (NH_4^+), (PO_4^{3-}), and color measurements. All samples were analysed in triplicate, and the mean of the three analytical measurements was reported. The concentrations of COD, (NH_4^+), and (PO_4^{3-}) were measured using standard methods (Autoridad Nacional del Servicio Civil, 2021). COD was determined using a DR2800 spectrophotometer (Hach, Canada) following the Hach reactor digestion Method 8000. The method incorporates a DI-water reagent blank, and the analytical range for higher concentration of (20 to 1500 mg/L) and for low concentration of (3 to 150 mg/L) were selected according to the sample expected concentration which was around 1200 mg/L. Samples exceeding

the applicable analytical range were diluted before measurement. Chloride interference was considered during COD analysis because chloride is a principal interference in the dichromate COD method. NH_4^+-N and orthophosphate were measured using a QuikChem 8500 flow-injection analyzer (Lachat Instruments, USA) following the corresponding method specific calibration procedures. True color was determined using the Platinum Cobalt standard method with a DR1900 spectrophotometer at 420 nm, with DI water used for zeroing. Chloride was determined using the Hach TNTplus iron(III)-thiocyanate method with a DR1900 spectrophotometer. pH was measured using an Oakton pH meter calibrated according to the manufacturer's procedure.

3.2.4 Experimental design and optimization of the reactor

The electrooxidation of leachate was carried out by five different current densities, i.e., 33, 45, 64, 95, 125 mA/cm^2, three distinct pH levels (pH 3, pH 5.5, and pH 8), and six different time intervals (30 minutes, 1 hr, 1.5 hr, 2 hr, 2.5 hr, and 3 hr.). The broader set of current densities and treatment times was initially evaluated as a preliminary screening step to establish the treatment kinetics and practical operating range. Based on these results, 64 and 125 mA/cm^2 were selected as the lower and upper current-density levels because they represented the effective boundaries of the investigated range, while 95 mA/cm^2 was used as the centre level. Similarly, pH 3 and 8 were selected to represent the acidic and alkaline limits of the investigated conditions. Treatment time was evaluated separately through the kinetic experiments and was therefore not included as an independent factor in the factorial design. In acidic conditions, pH dropped suddenly (3 to 1.8) as time and current densities increased, but in basic conditions, pH raised from (8 to 9.9) as time and current densities increased. However, each sample was taken at every 30-minute interval and then filtered to determine the effects of time and current densities on the removal of organic compounds. Samples were taken and filtered using a cellulose-based fiber paper in which the particle retention

was (1–5µm) with a diameter of 12.5 cm (Fisherbrand™). H_2S0_4 of (1 M) was used for adjusting the pH in the leachate sample.

However, when the result of a process is impacted by the relationship between multiple variables, utilizing statistical methods for experiment design is a suitable option for reducing resource consumption, testing costs, and time required (Contreras et al., 2007; Leili et al., 2020). When a combination of several independent variables and their interactions affects desired responses, response surface methodology (RSM) can effectively optimize the process (Leili et al., 2020). RSMs involve using statistical and mathematical techniques to fit a polynomial equation to experimental data, which can then be used to construct response pattern diagrams in the studied area (Leili et al., 2020). This approach comprises various techniques to determine the optimal values of the parameters that influence the response (Lenth, 2010). A validation spreadsheet of Factorial design with a central point (Teófilo & Ferreira, 2006) in association with RSM and desirability profile was used for the optimization of the two variables (current density (mA/cm^2) and pH) influencing the removal of COD, Color, $NH_4^{+,}$ and PO_4^{3-} from raw wastewater (**Table 1**). STATISTICA® software was used to design RSM and the desirability function. The analysis of variance (ANOVA) was employed to analyze the variance explained for the linear model. The degree of the model was determined by selecting the best-fitted model at each stage and at the final stage of the experiments.

3.2.5 Energy consumption

The energy consumption per volume of treated effluent was calculated using the average cell voltage during electrolysis. Energy consumption (Equation 1) can be expressed in kWh/dm^3 in **Eq. (3-1).**

$$Energy\ consumption = \frac{\Delta EC * I * t}{V} \quad (3\text{-}1)$$

Where ΔEc (V) and I (A) stand for the average cell voltage and the electrolysis current, respectively. Also, t is the electrolysis time (hr), and V is the sample volume (dm^3) (Rocha et al., 2012).

3.3 Results and discussion

The optimal condition for the treatment of landfill leachate matrix was investigated based on a factorial design. The results of experiments in the form of removal rate of COD, Color, NH_4^+, and PO_4^{3-} are provided in **Table 3-2**. The removal efficiency varied within the ranges of 44–71% (COD), 86–99% (Color), 17-80% (NH_4^+-N), and 12-56% (PO_4^{3-}). According to the results, experiment 4 (J=125 mA/cm^2 and pH 8) presents the most removal for COD and NH_4^+.

The statistical significance of the model, which includes the ratio of mean square variation due to regression and mean square standard error, was analyzed using ANOVA. The results obtained from ANOVA for the four responses evaluated are given in **appendix-A, Table S1.** For each regression, the Fisher (F) values were greater, to the same, as a low lack of fit in most cases, these suggest that most of the variation in the response can be explained by the regression equation. To confirm this, the associated p-value was used to estimate whether F is large enough to indicate statistical significance, where a p-value lower than 0.05 indicates that the model is statistically significant. The closer the coefficient correlation is, the better the proposed model is provided by the software. The % variance explained of the response variables followed the order of COD > Color > PO_4^{3-} > NH_4-N, the highest variance explained obtained for COD removal efficiency denotes that 93.4 % of the total variation could be represented by the established model, expressing a satisfactory quadratic fit. Moreover, ANOVA results revealed a satisfactory agreement between

the experimental results and predicted models with high significance, as the probability values in them are low ($p < 0.05$) for COD, Color, and PO_4^{3-}.

Table 3-2. Experimental results of factorial design 2^2 with central point experiments

Experiment	Variable		Response (removal %)			
	(mA/cm^2)	pH	% COD	% Color	% NH_4^+	% PO_4^{3-}
1	64	3	44.15	86.87	17.32	12
2	125	3	68.5	99.19	23.20	22.33
3	64	8	43.3	89.49	36.95	56.33
4	125	8	71.15	95.47	80.27	47.15
5	95	5.5	63.85	91.06	22.88	22.35
6	95	5.5	59.39	92.98	21	23.53
7	95	5.5	56.34	91.07	27.24	33.73

Reaction time: 1 hour and 30 minutes

The three-dimensional (3D) response surface of the model-predicted responses was obtained (**Figure 3-2**) and utilized to assess the interactive relationships between the process variables and treatment outputs for the electrochemical oxidation treatment of the leachate matrix. Percent COD removal efficiency obtained as a function of current density and pH in mature landfill leachate treatment, as depicted in **Figure 3-2a**, high removal efficiency is achieved with the highest current density, regardless of the pH range. High current density at low pH achieves better performance in color removal (**Figure 3-2b**) and for better NH_4^+-N (**Figure 3-2c**) and PO_4^{3-} (**Figure 3-2d**) removal performance, the basic pH (close to 8) was the value that presented the best results;

regarding NH_4^+-N, high current densities favor the removal and for PO_4^{3-} removal the current density does not have a substantial impact.

For COD, the removal efficiency increased from 43.3% to 71.5% (Figure 3-2a) with time because of increased current densities from 64 to 125 mA/ cm^2 and increasing pH. Many other researchers have shown a similar effect of current density on COD removal using landfill leachate as their treatment target (Fernandes et al., 2015). This might be caused by higher chlorine production at higher current density because chlorine is the precursor of hypochlorite (reactions R1 to R3), a strong oxidizing agent for organic pollutants (Quan et al., 2013). When the pH was kept constant (pH 8), color removal increased from 89.49% to 95.47% (Figure 3-2b) because of the increased current density from 64 mA/cm^2 to 125 mA/cm^2. But decreasing the pH from 8 to 3 causes an increase in color removal. The generation of chlorine or hypochlorite ions in alkali media encourages the development of chlorate or perchlorate, which might oxidize the coloured substances in the electrooxidation process, which is the major cause of this color removal from leachate (Feki et al., 2009). Because the chlorine/chloride contained in the solution was in the form of hypochlorous acid, which has a higher oxidation potential than hypochlorite, in an acidic medium with a pH of 3, the color removal percentage was high (**Eqs. 3-2 to 3-8**).

$$2Cl^- \rightarrow Cl_2 + 2e^- \quad \textbf{(3-2)}$$

$$Cl_2 + H_2O \rightarrow HClO + H^+ + Cl^- \quad \textbf{(3-3)}$$

$$HClO \rightarrow H^+ + OCl^- \quad \textbf{(3-4)}$$

$$6HOCl + 3\ H_2O \rightarrow 2ClO_3^- + 4\ Cl^- + 12H^+ + 3O_2 + 6e^- \quad \textbf{(3-5)}$$

$$6ClO^- + H_2O + 2e^- \rightarrow Cl^- + 2OH^- \quad \textbf{(3-6)}$$

$$6ClO^- + 3H_2O \rightarrow 2ClO_3^- + 4Cl^- + 6H^+ + 1.5O_2 + 6e^- \quad \textbf{(3-7)}$$

$$2H_2O + 2e^- \rightarrow 2OH^- + H_2 \quad \textbf{(3-8)}$$

$$R + HOCl \rightarrow P \quad \textbf{(3-9)}$$

Where R is the pollutant, and P is the product.

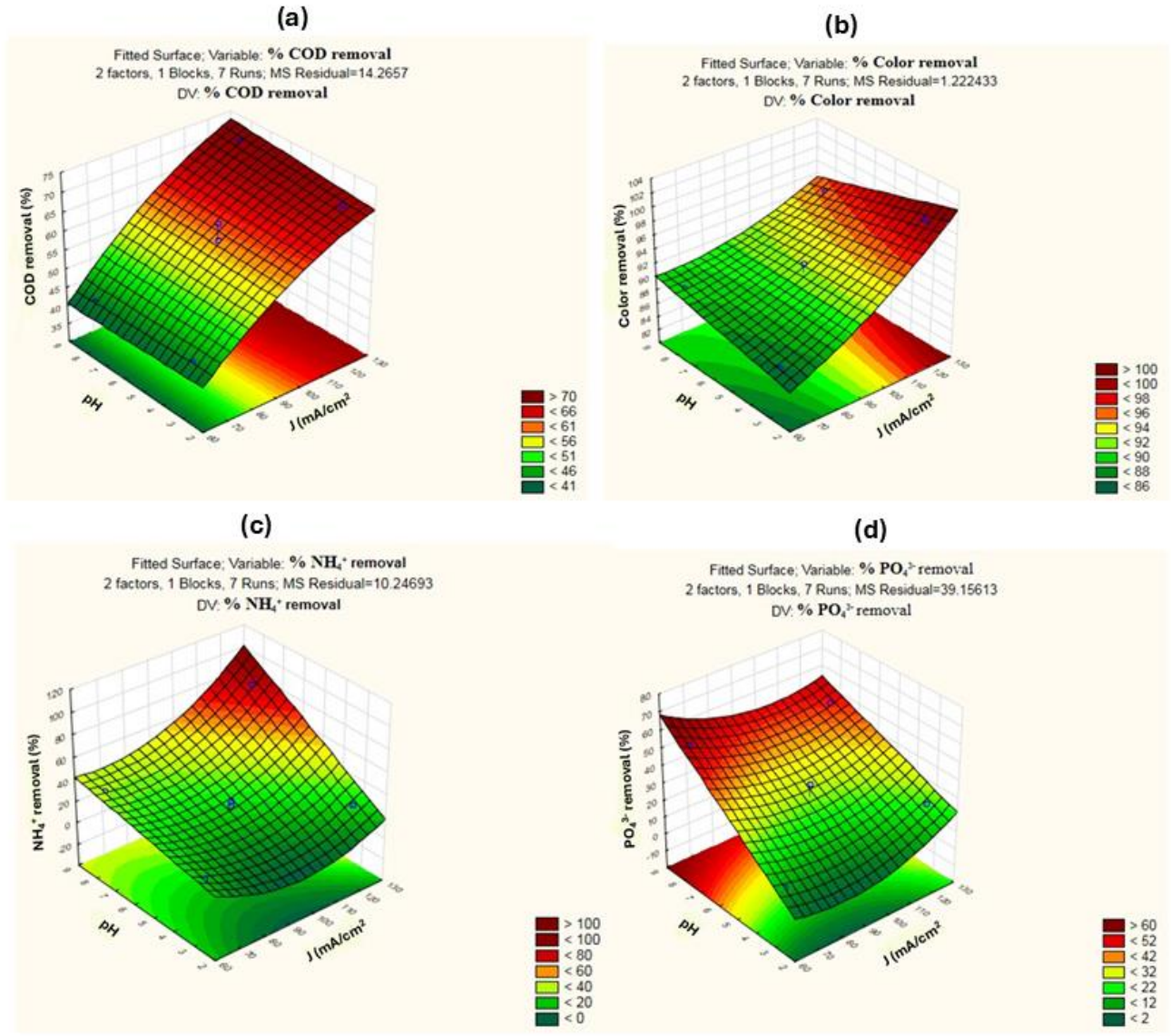

Figure 3- 6. Response surface model for (a) COD, (b) color, (c) NH_4^+-N, and (d) $PO4^{3-}$ removal

However, the desirability function was used to determine the optimal values of variables (current density and pH) that can give the optimum performance levels for the four responses (COD, color, NH_4^+-N, and PO_4^{3-}). The response is first converted into a specific desirability function, with desirability 1 being the most desirable value and 0 representing the least desirable condition (Sakkas et al., 2009). On the left side of **Figure 3-3** (below), the upper (left) section of the diagram displays each factor's current level in the model.

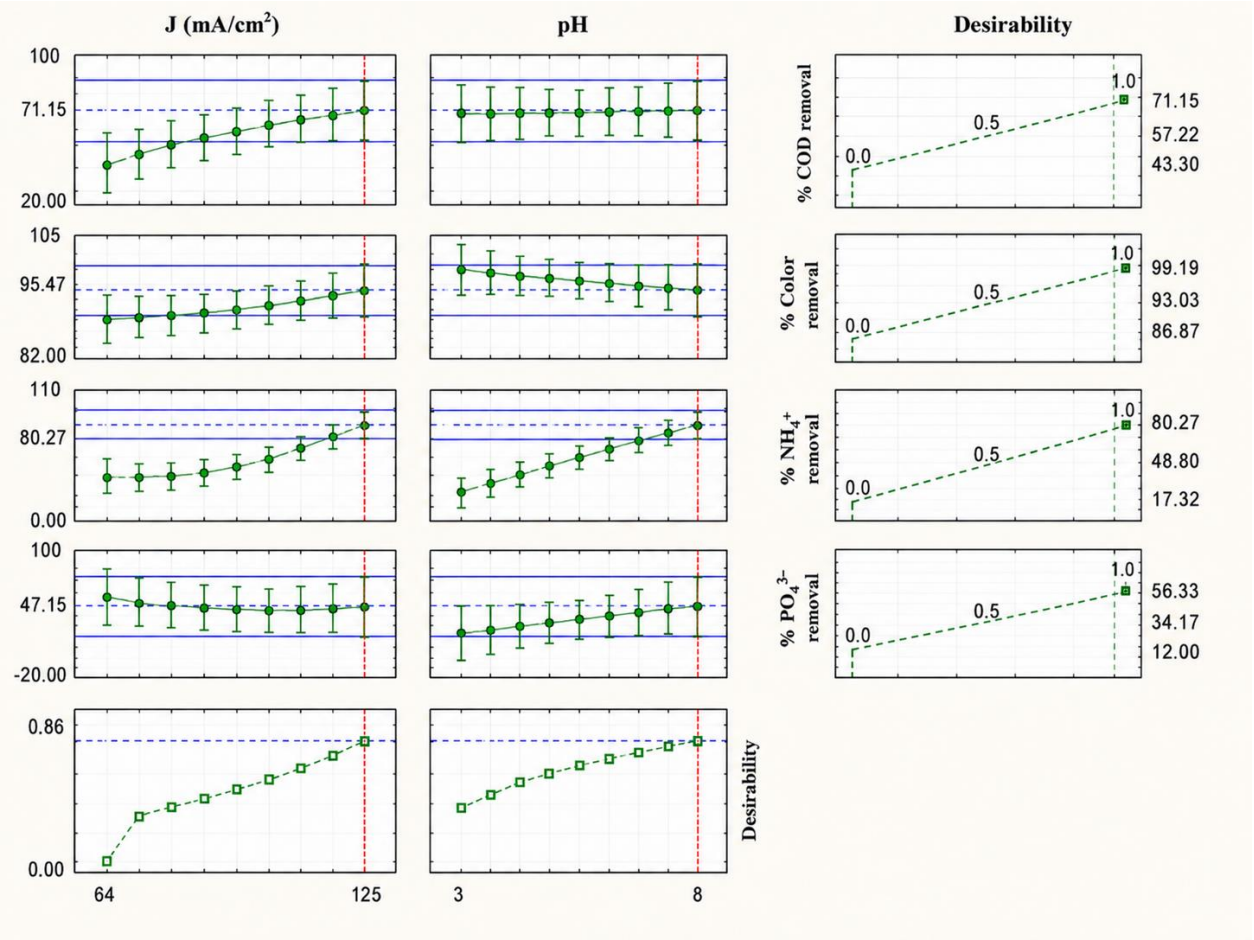

Figure 3- 7.Profile for predicted values and desirability in the four physicochemical parameters evaluated in mature landfill leachate

According to this study, all parameter removal percentages improved with increasing J and time during the electrooxidation process of landfill leachate, which is in accordance with previous research (Agustina et al., 2019; Anglada et al., 2011). The profile indicated that without color, the three responses are favored with an increase in pH values and an increase in current density, with the optimal condition in J = 125 mA/cm^2 at pH 8, which is in accordance with the factorial design data and response surface model. A previous study mentioned that increasing the contact time to some extent enhances the removal efficiency. This is because longer contact time generates more ozone and provides sufficient time for the destruction process (Rahmani, Nematollahi, et al., 2018).

However, the statistical model for ammonium removal showed comparatively weaker predictive reliability than the models for COD, color, and phosphate (Appendix A, Table S1). The model explained 72.3% of the observed variance, but the overall regression was not statistically significant (F = 5.22, p = 0.105). Although the lack of fit was non-significant (p = 0.114), the limited degrees of freedom restrict confidence in quantitative prediction. Accordingly, the model was used mainly to describe response trends within the investigated design space.

3.4 Electrooxidation of mature landfill leachate using BDD electrode

To evaluate the electrooxidation performance with the optimal conditions, the COD, color, NH_4^+-N, and PO_4^{3-} removal were measured against time (**Figure 3-4**).

An electron-transfer process is coupled as part of the electrochemical oxidation of landfill leachate. The mechanism responsible for COD, color, NH_4^+-N, and PO_4^{3-} removal could be described by: **(a)** discharge of water molecules to hydroxyl radicals **Eq. (3-10)**, **(b)** direct anodic oxidation where the pollutants are transformed to CO_2, H_2O, and other inorganic compounds **Eq. (3-11)**, **(c)** development of organic radicals (R*) by a dehydrogenation mechanism **Eq. (3-12)**and

(d) oxygen evolution and reaction with the organic radicals; **Eqs. (3-13 and 3-14)** (Alfaro et al., 2006; Sun et al., 2021).

$$BDD + H_2O \longrightarrow BDD(HO^{\cdot}) + H^+ + e^- \quad \textbf{(3-10)}$$

$$BDD(HO^{\cdot}) + R \longrightarrow BDD + mCO_2 + mH_2O + H^+ + e^- \quad \textbf{(3-11)}$$

$$RH + BDD(HO^{\cdot}) \longrightarrow R^* + H_2O + BDD \quad \textbf{(3-12)}$$

$$BDD(HO^{\cdot}) \longrightarrow BDD + \frac{1}{2}O_2 + H^+ + e^- \quad \textbf{(3-13)}$$

$$R^* + O_2 \longrightarrow ROO^* \quad \textbf{(3-14)}$$

Since the BDD anode allows to produce both •OH species in bulk solution and (BDD •OH)) on the surface, its usage facilitates more powerful oxidation. Due to a greater O_2 overvoltage, BDD(•OH) has a stronger oxidizing power than other anodes, making it easier to remove contaminants (Sirés et al., 2014b).

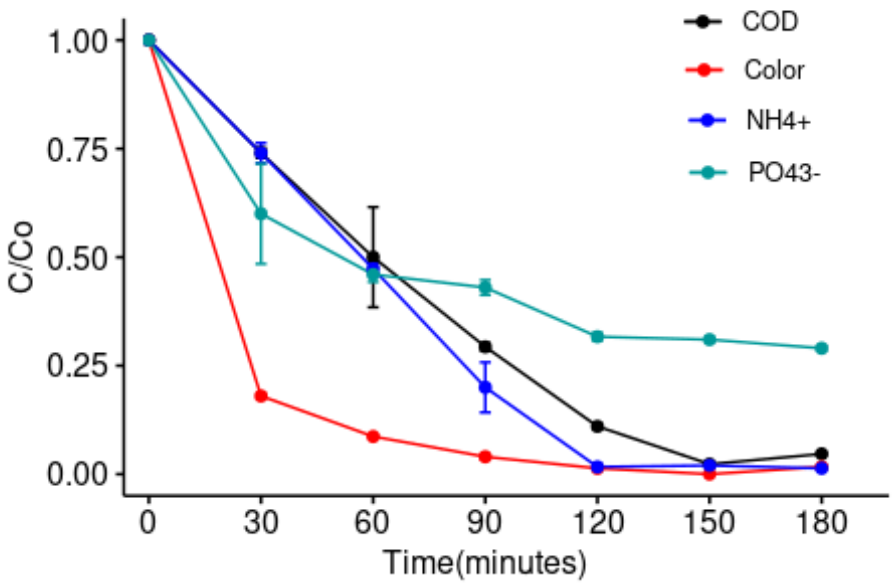

Figure 3- 8. Removal profile vs time for COD, Color, NH_4^+, PO_4^{3-} at the optimal conditions (J=125 mA/cm2 at pH 8)

As many researchers have already proved that oxidative degradation of COD, Color, NH_4^+, PO_4^{3-} at the BDD electrode only takes place in the potential region of water decomposition, the optimal value of applied current (125 mA/cm^2) attains the anodic potential higher than 2.3 V vs. SCE. It is quite apparent that complete mineralization could always be achievable due to the electrochemical decomposition of water molecules on the BDD surface that leads to the concomitant generation of hydroxyl radicals (•OH) (Agustina et al., 2019).

3.4.1 Effects on COD and Color removal

The COD (C_o=900 mg/L) removal increased with time, reaching 95.08 % after 2.5 hours of reactor operation. Also, the low content of solids contributes to mass-transport control in the process; it implies control in the oxidation from the bulk solution to the surface of the BDD electrode (Panizza

& Cerisola, 2008). (Agustina et al., 2019) found that electrooxidation of leachate removed 0.43 g, 0.53 g, and 0.72 g of COD at the original pH (8.5) in 6 hours, and the used current densities were 50, 75, and 100 mA/cm^2, respectively. In the present study, it was found that after 3 hours of electrooxidation, 0.61, 0.87, and 0.89 g COD were removed when applied current densities were 64, 95, and 125 mA cm^2, respectively. In both cases, COD removal increased with time and with current intensity. The COD removal performance for this research is higher owing to the increased generation of (BDD(•OH)) on the anode surface and the presence of •OH in the bulk solution during greater current density (Mandal et al., 2017). In addition, oxidation by (BDD(•OH)) and •OH radicals is not the only oxidation mechanism occurring in the system. When sulfates are present in landfill leachate, could develop the formation of some peroxodisulphates **Eq. (3-15)** (Panizza & Cerisola, 2008) can occur during electrolysis with BDD electrodes.

$$2SO_4^{2-} \longrightarrow S_2O_8^{2-} + 2e^- \quad \textbf{(3-15)}$$

After three hours of operation at current densities of 64, 95, and 125 mA/cm^2, the system's energy consumption was 0.02,0.03, and 0.05 kWh/dm^3 with COD removal of 68.44 %, 97.66 %, and 99.78 %, respectively. It can be mentioned that raising the current density from 95 mA/cm^2 to 125 mA/cm^2 did not significantly affect the COD removal in comparison with the energy consumption. Similar result trends for COD removal with current densities were also reported by, where they found 43 %, 53 %, and 72% of COD removal when the applied current density was 50, 75, and 100 mA/cm^2. This also implies that with a higher current density of 125 mA/cm^2, more energy was required not only for the oxidation of organic compounds but also for the oxidation of other ions in the leachate (mostly chloride ions), resulting in the indirect oxidation of organics, as measured with COD. In this study, it was found that when the pH was 3 and 8, the removal of COD was 97.66 and 99.77 %, respectively, with the same current density of 125 mA/cm^2. This

result indicates that with the same current, there is no considerable effect of pH on COD removal. Thus, the pH may not significantly affect the COD removal efficiency at a constant current, but with different concentrations of chloride. This to the fact that the electrochemical oxidation process generates reactive species, such as hydroxyl radicals, which are not pH-dependent and can oxidize organic pollutants at different pH values. Regarding the different concentrations of Cl^- observed at different pH values, it is possible that the electrochemical process may lead to the generation of chlorine-based species, such as hypochlorite or chlorine gas, which can increase the concentration of Cl^- in the treated wastewater. This could be influenced by the pH of the wastewater, as the formation and stability of these species depend on pH. In summary, while the pH may not significantly affect COD removal efficiency during electrochemical oxidation at a constant current, it may influence the formation of chlorine-based species and hence the concentration of Cl^- in the treated wastewater.

But when it comes to chloride, the solution's chloride content decreased as it went from basic, optimum conditions to acidic ones (from pH 8 to 3), **appendix-A** of **Table S2** of the supplementary information, which is because of the complete oxidation of the COD. For instance, the concentration of chloride using 125 mA/cm^2 current density (in pH 8) was 748 mg/L; in contrast, at pH 3 the chloride concentration was two-fold lower (339 mg/L). The twofold decrease in chloride concentration observed in experiment 2 (125 mA/cm^2) compared to experiment 1 (64 mA/cm^2) when keeping the pH constant at 3 in an electrooxidation process for leachate treatment can be explained by the difference in the rate of chloride oxidation at the anode. At higher current densities, the rate of oxidation of chloride ions can be expected to increase due to the increased rate of electron transfer at the anode. This means that more chloride ions will be converted to chlorine gas, which can lead to higher levels of chlorinated byproducts in the treated leachate.

However, at very high current densities, the rate of oxidation of water at the anode can become dominant, which can lead to a decrease in the rate of chloride oxidation. This phenomenon is known as the "competition effect" and can lead to a decrease in the concentration of chloride ions in the treated leachate.

Therefore, it is possible that the higher current density used in experiment 2 (125 mA/cm^2) caused the competition effect to become more pronounced, leading to a higher rate of water oxidation and a lower rate of chloride oxidation compared to experiment 1 (64 mA/cm^2). This would explain the observed decrease in chloride concentration in experiment 1.

According to the literature, adding sodium chloride in electrolysis for landfill leachate treatment enhances process performance by generating more chlorine or hypochlorite (Quan et al., 2013; Turro et al., 2012). Concurrently, for the treatment of landfill leachate, the current density can influence the chloride ions during leachate conversion into a significant quantity of active chlorine, which can increase the effectiveness of the treatment process (Moraes & Bertazzoli, 2005). Although adding Cl^- improves oxidation efficiency, it also increases the production of organochlorinated compounds, resulting in a final solution with substantial ecotoxicity (Turro et al., 2012). For the present study, when pH was adjusted by NaOH from acidic to basic pH (from 3 to 8) at 125 mA/cm^2 current density, the concentration of chloride was also increased to double in the electrooxidation process compared to the acidic condition. In that condition, the performance for COD removal was around 100% after 3 hours of operation. This result suggests that higher current densities and high pH increase chloride concentration and thus improve process performance for COD removal. According to previous research, the BDD/Nb electrodes with a current density of 50 mA/ cm^2 achieved 87.5% COD removal after 6 hours of operation (B. Zhou et al., 2016). Another study investigated the EO of biologically treated landfill leachate using

Ti/BDD anodes, achieving a maximum COD removal efficiency of 95.17% after 8 hours at 83 mA/ cm^2 (Luu, 2020). However, color removal was efficient within the first 60 minutes of the electrooxidation process, while removal effectiveness declined with time. Experimental data show that color removal efficiency was 99.65% within 1.5 hours of reaction time. During electrooxidation, more than 99.7 % of decolorization was achieved after about 3 hours of treatment. With increasing current density, the amount of the generated ozone increased, leading to an enhancement in color removal efficiency (Rahmani, Nematollahi, et al., 2018). In this case, the faster decolorization could be attributed to the high reaction of oxidative species with the π-π bond of molecules that absorb at 465 nm; these compounds are generally known to have a high molecular weight (Fan et al., 2006). According to a study, maintaining a constant pH of 6.5 and a time of 33 minutes resulted in an increase in color removal from 80% to 90% when the current density was raised from 2.02 mA/cm^2 to 4.05 mA/cm^2. However, further increasing the current density to 6.08 mA/cm^2 did not result in any increase in color removal (Veli et al., 2021). Moreover, when the pH was increased from 4 to 6.5, the color removal efficiency also increased from 74% to 90%. However, increasing the pH beyond 6.5 resulted in a decrease in color removal efficiency, dropping to 84% (Veli et al., 2021). Theoretical studies suggest that acidic conditions can decrease the concentration of carbonate and bicarbonate anions, leading to the destruction of hydroxyl radicals generated on anodes. This enhances oxidation. On the other hand, alkaline conditions may cause the redox circulation of Cl^- to enhance indirect oxidation (Deng & Englehardt, 2007). The variations in the composition of leachate are the likely cause of the inconsistent results reported by different authors (Mandal et al., 2017; Hui Zhang et al., 2011).

3.4.2 Effects on NH_4^+-N and PO_4^{3-} removal

Ammonia concentration reduced nearly linear over time (**Figure 4**), with full removal after 3-hour treatments at 125 mA/cm^2. In **Figure 2c** and **Figure 3** can be observed that oxidation of ammonium ion (initial concentration NH_4^+-N: 590 mg /L) is pH-dependent and follows the tendency of NH_3 formation (Kapałka et al., 2010). The experimental data confirm that ammonium ions oxidized on BDD achieved 83.15%, 98.24%, and 98.74% of removal in 3 hours of treatment at 64, 95, and 125 mA/cm^{2,} respectively. This value represents a better % removal in relation to treatment time in comparison with other studies, for instance, (Anglada et al., 2011) used a current density of 60 mA/cm^2 and reported an 8-hour treatment that removed 95% of the ammonia and (Zambrano & Min, 2020) by using BDD electrode to get 76.6% ammonia removal after a 3-h treatment at a current density of 100 mA/cm^2. Previous research studied the EO of landfill leachate by means of BDD electrodes using applied current densities (j) ranging from 150 to 900 mA/cm^2 (Cabeza, Urtiaga, & Ortiz, 2007; Cabeza, Primo, et al., 2007). The results of the studies showed that removal of N-NH_4^+ (ammonia) from landfill leachate using BDD electrodes followed zeroth-order kinetics at high j values, whereas, at low j values, the removal process was exponential-like decaying ammonia concentration. On the other hand, removal of N-NH_4^+ from landfill leachate by means of Ti/RuO_2–IrO_2 and Al electrodes indicated that in the case of COD removal, the rate constant of N-NH_4^+ increased with increasing applied j, and the value of the half-life consistently decreased (Juan Li et al., 2016). In the working conditions, the direct and active chlorine-mediated (indirect) electrooxidation of ammonia (NH_3 and NH_4^+) could be feasible on BDD at basic pH (>8); **Eqs. (3-16)** (Kapałka et al., 2010).

$$HOCl + NH_3 \longrightarrow NH_2Cl + H_2O \qquad k_1=3.07\cdot10^6\ M^{-1}s^{-1}\ (25ºC) \qquad \textbf{(3-16)}$$

In the present study, the concentration of chloride ions is relatively high, 1248 mg/L (**Table 1**), in the raw leachate. Thus, the formation of chlorine reactive species was expected in the anodic oxidation of leachate, and the (R15) reaction may happen in the system. Chloride may be oxidized at the BDD anode to active chlorine species, including Cl_2, HOCl, and OCl^-. In addition to contributing to leachates pollutant oxidation, these species can react with ammonium to form chloramines. Depending on the active chlorine exposure, pH, chloride to ammonium ratio, and competing chlorine demand, chloramines may persist as intermediate products or undergo further transformation to nitrogen gas, nitrate, and other nitrogen containing species. Active chlorine may also be further oxidized at the BDD surface to chlorate and perchlorate, while reactions with leachate pollutants, transformation products, and other organic constituents may generate organically bound chlorine measured collectively as AOX. Therefore, parent compound and ammonium depletion is not interpreted independently of the potential formation of halogenated and nitrogenous byproducts.

These byproducts were not quantified in the present study. Consequently, their absence cannot be established, and the environmental safety of the treated solution cannot be evaluated solely from parent compound removal efficiencies. The initial chloride concentration provides a conservative chlorine inventory boundary: on a molar chlorine-atom basis, the total amount of chlorine contained in active chlorine, chloramines, chlorate, perchlorate, AOX, and any volatile chlorine containing products cannot exceed the chloride initially present. Where chloride depletion is available, the net concentration of accumulated non chloride chlorine species is bounded by the amount of chloride consumed, subject to potential gaseous losses and chlorine recycling.

Based on the results of the current study, chloride concentration is mainly pH and current-dependent. The chloride content in the present experiment at pH 8 and 125 mA/cm^2 current was

748 mg/L, almost twofold when compared to the pH 3 (Table S2) conditions with the same electricity. Within a 1.5-hour reaction time, the removal of NH_4^+-N from leachate was 80.27% at pH 8. This is primarily because greater current densities with neutral pH compared to acidic pH result in increased Cl_2 generation and consequent increases in HOCl, which in turn cause higher ammonia oxidation rates. For this reason, a neutral pH is suggested for ammonia removal as it produces a higher HOCL. However, oxidation of ammonia may produce free chlorine (HOCl and OCl^-) and chloramines. Since free chlorine is the most efficient disinfectant, electrochemical treatment of the leachate will improve chlorine's potential to inhibit microbes in the leachate. From the present study, it was found that for the current density of 125 mA/cm^2 at pH 3 and pH 8, the chloride concentration was increased from 339 to 748 mg/L. With increasing chloride concentration, the increase of ammonium removal was achieved from 38% to >99%, which indicates that ammonia removal is affected by HClO formation, **Eq. (3-17)** (Pérez et al., 2012).

$$2NH_4^+ + 3HOCl \rightarrow N_2 + 3H_2O + 5H^+ + 3Cl^- \quad \textbf{(3-17)}$$

For the present study, it was found that at higher current densities (125 mA/cm^2), in acidic forms (at pH 3 and 5.5), the pH reduction rate was faster with the operation time, but for the basic condition at pH 8, it was reversed. Furthermore, when 3 hours of operation at constant current densities of 64, 95, and 125 mA/cm^2, ammonia removal was 83.15%, 98.24%, and 98.62%, respectively, with energy consumption of 0.02 kWh/dm^3, 0.03 kWh/dm^3, and 0.05 kWh/dm^3, respectively. The present research revealed that there are no significant changes in ammonia removal efficiency when the electricity is 95 and 125 mA/cm^2. The observed decrease in NH_4^+–N is therefore described as ammonium depletion or transformation rather than confirmed total nitrogen removal. Direct anodic oxidation may occur through oxidation of free NH_3, particularly at alkaline pH. In contrast, under acidic and near neutral conditions, where NH_4^+ predominates,

indirect oxidation by electrogenerated active chlorine is mechanistically more logical in a chloride containing electrolyte. Nevertheless, the current data cannot distinguish direct oxidation from active chlorine mediated reactions or confirm that breakpoint chlorination was reached. Such confirmation would require time resolved measurements of free chlorine, combined chlorine or individual chloramines, NH_4^+–N, NO_2^-–N, NO_3^-–N, total nitrogen, chloride, chlorate, perchlorate, AOX, and preferably gaseous nitrogen products.

However, the presence of phosphate has a negative effect on ammonia removal due to oxygen evolution (Mahvi et al., 2011; Vanlangendonck et al., 2005), the removal rate of ammonia is less if significant phosphate concentrations exist in the reactor. In our present study, phosphate did not affect ammonia removal, as the concentration of phosphate was not high in the reactor. The oxidation of phosphate on BDD can occur by direct oxidation on the anode surface (BDD(•OH)) or by the oxidation by •OH in the bulk solution, both mechanisms lead to the formation of phosphate radicals ($H_2PO_4^{\bullet}$, $HPO_4^{-\bullet}$, and $PO_4^{2-\bullet}$), which can combine to yield the peroxodiphosphate ion (2.07 V vs NHE) (C. R. Costa et al., 2009). When the anodic potential is less than 3.95 V vs. Ag/AgCl, the process that predominates is the direct oxidation of phosphate ions (C. R. Costa et al., 2009). In addition, the phosphate oxidation mechanism involves a proton exchange. Current oxidation is useful at high pH values, which means the oxidation reaction is faster in a basic solution. In addition, high electricity causes temperatures to rise over time, which accelerates electron transfer and helps the EO process to remove phosphate.

3.5 Energy consumption and energy yield

Energy demand is an important consideration for evaluating the practical feasibility of electrochemical treatment. In this study, two different energy performance metrics were considered, which are volumetric energy consumption and energy yield.

For the present study, volumetric energy consumption represents the electrical energy required to treat a unit volume of leachate and is expressed as kWh/m^3 and was calculated using **Eq. (3-18)**:

$$ECv = \frac{UIt}{1000\,VR} \quad \textbf{(3-18)}$$

where U is the cell voltage (V), I is the applied current (A), t is the treatment time (h), and V_R is the reactor volume (m^3). At the optimized condition of 125 mA/cm^2 and pH 8, the volumetric energy consumption was 50 kWh/m^3, equivalent to 0.05 kWh/ dm^3.

In contrast, the values expressed in g/Wh represent the energy yield, i.e., the mass of contaminant removed per unit of electrical energy supplied. The energy yield for each pollutant was calculated using **Eq. (3-19)**:

$$Yx = \frac{\Delta mx}{U.I.t} \quad \textbf{(3-19)}$$

where Y_x is the energy yield (g/Wh), Δmx is the mass of the respective pollutant removed (g), U is the cell voltage (V), I is the applied current (A), and t is the electrooxidation time (h). Thus, a higher g/Wh value indicates greater pollutant removal per unit energy, whereas a lower kWh/ m^3 value indicates lower volumetric energy demand. The energy yields of COD, NH_4^+, color, and PO_4^{3-} removal under factorial design conditions are presented in (**Table 3-3**).

Table 3-3. Energy yields for COD, NH_4^+-N, and PO_4^{3-} removal under factorial design conditions.

Experiment	**Variable**			**Energy consumption (g/Wh)**		
	Time (h)	**Current (A)**	**pH**	**COD energy yield (g/Wh)**	**NH_4^+-N energy yield (g/Wh)**	**PO_4^{3-} energy yield (g/Wh)**
1	3	10	3	0.0089	0.0026	0.0003

2	3	20	3	0.0050	0.0014	0.0001
3	3	10	8	0.0089	0.0071	0.0001
4	3	20	8	0.0052	0.0033	0.0005

The energy yield results demonstrate that increasing current did not necessarily improve the mass removed per unit energy. The highest COD energy yield was 0.0089 g/Wh at 10 A, while the highest NH_4^+-N energy yield was 0.0071 g/Wh at 10 A and pH 8. The highest PO_4^{3-} energy yield was 0.0005 g/Wh at 20 A and pH 8. These results indicate that greater electrical input can enhance overall removal while decreasing the efficiency with which the supplied energy is utilized for contaminant removal.

For comparison, (Zambrano & Min, 2020) investigated landfill-leachate electrooxidation using a Ti/Pt electrode over current densities of 50-150 mA/cm^2 and reported increasing energy requirements at higher applied current densities. The volumetric energy consumptions reported in the present study were approximately 20, 30, and 50 kWh/m^3 at 64, 95, and 125 mA/cm^2, respectively. At the optimized condition, 50 kWh/m^3 was associated with removals of 71.15% COD, 80.27% NH_4^+, 95.47% color, and 47.15% PO_4^{3-}. However, reported energy requirements are strongly influenced by electrode material, reactor design, operating conditions, and leachate composition. Therefore, the present comparison reflects the performance of the Nb/BDD system under the specific conditions investigated and is not interpreted as evidence of a universal energy advantage over Ti/Pt electrodes.

3.6 Conclusions

To conclude, the use of BDD electrodes for leachate treatment is considered novel due to their ability to achieve simultaneous removal of multiple pollutants, including COD, ammonium,

phosphate, and color, in a single treatment process. The high efficiency, long lifespan, and resistance to fouling and corrosion of BDD electrodes make it a promising technology for landfill leachate treatment. In this research, BDD electrodes were used in the electrooxidation process to treat landfill leachate, and the optimum conditions were used to assess the process performance. The key factors influencing the process in this investigation were current densities, effluent pH, and time. pH 8 and a current density of 125 mA/cm^2 were determined to be the optimum operating conditions. In this case, the COD removal was 71.15%, color removal 95.47%, NH_4^+ removal 80.27%, and PO_4^{3-} removal 47.15% within 1.5 hours of reaction time. From the experimental results, it was seen that the response of the model predicted for COD, color, $NH_4^{+,}$ and PO_4^{3-} were almost similar to the actual response obtained under the aforementioned optimal conditions. It was observed that increasing the response time and current density considerably increased treatment efficacy. Furthermore, pH has no significant influence on COD and ammonium removal. But color removal was high in the acidic condition at low pH, which is because the chloride present in the solution was in the form of hypochlorous acid, which possesses high oxidation potential compared with hypochlorite. This is recommended that further studies should be conducted for other factors, such as the electrode gap and stirring rate, to obtain the optimum operational conditions for the removal of a variety of pollutants, including pharmaceuticals, pesticides, and other recalcitrant compounds that can be removed by the electrooxidation process. Also, research is needed to optimize the use of BDD electrodes for different types of wastewater and pollutant mixtures.

Chapter 4: Manuscript no. 2

Influence of operational parameters on mixed pharmaceutical antibiotics removal from wastewater using Boron-doped diamond (BDD) electrooxidation

Abstract

This study evaluated the effectiveness of electrooxidation using a niobium-based boron-doped diamond (Nb/BDD) anode for removing mixtures of antibiotics, with particular focus on how key operational parameters influence parent-compound degradation and organic carbon reduction in wastewater. Sulfanilamide (SN), tetracycline-hydrochloride (TC-HCl), and sulfamethazine (SMZ) were selected as representative pollutants. Among the tested conditions, 35 mA/cm^2 current density produced the fastest removal on a time basis, whereas 15 mA/cm^2 provided the highest removal per unit charge at acidic pH (3.5). In addition, at Q/V = 2.0 A h L^{-1}, the 15 mA/cm^2 condition gave the maximum removal for all three antibiotics across every tested pH concentration combination. At pH 3.5, an initial concentration of 4000 µg/L, and 60 min of electrolysis, TC-HCl removal reached 77–80%, while SN and SMZ achieved ~77% and 79% removal, respectively. Degradation efficiencies declined under neutral and alkaline conditions, which confirms the strong influence of solution chemistry on oxidation behavior. TOC mineralization was highest at pH 3.5 and 35 mA/cm^2; TOC decreased from 160 mg/L to 75 mg/L after 60 min, corresponding to a TOC mineralization efficiency of 53.13%. These findings demonstrate that Nb/BDD electrooxidation not only effectively removes parent pharmaceuticals but also achieves significant total organic carbon removal within a short period of time. The highest treatment performance is achieved due to the generation of strongly oxidizing species, particularly hydroxyl radicals (•OH), at the Nb/BDD surface and shows excellent performance for treating wastewater containing mixed

pharmaceuticals. Future research should integrate modeling and experimental approaches to optimize system performance, manage byproducts formation, assess toxicity evolution, and validate performance under real wastewater conditions at pilot scale.

Keywords: Nb/BDD electrooxidation, pharmaceutical antibiotics in wastewater, Electrooxidation processes, Hydroxyl radicals, Mineralization, Current density, pH and time.

4.1 Introduction

Pharmaceuticals are emerging wastewater pollutants, and among them, antibiotics are one of the largest classes of pharmaceuticals commonly used in both human and veterinary therapy for treating infections and supporting animal growth (Hai et al., 2020a; Vasilie et al., 2018). Some of these antibiotics are partially metabolized and excreted through urine and feces, thus released into the wastewater treatment systems (Hai et al., 2020a; Wroński et al., 2025). Their continuous release in surface waters at trace to sub-trace levels and partial elimination is commonly associated with ecological risk and the development of antibiotic-resistant bacterial populations (Kaplan et al., 2013; Robinson et al., 2005; Wroński et al., 2025). The current research aimed at three antibiotics that belong to two major classes: (i) Sulfonamides (sulfanilamide and sulfamethazine) and (ii) Tetracyclines (Tetracycline Hydrochloride (TC- HCl)) as targeted pollutants in wastewater. All these antibiotics are significant due to their environmental occurrence and persistence and are found in almost all kinds of surface water and the effluent of wastewater treatment plants (WWTPs) (L. Chen et al., 2025). Therefore, effective and economic methods for the removal of these specific antibiotics from wastewater are urgently required (L. Chen et al., 2025; Hai et al., 2020a).

Several physicochemical methods have been developed for the removal of antibiotics, such as adsorption (Tian et al., 2019), ozone oxidation (Iakovides et al., 2019), photo-catalytic oxidation (Hussain et al., 2017a), Fenton reaction (Liu et al., 2018), and electrochemical oxidation process (Bari et al., 2025; L. Chen et al., 2025; Teng et al., 2020). However, the conventional treatment methods such as adsorption and membrane-based separation can decrease the concentrations of antibiotics in wastewater, although in most cases they do not eliminate them but simply transfer them to another phase. For this, more attention has been paid to advanced oxidation processes,

specially electro-advanced oxidation processes for antibiotic removal from wastewater (Hu et al., 2025a; Jaiswal et al., 2025; Wroński et al., 2025). In the electrooxidation process, operating parameters that include electrode material, current density, pH, electrolyte composition, operating time, pollutant concentration, and water-matrix effects are major controlling factors of the overall treatment outcome, which can also affect the energy demand and byproduct formation (Wroński et al., 2025; Yuan et al., 2023). Among the available materials, boron-doped diamond (BDD) electrodes have attracted particular attention because of their unique properties, including high chemical stability, long-term durability, broad potential window, strong resistance to passivation, low capacitive current, and high direct and indirect oxidation ability (Hasnine et al., 2023; Hu et al., 2025b; Jaiswal et al., 2025; Vasilie et al., 2018).

The existing literature on the target antibiotics suggests that the treatment based on BDD is strongly feasible; at the same time, research evidence suggests that the optimization of the operations is required (Bari et al., 2025; García-Espinoza & Nacheva, 2019; Hu et al., 2025c; Oturan & Aaron, 2014). The optimization is important for balancing the degradation performance, mineralization degree, and the energy demand (Vasilie et al., 2018). Despite the proven efficiency of BDD electrooxidation of individual antibiotics and larger combinations of mixtures of micropollutants, there are still two gaps that are highly important to engineering design and scale-up. First, mixed-antibiotic systems still need to be mapped in a systematic way, as competitive scavenging, different speciation, and oxidant schemes by matrices can cause apparent rate control and change the hierarchy of removal among different compounds (Wroński et al., 2025). Second, feasibility is strongly influenced by energy consumption and local electricity cost, where electrooxidation performance usually increases with the current density and treatment duration, but these two variables tend to increase energy consumption and decrease current efficiency by

encouraging parasitic reactions (Vasilie et al., 2018). This trade-off is especially applicable in the jurisdiction of Manitoba, Canada, whereby fairly low cost of electricity units can increase the economic viability of the electrochemical polishing processes, yet the current rate structure, including energy and demand charges, still requires close optimization of the operating conditions to reduce the overall cost of treatment.

The novelty of the present study lies in the systematic investigation of Nb/BDD electrooxidation for the simultaneous removal of a ternary antibiotic mixture comprising sulfanilamide, tetracycline-HCl, and sulfamethazine. These structurally different compounds offer different acid and alkaline base speciation and oxidation behaviour. Instead of focusing on a specific pharmaceutical or a limited operational range, the present study determined the influence of pH, current density, duration of treatment, and initial concentration on the mixed pharmaceutical antibiotics removal. Thus, the study provides comparative information on major operational factors for their removal performance and useful recommendations on competitive oxidation in a multi-antibiotic system. The second novelty is the application of high influent concentrations as an urgency test to describe process performance. In municipal wastewater, antibiotics are typically found in trace to low μg/L concentrations; the range of mg/L used here can be interpreted as a source-strength or worst-case scenario that allows a more reliable characterisation of removal energy trade-offs and a more definitive definition of operational limits, including the potential risk of by-products in wastewaters with chloride and carbonate alkalinity (Garcia-Segura et al., 2015). Furthermore, these higher concentrations were chosen to provide reliable HPLC quantification and clear differences in treatment response. They also allowed the Nb/BDD process to be evaluated under high mixed-antibiotic loading. Such concentrations are more relevant to concentrated pharmaceutical or point-source wastewaters than to conventional municipal wastewater.

Overall, this research provides mechanistic understanding and practical engineering guidance for applying Nb/BDD electrooxidation as an advanced treatment step or as a targeted treatment option for high-strength pharmaceuticals in wastewater processes.

The main objectives of this research were to: (i) measure the removal-efficiency trends of individual antibiotics at different initial concentration, pH, current density and operating electrolysis time; (ii) identify the main operational parameters that determine the removal in mixed-antibiotic wastewater; and (iii) contextualise energy use and operating electricity cost on a Manitoba, Canada based distribution scenario with updated commercial tariff price by Manitoba hydro.

The main hypotheses of this research were that: (a) the most significant operational factor would be the treatment time; (b) the higher the current density, the higher the removal rate, but the improvement become less with the increase of parasitic reactions; (c) the acidic pH usually would favour the higher oxidation rate because of hydroxyl radicals (•OH) whereas the alkaline pH would potentially inhibit the radical activity by scavenging; (d) an increase in the initial pollutant concentration generally lowers the overall removal percentage when treatment time and current are kept constant. However, a higher starting concentration can temporarily improve current efficiency because the majority of the applied current is directed toward oxidizing the pollutant rather than increasing parasitic side reactions.

4.2 Materials and Methods

Sulfanilamide ($pKa_1 \approx 1.8$, $pKa_2 \approx 10.5$), tetracycline hydrochloride TC-HCl (pKa 3.3, 7.7, 9.7), and sulfamethazine ($pKa_1 \approx 2.07$, $pKa_2 \approx 7.4$) (Hu et al., 2025c) were selected as a targeted

antibiotics in wastewater and electrooxidation experiments were conducted in a three litre batch reactor using a Nb/BDD anode under constant applied current density (15, 25 and 35) mA/cm^2 with periodic sample analysis through high-performance liquid chromatography (HPLC) to determine the residual concentrations. The antibiotic removal efficiency was calculated with the following equation, **Eq. (4-1):**

$$\text{Removal efficiency (\%)} = \left(1 - \frac{C_t}{C_0}\right) \times 100\% \quad \textbf{(4-1)}$$

where C_0 is initial concentration at time zero and C_t is the final concentration at time t. All the experiments were conducted in triplicate (n = 3) to ensure reproducibility.

4.2.1 Chemicals and Reagents

Sulfamethazine (SMZ, $C_{12}H_{14}N_4O_2S$; ≥ 99 % assay) and Sulfanilamide (SN, $C_6H_8N_2O_2S$; ≥ 99% assay) were obtained from Sigma-Aldrich. Tetracycline Hydrochloride (TC-HCl, $C_{22}H_{24}N_2O_8 \cdot$ HCl; > 98% assay) was purchased from TCI America. These three compounds were selected as the targeted pharmaceutical pollutants. Analytical grade sulfuric acid (H_2SO_4, 98%) and sodium hydroxide (NaOH) were used for pH adjustment.

For High-Performance Liquid Chromatography (HPLC) analysis, HPLC-grade methanol (CH_3OH), acetonitrile, and 0.5% formic acid solution (CH_2O_2) were used, purchased from Fisher Scientific in Canada. All aqueous solutions were prepared using deionized water (conductivity <1 µS/cm). To ensure contaminant-free analysis, all glassware was rigorously cleaned by soaking in 10% HCl followed by thorough rinsing with deionized water before use.

4.2.2 Wastewater Matrix Preparation and Characterization

A defined synthetic wastewater was used as the feed for laboratory-scale granular sequencing batch reactors (GSBRs). The biologically treated effluent discharged from the GSBRs was collected and

used as the influent matrix for the subsequent electrooxidation (EO) experiments. Thus, the experimental matrix was classified as biologically treated synthetic wastewater, rather than real municipal or industrial wastewater. The composition of the synthetic feed and the measured characteristics of the GSBR effluent are summarized in **Table 4-1.**

Table 4-1: Composition of the synthetic GSBR feed and influent characteristics for the electrooxidation (EO) experiments

Component/Parameter	**Concentration (mg/L)**
Yeast extract	380
NH_4Cl	29
$K_2HPO_4 \cdot 3H_2O$	17
$MgSO_4$	2
EDTA	1
Mineral/ trace solution	0.10
TCOD	425 ± 16
sCOD	380 ± 15
TOC	160 ± 5
Total nitrogen (TN)	47 ± 4
Total Ammoniacal Nitrogen (TAN)	10 ± 0.6
Total phosphorus (TP)	8 ± 1.2
Soluble Phosphorus (SP)	5 ± 1.1
pH	6.8 (no unit)

Values for the GSBR effluent are reported as mean ± standard deviation. Each sample was analyzed in triplicate, and the average of the analytical replicates was treated as one independent observation. TCOD: total chemical oxygen demand; sCOD: soluble chemical oxygen demand;

TOC: total organic carbon; TN: total nitrogen; TAN: total ammoniacal nitrogen; TP: total phosphorus; SP: soluble phosphorus.

Chloride was present in the experimental matrix because NH_4Cl was used in the synthetic wastewater supplied to the GSBRs. The addition of 29 mg/L NH_4Cl provided a nominal chloride concentration of approximately 19.26 mg Cl^-/L, excluding any additional chloride introduced by the yeast extract, trace-element solution, preparation water, or other reagents. During electrooxidation, chloride may undergo anodic oxidation and generate reactive chlorine species, including Cl_2, HOCl, and OCl^-. These species may contribute to antibiotic removal through indirect oxidation. However, their further oxidation may result in the formation of chlorate and perchlorate, which represent important safety endpoints for the electrochemical treatment of chloride-containing wastewater. Chlorate and perchlorate formation is influenced by the anode material, chloride concentration, current density, wastewater composition, and electrolysis duration (L. Wang et al., 2022). In this study, chloride, free chlorine, chlorate, and perchlorate were not directly measured. Therefore, the contribution of active chlorine to antibiotic degradation and the formation of chlorate or perchlorate could not be confirmed. Chlorine-mediated oxidation is therefore presented as a potential hypothetical pathway in Figure 1 rather than an experimentally verified mechanism.

4.2.3 Experimental setup and Electrochemical Reactor

The experiments were conducted with the CONDIAPURE® test system (CONDIAS GmbH, Itzehoe, Germany) and a DIACHEM® electrode stack (CONDIAS). Four boron-doped diamond electrodes were used as anode/cathode; dimensions of the electrode (2 × 26 × 230) mm (thickness × width × length) per anode with a total active area of the 2 anodes (A) ≈ 400 cm^2. The inter-electrode gap between the electrodes were 3mm, and the electrodes were placed in a vertical

position parallel to each other. The reactor was a single-cell acrylic reactor with a cylindrical geometry. The height and diameter of the reactor were 23 cm and 19.51 cm, respectively. The selected pharmaceutical compounds were mixed thoroughly by placing the reactor in a magnetic stirrer (Fisher Scientific, model 11-100-49S) operating at 450 rpm. Power was supplied by a DC switching power supply (B&K Precision 1901-B) capable of a maximum output of 30 A/ 32V, with real-time current-voltage monitoring. **Figure 4-1** illustrates the electrochemical cell assembly, electrode arrangement, and hypothetically proposed reactive pathways, which includes the generation of surface-bound •OH at the non-active Nb/BDD anode surface and their subsequent role in the non-selective oxidative degradation of target micropollutants toward complete mineralization end-products (CO_2, H_2O, and inorganic ions).

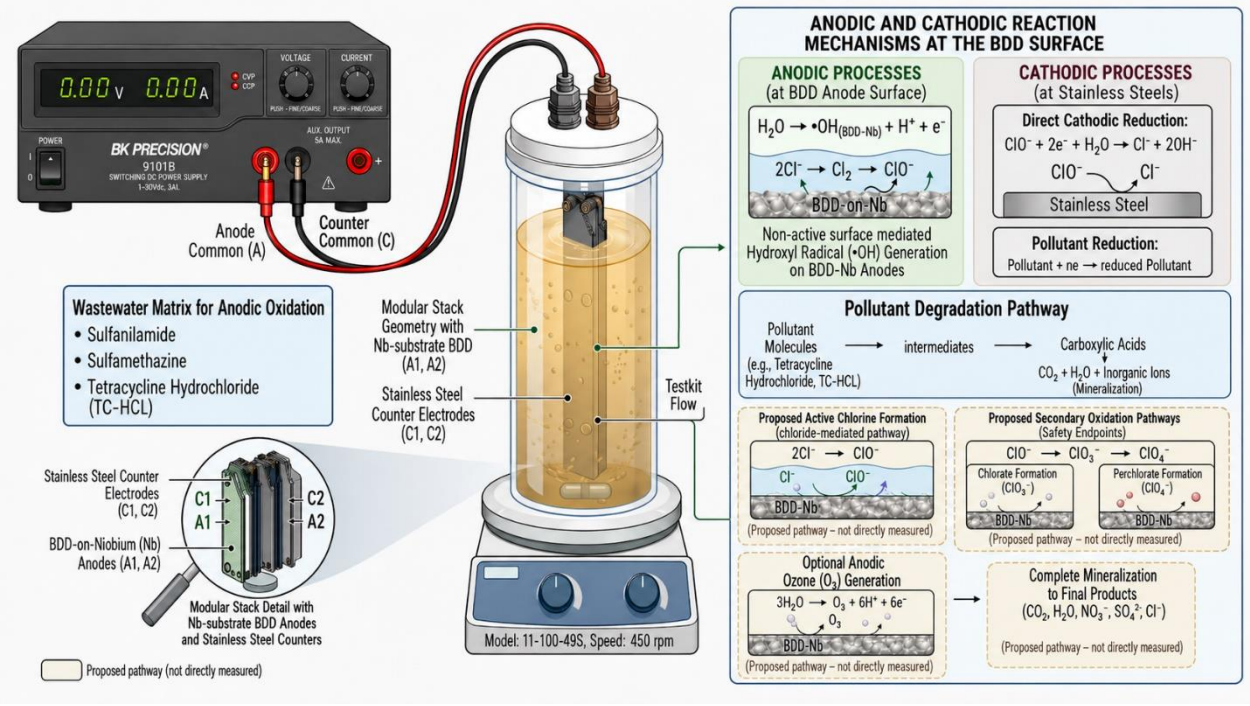

Figure 4-1 Schematic representation of the bench-scale Nb/BDD electrochemical oxidation system and the proposed anodic and cathodic reaction pathways for antibiotic degradation in synthetic wastewater. Pollutant removal is attributed primarily to direct and hydroxyl-radical-

mediated oxidation at the BDD surface, while chloride-mediated active chlorine formation, subsequent chlorate and perchlorate generation, and anodic ozone production are presented as proposed secondary pathways and potential electrochemical safety endpoints rather than confirmed reactions.

4.2.4 Sampling procedure and preparation

Before each EO experiment, the selected antibiotics were precisely weighed using a Denver Instruments PI-214 analytical balance and spiked into the collected GSBR effluent to get target initial concentrations of (4000, 8000, and 12000) µg/L. To ensure accurate dosing of the ternary mixture, a concentrated Combined Stock Solution (1000 mg/L) was prepared. SMZ (100 mg), SN (100 mg), and TC-HCl (100 mg) were weighed into a 100 mL volumetric flask. Approximately 50 mL of water was added, followed by the dropwise addition of 1 M NaOH to facilitate the dissolution of the hydrophobic SMZ. The solution was then diluted to volume with deionized water. Fresh stock solutions were prepared daily to prevent the hydrolytic degradation of TC-HCl. To achieve the target initial concentrations of 4000, 8000, and 12000 µg/L (for each component), aliquots of 12 mL, 24 mL, and 36 mL of the combined Stock Solution were added, respectively, to the 3.0 L electrolyte volume.

The reactor was run in different pH conditions (3.5, 7, and 9), and solution pH was adjusted before each experimental run using a calibrated pH meter (Oakton pH 6 Acorn Series) through incremental addition of 0.1 M NaOH or H_2SO_4. The prepared mixed pharmaceutical wastewater and the electrooxidation were performed under galvanostatic conditions in the batch reactor at three different current densities (15, 25, and 35) mA/cm^2. The solution was continuously stirred at 450 rpm using a magnetic stirrer to ensure homogeneity. Electro-oxidation was initiated by activating the power supply at the designed current densities; the initial pH was adjusted to the

investigated values of pH (3.5,7 and 9), the initial concentration was set to (4000, 8000, 12000) µg/l and the time was (15, 30, 45, 60) minutes. After each run, samples were collected from the center of the reactor at 15-minute intervals up to 60 minutes using a 100 mL glass pipette equipped with a rubber bulb for subsequent analysis.

To ensure the removal of suspended solids and precipitate, a multi-step purification protocol was established. The collected aliquots were first filtered through Fisherbrand™ cellulose-based fiber filter paper (particle retention 1-5 µm, diameter 12.5 cm) into 50 mL polypropylene conical tubes. The filtrate was then centrifuged at 12,000 rpm for 10 minutes using a Thermo-Scientific centrifuge to settle any remaining fine particulates. Following centrifugation, the supernatant was then filtered through a Sartorius RC (Regenerated Cellulose) 0.20 µm syringe filter. The final purified samples were transferred into Fisherbrand™ 9 mm screw-thread glass vials (2 mL volume) for HPLC analysis.

4.2.5 Analytical methods and concentration determination

The concentration of SMZ, SN, and TC-HCl was determined using a High-Performance Liquid Chromatography (HPLC) system that included a Waters 2695 Separation Module coupled with a 2998 Photodiode Array (PDA) Detector. The separation was achieved using a LiChrosorb® RP-18 column (5 µm particle size, 250 × 4.6 mm). The column temperature was maintained at 40ºC, and the sample temperature was kept at 5ºC to ensure that thermal degradation of the analytes was minimised.

Mobile phase solvents were filtered through Sterlitech PES (polyethersulfone) membrane filters (0.45 µm pore size, 47 mm diameter). Concentration analysis was done in the HPLC system using two mobile phases. Mobile phase A was comprised of methanol: 0.5% formic acid: acetonitrile (10:80:10 v/v/v), adjusted to pH 2.6. Mobile phase B was comprised of methanol: 0.5% formic

acid (80:20, v/v); the pH was adjusted to 3.30. The system was operated in the gradient elution mode with the use of both phases. The flow rate was set to 1.0 mL/min, and the injection volume was 10 μL. The detection was monitored at an absorbance wavelength of λ_{max}= 254 nm. The gradient program was set up as follows described in **Table 4-2**.

Table 4-2: HPLC gradient profile showing mobile-phase composition, time, flow rate, and analytical conditions

Time (min)	**Flow (mL/min)**	**Mobile phase A (%)**	**Mobile phase B (%)**	**Condition**
0	1.0	85	15	Initial Equilibrium
3.0	1.0	85	15	Isocratic Hold
3.5	1.0	15	85	Linear Gradient Ramp
5.5	1.0	15	85	Organic Hold (Elution)
6.0	1.0	100	0	Column Wash/Reset
10	1.0	100	0	End of Run

Before the analysis, the system was conditioned for 30 minutes at a low flow rate of 0.2 mL/min to stabilize the column pressure at approximately 1400 psi (≈ 96.5 bar). Analytical runs were performed at a flow rate of 1.0 mL/min for a duration of 10 minutes. After each run, 30% isopropanol was used to clean the injection needle to avoid any sample carryover, and a deionized water blank sample was injected between sample analyses. The separation was observed at a wavelength of 254 nm. Under these conditions, the target compounds were separated with retention times (t_R) of 2.2 min for Sulfanilamide (SN), 4.4 min for Tetracycline Hydrochloride (TC-HCl), and 4.9 min for Sulfamethazine (SMZ), as shown in **Figure 4-2**.

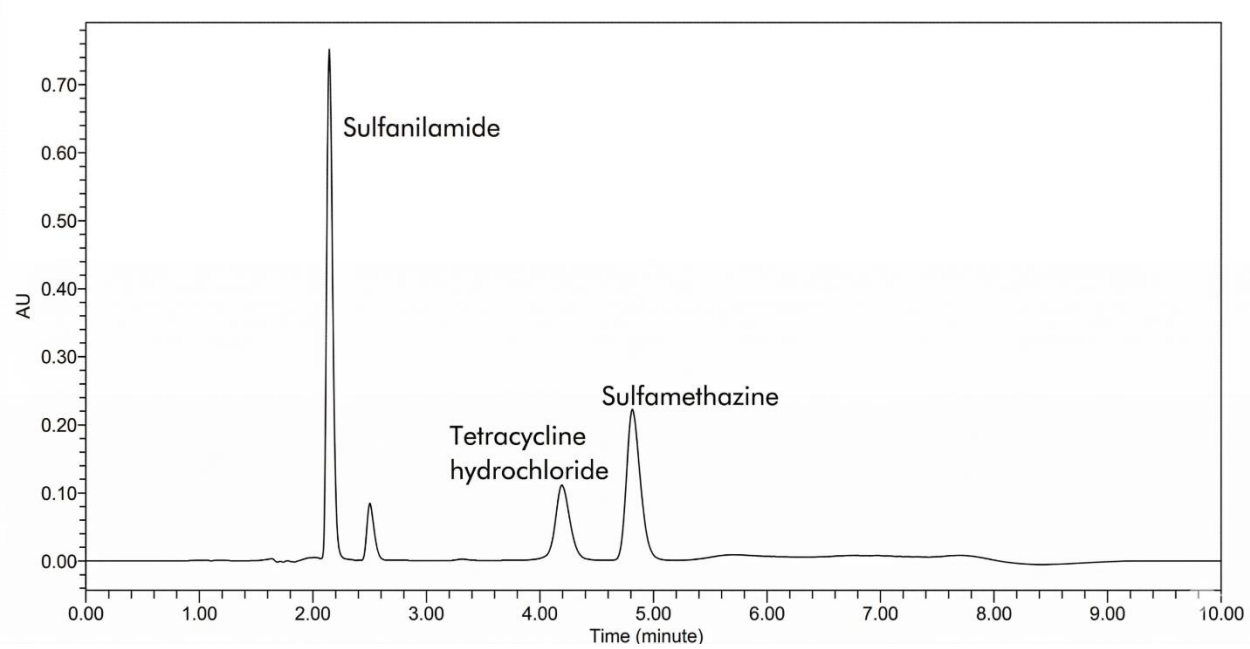

Figure 4-2. High-performance liquid chromatography (HPLC) chromatogram detailing the separation and simultaneous determination of the selected pharmaceutical mixture.

The separation was achieved using UV absorbance detection at a wavelength of 254 nm. Peak identifications and corresponding observed retention times (t_R) are as follows: Sulfanilamide (SN) at 2.2 min; Tetracycline Hydrochloride (TC-HCl) at 4.4 min; and Sulfamethazine (SMT) at 4.9 min. Peak intensity is recorded in Absorbance Units (AU) versus elution time in minutes.

4.2.6 Method Performance and QA/QC Procedures

External calibration curves were prepared from freshly prepared mixed standard solutions over the nominal range of 325 to 10,000 µg/L or 0.3125 to 10 mg/L for the selected mixed antibiotics. Each calibration level was injected in triplicate, and the mean peak area was used for least-squares regression. In accordance with ICH Q2 recommendations, linearity was evaluated from the regression equation, coefficient of determination, slope, intercept, and residual pattern across the calibration range (Ermer, 2025). The resulting calibration equations were ($y = 36.2155x + 62,266.8$) for SN (($R^2 = 0.9901$)), ($y = 13.4059x - 7,370.3$) for TC-HCl (($R^2 = 0.9963$)), and ($y =$

29.1986x + 6,689.9) for SMZ ((R^2= 0.9922)) as shown in appendix-B of the **supplementary Table S1 and Figure S1.** Retention times were stable across the calibration sequence, with mean values of 2.162 min for SN, 4.201 min for TC-HCl, and 4.860 min for SMZ. Estimated LOD and LOQ values were obtained from the calibration-curve approach as (3.3× (σ/S) and (10× (σ/S), respectively, as shown in **appendix-B of the supplementary Table S2,** where (σ) is the standard deviation of the response and (S) is the slope of the regression line, and these values are reported as regression-derived estimates.

However, matrix spike-recovery experiments were not performed in the original analytical measurement. Accordingly, the present HPLC datasets are interpreted as an externally calibrated quantification method validated for trend analysis of parent-compound removal within the studied matrix, while matrix-specific accuracy remains to be established by future spike-recovery experiments, which is one of the limitations of the present study.

4.2.7 Total Organic Carbon (TOC) measurement

TOC was measured using a Shimadzu TOC-L analyzer (Shimadzu Corporation, Kyoto, Japan) based on the high-temperature catalytic combustion (680ºC) method. Inorganic carbon was removed before analysis, and TOC concentrations were determined as non-purgeable organic carbon (NPOC). Instrument calibration was verified periodically using independent quality-control standards, and blank analyses were included to assess background carbon levels. The method reporting range of the instrument was within the manufacturer-specified operating limits (approximately 4 µg/L to 30,000 mg/L TOC). Samples were analyzed in triplicate, and TOC concentrations are reported as mean ± standard deviation (SD). TOC served as an operational measure of overall organic carbon removal, and the TOC mineralization was calculated as:

$$\text{TOC Mineralization efficiency (\%)} = \frac{\text{TOC}_0 - \text{TOC}_t}{\text{TOC}_0} \times 100$$

where TOC_0 and TOC_t represent the initial and final TOC concentrations, respectively.

4.2.8 Volumetric Specific Charge and Equal-Charge Comparison

To distinguish the effect of current density from the electrical dose delivered during electrolysis, pollutant-removal data were additionally expressed as a function of the volumetric specific charge,

$q_v = Q/V = It/V$

Where I is the applied current (A), t is the electrolysis time, and V is the working solution volume. Specific charge was reported in A h L^{-1} and C L^{-1}. Electrical dose delivered after 60 minutes is shown in appendix B of the supplementary Table S3. Equal-charge comparisons were performed at 1.5 and 2.0 A h L^{-1}, which were within the overlapping charge range of the three current-density conditions. At an equal specific charge of 2.0 A h L^{-1}, averaged removals are shown in appendix B of the supplementary Table S4. When a selected charge did not coincide with a sampling time, the removal value was calculated by piecewise linear interpolation between the two adjacent measured time points for each replicate. Charge-normalized removal was further evaluated using a quadratic analysis-of-covariance model containing specific charge, current density, pH, initial concentration, and current-density × charge interactions, with cluster-robust standard errors calculated for each experimental time period.

4.2.9 Statistical analysis

Each experiment was conducted in triplicate (n=3), where the response variable was the removal efficiency (%) of sulfanilamide, tetracycline-HCl, and sulfamethazine. Statistical differences among current densities in **Figure 4-3** were evaluated using one-way ANOVA within each compound × pH × time condition. Further post-hoc pairwise comparisons were conducted with the Tukey honestly significant difference (HSD) test where the contrasts were compared with respect to 15 mA/cm^2 as the reference level.

The main factorial data were conducted with a constant current density of 35 mA/cm^2, across three initial concentrations (4000, 8000, 12000 µg/ L), four electrolysis times (15, 30, 45, 60 min), and three pH levels (3.5, 7.0, 9.0). Python was used to perform statistical analyses using NumPy, Pandas, SciPy, and the Statsmodels library. Factorial ANOVA models were used in the 35 mA/cm^2 factorial dataset to determine the magnitude of the main and interaction effects of the operating variables. In particular, a three-way ANOVA (pH × time × concentration) was applied to evaluate the combined effects within the full design space, where time was found to be the most dominant factor **(Figure 4-5).** In addition, two-way ANOVA models were used for the targeted specific comparisons (i) time × concentration effect within each pH level and (ii) pH × time effect within each concentration level; pH levels were also compared within each compound × concentration × time stratum **(Figure 4-6).**

The model assumptions were checked by Shapiro-Wilk tests on the residuals (normality) and Levene's tests on the homogeneity of variances. When there is a significant effect determined by ANOVA, post hoc multiple comparisons were done with Tukey HSD at $\alpha = 0.05$ to control the family-wise error rate; also, time-stratified pH contrasts were made where necessary. The results are presented in the form of F -statistics (with degrees of freedom) and p -values. The level of statistical significance was denoted as ns ($p \geq 0.05$), * ($p < 0.05$), ** ($p < 0.01$), and *** ($p < 0.001$), where significant partial eta -squared (η^2) was used to describe effect sizes.

4.3 Results and Discussion

Nb/BDD is commonly characterized as a non-active anode where the oxidation takes place through the dissociation of surface-associated hydroxyl radical chemistry (·OH), which provides extensive reactivity to pharmaceuticals and antibiotics (Brinzila et al., 2014; Grebel et al., 2010; Panizza &

Cerisola, 2009). Recent peer-reviewed reviews and studies that focus on antibiotics have highlighted that the BDD electrooxidation kinetics and products are controlled together by time, current density, solution chemistry (including pH and inorganic scavengers), and pollutant loading (Jiang et al., 2021; Panizza & Cerisola, 2009). In the current study, the removal efficiencies of sulfanilamide, tetracycline -HCl and sulfamethazine were tested using Nb/BDD electrooxidation in pH 3.5, pH 7.0 and pH 9.0, initial concentration of 4000, 8000, 12000 µg/L and electrolysis time ranging 15 to 60 minutes with a set current density of (15, 25 and 35) mA/cm^2, emphasis on the dominant operating current density of 35 mA/cm^2.

4.3.1 Effect of Current Density

The applied current density is a major operational parameter in electrooxidation that influences both treatment efficiency and overall energy demand. The selected current-density range was chosen to ensure that degradation and mineralization of the target antibiotics such as Sulfamethazine (SMZ), Sulfanilamide (SN), and Tetracycline-HCl (TC-HCl) may occur through hydroxyl radicals generated on or adsorbed at the Nb/BDD electrode surface. In this study, current densities were also selected by economic considerations related to specific energy consumption. As a result, current densities of 15, 25, and 35 mA/cm^2 were employed, which are comparatively lower than those commonly reported in previous studies (Brinzila et al., 2014; T. S. Chen et al., 2014; Hu et al., 2025c).

For our research, the efficiency of sulfanilamide, tetracycline-HCl, and sulfamethazine in a wastewater solution was initially statistically proven to be significant at the applied current density using Nb/BDD electrodes in electrochemical oxidation **(Figure 4-3).** In all the experimented pH values (3.5, 7.0, and 9.0) and reaction times (15 to 60 min), removal efficiency increased with increasing applied current density of 15 < 25 < 35 mA/cm^2, which was also strongly supported by

the statistical analysis. Tukey HSD tests on each compound × pH × time combination demonstrated that 35 mA/cm^2 gave significantly higher removal compared to 15 mA/cm^2 in over 80% of all comparisons ($p < 0.05$ to $p < 0.001$), but the effect of 25 mA/cm^2 was moderate and only significant at longer reaction times at lower pH **(appendix-B, Supplementary Table S5).** Such findings are aline with BDD behavior, in which increased current densities increase hydroxyl radical (•OH) production and boost direct electron-transfer reactions, thus aiding faster cleavage of aromatic rings and heterocyclic groups found in sulfonamides and tetracyclines (Brinzila et al., 2012; H. Li et al., 2019).

For TC-HCl, initially hydroxyl-radical could attack the phenolic ketone groups; afterwards, oxidation of the chromophore ring system, which contains the tricarbonylamide and dimethylamine substituents. Similar studies have reported that the degradation of phenolic ketone is less affected by the current density value, whereas the cleavage of substituents-bearing rings is strongly influenced by the current density (Vasilie et al., 2018).

In a BDD electrode, the oxidation process is directed by the following reactions from reaction **Eq. (4-2) to Eq. (4-5)** (Brillas et al., 2010).

$$2H_2O \rightarrow O_2 + 4H^+ + 4e^- \quad \textbf{(4-2)}$$

$$BDD + H_2O \rightarrow BDD\ (\bullet OH) + 2H^+ + 2e^- \quad \textbf{(4-3)}$$

$$2BDD\ (\bullet OH) \rightarrow 2BDD + H_2O_2 \quad \textbf{(4-4)}$$

$$H_2O_2 + BDD\ (\bullet OH) \rightarrow BDD\ (HO\bullet_2) + H_2O \quad \textbf{(4-5)}$$

However, in our research, some conditions did not show significant differences (reported as “ns”) at 15 minutes, indicating the initial lag of radical generation prior to the accumulation of enough oxidant on the electrode surface. A similar effect is observed with recalcitrant antibiotics in other BDD systems (Wachter et al., 2019). After 45 to 60 min, almost all conditions showed significant

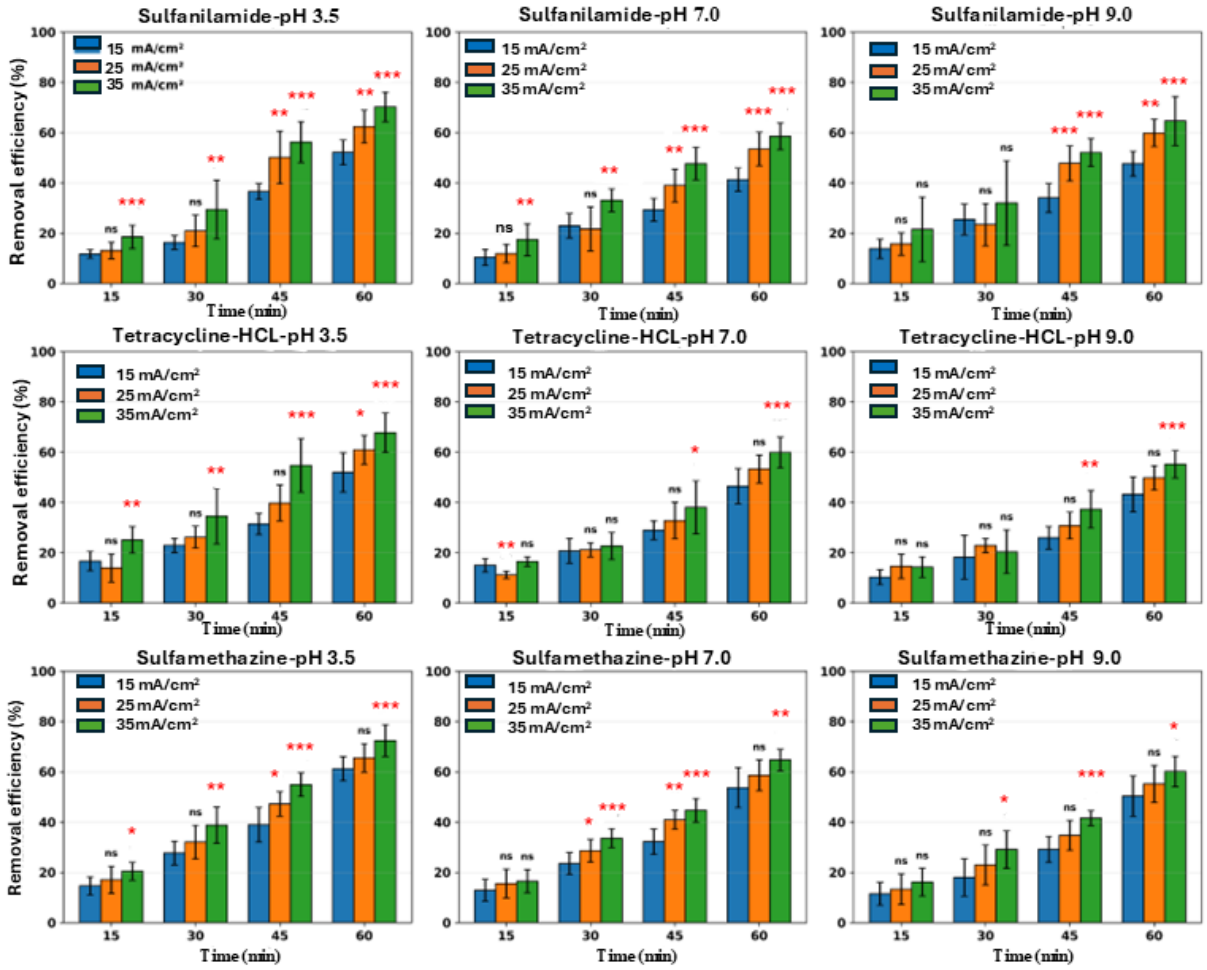

Figure 4-3. Effects of current density on the electrochemical oxidation of sulfanilamide, tetracycline-HCl, and sulfamethazine using a boron-doped diamond (Nb/BDD) anode across pH 3.5, 7.0, and 9.0. Bars show mean removal efficiency (%) averaged over all three initial concentrations (4000, 8000, and 12,000 µg/ L) at 15, 30, 45, and 60 min; error bars are standard deviations of pooled replicates. Statistical differences among current densities were evaluated using one-way ANOVA followed by Tukey HSD at each compound × pH × time condition. Tukey annotations are shown relative to 15 mA/cm² (reference): *$p < 0.05$; **$p < 0.01$; ***$p < 0.001$; ns = $p \geq 0.05$ (Tukey-adjusted)

statistical difference between 15 and 35 mA/cm^2 current densities, confirming that progressive oxidation kinetics are dominated by cumulative charge loading, and not instantaneous current only. These statistical results support the mechanistic explanation of the fact that an increase in the current density leads to an increase of direct and indirect oxidation pathways, which may involve the generation of secondary oxidants like sulfate radicals and peroxodisulfate in the presence of sulfates (Divyapriya & Nidheesh, 2021).

However, sulfate availability alone is insufficient to establish their formation or contribution (L. Chen et al., 2018). Accordingly, sulfate-radical and peroxodisulfate pathways are treated only as literature-supported hypotheses. Therefore, the mechanistic scheme could be interpreted as a representation of plausible electrochemical pathways rather than experimentally resolved reaction mechanisms.

Altogether, the statistical and mechanistic evidence shows that 35 mA/cm^2 provides the highest antibiotic removal within a fixed 60-minute treatment period; and 15 mA/cm^2 provided the highest removal per unit of applied charge and was therefore the most charge-efficient current-density condition. The influence of current density was also evaluated using the volumetric specific charge to avoid confounding current density with the total electrical dose delivered during a fixed electrolysis period, as shown in **Figure 4-4.**

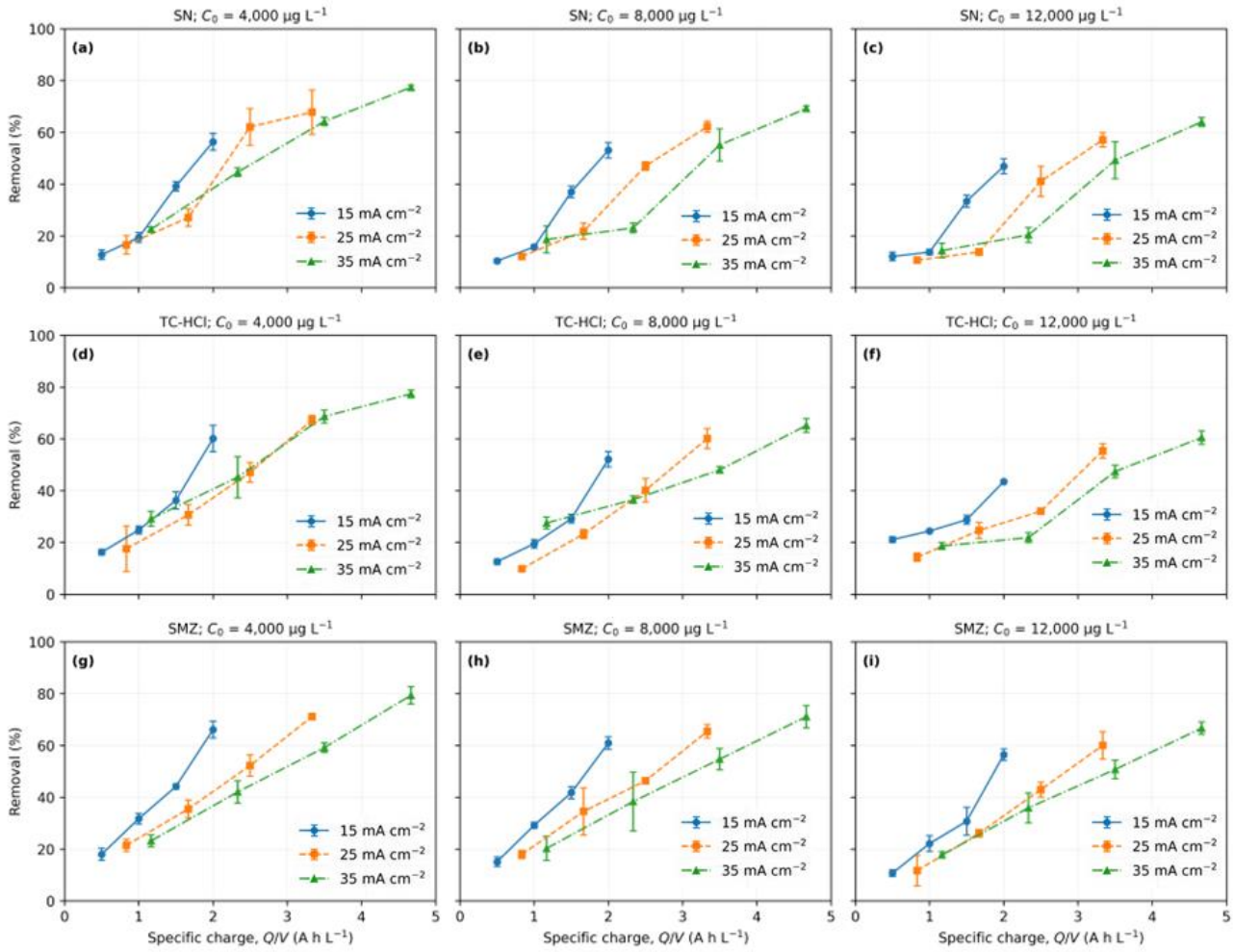

Figure 4-4: Removal of sulfanilamide (SN), tetracycline hydrochloride (TC-HCl), and sulfamethazine (SMZ) as a function of volumetric specific charge at pH 3.5 and initial concentrations of 4000, 8000, and 12000 µg/L. Symbols and error bars represent the mean ± standard deviation of triplicate measurements. Current density series correspond to 15, 25, and 35 mA/cm^2. Equivalent figures for pH 7 and 9 are supplied as (Appendix-B, supplementary Figures S2 and S3).

When removal was expressed as a function of treatment time, 35 mA/cm^2 produced the fastest removal in the target-antibiotic concentrations. However, the charge-normalized profiles showed

a different ranking. Within the common charge interval, 15 mA/cm^2 consistently produced greater removal per unit charge than 25 and 35 mA/cm^{2,} as shown in **Figure 4-4.**

At Q/V = 2.0 A h L^{-1}, the condition-averaged removals at 15, 25, and 35 mA/cm^2 were (46.97, 31.42, and 27.95) % for SN; (47.20, 27.83, and 23.80) % for TC-HCl; and (55.03, 33.06, and 29.17) % for SMZ, respectively. The charge-adjusted models explained 88.4, 89.1, and 93.5% of the variability in SN, TC-HCl, and SMZ removal, respectively. At Q/V = 2.0 A h L^{-1}, the model-adjusted removal at 25 and 35 mA /cm^2 were significantly lower than that at 15 mA /cm^2 for all three compounds ($p < 0.001$). These results demonstrate that increasing current density accelerated degradation on a treatment-time basis but reduced charge-utilization efficiency. Similar behaviour has been reported for BDD oxidation systems, in which higher current densities increase the apparent oxidation rate while decreasing current efficiency because of mass-transfer constraints and competing anodic reactions (Costa et al., 2010; Valladares et al., 2023). Previous literature mentioned that increasing the current density may reduce the total efficiency of current through parasitic reactions, thus making optimal removal and optimal energetic efficiency two distinct optimization objectives (Brinzila et al., 2014; Panizza & Cerisola, 2009). The relevance of this trade-off in antibiotic-based BDD studies supports the practical importance of this process, such as the removal of sulfamethazine is sensitive to the presence of •OH, which was proven by EPR analysis, and high current density and sufficiently long electrolysis times are highly effective (Du et al., 2021), and tetracycline removal is highly current-intensity and pH dependent (Brinzila et al., 2014).

However, during the treatment process of pharmaceuticals in wastewater, organic compounds may interfere with the electrooxidation process. These organic compounds contained in the wastewater solution are oxidized at the anode (M) surface by direct charge transfer, and the majority of

M(•OH) is physisorbed on the solution at high current densities through the reaction equation **Eq. (4-6)** of water oxidation (El-Ghenymy, Garrido, et al., 2013a).

$$M + H_2O \rightarrow M(\cdot OH) + H^+ + e^- \quad \textbf{(4-6)}$$

When the oxidation of organic compounds is less favorable, parasitic reactions may occur simultaneously and consume the generated oxidizing species. These competing pathways include (i) the conversion of adsorbed hydroxyl radicals, M(•OH), to H_2O_2 **(Eq.4-7),** (ii) the electrooxidation of M(•OH) accompanied by oxygen evolution reaction (OER) **(Eq. 4-8),** and (iii) the dimerization of hydroxyl radicals in solution to form H_2O_2 **(Eq. 4-9)** (Comninellis, 1994a; Moreira et al., 2017).

$$MO_x(\cdot OH)_{ads} \rightarrow MO_x + H_2O_2 \quad \textbf{(4-7)}$$

$$MO_x(\cdot OH)_{ads} \rightarrow MO_x + \tfrac{1}{2} O_2 + H^+ + e^- \quad \textbf{(4-8)}$$

$$2\bullet OH \rightarrow H_2O_2 \quad \textbf{(4-9)}$$

OER occurs simultaneously with the pharmaceuticals in the electrooxidation process and reduces the current efficiency because part of the applied current is consumed by the side reaction. Also, it plays an important role in preventing poisoning of the electrode surface, which helps control the polymerization of organic compounds on the electrode during pollutant oxidation (Comninellis, 1994a; Moreira et al., 2017). Surface passivation can be limited by the generation of hydroxyl radicals in the oxidation of organic compounds on electrodes, which rapidly react with intermediate organic species and thereby reduce the possibility of polymer formation (Santos et al., 2021a). In addition, in the case of OER, the reduction in passivation is mainly associated with the mechanical effect of gas evolution, which helps remove oxidized organic molecules from the electrode surface into the bulk solution and thus prevents their accumulation and deposition on the electrode surface (Panizza & Cerisola, 2009; Rice et al., 2018; Santos et al., 2021b). For our

present research, we found the same, as there was no deposition or accumulation on the electrode surface and the electrode performed without any fouling.

In this study, a steady decline in cell voltage was observed during the treatment period at all applied current densities. For instance, at 35 mA/cm^2, the voltage decreased from 12.8 V to 8.1 V, and at 15 mA/cm^{2,} the voltage decreased from 8.5 V to 6 V between 15 and 60 minutes. The decrease in cell voltage during electrolysis was likely related to the increase in solution temperature. Because the experiments were operated at constant current, a rise in temperature would increase ion mobility and improve the electrical conductivity of the solution. This reduces the internal resistance of the electrolyte. As a result, a lower voltage is required to maintain the same current. Changes in solution composition and electrode polarization during treatment may also have contributed. Therefore, the decrease in voltage observed during the experiment may result from reduced overall cell resistance, to which the rise in temperature may have contributed significantly.

4.3.2 Effect of Electrolysis Time

According to two-way ANOVA (Per compound × concentration, EC 35 mA/cm²) and based on the large-size effects (partial $\eta^2 = 0.88$ to 0.98), the duration of the electrolysis time was found to be the significant factor for the removal of all three pharmaceuticals **(Figure 4-5)** and achieved highly significant removal ($p \ll 0.001$) **(appendix-B, Tables S7-S19).** This dominance was supported in the three-way ANOVA (Time × pH × Concentration) in which time remains the major determinant for all of the selected three compounds (partial $\eta^2 \approx 0.93$-0.97; **appendix-B, Tables S21-S23).** These results are mechanistically consistent with the paradigm of BDD anodic oxidation as a time/ charge-controlled process that is run under constant current density, in which the cumulative oxidant contact increases with longer electrolysis times (Comninellis, 1994b; Jiang et al., 2021; Panizza & Cerisola, 2009).

In the case of sulfanilamide, the time effect was also very significant at all pH levels ($p < 0.001$), and the effect was the strongest at pH 3.5 ($F(3,24) = 416.23$, $p < 0.001$) (**appendix-B, Tables S6).** These were supported by Tukey post-hoc analyses that showed that removal at 60 min was more than that of 15 min at pH 3.5 by about 40-52% and at pH 7.0 by about 41% ($p < 0.001$ at 60 min vs 15 minutes). The difference between the 15 and the 30 min time was statistically significant at pH 3.5 ($p \approx 0.035$) and pH 7.0 ($p < 0.001$), but the corresponding difference at pH 9.0 was nonsignificant ($p = 0.27$), reflecting a smaller and more variable early time gain (~10%). At 45 min and beyond, the removal efficiencies in all the pH conditions were much higher than those of the 15-minute interval ($p < 0.001$).

Tetracycline-HCl had an overall strong correlation with elapsed time (e.g., at pH 3.5: F_ (3,24) =351.68, $p < 0.001$). However, it exhibited a different early time response because removal after 60 min was much higher than after 15 min, and absolute removal was about 40 to 43% ($p < 0.001$). Conversely, the 15 to 30min interval was not found to be significant at pH 3.5 and 7.0 ($p \approx 0.14$ to 0.23), but the 15 to 45 min interval was significant ($p < 0.001$). This profile indicates a lag phase, then accelerated removal following the first 30 min, which is the same as multistep oxidation mechanisms that have been reported repeatedly in structurally complex antibiotics subjected to intense anodic oxidation (Brinzila et al., 2014; S. W. da Silva et al., 2019).

In the case of sulfamethazine, time was found to be highly significant at pH 7.0 where ($F(3,24) = 605.39$, $^{**}p < 0.001$). At this pH, the removal efficiency increased from 20 to 23% at 15 min to 69 to 72% at 60 min, with a concentration difference, yielding a gain of about 48% (15 min vs 60 min, $p < 0.001$). The 15 to 30 min increment was also statistically significant at most pH levels with sulfamethazine (e.g., +17 % at pH 7.0, $p < 0.001$). This high, monotonic time response

corresponds to the results of BDD systems, where rapid oxidant production facilitates an increasingly large removal with increasing treatment time (Du et al., 2021).

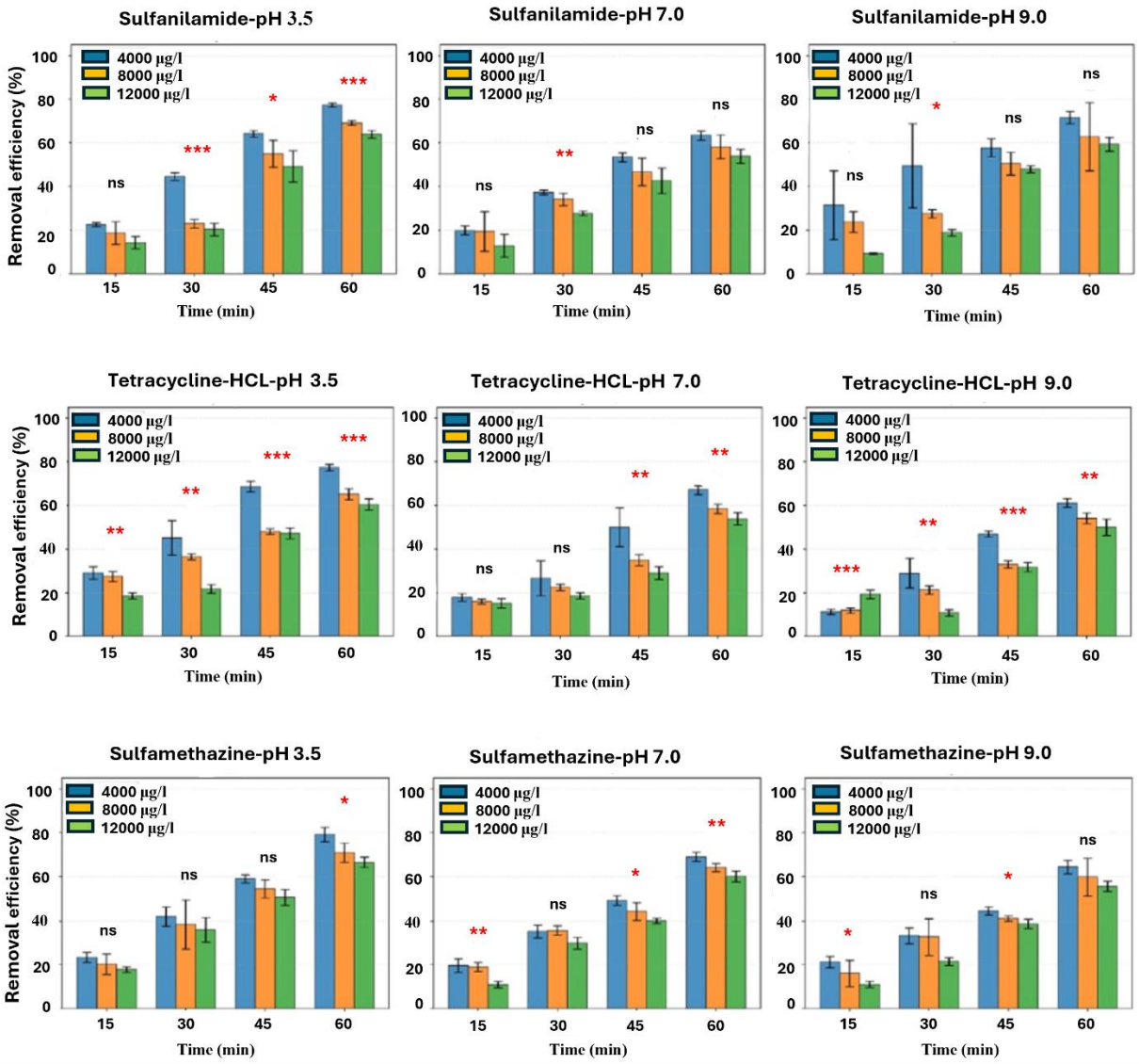

Figure 4-5. Effects of time and different concentrations on removal efficiency at 35 mA/cm^2 current densities (15- 60 minutes).

Note:

- ns = non-significant ($p \geq 0.05$) - No statistical difference between concentrations
- * = Significant ($p < 0.05$) - Concentrations differ significantly
- ** = Highly significant ($p < 0.01$) – Strong statistical differences

- *** = Very highly significant ($p < 0.001$) - Very strong statistical differences

4.3.3 Effect of Initial Concentration

The effect of concentration was statistically significant in all three compounds and consistent in direction, where greater concentrations decreased removal efficiencies in the fixed 15 to 60 minutes treatment window. This type of trend is expected under the conditions of constant current density since the ratio of the oxidant to the pollutant decreases as the initial load increases, which enhances the competition between reactive oxidants and slows down the apparent removal (Panizza & Cerisola, 2009; X. Wang et al., 2025). This interpretation is consistent with previous BDD electrooxidation studies reporting that degradation kinetics are strongly influenced by substrate concentration. Because under galvanostatic conditions, oxidant generation remains limited, and increasing pollutant loading similarly decreases the proportion of molecules that can be effectively oxidized within a given treatment period (Hai et al., 2020a; H. Li et al., 2019).

In the case of sulfanilamide, initial concentration and time both were important main effects at any pH (p<0.001). The concentration effect was high at pH 3.5 ($F_{(2,24)} = 59.81$, $p < 0.001$), and resulted in decreased removal with increasing concentration. At any given time, the mean removal at 12,000 µg/L was ~ (10 to 19 %) lower than the mean removal at 4,000 µg/L, by pH. The post-hoc test of overall means by Tukey did not indicate a statistically significant difference in the pairwise comparisons at pH 7.0 or 9.0, probably because of variability, but the pattern remained the same, with 4,000 ug/L giving the highest removal, 12,000 ug/L the lowest removal, and 8,000 ug/L intermediate **(Figure 4-5).** The observed behavior agrees with BDD-based studies on sulfonamide oxidation, which consistently reported lower removal at higher initial concentrations. Even when overall degradation remains effective, increasing the pollutant load distributes the amount of available •OH radicals across a larger number of parent molecules and intermediates.

As a result, the fraction of species that can be oxidized at any given moment is reduced (Fabiańska et al., 2014; H. Li et al., 2019).

In the case of Tetracycline-HCl, the removal efficiency showed a strong dependence on initial concentration across all pH levels ($p < 0.001$), with the largest effect observed at pH 3.5 ($F_{2, 24} = 103.67$, $p < 0.001$). At this pH, mean removals were approximately 54% and 36% for 4000 μg/L and 12000 μg/L, respectively, and Tukey's test confirmed the significance of this difference ($p = 0.0498$). Although pairwise comparisons were not significant at pH 7.0 and 9.0, the same decreasing trend with increasing concentration (4000 > 8000 > 12000 μg/L) was consistently observed. These results align with the expected behavior of a mass-transport-controlled electrooxidation process. The removal percentage become less in higher initial TC concentrations because the fixed current and treatment time limit the amount of available •OH for oxidation. At higher concentrations, the steeper concentration gradient increases the absolute amount of TC degradation, but the fractional removal decreases at that time. This is consistent with previous studies where they have shown that phenolic ketone oxidation is relatively unaffected by operating conditions, whereas cleavage of substituent-carrying rings is strongly affected (Vasilie et al., 2018). In the electrooxidation process, •OH production usually remains constant under galvanostatic control, and for this reason, higher TC concentrations could lead to greater accumulation of intermediates at the electrode surface. These intermediates compete for hydroxyl radicals, reducing apparent degradation efficiency at higher pollutant loads, as reported in previous research (T. S. Chen et al., 2014; Vasilie et al., 2018). However, for our study, mineralization was not significantly affected at higher concentrations, and there was no persistent lag, which is a sign of a clean electrode surface, confirming that electrode fouling did not occur at any of the tested concentrations. This is supported by tetracycline-specific BDD studies reporting that tetracycline

removal is strongly concentration dependent. Higher initial loads reduce the apparent degradation efficiency under fixed operating time and current density, even though the BDD anode remains highly effective at oxidizing TC-HCl through hydroxyl-radical facilitated pathways (Brinzila et al., 2014; T. S. Chen et al., 2014).

In the case of sulfamethazine, initial concentration played a significant role at all pH values ($p \leq 0.01$). The strong concentration effect was repeated at pH 7.0 (F_(2, 24) = 33.76, $^{**}p < 0.001$), with the highest mean removal being 4,000 μg/L, and the lowest being 12,000 μg/L. Similar to sulfanilamide, Tukey post-hoc tests failed to find statistically significant pairwise differences at pH 7.0 when a noticeable monotonic trend is present (4000 > 8000 > 12000 μg/L). This observation aligns with previous sulfonamide electrooxidation literature, where initial concentration has a strong net effect on removal, but pairwise removal is often conditional on the operating window. In BDD systems, degradation typically occurs faster than on "active" anodes, although run-to-run variability and formation of intermediates can complicate pairwise contrast (H. Li et al., 2019; X. Wang et al., 2025). In the BDD electrode, sulfonamides are degraded more rapidly compared to other less oxidizing anodes, and the degradation remains concentration sensitive because the oxidizing capacity of the BDD electrode is fixed under constant current operation (Hu et al., 2025c; H. Li et al., 2019).

4.3.4 Effect of pH

Though removal was primarily time-dependent, pH also has significant effects across all concentration levels from 4000 to 12000 μg/L, especially in the case of TC-HCl and sulfamethazine ($p < 0.01$). Time-stratified Tukey tests showed that the differences in pH were obtained primarily at 45 to 60 minutes, with the acidic conditions promoting removal **Figure 4-6;**

appendix-B, Tables S7-S19). There are significant pairwise differences with the following *p*-values: *$p < 0.05$; **$p < 0.01$; and ***$p < 0.001$.

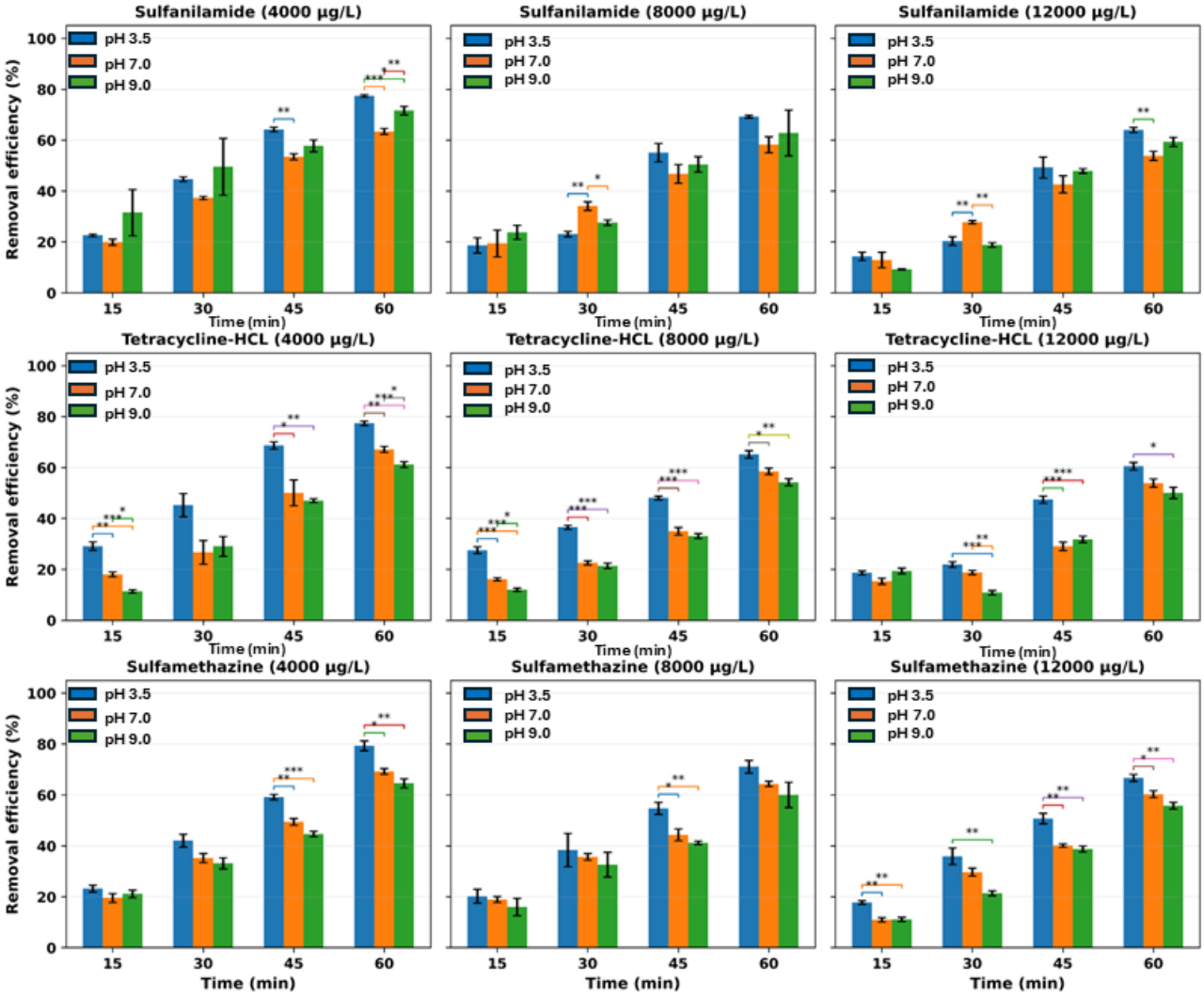

Figure 4-6. Effect of pH on the electrooxidation (EO) removal efficiency of sulfanilamide, Tetracycline-HCl, and sulfamethazine at 35 mA/cm^2 across initial concentrations of 4000, 8000, and 12000 µg/ L. Bars represent mean removal efficiency (%) where (n=3) and error bars indicate standard deviation (SD).

For sulfanilamide, the pH effects became most evident with longer time, and a significant pH-time interaction was observed at 12000 µg/L (p = 0.0048; **appendix-B, Table S9).** Removal at pH 3.5 at 60 min was significant compared to pH 7 (Tukey p_adj = 0.0092; **appendix-B, Table S12**).

However, the strong pH dependence of TC-HCl is in line with the pH-sensitive speciation of tetracycline and with the oxidation process of BDD electrooxidation. Tetracycline has various ionizable functional groups with its reported pKa values around 3.3, 7.7 and 9.7, which means that pH changes can cause the protonation of key reactive sites and, consequently, their susceptibility to oxidation (Dong et al., 2018). Specifically, the phenolic diketone moiety is less protonated at pHs above 7.7, and this can change its reactivity with respect to attack by hydroxyl radicals.

The overall pH dependence of tetracycline-HCl had the largest effect sizes (partial η^2 up to ~0.94 at 8000 µg/L) and the pH × time interaction was highly significant at 12000 µg/L ($p \ll 0.001$; **appendix-B**, Tables **S14-S15).** In this case, at 45 min, pH 3.5 was significantly more effective than pH 7 and 9, whereas at 60 min, pH 3.5 was significantly higher again compared to pH 9. This indicates that slightly acidic conditions were conducive to the rapid initial transformation of TCL-HCL under experimental conditions. This could reflect a more favourable ratio between tetracycline speciation and effective use of oxidants at acidic pH, and at neutral to alkaline pH the reaction was slower or time dependent. Since tetracycline has several reactive sites, such as phenolic, amine, and unsaturated sites, this observation is understandable and justifies the opinion that the kinetics of degradation are regulated by both molecular speciation and accessibility of oxidants. In other research, they observed that at pH 2, yield the highest removal of chemical oxygen demand (COD) that indicate more effective tetracycline breakdown, although total organic carbon (TOC) removal and mineralization are favored near the natural pH (~5.6) of the solution (Brinzila et al., 2014). For this reason, pH optimization is important for TC-HCl, particularly at

higher starting concentrations, where even a small change in reaction environment can result in significant changes in removal performance over time.

Sulfamethazine also exhibited significant pH effects, with a significant pH × time interaction, at 4000 µg/L (p = 0.0189; **appendix-B, Table S17);** at 60 min, pH 3.5 was again significantly more effective than pH 7 and pH 9. The trend in the direction of the pH response was the same for all the selected compounds, and at acidic pH, removal is the highest. This tendency follows the hydroxyl radical oxidation mechanism of complex aqueous matrices, with carbonate and bicarbonate competing to take over the •OH, shifting radical budgets, and forming carbonate radical chemistry, which can be more selective than the •OH (Cai et al., 2026; Grebel et al., 2010; Yan et al., 2019). The fact that pH effects were most evident at 45-60 min indicates that initial stages are controlled by the large time/oxidant flux at 35 mA/cm², but subsequent stage become more oxidant scavenging sensitive and the evolving reactivity of remaining parent compound and intermediates are consistent and align with BDD oxidation models and antibiotic electrooxidation literature (Panizza & Cerisola, 2009; X. Wang et al., 2025).

4.4 Compound-specific interaction effects

The present study shows that the three antibiotics did not respond to Nb/BDD electrooxidation as a uniform chemical class, and their observed behavior reflected clear compound-specific interaction patterns among time, concentration, current densities, and pH. This outcome is consistent with BDD-based electrooxidation literature in which degradation kinetics occur not only by the applied current and oxidant flux, but also by molecular structure, ionization state, and the accessibility of oxidizable functional groups (Brinzila et al., 2014; Castillo-Cabrera et al., 2023; Fabiańska et al., 2014).

Tetracycline-HCl showed more condition-dependent kinetics and interaction behavior relative to sulfanilamide and sulfamethazine under identical electrochemical conditions, especially in the concentration × time interaction at all pH values. This is because tetracycline has a polyfunctional, polycyclic scaffold with multiple reactive sites, including phenolic, enolic, amide, and dimethylamino moieties, which may create various competing oxidation pathways and make its apparent rate highly dependent on radical availability (Brinzila et al., 2014; Ivantsova et al., 2025). BDD oxidation of tetracycline usually occurs through •OH attack and related reactive oxygen species (ROS), with degradation behavior strongly influenced by solution pH and applied current (Brinzila et al., 2012, 2014). The significant effects of concentration × time interactions indicate that increasing TC-HCL concentration not only reduces the removal percentage; it may slow down the apparent degradation rate. The behavior is expected when the amount of generated oxidant stays the same while more reactive sites become available. In this situation, the generated •OH may quickly be utilized by the target compound and by competing side reactions, which reduces the effective oxidizing power available for each molecule. Similar trends have been observed during electrochemical oxidation of other structurally related antimicrobial compounds treated with a BDD anode and some other comparable advanced oxidation processes (Castillo-Cabrera et al., 2023; Wachter et al., 2019).

In the case of sulfamethazine, this compound responded in a more regular and near-additive manner, with time and concentration affecting removal but without significant concentration × time interactions. This suggests that once the oxidation occurred near the anode surface, sulfamethazine removal was directed mainly by overall exposure time and pollutant loading, rather than by strong nonlinear competition among pathways. In BDD systems, sulfamethazine degradation typically occurred through •OH radical attack, followed by ring hydroxylation,

cleavage, and stepwise mineralization (Hu et al., 2025c). These transformations are efficient but usually less sensitive to pH-driven speciation effects compared to tetracycline because the ionization distribution of sulfamethazine is simpler and its reactive centers are less heterogeneous (Brinzila et al., 2014; Hu et al., 2025b). The strong time effects observed for sulfamethazine are consistent with previous findings showing that BDD electrooxidation depends mainly on treatment duration, as continuous anodic operation progressively regenerates oxidants at the electrode surface (Castillo-Cabrera et al., 2023; Hu et al., 2025b). This effect mainly happens under moderate current densities, where radical formation remains the major pathway over oxygen evolution or electrode passivation (Castillo-Cabrera et al., 2023; Hu et al., 2025b).

Compared with tetracycline and sulfamethazine, however, sulfanilamide has a simpler aromatic structure and fewer competing electron-rich sites, which reduces the chances of condition-dependent pathway switching. For the present study, sulfanilamide behaved as the least interactive compound, with its strong main effects and limited higher-order dependence, which indicates that its degradation could follow a more straightforward kinetic pattern. This is consistent with BDD electrooxidation studies on sulfonamides showing that oxidation often begins with •OH attack on the aromatic amine and sulfonamide linkage by producing intermediates which are then slowly mineralized (Fabiańska et al., 2014; H. Li et al., 2019). The relatively small concentration × time interaction observed under acidic conditions suggests that protonation may have slightly improved the sensitivity of sulfanilamide to anodic oxidation, though it was not enough to produce strong nonlinear kinetics. In acidic media, BDD systems often promote •OH generation and limit radical scavenging by OH^- ions, which can enhance overall oxidation efficiency (El-Ghenymy, Garrido, et al., 2013b). Though sulfanilamide is structurally simpler and less demanding to oxidize than tetracycline, its degradation may remain comparatively insensitive to such interactive effects once

an adequate oxidant flux is maintained. The overall trend for the present study suggests that sulfanilamide degradation could be driven primarily by cumulative oxidant exposure rather than by strong shifts associated with its specific molecular speciation. This interpretation is consistent with previous BDD studies on sulfonamides, where oxidation kinetics are commonly characterized by first-order or pseudo-first-order behavior under fixed operating conditions (El-Ghenymy, Garrido, et al., 2013b). The findings collectively show that while BDD electrooxidation was effective for all three antibiotics, the degradation mechanisms were strongly compound-specific, with tetracycline-HCl exhibiting the greatest sensitivity to combined operating conditions.

Furthermore, the reported second-order rate constants for reaction with •OH are of the order of 10^9 M^{-1} s^{-1} for all three antibiotics. Literature values are approximately 4.5 $\times 10^9$ M^{-1} s^{-1} for SN, 6.3 $\times 10^9$ M^{-1} s^{-1} for TC, and 5.27 to 6.07 $\times 10^9$ M^{-1} s^{-1} for SMZ, depending on the experimental conditions and determination method (Jeong et al., 2010; Mezyk et al., 2007; Sági et al., 2015). Thus, the intrinsic •OH reactivity broadly follows TC > SMZ > SN. In contrast, the experimentally observed removal at the optimized condition followed SN (97.0%) > TC-HCl (95.5%) > SMZ (88.0%). This difference indicates that the removal behaviour cannot be explained by •OH reaction constants alone. In BDD electrooxidation, hydroxyl radicals are generated close to the anode surface, and pollutant removal may also involve direct anodic oxidation, mass-transfer effects, compound speciation, and competitive reactions among the parent antibiotics and their transformation products (Groenen-Serrano et al., 2013). Therefore, the literature K_{OH} values support the potential involvement of hydroxyl radicals but do not predict the observed removal ranking. Because radical scavenging or probe experiments were not conducted and for this reason the relative contribution of •OH oxidation cannot be quantified from the present study.

4.5 TOC mineralization and hypothetical degradation pathway

TOC mineralization increased with the delivered specific charge and was highest at pH 3.5. However, the equal-charge comparison demonstrated that increasing current density did not improve charge utilization. At $Q/V = 2.0$ A h L^{-1}, TOC mineralization at pH 3.5 decreased from 31.3% at 15 mA/cm^2 to 26.9% and 23.7% at 25 and 35 mA/cm^{2,} respectively have shown in **Figure 4-7.**

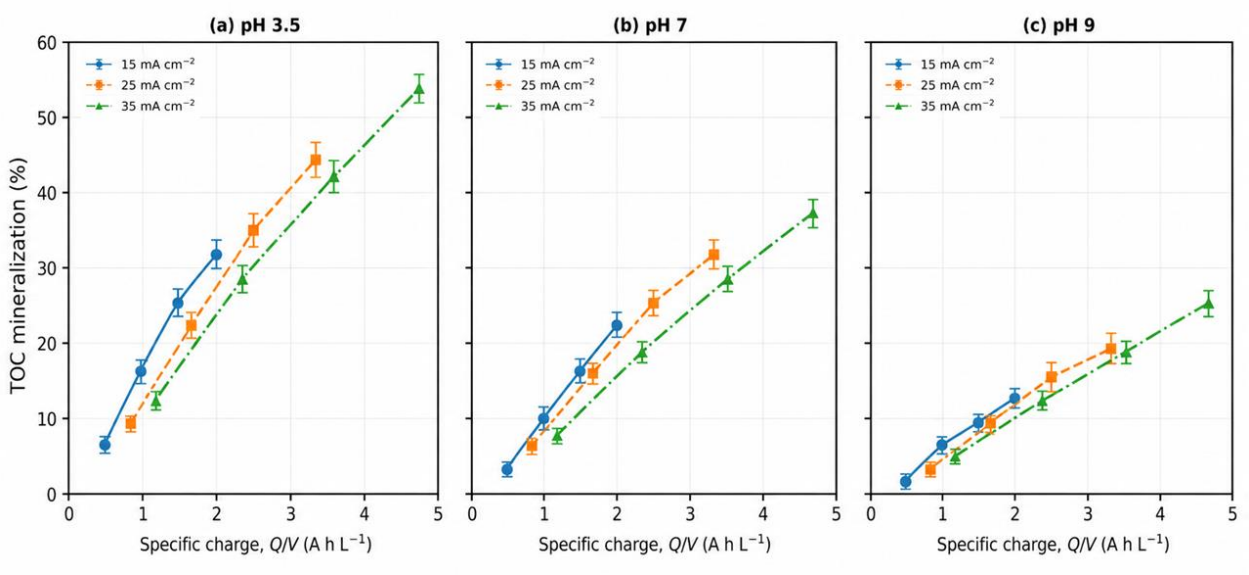

Figure 4-7: Charge-normalized TOC mineralization during Nb/BDD electrochemical oxidation under different pH conditions. TOC mineralization is presented as a function of volumetric specific charge, Q/V, at (a) pH 3.5, (b) pH 7, and (c) pH 9 for applied current densities of 15, 25, and 35 mA/cm^2. Specific charge was calculated as $Q/V = It/V$, where I is the applied current, t is the electrolysis time, and V is the working solution volume. Data are reported as mean ± standard deviation of triplicate measurements ($n = 3$).

Corresponding values were 21.9%, 19.4%, and 15.6% at pH 7 and 12.5%, 11.9%, and 10.4% at pH 9. The charge-normalized TOC removal yield showed the same trend, indicating that 15 mA/cm^2 provided the most efficient use of the supplied charge, whereas 35 mA/cm^2 mainly

increased the mineralization rate by delivering a greater electrical dose, as shown in **Figure 4-8.** At higher current densities, the current efficiency drops because more electricity proceeds to produce oxygen instead of oxidizing the pollutants, and the system is pushed beyond the limit where mass transfer can supply enough reactants to the electrode.

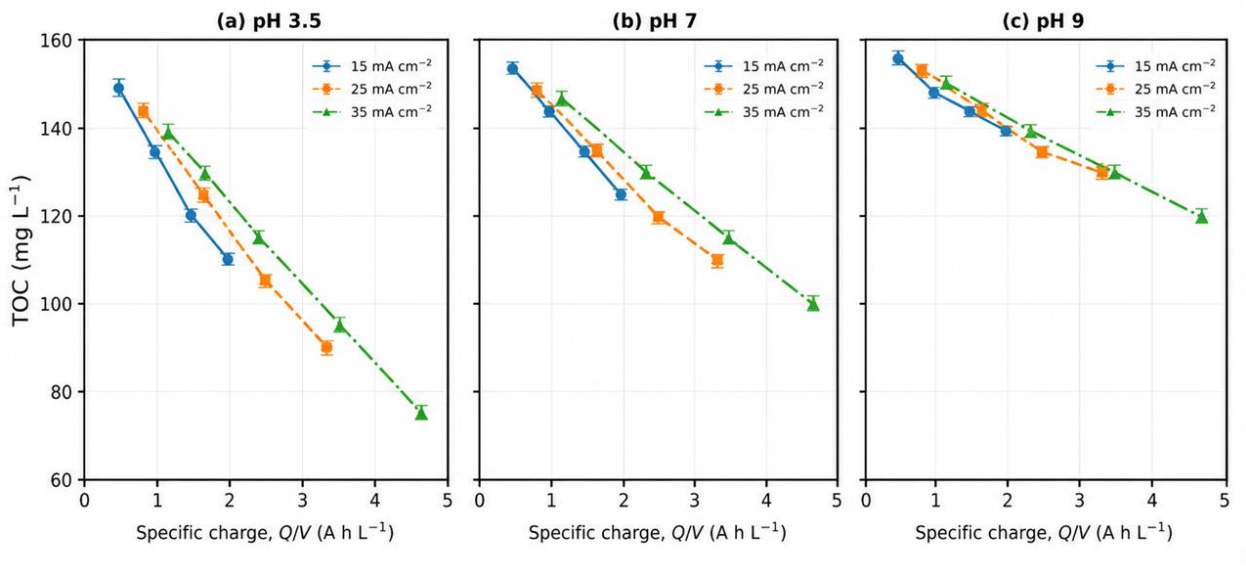

Figure 4-8. Variation of total organic carbon concentration with volumetric specific charge during Nb/BDD electrochemical oxidation**.** TOC concentrations are plotted against Q/V at (a) pH 3.5, (b) pH 7, and (c) pH 9 for current densities of 15, 25, and 35 mA/cm^2. Error bars represent the standard deviation of triplicate TOC measurements ($n = 3$). The decreasing TOC profiles indicate progressive TOC mineralization of the organic matrix with increasing charge input, while the differences among pH conditions reflect the influence of solution acidity on overall TOC mineralization performance.

Furthermore, Equal-charge comparison of TOC mineralization at a volumetric specific charge of 2.0 A h L^{-1} is shown in **Figure 4-9.**

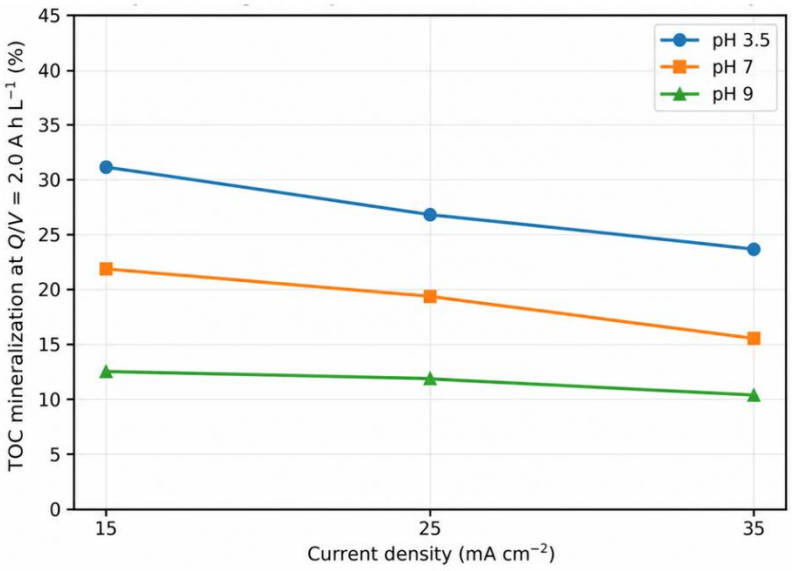

Figure 4-9: Equal-charge comparison of TOC mineralization at a volumetric specific charge of 2.0 A h L^{-1}**.** TOC mineralization at pH 3.5, 7, and 9 is compared across current densities of 15, 25, and 35 mA/cm^2 at the same charge input. Values at 15 mA/cm^2 correspond to the measured 60-min data, whereas the values at 25 and 35 mA/cm^2 were obtained by linear interpolation between the two nearest experimental points. The comparison distinguishes the effect of current density from the effect of unequal total charge delivery and demonstrates charge-normalized TOC mineralization performance under the investigated operating conditions.

In addition, TOC mineralization results also indicate that the amount of bulk carbon removal is much lower than parent-compound degradation. Because in the BDD electrooxidation system, the rapid, non-selective attack by hydroxyl radicals may initiate degradation and transformation of the parent pharmaceuticals, while the subsequent oxidation of the resulting refractory intermediates to CO_2 proceeds at a considerably slower rate (Brinzila et al., 2014; Sirés & Brillas, 2012). In the present mixed-pharmaceuticals wastewater matrix, the moderate TOC removal indicates that the electrogenerated oxidizing flux may be shared among TC-HCl, sulfanilamide, sulfamethazine, and their continuously evolving intermediates, thereby limiting the fraction of current available for

direct mineralization. This interpretation is mechanistically reasonable because tetracycline-HCl is known to display greater structural complexity and stronger condition dependence than sulfonamides, whereas sulfanilamide and sulfamethazine generally show more regular anodic oxidation behavior under acidic conditions in the BDD electrooxidation system (Brinzila et al., 2014; El-Ghenymy, Cabot, et al., 2013; El-Ghenymy, Garrido, et al., 2013b).

Therefore, the observed TOC removal provides useful information regarding the range of organic carbon removal; however, it does not confirm complete mineralization of the antibiotic molecule into inorganic end products or detoxification. Previous studies on antibiotic treatment processes have shown that significant parent-compound removal can occur while transformation products persist, and toxicity may either decrease or temporarily increase during degradation pathways (Z. Li et al., 2024; Sun et al., 2024). Accordingly, the absence of transformation-product and toxicity analyses represents a limitation of the present work.

From an engineering perspective, the overall findings indicate that the selected operating conditions were sufficient to promote oxidative breakdown of the mixed pharmaceutical matrix, but not yet optimized for deep carbon abatement, which would likely require longer electrolysis time and further refinement of current density and reactor operation.

Hypothetical degradation pathway

Sulfanilamide and sulfamethazine may be degraded by Nb/BDD electrooxidation through a radical-driven mineralization process, though their exact degradation steps are not the same. However, •OH was not quantified in the present study; therefore, their contribution relative to direct electron transfer or other mediated pathways is not explained here experimentally, but rather hypothetically. Each compound may be involved in aromatic oxidation and then forms short-chain carboxylic acids (El-Ghenymy, Cabot, et al., 2013; El-Ghenymy, Garrido, et al., 2013b). Because

sulfamethazine has a more complex structure, it also produces extra intermediates related to its heterocyclic ring (El-Ghenymy, Garrido, et al., 2013b). For sulfanilamide, the primary aromatic intermediates may be formed during the oxidation, which include 1,2-benzenediol, 1,3-benzenediol, and p-benzoquinone (El-Ghenymy, Garrido, et al., 2013b). The oxidation process may involve in producing several carboxylic acid intermediates, including maleic, fumaric, acetic, formic, oxalic, and oxamic acids. Therefore, sulfanilamide could first undergo hydroxylation and oxidation of its aromatic ring, followed by ring cleavage and the formation of low-molecular-weight carboxylic acids, which may then further oxidize during the mineralization process. Based on the literature, for the present study, we propose a hypothetical possible pathway for sulfanilamide degradation and mineralization in an acidic medium during anodic oxidation with Nb/BDD, shown in **Figure 4-10.**

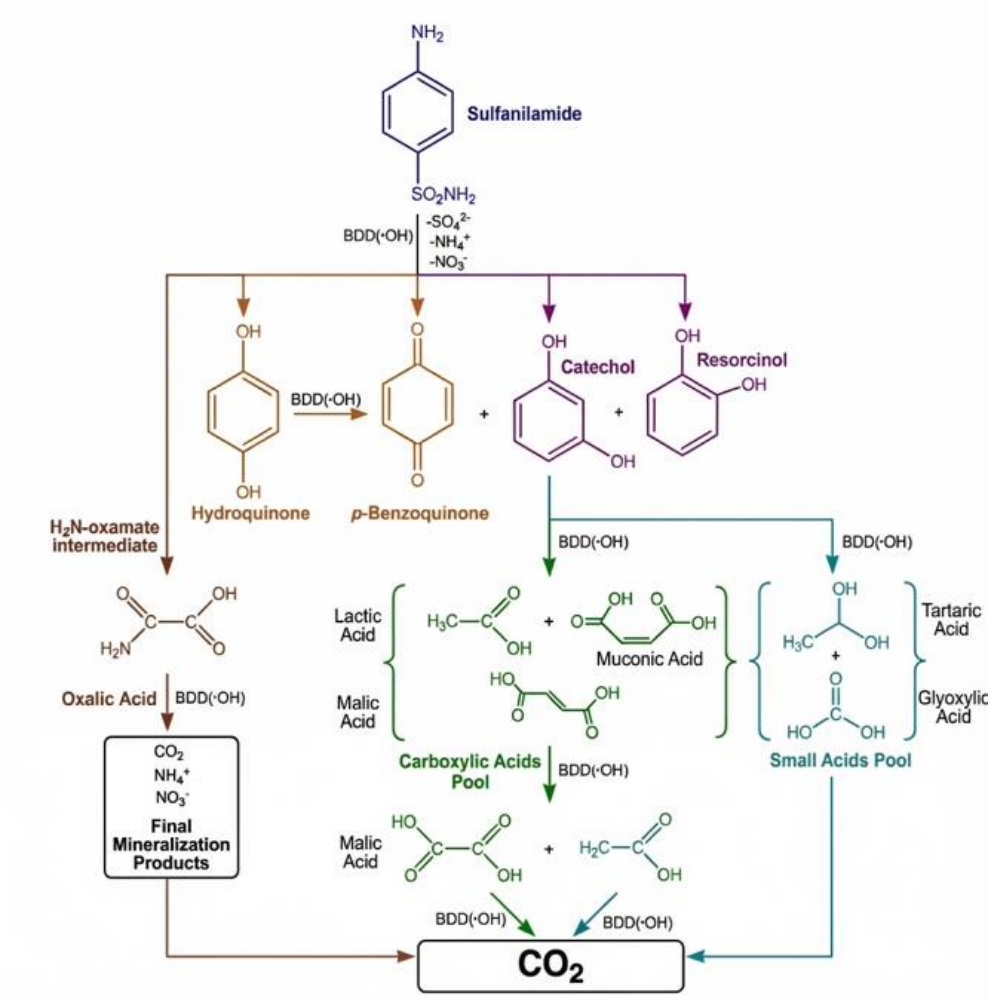

Figure 4-10: Hypothetically proposed degradation and mineralization pathway of sulfanilamide in wastewater by anodic oxidation (AO) with a Nb/BDD electrode, modified from (El-Ghenymy, Garrido, et al., 2013b).

In this hypothetical pathway, the Nb/BDD(•OH) radical generated from reaction (4-6) could be considered the main oxidizing species. The degradation pathway may start with radical attack on sulfanilamide, which leads to deamination, cleavage of the $–SO_2NH_2$ group, and formation of dihydroxylated aromatic intermediates such as 1,2-benzenediol, 1,3-benzenediol, and 1,4-benzenediol. These intermediates may further oxidize to p-benzoquinone. Deamination and breakdown of the $–SO_2NH_2$ group, followed by sulfur oxidation to sulfate, contribute to nitrogen

mineralization primarily as NH_4^+. Release of the $–SO_2NH_2$ group could also form N-containing intermediates that form oxamic acid, which could subsequently convert to CO_2, NH_4^+, and $NO_3^–$. Further oxidation of the aromatic intermediates may lead to cleavage of the benzene ring and formation of short-chain carboxylic acids, including maleic, fumaric, and acetic acids. Afterward, they may oxidize to the final intermediates, oxalic and formic acids, which may ultimately mineralize to CO_2. These proposed reaction pathways are similar to previous research on degradation of SMX through a Ti/SnO_2-Sb/Ce-PbO_2 anode (Hussain et al., 2017b; Lin et al., 2013).

However, in the case of Tetracycline-HCl, mineralization under anodic oxidation at a BDD electrode proceeds through a step-by-step oxidative pathway rather than a single direct conversion process (Körbahti & Alaca, 2021). For TC-HCl, the parent molecule may initially convert into hydroxylated and demethylated intermediates, followed by ring opening. Over time, it could be more oxidized into smaller carboxylic acids, eventually breaking down into inorganic end products, thus mineralized (X. Li et al., 2022; J. Wang et al., 2018). (Brinzila et al., 2014) reported that TC degradation at BDD was enhanced at low initial pH and higher current density, whereas TOC removal remained slower than parent-compound removal, which indicates that rapid TC removal does not necessarily correspond to immediate complete mineralization, which is consistent with our present studies where TOC removal is much slower than the parent compounds. Previous studies have identified major oxidation byproducts from TC-HCl that include oxalic, oxamic, and maleic acids, supporting the interpretation that mineralization proceeds gradually through multiple degradation steps rather than by direct one-step destruction of the parent molecule (Brinzila et al., 2014; X. Li et al., 2022). Similar findings have been found in other BDD-based studies, where reaction intermediates accumulated at early electrolysis stages and were only

further oxidized during prolonged treatment (Körbahti & Alaca, 2021). These suggest that mineralization occurred through successive intermediate conversion and is strongly influenced by current density, electrolyte composition, and solution pH for TC-HCl.

4.6 Electrical energy consumption and cost analysis

The economic feasibility of this research is mainly determined by electrical energy consumption, which is the primary determinant of the cost of electrochemical advanced oxidation processes (EAOPs). For the present research, the specific energy consumption (SEC) and operational cost were evaluated to see the economic feasibility for the degradation of selected mixed pharmaceutical compounds (sulfamethazine, sulfanilamide, and tetracycline hydrochloride) in wastewater using the Nb/BDD electrodes.

4.6.1 Specific Energy Consumption (SEC)

The applied current density (j) is an important parameter that influences both the degradation kinetics and the energy efficiency of the system. The specific energy consumption per unit volume of treated wastewater (SEC, kWh/m^3) was calculated based on the applied current densities (j) that are (15, 25, and 35) mA/cm^2 by using the following **Eq. (4-10)**:

$$\mathrm{SEC} = \frac{U*I*t}{V*1000} \qquad \textbf{(4-10)}$$

Where U is the average cell voltage (V), I is the applied current (A), t is the electrolysis time (h), and V is the treated volume (m^3). As can be seen in **Table 4-3**, the energy consumption increases with the increase in current density.

Table 4-3. Summary of electrical energy consumption and electricity cost at different current densities (t = 1 hour)

Current Density (*j*) [mA/cm^2]	**Applied Current (*I*) [A]**	**Avg. Cell Voltage *(U)* [V]***	**Power (*P*) [kW]**	**SEC [kWh/m^3]**	**Operational cost [CAD/ m^3] (**)**
15	6	8.5	0.051	17.0	1.68
25	10	10.7	0.107	35.66	3.52
35	14	12.8	0.179	59.67	5.88

*Average cell voltage *(U)* was calculated based on the arithmetic mean of the recorded voltage for each applied current *(I)* with an equal time interval during the experiment

** Operational cost calculated based on Manitoba Hydro industrial rates, which is 9.864 ¢/kWh (*electricity rates effective approved in*, 2026).

For our research, the treatment process required 17.0 kWh/m^3 of energy at 15 mA/cm^2. Increasing the current density to 35 mA/cm^2 required 3.5 times higher energy, at 59.67 kWh/m^3. The cost of energy is, therefore, nearly proportional to the current density due to increased power consumption. A similar trend was observed in previous studies where, in a BDD electrode, the SEC was increased to 30% with an increased current density from 29.2 mA/cm^2 to 33.3 mA/cm^2 (Bagastyo et al., 2022). The faster rate is related to parasitic reactions because oxygen evolution processes become dominant at higher current densities, and it reduces the faradaic efficiency in the oxidation of pollutants (Panizza & Cerisola, 2009). These findings emphasize that increased energy needs to be used only to fully mineralize the complex pharmaceutical compounds.

From the literature, it was found that BDD electrooxidation of antibiotics normally consumes tens of kWh/kg of contaminant. For instance, (Hai et al., 2020b) reported 72 kWh/kg COD of

sulfamethoxazole at 30 mA/cm^2, and Nb/BDD anodes reported 66.5 kWh/kg COD at 20 mA/cm^2 (S. da Silva et al., 2019). When normalized to the mass of antibiotic removed, the SEC of our system is within a comparable range. The energy requirements are due to the recalcitrant structures of sulfonamides and tetracyclines, and the reduction in current efficiency happens due to increasing current, which enhances parasitic oxygen evolution as well as other side reactions, thus raising the energy per unit pollutant removed. Though higher currents accelerate the efficiency of pharmaceutical removal, it consumes more energy and lose it mainly as heat. At 35 mA/cm², the anodic potential could exceed the thermodynamic threshold for oxygen evolution, which may develop a highly competitive, parasitic side reaction mentioned in **Eq. (4-11).**

$$2H_2O \rightarrow O_2 + 4H^+ + 4e^- \quad \textbf{(4-11)}$$

At high current densities, water splitting causes much of the applied current to be lost to the production of oxygen gas and not on the oxidation of pollutants or the dissolution of metals. For our research, the design of the reactor is a cylindrical cell with an inter-electrode distance of 3-mm maintained moderate voltages compared to standard wide-gap designs, which contributed to excellent energy efficiency at all selected current densities.

4.6. 2 Economic Assessment

The operational cost was calculated based on SEC, and no cost was added for electrode amortization and chemical additives. One of the strongest advantages of this study's location is the fact that electricity rates are low in Manitoba, Canada due to the availability of hydroelectric power. This highlights the strategic benefit of implementing electrooxidation in areas that have renewable and low-cost energy grids, such as in Manitoba. In our study, we applied an electricity rate with an average industrial rate of 9.864 ¢/kWh or $0.0986 CAD/kWh sourced from Manitoba

Hydro, 2026 was applied (electricity rates effective approved in, 2026). **Table 4-3** indicates that the treatment cost varies between 1.68/m^3 at 15 mA/cm^2 and 5.88/m^3 at 35 mA/cm^2 and is lower than other AOPs such as O_3/UV, which costs from $5.00 to $10.00/$m^3$ for high-load pharmaceutical wastewater (Kim et al., 2009).

However, full-scale treatment would require larger volumes and longer times, and the overall cost might increase. In practice, the trade-off between current density and removal efficiency is very important since the higher the current, the faster the degradation, the lower the energy efficiency, and the higher the kWh consumed. Therefore, the selection of an optimal current is essential to reduce SEC. In general, the calculated SEC and operational costs are relatively lower when compared with previous BDD-antibiotic research. The energy requirements indicate the difficulty of mineralizing persistent pharmaceutical molecules, but the application of BDD with its high oxidation potential and Manitoba's low energy rates can reduce operating costs in practice.

4.7 Conclusion and future recommendations

This research supports the significant effectiveness of Nb/BDD electrooxidation as a treatment method in removing a ternary antibiotic mixture of sulfanilamide, tetracycline-HCl, and sulfamethazine over a broad range of operating parameters. In the studied ranges of initial concentration (4000-12000 µg/L), solution pH (3.5-9.0), treatment time (15-60 min), and applied current density (15-35 mA/cm^2), the treatment time was found to be the most important operating variable, which determined the efficiency of pollutant removal. Removal was significantly higher at 60 min as compared to 15 min in all the experimental conditions that were tested. Among the investigated conditions, 35 mA/cm^2 achieved the highest antibiotic removal within the fixed 60 min treatment period; however, charge-normalized analysis confirmed that 15 mA/cm^2 provided

the maximum removal per unit of applied charge and was therefore the most charge-efficient current-density condition. In terms of TOC mineralization, the absence of transformation-product identification, inorganic nitrogen/sulfur speciation, and toxicity measurements constitutes a limitation of the current study. Therefore, the results are not interpreted as evidence of complete mineralization or detoxification. Rather, the present work provides a preliminary operational mapping of process performance and establishes a basis for future studies aimed at explaining degradation pathways, byproduct formation, and environmental safety.

Furthermore, in terms of compound-specific behavior, TC-HCl was the most sensitive to the interactions of parameters, and the degradation of sulfanilamide and sulfamethazine was largely controlled by the primary impact of treatment time, the pH of the solution, and the initial concentration. A lower pollutant load concentration (4000 μg/L) consistently exhibited better removal when compared to a higher load (12000 μg/L), with the greatest differences being observed at longer electrolysis times. This happened particularly for TC-HCl, where the concentration-dependent difference in removal efficiency increased significantly with time (e.g., at 60 min, at pH 7, ~67% vs ~50%). Solution pH is another factor whose effect is most significant at extended time periods. In all target compounds, removal efficiency was increased by acidic conditions, with the most significant effect noted with TC-HCl, which reached about 77-80% at 60 min at 4000 μg/L and pH 3.5, decreasing to about 66-70% at pH 7.0 and approximately 60-62% max at pH 9.0. Sulfanilamide also showed its highest performance at acidic conditions with a removal of about 77% at pH 3.5 (4000 μg/L, 60 min), which is better than the removal at neutral pH, approximately 63%, and removal at pH 9 (~72%) under the same conditions. A similar pattern was observed with sulfamethazine, with a removal of about 79% at pH 3.5 (4000 μg/L, 60 min) compared to about 65% at pH 9.0.

The observed degradation is consistent with oxidative processes generally associated with BDD anodes; however, the relative contributions of direct anodic oxidation, BDD-associated hydroxyl species, and other matrix-mediated oxidants could not be resolved because individual oxidant species were not quantified in the present study. Therefore, it highlights the importance of matrix-dependent radical scavenging and pollutant speciation effects for future studies. From an implementation perspective, specific energy consumption (SEC) should be considered as a co-equal performance measure alongside contaminant removal efficiency since more complex and stronger matrices could require more energy input due to competing oxidant sinks and parasitic electrochemical reactions. In this regard, the current Manitoba electricity tariff system, which is already in effect from January 1, 2026, could provide a relatively good economic framework to implement our treatment process. The energy-charge component covers a range of about 3.917-9.864 ¢/kWh under typical commercial rate classes, which means that the price of electricity is directly proportional to the measured SEC. This tariff range is beneficial to Manitoba as relatively inexpensive compared to the more expensive electricity grids in North America and, therefore, supports the engineering feasibility of Nb/BDD electrooxidation as a specific polishing or source-treatment technology when optimized for charge efficiency.

For full-scale implementation, the following recommendations are provided for future studies:

Process optimization: Future studies need to prioritize the optimization of charge utilization to facilitate full-scale implementation. Balancing target pollutant removal efficiency against specific energy consumption (SEC) is vital for full-scale implementation.

Predictive modeling: The establishment of integrated kinetic and reactor-scale models is required. This predictive modeling will help outline strong operating windows suitable for scale-up applications.

Matrix validation: All proposed process models and performance metrics must be experimentally validated in real wastewater matrices to ensure practical relevance.

By-product and toxicity analysis: Comprehensive transformation by-product and ecotoxicological analyses are essential. These evaluations are necessary to confirm the environmental safety of the treated effluent.

Chlorine speciation tracking: Future experiments must systematically quantify chloride, free and total chlorine, chlorate, and perchlorate. Measuring these specific species before and after electrooxidation is vital to evaluating overall treatment performance and process safety.

Chapter 5: Manuscript no. 3

Application of response surface methodology for optimization and electrochemical oxidation of three mixed antibiotics at Boron-doped diamond electrodes

Abstract

This study investigated hydrogen peroxide (H_2O_2) supported electrooxidation using niobium-based boron-doped diamond (Nb/BDD) electrodes for the simultaneous removal of sulfanilamide (SN), tetracycline hydrochloride (TC-HCl), and sulfamethazine (SMZ) from biologically treated synthetic wastewater. Response surface methodology based on central composite design was applied to evaluate the effects of current density, pH, H_2O_2 dose, and initial antibiotic concentration on removal performance. The selected operating condition provided a chemically relevant design space by capturing the effects of antibiotic speciation, oxidant generation, radical availability, and pollutant loading. The optimized condition was identified at a current density of 30 mA/cm^2, pH 4.95, H_2O_2 dose of 2.5 mM, and initial antibiotic concentration of 6000 µg/ L at 90 minutes. Under these conditions, the model predicted removal efficiencies of 95.32%, 92.35%, and 86.16% for SN, TC-HCl, and SMZ, respectively, with an overall desirability of 0.817. Experimental validation confirmed removals of 97%, 95.50%, and 88%, respectively, which is an indication of good performance between predicted and observed values. TOC decreased from 85 to 20 mg/L after 90 min, corresponding to a mineralization efficiency of 76.47%, which confirmed that the process promoted better oxidation beyond parent-compound degradation. Under the optimized operating conditions, the process required 0.198 kWh to treat a 3.0 L batch, equivalent to a specific energy consumption of 66 kWh/m^3 and an estimated electrical cost of 6.51 CAD/m^3. Overall, the findings demonstrate that H_2O_2-assisted Nb/BDD electrooxidation is an effective advanced treatment strategy for antibiotic-

containing wastewater, particularly when simultaneous parent-compound removal and mineralization are required.

Keywords: H_2O_2-supplemented electrooxidation; ternary antibiotic mixture; pharmaceutical-contaminated wastewater; oxidative removal; central composite design; multi-response optimization.

5.1 Introduction

The presence of pharmaceutical antibiotics in wastewater can create the development of antimicrobial resistance, and the treatment of this antibiotic-contaminated wastewater remains a major environmental challenge (Akbari et al., 2021; Xinyu Wang et al., 2025). Since pharmaceuticals are not usually discharged as isolated compounds, rather, they enter treatment systems as complex multi-component mixtures. Therefore, effective treatment strategies need to be developed to address simultaneous degradation, complete mineralization, and energy efficiency within an integrated process design framework (Akbari et al., 2021; Xinyu Wang et al., 2025).

Advanced electrochemical oxidation using boron-doped diamond (BDD) anodes has become a promising treatment option because of its high overpotential for oxygen evolution, strong generation of hydroxyl radicals (•OH), and a confirmed ability to support deep oxidation and complete mineralization of recalcitrant organic micropollutants (M. T. Hasnine et al., 2025; Loos et al., 2018; Yuan et al., 2023). Previous studies have shown direct experimental evidence for •OH formation on BDD anodes, with the extent of radical production to correlate directly with degradation and mineralization performance (Espinoza et al., 2018). Other BDD-based studies have shown that both parent-compound removal and total organic carbon (TOC) reduction are strongly dependant by operating parameters, including current density, initial pH, added oxidant dose, and electrolysis time (García-Espinoza & Nacheva, 2019; M. T. Hasnine et al., 2022; T. Hasnine et al., 2023; Nashat et al., 2022).

The optimization of BDD-based electrooxidation therefore requires a multivariable experimental strategy rather than a one factor at a time approach. Statistical modelling has been increasingly applied to evaluate the combined effects of operating variables in electrochemical wastewater treatment. (S. U. Khan et al., 2020) used a central composite design and artificial neural network

modelling to optimize Synozol Red degradation as a function of pH, current density, electrolyte concentration, and electrolysis time. The study showed that these parameters had nonlinear and interactive effects on electrochemical treatment performance. (H. Khan et al., 2022) subsequently applied response surface and machine-learning models to Nb/BDD oxidation of Navy-blue dye. Their multi-response approach simultaneously considered dye removal and energy consumption. However, similar multi-response optimization remains limited for the simultaneous treatment of mixed pharmaceutical compounds using H_2O_2 assisted Nb/BDD electrooxidation. Response surface methodology (RSM) provides a statistically structured framework that evaluates linear, quadratic, and interaction effects while reducing the number of experimental runs required for process optimization (Körbahti & Taşyürek, 2016). In electrochemical wastewater treatment, RSM has been used to connect operating conditions with degradation efficiency, mineralization, and energy-related responses, which makes the process valuable for both mechanistic interpretation and engineering design and scale-up (Körbahti & Taşyürek, 2015, 2016). For example, RSM successfully optimized ampicillin degradation using BDD electrodes and RSM by evaluating the effects of current density, supporting electrolyte concentration, temperature, and initial antibiotic concentration on degradation performance and energy demand (J. Hu et al., 2020). Similar RSM-based electrochemical studies have shown that central composite and related experimental designs can capture nonlinear effects and interactions that are difficult to resolve using conventional single-variable testing, particularly when multiple parameters are required to optimize simultaneously (T. Hasnine et al., 2023; Körbahti & Taşyürek, 2015).

In addition to these methodological advances, the published literature mostly focused on single-contaminant systems or restricted sets of treatment conditions, which results in a significant gap in the knowledge base for optimizing mixed-antibiotic systems under combined oxidant-assisted BDD

electrooxidation. To address this gap, the present study investigates the simultaneous electrochemical treatment of a synthetic mixed-pharmaceutical matrix containing sulfanilamide (SN), sulfamethazine (SMZ), and tetracycline-HCl (TC-HCl) using H_2O_2-assisted BDD electrooxidation. This approach is motivated by the growing recognition that H_2O_2-based advanced oxidation processes offer strong oxidative capacity for antibiotic degradation, and that in situ H_2O_2 generation and activation can significantly improve both degradation kinetics and mineralization efficiency (Xuechun Wang et al., 2023). Moreover, recent research has established that BDD electrodes can serve not only as strong anodic oxidation materials but also as multipurpose electro -synthetic platforms for simultaneous oxidant generation, which further strengthens their engineering potential for advanced pharmaceutical wastewater treatment (Espinoza-Montero et al., 2022; M. D. T. Hasnine et al., 2024). The principal novelty of the present work lies in integrating compound-specific contaminant removal, interaction modeling within a single, cohesive RSM optimization framework, and later extending the RSM-derived optimum condition to evaluate TOC mineralization, energy demand, and operational cost analysis. Together, these components provide a more realistic representation of the complexity involved in designing treatment strategies for real wastewater systems.

The primary objective of this study is therefore to optimize the simultaneous removal of sulfanilamide, sulfamethazine, and tetracycline-HCl from synthetic wastewater using H_2O_2-supplementation BDD electrooxidation, conducted by a central composite design RSM. Specifically, the study aims to: (i) quantify the individual, quadratic, and interaction effects of current density, initial solution pH, electrolysis time, initial pharmaceutical concentration, and H_2O_2 dose on antibiotic removal efficiency, TOC mineralization, and specific energy consumption; (ii) derive and validate predictive response surface models for each performance indicator; and (iii)

identify optimized operating conditions that simultaneously maximize contaminant removal and minimize energy demand. From an engineering perspective, the findings are expected to provide quantitative design guidance for scalable electrochemical treatment systems targeting mixed pharmaceutical wastewater streams.

5.2 Experimental methods

5.2.1 Chemicals and Synthetic Wastewater Preparation

SN, SMZ, and TC-HCl were selected as representative antibiotics for the present research. All antibiotics and other chemicals used were purchased in analytical-grade form. Sulfuric acid (H_2SO_4, 98%) and sodium hydroxide (NaOH) were used for pH adjustment. ACS-grade hydrogen peroxide solution (H_2O_2, 30%) was used as an oxidant-supporting factor in the reactor. HPLC-grade methanol, acetonitrile, and 0.5% formic acid were also used, and all solutions were prepared using deionized (DI) water with conductivity <1 μS/cm. All glassware was acid-washed with 10% HCl and rinsed thoroughly with DI water before each use in experimental analysis.

Synthetic wastewater was used as the main matrix for the present research. This approach reduced matrix variability and allowed the effects of current density, pH, H_2O_2 concentration, and initial pharmaceutical concentration to be evaluated systematically. The characteristics of the high-strength synthetic wastewater used as an influent for the biological reactor were Yeast extract 1250 mg/L, NH_4Cl 33 mg/L, $K_2HPO_4.3H_2O$ 125 mg/L, TCOD 1400 mg/L, soluble chemical oxygen demand (sCOD) 1250 mg/L, TN 140 mg/L, total ammonia nitrogen (TAN) 117 mg/L, TP 42 mg/L, and soluble phosphorus (SP) of 20 mg/L. After the biological treatment, the effluent, which is used as influent for the present research, was (sCOD) 150 mg/L, (TOC) 85 mg/L, (TAN) 14 mg/L, and (SP) 2.2 mg/L. The target antibiotics were spiked into this biologically treated effluent to obtain the desired initial concentrations of antibiotics for CCD-RSM analysis.

A combined antibiotic stock solution was prepared by dissolving 100 mg each of SN, TC-HCl, and SMZ in a 100 mL volumetric flask. This results in a nominal concentration of 1000 mg/L for each antibiotic. Approximately 50 mL of deionized water was first added, followed by dropwise addition of 1 M NaOH to improve SMZ dissolution, and the solution was then diluted to the final volume with deionized water. Fresh stock solutions were prepared daily to minimize hydrolytic degradation of TC-HCl. For a 3.0 L working volume, aliquots of 18, 24, 30, and 36 mL of the combined stock solution were added to obtain initial concentrations of 6000, 8000, 10000, and 12000 µg/L, respectively, for each antibiotic. Based on the experimental design, the reactor was run in different pH conditions, and the pH was adjusted to 3.60, 4.95, 6.30, 7.65, and 9.00 before electrooxidation using 0.1 M H_2SO_4 or 1 M NaOH.

Furthermore, 30% H_2O_2 was added at target doses of 1.0, 1.5, 2.0, 2.5, and 3.0 mM before each reactor run. As the approximate molarity for 30% H_2O_2 was 9.8 M, the corresponding H_2O_2 volumes for a 3.0 L reactor were approximately 0.31, 0.46, 0.61, 0.77, and 0.92 mL, respectively. However, in situ H_2O_2 production generally requires a cathode selective toward the two-electron oxygen-reduction reaction and an adequate oxygen supply (Ali et al., 2022; Espinoza-Montero et al., 2022). The stainless-steel cathodes used in the present reactor were not specifically designed for controlled H_2O_2 electrogeneration. Therefore, H_2O_2 was externally added and considered H_2O_2 assisted Nb/BDD electrooxidation to provide a known and reproducible initial concentration which allowed its individual, interaction, and quadratic effects on antibiotic removal. The H_2O_2 dose was optimized because excessive addition may promote non productive oxidant consumption and radical scavenging reactions (Miklos et al., 2018).

5.2.2 Electrochemical reactor setup

Electrooxidation experiments were performed using Nb/BDD electrodes. A schematic representation of the electrochemical reactor configuration, including the electrode arrangement, power supply connection, mixing system, and the anodic oxidation pathway are presented in **Figure 5-1.**

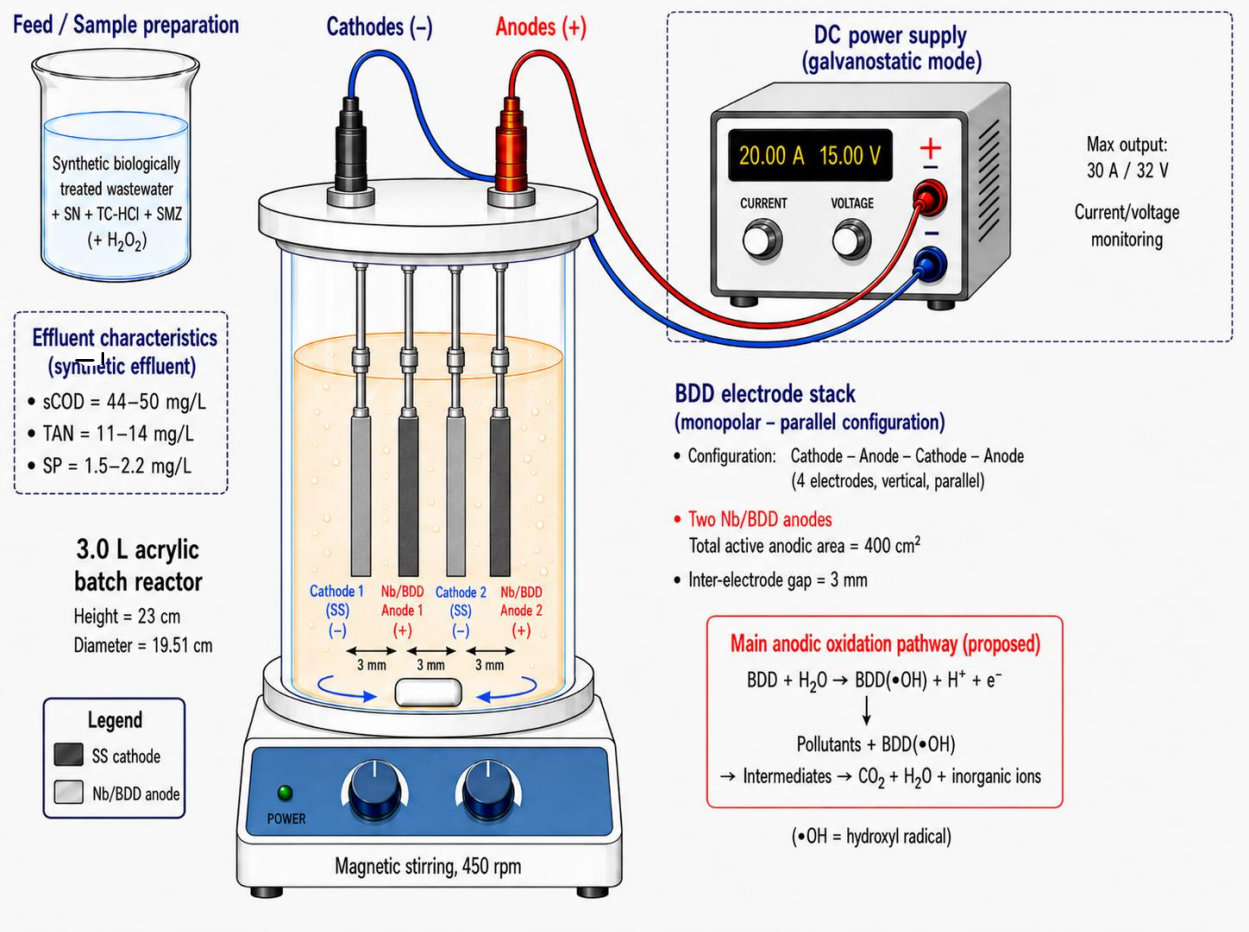

Figure 5-1: Schematic diagram of the Nb/BDD electrooxidation system used for the removal of SN, TC-HCl, and SMZ from synthetic wastewater. The setup includes a 3.0 L acrylic batch reactor, vertically arranged BDD electrode stack, DC power supply operated under galvanostatic mode, magnetic stirring system, and the main anodic oxidation pathway through •OH generation at the Nb/BDD anode surface.

The antibiotic-spiked wastewater, along with the addition of H_2O_2 as an oxidant, was run in a stirred 3.0 L batch reactor. The mixed antibiotic solution was continuously mixed at 450 rpm using a magnetic stirrer to maintain solution homogeneity. The reactor consisted of two Nb/BDD anodes and two cathodes with an active anodic area of 400 cm², arranged vertically with a 3 mm inter-electrode gap. This configuration provided the required electrode area within a compact reactor while maintaining a fixed interelectrode distance. It also distributed the active electrode surfaces across the treated liquid volume. Electrode area to volume ratio, spacing, current distribution, and reactor hydrodynamics are important factors which control mass transfer and electrochemical oxidation performance (Mandal et al., 2017; Sandoval et al., 2022). Although a single electrode with an equivalent surface area could simplify the reactor assembly, it would require a different reactor geometry and hydrodynamic assessment. However, the reactor was operated using a DC power supply (B&K Precision 1901-B, 30 A/32 V), and the samples were collected for antibiotic concentration analysis in HPLC and for TOC analyses. The main oxidation mechanism involves water oxidation at the BDD anode to generate surface-bound •OH, which degrades the target antibiotics into oxidation intermediates and final mineralization products.

Based on the experimental design, fixed applied currents of 6, 8, 10, 12, and 14 A were used in the present study. Considering the total active anodic area of 400 cm^2, the subsequent current densities were calculated using $j = \frac{I}{A}$, where j is the current density, I is the applied current, and A is the active anodic area. From the calculation, the measured current densities were (15, 20, 25, 30, and 35 mA/ cm^2) for the applied currents of (6, 8, 10, 12, and 14 A), respectively.

However, electrooxidation was carried out at different reaction times of 30, 60, 90, and 120 min during preliminary evaluation. However, for the response surface methodology study, the 90 min treatment time was selected because it provided more consistent and higher removal efficiencies

compared with the shorter treatment periods while avoiding unnecessary extension of electrolysis time. Therefore, removal efficiencies at 90 min were used as the response variables for the RSM model.

The occurrence of electrooxidative degradation of the selected antibiotics is due to the generation of weakly adsorbed hydroxyl radicals at the non-active Nb/BDD anode surface. This radical subsequently oxidized the target antibiotics through non-selective oxidation pathways, as mentioned in **Eq. (5-1)** and **Eq. (5-2).** where R represents SN, TC-HCl, and SMZ.

$$BDD + H_2O \rightarrow BDD(\bullet OH) + H^+ + e^- \quad \textbf{(5-1)}$$

$$R + BDD(\bullet OH) \rightarrow \text{oxidation intermediates} \rightarrow CO_2 + H_2O + \text{inorganic ions} \quad \textbf{(5-2)}$$

Removal efficiency was calculated using **Eqs. (5-3).** where C_0 is the initial concentration and $C_t$is the concentration after electrooxidation time t.

$$\text{Removal efficiency}(\%) = \left(1-\frac{C_t}{C_0}\right) \times 100 \quad \textbf{(5-3)}$$

All experimental runs were performed in triplicate to ensure reproducibility.

5.2.3 Analytical procedure

After electrooxidation, samples were collected from the reactor for antibiotics concentration analysis in high-performance liquid chromatography (HPLC). The collected samples were then subjected to a multi-step preparation procedure to remove suspended solids and fine particulates from the treated effluents to minimize matrix interference during HPLC analysis. Therefore, the sample preparation procedure improved the reliability and accuracy of the instrumental analysis. The sequential steps involved in the sample preparation process are summarized in (**Figure 5-2).**

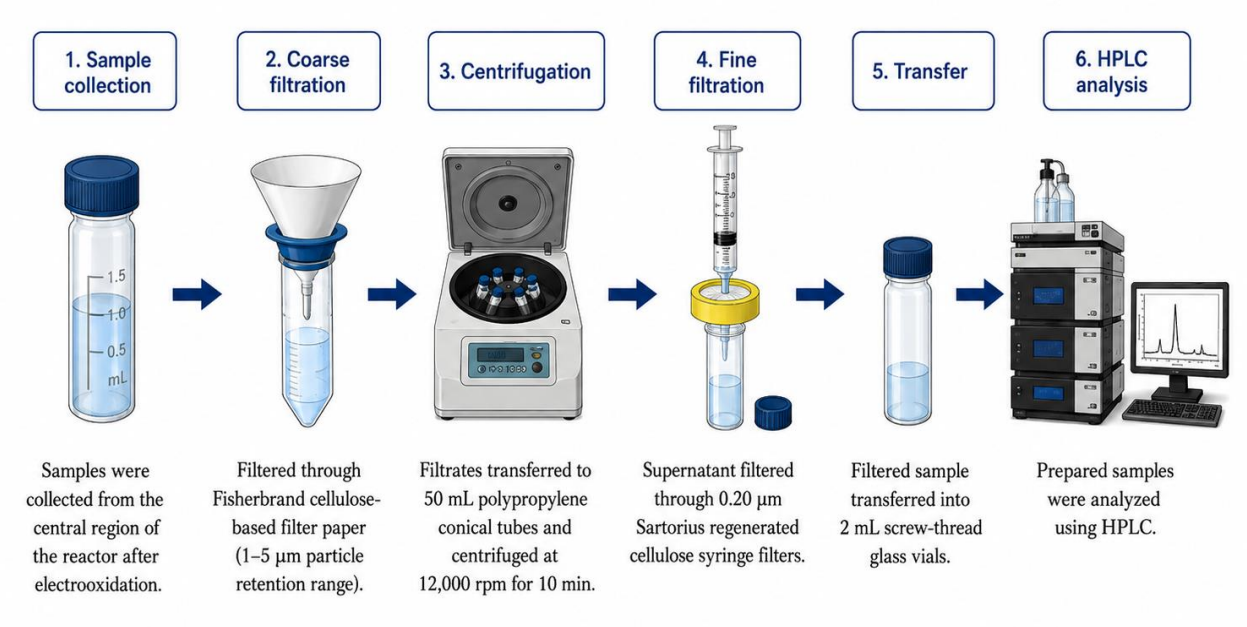

Figure 5-2. Flow chart of the post-electrooxidation sample preparation to minimize particulate interference before HPLC analysis

After the post-electrooxidation sample preparation steps, the prepared samples were analyzed using a Waters brand HPLC system under gradient elution with UV detection at 254 nm. In addition, the TOC was measured using a Shimadzu TOC-L analyzer operated by high-temperature catalytic combustion at 680°C. The flowchart in (**Figure 5-3**) summarizes the analytical workflow used for quantifying the concentration of SN, TC-HCl, and SMZ by HPLC-PDA and evaluating the total organic carbon removal by TOC analysis.

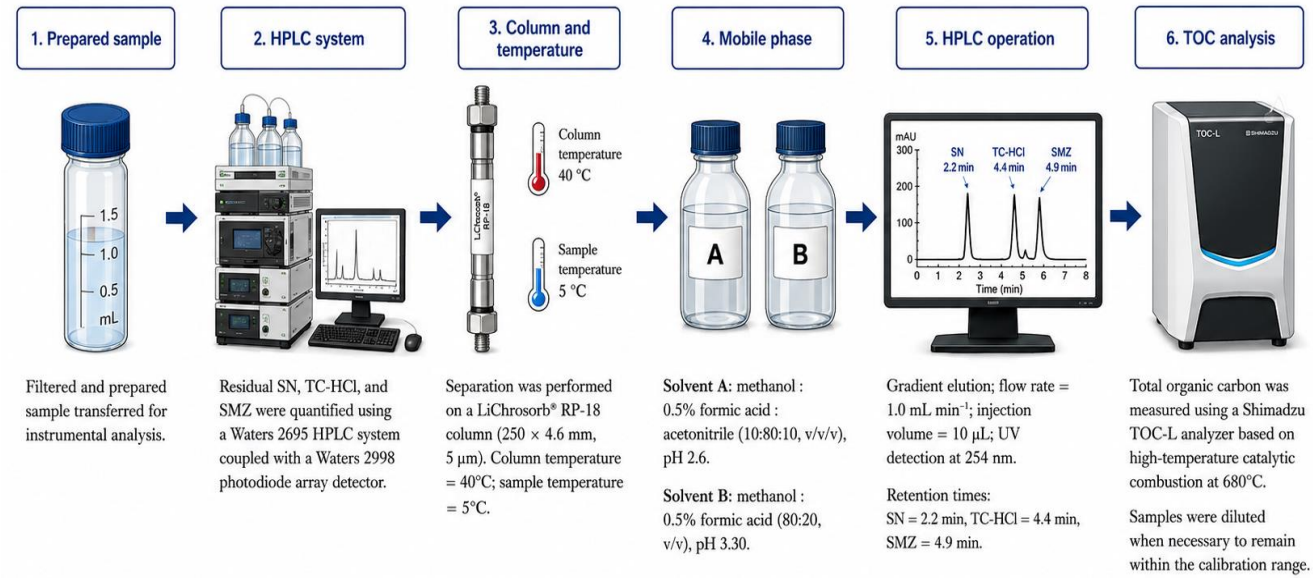

Figure 5-3. Flow chart of the analytical procedure used for chromatographic determination of sulfanilamide (SN), tetracycline hydrochloride (TC-HCL), and sulfamethazine (SMZ), together with total organic carbon (TOC) measurement. Residual antibiotics were quantified by HPLC-PDA under gradient elution conditions, while TOC measurement was evaluated using a Shimadzu TOC-L analyzer operated by high-temperature catalytic combustion.

5.2.4 Selection of operating conditions and CCD for experimental design

RSM is a statistically based optimization technique that applies polynomial regression models, commonly second-order quadratic equations, to evaluate the effects of multiple independent variables and their interactions on selected responses (Khorram & Fallah, 2018). It has been widely applied in process engineering and industrial research because it enables systematic interpretation of factor interactions, prediction of response behavior, and identification of optimum operating conditions with a reduced number of experimental runs (J. Hu et al., 2020). In the present study, the experimental factors were investigated within a predefined operating domain; therefore, a central composite design (CCD) was selected to efficiently generate the experimental design along with

maintaining sufficient model accuracy and predictive capability (Khodadoost et al., 2017). For the present research, the experimental design, regression modelling, analysis of variance, response surface generation, and optimization were performed using Design-Expert software version 7.0.0 (Stat-Ease Inc., Minneapolis, MN, USA).

The selected pH, current density, H_2O_2 dose, and initial concentration have a significant impact on establishing a chemically appropriate and statistically reliable design space for RSM optimization of Nb/BDD electrooxidation. These factors enabled the evaluation of key individual and interaction effects that control the simultaneous removal of SN, TC-HCl, and SMZ. The pH range of 3.60 to 9.00 was chosen to cover acidic, near-neutral, and alkaline conditions because pH strongly affects the ionization state of SN, TC-HCl, and SMZ, as well as the reactivity and stability of electro-generated oxidants. The selected range also includes conditions around the pKa values of the targeted antibiotics, where changes in molecular charge may influence their susceptibility to •OH attack and electrochemical oxidation. The initial concentration range of 6000 to 12000 µg/L was selected to evaluate the influence of pollutant loading on treatment efficiency while maintaining reliable HPLC quantification. This also allows assessment of the oxidant-to-contaminant ratio under controlled stress-test conditions. Current density was varied from 15 to 35 mA/cm2 because it directly regulates the formation rate of •OH at the non-active Nb/BDD anode surface. Lower current densities may produce insufficient oxidant flux, whereas higher current densities can enhance degradation but may also promote competing reactions such as oxygen evolution and radical recombination. The H_2O_2 dose range of 1.0 to 3.0 mM was selected to assess its role as an additional oxidant and radical mediator. Moderate H_2O_2 addition may improve oxidative degradation, while excessive dosing can consume •OH and reduce process efficiency. Thus, these ranges provided a suitable experimental

domain for developing quadratic RSM models and identifying optimum conditions for the simultaneous removal of SN, TC-HCl, and SMZ.

However, in RSM, the independent variables were coded as X_1, X_2, X_3, and X_4, representing current density, pH, H_2O_2 dose, and initial concentration, respectively. The removal efficiencies of sulfanilamide, TC-HCl, and sulfamethazine at 90 min were fitted using a quadratic response surface model mentioned in **Table 5-1** using a second-order polynomial **Eq. (5-4)** which usually describe the effects of various factors on a response based on experimental results from a central composite design. Multi-response optimization was performed using the desirability function approach by maximizing the removal efficiencies of the three target compounds simultaneously. The general quadratic model was expressed as:

$$Y = \beta_0 + \sum_{i=1}^{k} \beta_i X_i + \sum_{i=1}^{k} \beta_{ii} X_i^2 + \sum_{i<j} \beta_{ij} X_i X_j \quad \textbf{(5-4)}$$

where y is the predicted response, β_0 is the constant, β_i is the linear coefficient, β_{ii} is quadratic coefficient, β_{ij} is the interactive coefficient and x_i is the coded factor level.

Table 5-1. Independent variables and their coded and actual levels used in the central composite design

Variables	Units	Low level (-1)	Medium level (0)	High level (+1)	-alpha	+ alpha
X_1: Current densities	mA/cm^2	20.38	25.19	30	15.57	34.81
X_2: pH		4.95	6.3	7.65	3.5	9.0
X_3: H_2O_2	mM	1.5	2.0	2.5	1.0	3.0
X_4: Initial Concentration	ug/L	6000	8000	10000	4000	12000

5.3 Results and discussion

5.3.1 Statistical analysis and analysis of variance

For our present research, central composite design (CCD) under response surface methodology (RSM) was employed to determine the optimum values of the selected operational variables. The effects of current density, pH, H_2O_2 dose, and initial concentration on the removal efficiencies of sulfanilamide, TC-HCl, and sulfamethazine were evaluated using 3D response surface plots and a quadratic polynomial model, and analysis of variance was used to evaluate model significance, individual model terms, and lack of fit.

The experimental runs generated by Design-Expert software, along with the corresponding removal efficiencies, are presented in **Table 5-2.**

Table 5-2. Central composite design matrix showing the coded and experimental runs and the corresponding observed removal efficiencies of sulfanilamide, tetracycline hydrochloride, and sulfamethazine

Std	Runs	A	B	C	D	SN removal (%)	TC-HCL removal (%)	SMZ removal (%)
29	1	0	0	0	0	75	88	68
13	2	-1	-1	1	1	52	86	59
19	3	0	-2	0	0	80	89	67
24	4	0	0	0	2	45	81	58
30	5	0	0	0	0	74	89	65
2	6	1	-1	-1	-1	92	91	86
3	7	-1	1	-1	-1	81	80	60

25	8	0	0	0	0	73	91	64
9	9	-1	-1	-1	1	51	84	58
21	10	0	0	-2	0	72	82	79
22	11	0	0	2	0	76	83	85
14	12	1	-1	1	1	65	83	66
17	13	-2	0	0	0	59	79	52
16	14	1	1	1	1	48	77	73
27	15	0	0	0	0	73	89	66
23	16	0	0	0	-2	97	94	74
1	17	-1	-1	-1	-1	82	77	65
12	18	1	1	-1	1	59	79	67
4	19	1	1	-1	-1	77	86	74
7	20	-1	1	1	-1	81	88	71
5	21	-1	-1	1	-1	90	85	65
10	22	1	-1	-1	1	68	86	75
11	23	-1	1	-1	1	49	83	60
6	24	1	-1	1	-1	97	92	88
26	25	0	0	0	0	70	86	65
18	26	2	0	0	0	72	83	80
28	27	0	0	0	0	72	90	64
20	28	0	2	0	0	68	84	68
8	29	1	1	1	-1	74	88	87
15	30	-1	1	1	1	52	89	69

The fitted quadratic regression equation in terms of coded factors for sulfanilamide, Tetracycline hydrochloride, and sulfamethazine removal efficiency at 90 min was expressed in **Eqs. (5-5), (5-6),** and **(5-7)** respectively.

$$Y_1 = 72.83 + 2.83X_1 - 4.17X_2 + 0.33X_3 - 13.92X_4 - 3.25X_{1X_2} - 1.50X_{1X_3} + 1.88X_{1X_4} - 1.37X_{2X_3} + 1.25X_{2X_4} - 1.25X_{3X_4} - 2.04X_1^2 + 0.083X_2^2 + 0.083X_3^2 - 0.67X_4^2 \quad \textbf{(5-5)}$$

$$Y_2 = 88.83 + 0.75X_1 - 1.00X_2 + 1.00X_3 - 1.92X_4 - 1.87X_{1X_2} - 1.62X_{1X_3} - 2.75X_{1X_4} + 0.38X_{2X_3} - 0.50X_{2X_4} - 1.00X_{3X_4} - 1.92X_1^2 - 0.54X_2^2 - 1.54X_3^2 - 0.29X_4^2 \quad \textbf{(5-6)}$$

$$Y_3 = 65.33 + 6.88X_1 + 0.042X_2 + 1.87X_3 - 4.21X_4 - 1.69X_{1X_2} - 0.56X_{1X_3} - 2.44X_{1X_4} + 2.81X_{2X_3} + 1.44X_{2X_4} - 1.19X_{3X_4} + 0.14X_1^2 + 0.51X_2^2 + 4.14X_3^2 + 0.14X_4^2 \quad \textbf{(5-7)}$$

where (Y_1, Y_2, Y_3) are the predicted sulfanilamide, tetracycline hydrochloride, and sulfamethazine removal efficiency (%), while (X_1, X_2, X_3, X_4) denotes the coded values of current density, pH, H_2O_2 dose, and initial concentration, respectively.

However, the relationship between the actual and model-predicted removal efficiencies of SN, TC-HCl, and SMZ are shown in the following **Figure 5-4.**

The data points are distributed closely around the 45° straight line, which indicates strong agreement between experimental and predicted values. This consistency confirms that the main

model assumptions were valid and that the selected quadratic models adequately describe the removal behaviour within the studied design space (Gaetan et al., 2025).

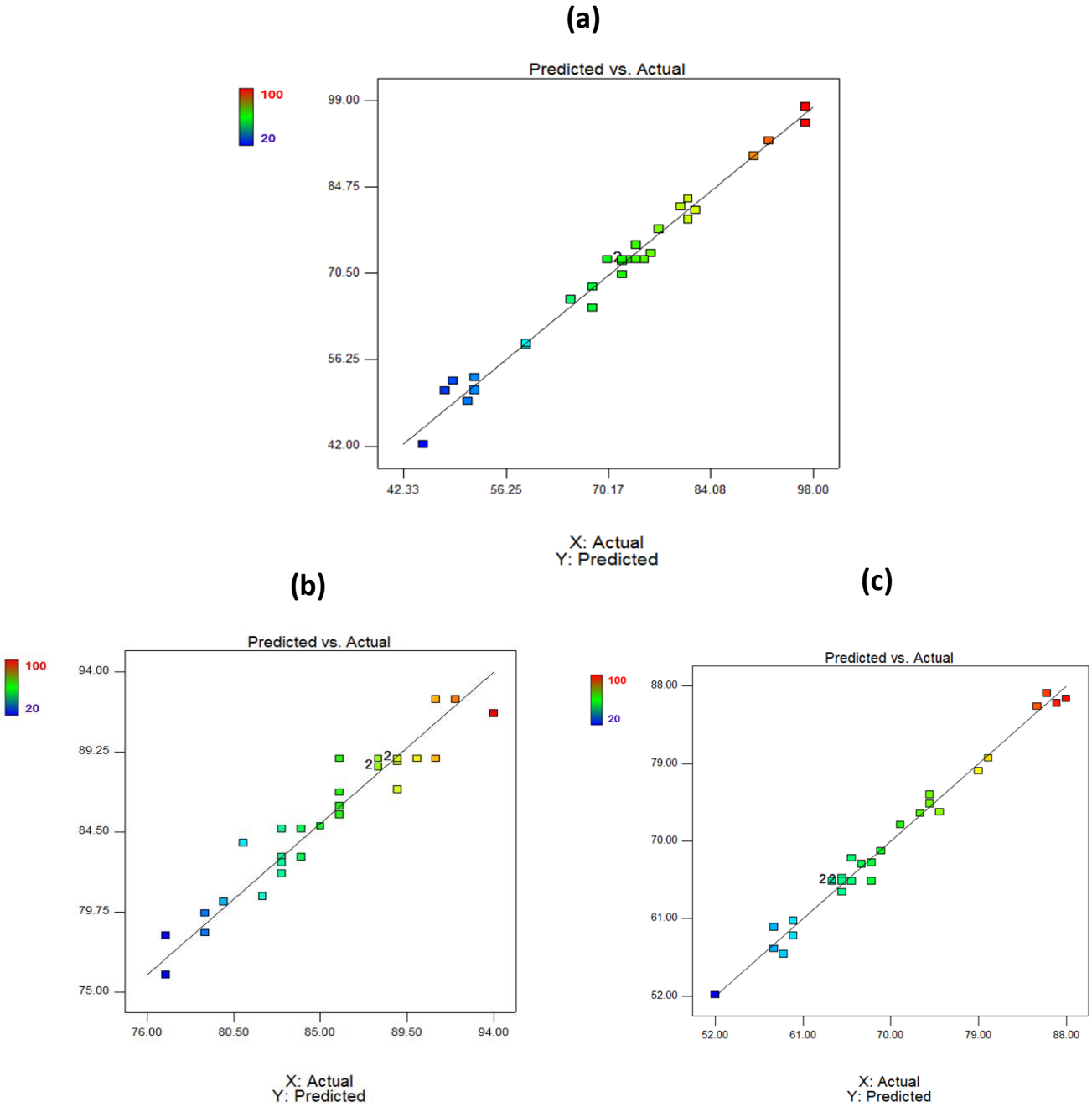

Figure 5-4. Actual vs predicted plots for SN (a), TC-HCL (b), and SMZ (c) at 90 minutes using the quadratic response surface models.

Furthermore, the diagnostic residual plots used to assess model adequacy are provided in the **appendix-C**, supplementary information. Residuals versus predicted values and residuals versus run order for SN, TC-, HCl, and SMZ are shown in **appendix-C, Fig. S1**and **S2.** In all cases, the residuals were randomly scattered around the zero line with no obvious pattern, and this indicates that the fitted models appropriately captured the experimental response behaviour. The absence of trends in the residuals versus run order further confirms the independence of experimental errors and the lack of time-dependent bias during the runs. These diagnostics show that the response surface models reliably predict the removal efficiencies of SN, TC-, HCl, and SMZ within the studied design region.

The statistical significance and adequacy of the developed response surface models were evaluated using analysis of variance (ANOVA), summarized in **appendix-C, Table S3.**

Table 5-3. Analysis of Variance **(**ANOVA) summary for the fitted response surface quadratic model

Response	**Model F value**	**Model *p*- value**	**Significant terms**	**Lack of fit *p*- values**	**Status**
Y_1: SN	71.58	< 0.0001	X_1, X_2, X_4, X_1X_2	0.174	
Y_2: TC-HCL	12.27	< 0.0001	X_4, X_1X_4, X_1^2	0.4949	Significant model; non-significant lack of fit

Y_3: SMZ	67.77	< 0.0001	X_1,X_3,X_4, X_1X_4, X_2X_3	0.4415

In general, model terms with *p*-values <0.05 are considered statistically significant, whereas terms with *p*-values >0.10 are usually regarded as insignificant at the selected confidence level (Asadollahzadeh et al., 2014). As shown in detail in **appendix-C,** Tables **S1 to S3**, the overall model *p*-values for all three responses, namely Y_1, Y_2, and Y_3, were <0.05, which confirms that the fitted models were statistically significant. This indicates that the proposed regression models are reliable and capable of describing the experimental response behaviour with acceptable accuracy (Kaur et al., 2018).

For response Y_1, the linear terms X_1, X_2, and X_4, together with the interaction term X_1X_2, showed statistically significant effects, which suggests that these factors played a dominant role in controlling the response. In the case of Y_2, the linear term X_4 and the model terms X_1X_4 and X_1^2 were identified as significant contributors. This indicates that both the individual effect of X_4 and the nonlinear contribution of X_1 strongly influenced the response. For Y_3, the linear effects of X_1, X_3, and X_4, along with the interaction terms X_1X_4 and X_2X_3 and the quadratic term X_3^2, were statistically significant. These results, summarized in **Table 5-3**, demonstrate that the response behaviour was directed not only by the individual process variables but also by their interactive and curvature effects.

The goodness-of-fit of the models was further confirmed by the coefficient of determination values, summarized in **Table 5-4.**

Table 5-4. Summary of model performance statistics for responses Y_1 (SN), Y_2 (TC-HCl), and Y_3 (SMZ), including major indicators of model fit, predictive accuracy, and adequacy

Statistics	**Y_1: SN**	**Y_2: TC-HCL**	**Y_3: SMZ**
Standard Deviation	2.39	1.77	1.61
Mean	70.8	85.40	69.27
C.V. (%)	3.38	2.07	2.32
PRESS	429.84	206.64	174.24
R-Squared	0.9853	0.9197	0.9844
Adj. R-Squared	0.9715	0.8447	0.9699
Pred. R-Squared	0.9261	0.6469	0.9300
Adeq. Precision	32.926	13.049	30.833

The R^2 values obtained for Y_1, Y_2, and Y_3 were 0.985, 0.919, and 0.984, respectively, indicating that 98.5%, 91.9%, and 98.4% of the total variability in the corresponding responses could be explained by the fitted models. Similarly, the adjusted R^2 values were 0.971, 0.844, and 0.969 for Y_1, Y_2, and Y_3, respectively. However, for TC-HCl, the low coefficient of variation (2.07%) and standard deviation (1.77) indicate good experimental precision, while the adequate precision value of 13.04, substantially >4, confirms an adequate model signal. Thus, the lower predicted (R^2) is more appropriately interpreted as reduced predictive robustness rather than excessive experimental variability. Consequently, the TC-HCl model remains useful for interpreting factor effects and guiding optimization within the investigated design space. But its predictions can not be considered with greater uncertainty than those of the SN and SMZ models, particularly when approaching the boundaries of or extrapolating beyond the experimental domain. However, overall

for all three compounds, the close agreement between R^2 and adjusted R^2 confirms that the models were not overfitted and that the selected terms adequately represented the relationship between the independent variables and the responses (J. Hu et al., 2020). Therefore, the regression equations can be considered statistically valid for interpreting the multi-factor experimental system and for predicting response values within the investigated design space.

5.3.2 CCD based response surface graphs, and their interaction patterns

The center-point response surface plots were first used to evaluate the general interaction patterns within the experimental domain. These plots were generated by varying two factors while holding the remaining variables at their central levels. These plots were used to visualize the local behavior of the model under the most favorable operating conditions for the selected three compounds, as shown in (**Figure 5-5).**

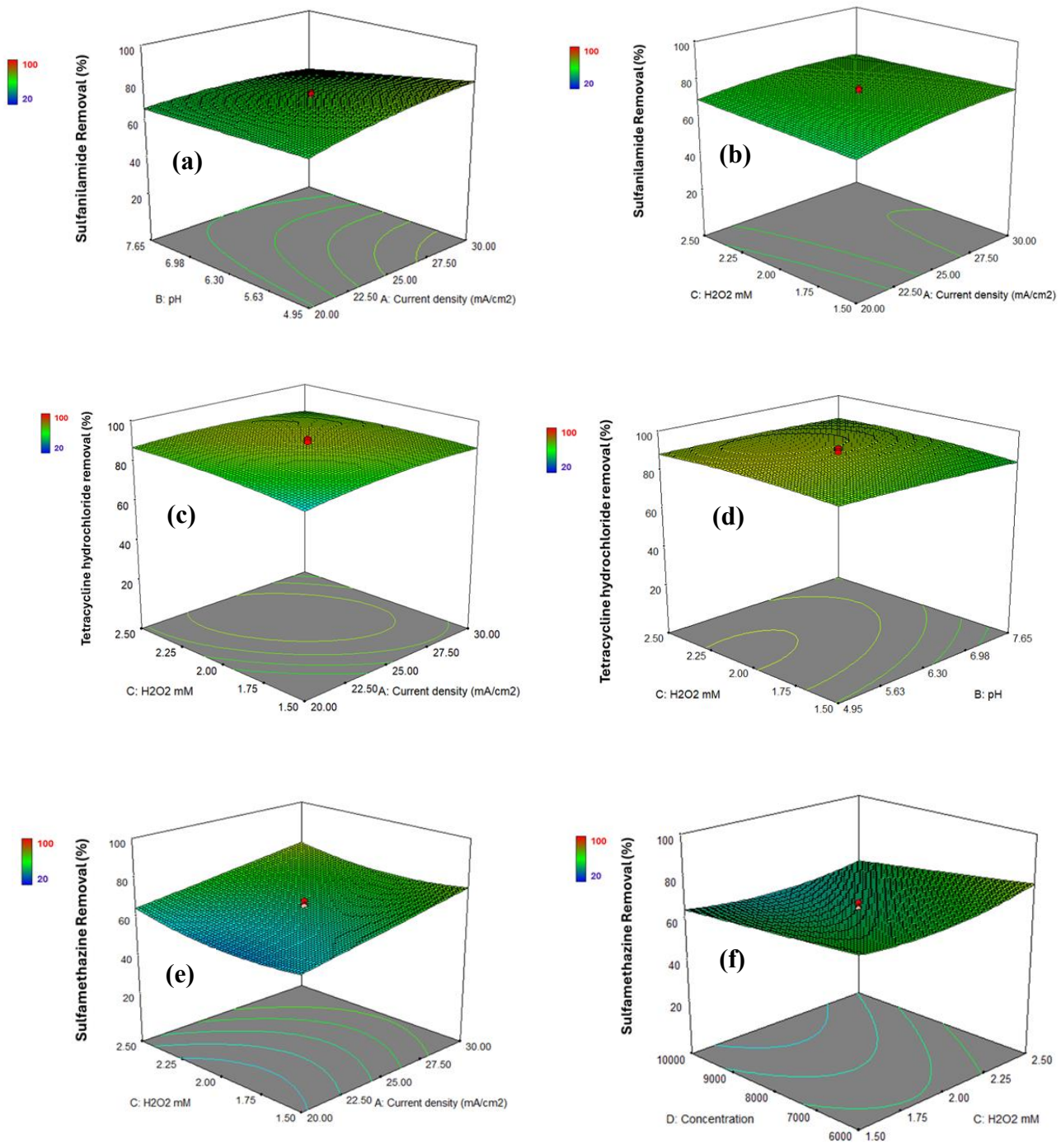

Figure 5-5. Response surface plots showing the interaction effects of current density, pH, H_2O_2 dose, and initial concentration on the removal efficiencies of SN, TC-HCl, and SMZ under centre-point conditions.

The subplots represent: (a) SN removal as a function of current density and pH at fixed, H_2O_2 dose = 2 mM and initial concentration = 8000 µg/L; (b) SN removal as a function of current density and, H_2O_2 dose at fixed pH = 6.30 and initial concentration = 8000 µg/L; (c) TC-HCl removal as a function of current density and, H_2O_2 dose at fixed pH = 6.30 and initial concentration = 8000 µg/ L; (d) TC-HCl removal as a function of pH and, H_2O_2 dose at fixed current density = 25.19 mA/cm^2 and initial concentration = 8000 µg/L; (e) SMZ removal as a function of current density and, H_2O_2 dose at fixed pH = 6.30 and initial concentration = 8000 µg/ L; and (f) SMZ removal as a function of, H_2O_2 dose and initial concentration at fixed current density = 25.19 mA/ cm^2 and pH = 6.30.

The response surface plots were generated by varying two independent variables at a time while keeping the remaining factors fixed. For general interaction interpretation, the unplotted factors were initially maintained at their center-point levels. Additional optimization-oriented plots were then generated by fixing the unplotted factors, which are near the predicted optimum condition. This approach allowed both the general curvature of the response surface and the local behavior around the optimum region to be evaluated. The 90 min removal efficiencies were selected for RSM modelling because this treatment interval provided sufficient response variation.

Figure 5-5 of the response surface plots showed compound-specific differences in removal behavior at centre-point conditions of 25 mA/ cm^2, pH 6.30, 2.0 mM H_2O_2, and 8000 µg/L initial antibiotic concentration. From **figures 5-5(a) and 5-5(b),** the response surfaces for SN appear comparatively flat, indicating weak curvature and modest interaction between current density and pH or H_2O_2 dose. This suggests that sulfanilamide removal in the investigated region is relatively strong and mainly influenced by the main effect of current density, with pH contributing a secondary influence. This type of behavior is consistent with the dual contribution of direct electro-

oxidation and hydroxyl-radical attack to sulfanilamide degradation, together with the known susceptibility of sulfonamides to aromatic hydroxylation and S–N/C–S bond cleavage (Kim et al., 2024).

In contrast, TC-HCl showed the highest response levels and the strongest quadratic dependence among the three antibiotics. The dome-shaped surfaces and closed elliptical contours in panels **5-5(c) and 5-5(d)** indicate that both current density and H_2O_2 dose contribute positively up to an optimum region, while deviations occurred toward lower oxidant supply or suboptimal conditions, pH reduces removal. The broad high-response region around the centre point indicates that TC-HCL is highly responsive to peroxide-assisted electrochemical degradation in this operating window. This interpretation is supported by recent tetracycline studies, which showed improved removal with increasing H_2O_2 dosage and noticeable transformation through hydroxylation, demethylation, deamination, and ring-opening reactions (Espinoza-Montero et al., 2022; Xiaobao Li et al., 2022; Nguyen et al., 2025; N. Oturan et al., 2013).

The SMZ plots exhibited the strongest dependence on oxidant availability relative to pollutant loading. While panel **5-5(e)** shows that increasing current density progressively enhances sulfamethazine removal, panel **5-5(f)** demonstrates a marked interaction between H_2O_2 dose and initial concentration. For SMZ, the highest removal was obtained at high oxidant dosage and low initial SMZ concentration. The downward slope at higher concentration confirms that SMZ removal is limited by the available oxidant-to-substrate ratio under centre-point current density and pH conditions. This behavior is consistent with the hydroxyl-radical-dominated degradation of sulfamethazine reported in recent Electro Fenton (EF) and photo-Fenton-like studies, in which bond cleavage, hydroxylation, deamination, and ring opening were identified as the dominant

transformation routes (El-Ghenymy, Cabot, et al., 2013; W. Wang et al., 2020; Xuechun Wang et al., 2023).

Across the tested factor space, **Figure 5-5** reveals a clear reactivity order of TC-HCl > SN > SMZ, with TC-HCl displaying the largest high-efficiency domain. On the other hand, SN exhibited the most stable but less strongly curved response, and SMZ showed the greatest sensitivity to oxidant dosage and pollutant loading. Therefore, from a process-optimization perspective, current density appears to be the most influential shared factor, whereas the definite secondary variable is pH for TC-HCl and H_2O_2 dose/initial concentration balance for SMZ. This pattern is fully consistent with other advanced electro literature, which identifies pH, current density, H_2O_2 generation, and substrate concentration as the main variables controlling hydroxyl-radical flux, thus, antibiotic removal efficiency (Espinoza-Montero et al., 2022; Xiaobao Li et al., 2022; Nguyen et al., 2025; N. Oturan et al., 2013).

However, applying too much higher current density may reduce electrolysis efficiency due to intensified side reactions, such as hydrogen and oxygen evolution, radical recombination, and interfacial Joule heating, which can alter radical availability, reaction kinetics, and mass-transfer behavior, on the BDD electrode, expressed by **Eq. (5-8) and Eq. (5-9)** (J. Hu et al., 2020; Pei et al., 2019; H. Qi et al., 2023).

$$2H_2O + 2e^- \rightarrow H_2 + 2OH^- \quad \textbf{(5-8)}$$

$$2H_2O \rightarrow O_2 + 4H^+ 4e^- \quad \textbf{(5-9)}$$

Thus, the effect of current density is beneficial only within an appropriate operating range that supports the need for RSM-based optimization rather than simply applying the highest current density. However, in the present research, it has been observed that the removal efficiency for antibiotics removal is much higher in low pH conditions. The increased antibiotic removal at lower

pH is due to the higher oxidation potential of •OH and the reduced loss of reactive radicals through oxygen evolution (Schranck & Doudrick, 2020). Because •OH were not easily converted into oxygen according to **Eq. (5-10).**

$$2 \bullet OH + H_2O \rightarrow O_2 + 3H^+ + 3e^- \quad \textbf{(5-10)}$$

Furthermore, acid catalysis increases the generation of $S_2O_8^{2-}$, which later boosts the production of SO_4^{-}• and contributes to enhancing the oxidative degradation of SN, TC-HCL, and SMZ **Eq. (5-11) and Eq. (5-12)** (Nashat et al., 2022). Also, in low pH conditions, the BDD electrode edge undergoes a two-electron oxygen reduction reaction ($2e^-$ORR), which is more conducive for producing H_2O_2(aq)), represented in **Eq. (13)** (S. Hu et al., 2025a)**.** This, H_2O_2, is more easily decomposed to produce •OH and other active substances under acidic conditions.

$$H^+ + S_2O_8^{2-} \rightarrow HS_2O_8^- \quad \textbf{(5-11)}$$

$$HS_2O_8^- + e^- \rightarrow H^+ + SO_4^{2-} + SO_4^- \bullet \quad \textbf{(5-12)}$$

$$H_2O_2\ (O_2(g) + 2H^+(aq) + 2e^- \rightarrow H_2O_2(aq)) \quad \textbf{(5-13)}$$

As pH increases, the oxidative potential decreases according to **Eq. (5-14)**, which may reduce the ability of the BDD-generated oxidants to attack SN, TC-HCl, SMZ, and their transformation products (J. Hu et al., 2020; Schranck & Doudrick, 2020).

$$E = 2.59 - 0.059 \times pH \quad \textbf{(5-14)}$$

This supports the observed improvement in removal efficiency under acidic-to-mildly acidic conditions in the optimized Nb/BDD electrooxidation system.

5.4 Optimization criteria and verification of the optimal condition

The optimization criteria were selected to maximize the simultaneous removal efficiencies of SN, TC-HCl, and SMZ while maintaining the operational variables within the experimentally investigated CCD range, as summarized in **Table 5-5.** Therefore, verifying model accuracy is an

important step in response surface methodology, as it confirms the predictive reliability of the optimized conditions before experimental confirmation (Nekouei & Nekouei, 2017)**.**

Table 5-5. Optimization criteria used for multi-response desirability analysis of SN, TC-HCl, and SMZ removal under the CCD-RSM framework

Variable/response	**Goal**	**Lower Limit**	**Upper Limit**	**Weight**	**Weight**	**Importance**
X_1: Current densities	is in range	20.38	30	1	1	3
X_2: pH	is in range	4.95	7.65	1	1	3
X_3: H_2O_2	is in range	1.5	2.5	1	1	3
X_4: Concentration	is in range	6000	10000	1	1	3
Y_1: SN removal	maximize	60	98	1	1	3
Y_2: TC-HCL removal	maximize	60	98	1	1	3
Y_3: SMZ removal	maximize	60	98	1	1	3

To verify the accuracy of the model, the optimal parameters calculated by the model were selected for the verification experiment. The experimental validation was conducted under the optimized operating condition predicted by the multi-response desirability function with a current density of 30 mA/ cm^2, pH 4.95, H_2O_2 dose of 2.5 mM, and initial antibiotic concentration of 6000 µg/ L. At this condition, the quadratic RSM model predicted removal efficiencies are 95.32%, 92.35%, and 86.16% for sulfanilamide, TC-HCl, and sulfamethazine, respectively. For the present study, the individual desirability for maximization and overall desirability were calculated by Derringer and Suich's desirability function approach, where each response was transformed into an individual

desirability function ranging from 0 to 1 (Derringer & Suich, 1980). For maximization responses, the individual desirability was calculated by the following **Eqs. (5-15).**

$$d_i = \left(\frac{Y_i - L_i}{T_i - L_i}\right)^{\{w_i\}} \quad \textbf{(5-15)}$$

where $Y_i$is the predicted response, $L_i$is the lower acceptable limit, $T_i$is the target value, and $w_i$is the weighting factor. The overall desirability was determined using the geometric mean of all individual desirabilities, as shown in the following **Eqs. (5-16).**

$$D = (d_1 \times d_2 \times d_3 \times \ldots \times d_n)^{\frac{1}{n}} \quad \textbf{(5-16)}$$

In the present study, the lower and upper target limits for antibiotic removal efficiencies were fixed at 60% and 98%, respectively, and equal importance was assigned to all responses. Based on the optimization criteria selection and the above **Eqs. (5-15) and (5-16)** implementation, the individual desirability for SN, TC-HCL, and SMZ was found to be 0.929, 0.851, and 0.688, respectively, as summarized in **Table 5-6,** and the overall desirability was 0.817 as shown in **(Figure 5-6).**

Table 5-6: Experimental validation of the optimal condition

Response	**Predicted removal (%)**	**Experimental removal (%)**	**Error (%)**	**Individual Desirability (*di*)**
SN	95.32	97.00	1.73	0.929
TC-HCl	92.35	95.50	4.30	0.851
SMZ	86.16	88.00	4.27	0.688

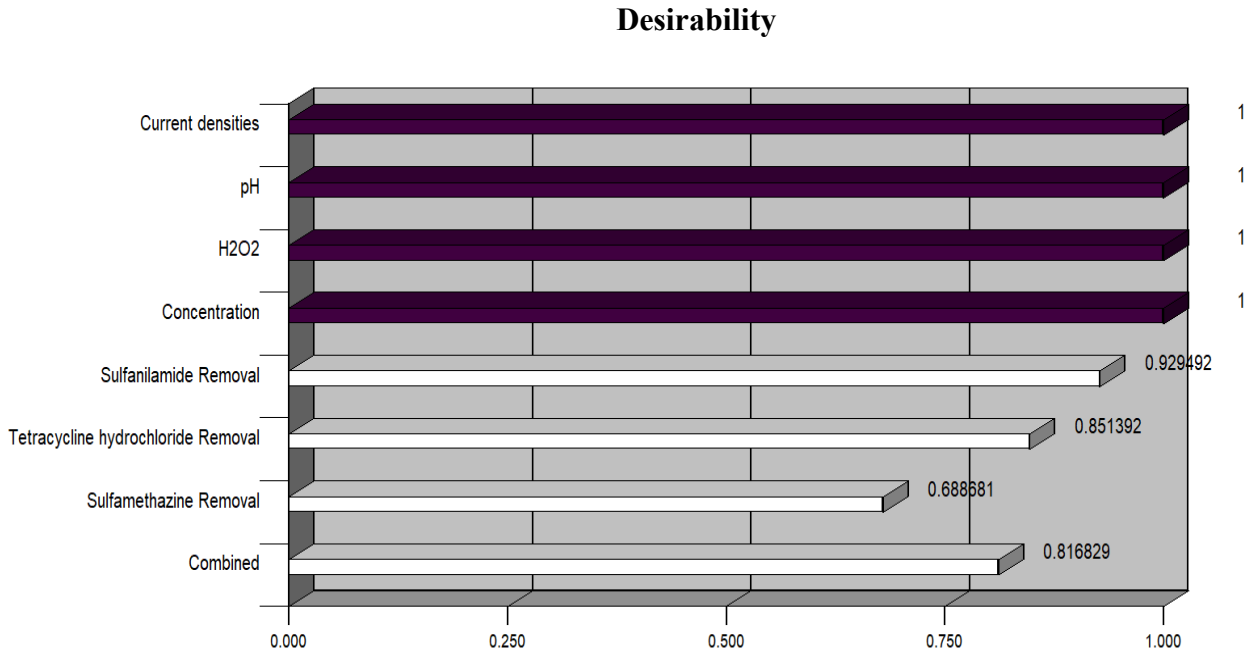

Figure 5-6: Bar graph of individual and overall desirability values obtained from the multi-response optimization of SN, TC-HCl, and SMZ removal under the selected CCD-RSM optimum condition**.**

However, the corresponding experimental removal efficiencies in the optimum conditions were found to be 97%, 96.50%, and 90% for SN, TC-HCl, and SMZ, respectively. These removal efficiencies confirm the close agreement between the predicted and observed responses. The prediction error was calculated using the following formula **(5-17).**

$$\boldsymbol{Error}\ (\%) = \frac{|\text{Experimental value} - \text{Predicted value}|}{\text{Experimental value}} \times 100 \qquad \textbf{(5-17)}$$

The relatively high desirability value indicates that the selected condition provides a balanced compromise for the simultaneous removal of the three target antibiotics rather than maximizing a single response independently. A detailed optimum operating condition (X_1–X_4) and predicted removal efficiencies (Y_1–Y_3) with overall desirability have been shown in **appendix-C, Table S4** of the supplementary information.

The calculated errors were 1.73% for sulfanilamide, 4.30% for TC-HCl, and 4.27% for sulfamethazine and are summarized in the above **Table 5-6** as experimental validation of the optimal conditions. These low error values and individual desirability close to 1 indicate that the developed quadratic models provided a reliable prediction of the removal efficiencies within the selected experimental domain. The close agreement between the model-predicted and experimentally validated results further confirms the adequacy of the CCD-based RSM approach for optimizing the simultaneous electrochemical removal of the three targeted antibiotics.

The optimized condition suggests that improved degradation was favored under higher current density, particularly at 30 mA/cm^2, acidic pH at 4.95, and moderate H_2O_2 addition. The positive role of current density can be attributed to enhanced electrochemical generation of oxidizing species at the BDD surface, while the acidic condition likely improved the oxidative environment for antibiotic degradation. However, increasing current density beyond this 30 mA/cm^2 could be economically not favorable because higher current can increase energy consumption and promote parasitic reactions such as oxygen evolution.

Previous research showed that, the second order rate constants for reaction with •OH are of the order of 10^9 M^{-1} s^{-1} for all three antibiotics. Literature values are approximately 4.5 $\times 10^9$ M^{-1} s^{-1} for SN, 6.3 $\times 10^9$ M^{-1} s^{-1} for TC, and 5.27 to 6.07 $\times 10^9$ M^{-1} s^{-1} for SMZ, depending on experimental conditions (Jeong et al., 2010; Mezyk et al., 2007; Sági et al., 2015). Thus, all three are highly

reactive toward hydroxyl radicals. However, these intrinsic rate constants are not directly equated with our observed removal efficiencies because the BDD system is controlled by radical availability, pH-dependent speciation, mass transfer, competitive scavenging, direct anodic oxidation, and other oxidation pathways. Thus, from the literature, the intrinsic •OH reactivity broadly follows TC > SMZ > SN. In contrast, for the present study, the experimentally observed removal at the optimized condition followed SN (97.0%) > TC-HCl (95.5%) > SMZ (88.0%). This difference indicates that the removal behaviour cannot be explained by •OH reaction constants alone. In BDD electrooxidation, hydroxyl radicals are generated close to the anode surface, and pollutant removal may also involve direct anodic oxidation, mass-transfer effects, compound speciation, and competitive reactions among the parent antibiotics and their transformation products (Groenen-Serrano et al., 2013). Therefore, the literature K_{OH} values support the potential involvement of hydroxyl radicals but do not predict the observed removal ranking. Because radical scavenging or probe experiments were not conducted and for this reason the relative contribution of •OH oxidation cannot be quantified from the present study.

Furthermore, the developed CCD based RSM models describe the effect of H_2O_2 only within the investigated experimental range of 1 to 3 mM and did not include a zero H_2O_2 condition. This H_2O_2 was not used to quantify improvement relative to electrooxidation alone. Similarly, mineralization and energy efficiency were not compared under matched conditions with and without H_2O_2. This type of comparison would require identical operating conditions and consideration of both electrical energy consumption and chemical oxidant demand (Miklos et al., 2018). The present results therefore be interpreted as optimization of H_2O_2 assisted Nb/BDD electrooxidation rather than evidence of its superiority over electrooxidation alone. The selected H_2O_2 dose of 2.5 mM indicates that moderate oxidant addition was beneficial, whereas excessive

oxidant addition may not be necessary and could potentially reduce process efficiency through radical scavenging. Similarly, the lower initial concentration of 6000 μg/L favored higher percentage removal, reflecting the greater availability of oxidizing species relative to the contaminant load. Overall, the optimized condition represents an effective operating window for simultaneous treatment of sulfanilamide, TC-HCl, and sulfamethazine using the CCD-based quadratic RSM model.

5.5 Short-term reproducibility of the Nb/BDD electrode system

The close agreement between the CCD-RSM predicted and experimentally validated removal efficiencies, with relative deviations of 1.76–3.41%, indicated satisfactory short-term reproducibility of the Nb/BDD electrode reactor system. No significant reduction in removal performance was evident during the experimental run. However, the central composite design evaluated current density, pH, H_2O_2 concentration, and initial antibiotic concentration and did not include electrode use cycle or cumulative operating time as independent factors. Therefore, the RSM results confirm process reproducibility but do not constitute a direct assessment of long-term electrode durability.

BDD electrodes are generally characterized by high chemical and electrochemical stability, high oxygen-evolution overpotential, and relatively strong resistance to organic fouling which make them suitable for the electrochemical oxidation of refractory organic contaminants (Carolina Espinoza et al., 2021; Karim et al., 2021; Panizza et al., 2002). However, their practical stability mainly depends on the boron-doping level, sp^3/sp^2 carbon content, diamond film integrity, substrate properties, surface chemistry, and composition of the treated water (Carolina Espinoza et al., 2021; Karim et al., 2021; Panizza et al., 2002). Although •OH mediated oxidation in the oxygen evolution region can limit the accumulation of organic deposits, direct oxidation of certain

aromatic compounds may produce polymeric films and cause surface fouling under some operating conditions (Panizza et al., 2002). For the present study, no consecutive reuse experiments under identical conditions or pre and post use surface analyses were performed. Therefore, minor electrode fouling or gradual activity loss cannot be completely excluded. Further studies require to assess repeated treatment cycles together with cell voltage monitoring and electrochemical or surface characterization.

5.6 TOC Mineralization, energy consumption, and cost estimates

For the present research, RSM optimization was developed using the removal efficiencies of SN, TC-HCl, and SMZ as the primary responses. Based on the RSM optimization condition for the parent compound removal, TOC analysis was also performed to evaluate the TOC mineralization efficiency. Total organic carbon (TOC) represents the concentration of carbon contained in the organic constituents of a water sample and is expressed as mg C/L. In contrast, chemical oxygen demand (COD) represents the oxygen equivalent required for chemical oxidation of oxidizable compounds and is expressed as mg O_2/L. In the present study, HPLC was used to quantify the parent antibiotics, whereas TOC was used as an indicator of mineralization. Although TOC and COD both indicate bulk organic contamination, their relationship is matrix-specific and may change during oxidation. Therefore, TOC values were not converted to COD in the absence of a validated experimental correlation (Al-Qodah, Al-Shannag, et al., 2024; Wojnárovits et al., 2024). However, for the present study, in the optimized condition at 30 mA/cm^2, pH 4.95, H_2O_2 dose of 2.5 mM, initial antibiotic concentration of 6000 µg/L, and 90 min treatment time, the experimental removals of SN, TC-HCl, and SMZ were 97%, 95.50%, and 88%, respectively. These results confirm high parent-compound removal; however, TOC analysis was required to assess whether oxidation proceeded towards mineralization or generated further transformation of the parent

antibiotics. Because in the electrooxidation process, it may generate transformation products before conversion to CO_2, H_2O, and inorganic ions. Additionally, hydroxyl radical-mediated oxidation, such as the BDD electrode, usually proceeds through sequential hydroxylation, bond cleavage, ring opening, and formation of low-molecular-weight organic acids before final mineralization (El-Ghenymy et al., 2013). Therefore, TOC removal at the optimum condition was used as a supporting indicator of the mineralization efficiency of the Nb/BDD electrooxidation process. Previous BDD-based studies have reported that parent-antibiotic removal can be faster than TOC reduction because TOC mineralization requires further oxidation of aromatic and short-chain intermediates (Brinzila et al., 2014; Fabiańska et al., 2014; J. Hu et al., 2020). TOC removal was calculated using the following **Eq. (5-18):**

$$TOC\ removal\ (\%) = \left(\frac{TOC_0 - TOC_t}{TOC_0}\right) \times 100 \quad \textbf{(5-18)}$$

where TOC_0 is the initial TOC before electrooxidation and TOC_t is the TOC after treatment at the optimum time. Under the optimum operating conditions, the influent TOC (TOC_0) was 85 mg/L and effluent (TOC_t) was 20 mg/L after 90 minutes of electrooxidation with an overall TOC removal efficiency of 76.47%.

The result of TOC reduction indicates that the Nb/BDD electrooxidation process not only degrades SN, TC-HCl, and SMZ into intermediate products but also promotes higher mineralization of dissolved organic carbon. This interpretation is consistent with the known behavior of BDD anodes highlighted in previous research and is effective for mineralization because of their high oxygen evolution overpotential, low adsorption behavior, electrochemical stability, and efficient generation of •OH at the anode surface (Mehrkhah et al., 2025). The TOC removal observed in the present study is also consistent with the previous BDD-based antibiotic degradation studies, where parent-compound removal occurred rapidly but the TOC reduction is comparatively low and

required longer oxidation (S. Hu et al., 2025). This occurs due to transformation products and low-molecular-weight organic acids, which are not easily degradable during electrolysis. The high TOC removal also suggests that the H_2O_2 assisted Nb/BDD system provided sufficient oxidative capacity for deeper degradation of the antibiotic mixture. Therefore, the TOC decrease from 85 to 20 mg/L provides important supporting evidence for TOC mineralization beyond HPLC-based parent-antibiotic removal. Recent review also mentioned that antibiotic degradation in EAOPs is controlled by electrode material, initial concentration, electrolyte composition, operating conditions, and water matrix, all of which influence degradation pathways, intermediate formation, and toxicity evolution (Yuan et al., 2023).

From an engineering perspective, the combined parent-compound removal and TOC results demonstrate that the optimized Nb/BDD electrooxidation process achieved both high antibiotic removal and significant TOC mineralization within 90 min. This level of mineralization is comparable to recent BDD-based antibiotic oxidation studies, where high COD or TOC removal was achieved when sufficient current density and treatment time were applied (Gaetan et al., 2025; Hai et al., 2020). For example, BDD oxidation of sulfamethoxazole achieved complete parent-compound removal after 3 hours of operation, and COD removal was 65.6% under optimized conditions (Hai et al., 2020). Similarly, BDD pulsed electrooxidation of levofloxacin achieved 94.4% COD removal within 120 min with an energy consumption of 81.43 kWh/m^3. This result indicates the relation of mineralization performance with energy demand in evaluating antibiotic wastewater treatment (Xu et al., 2023). (Al-Qodah, Al-Zghoul, et al., 2024) achieved 95.5% COD removal using an integrated electrocoagulation–adsorption system for pharmaceutical wastewater. Similarly, (Al-Qodah, Al-Shannag, et al., 2025) reported 97.1% overall TOC removal using sequential chemical coagulation, solar-powered electrocoagulation, and adsorption for dairy

wastewater. Electrocoagulation may be considered as a pretreatment step when the process is applied to real wastewater with high TOC, suspended solids, or colloidal matter. However, the technical and economic benefits of combining electrocoagulation with Nb/BDD electrooxidation require separate validation using real municipal or hospital wastewater.

Overall, the TOC result from our study supports the optimized condition and confirms the practical application of H_2O_2 assisted Nb/BDD electrooxidation as an advanced oxidation process for mixed pharmaceutical removal from wastewater. However, the mineralization current efficiency was calculated based on the TOC basis, and the efficiency was found to be ~9.7% calculated by the following **Eqs. (5-19).**

$$MCE\ (\%) = \left(\frac{4FV\Delta TOC}{12It}\right) \times 100 \quad \textbf{(5-19)}$$

Where, $F = 96485$ C/mol, $V = 3$ L, ΔTOC $= 0.065$ g/L, $I = 12$ A and $t = 5400$ s

The total electrical energy consumed by the EO reactor during the 90-minute run was found to be 0.198 kWh through the following **Eqs. (5-20)** and the specific energy consumption per unit volume of treated wastewater (SEC, kWh/m^3) was found to be 66 kWh/m^3 from the following Eqs. **(5-21).**

$$P = UI = 11 \times 12 = 132\ \text{W} \quad \textbf{(5-20)}$$

$$E = P \times t = 132\ \text{W} \times 1.5\ \text{h} = 198\ \text{Wh} = 0.198\ \text{kWh}$$

$$SEC = \left(\frac{UIT}{V \times 1000}\right) \quad \textbf{(5-21)}$$

Where U is the average cell voltage (V), I is the applied current (A), t is the electrolysis time (h), and V is the treated volume (m^3).

The electrooxidation process removed 195 mg (0.195 g) of TOC, corresponding to a specific energy consumption of 1015 kWh/kg of TOC removed.

$m_{\text{TOC, removed}} = 65\ \text{mg/L} \times 3\ \text{L} = 195\ \text{mg} = 0.195\ \text{g} = 1.95 \times 10^{-4}\ \text{kg}$

$$\text{EC}_{\text{TOC}} = \frac{0.198}{1.95 \times 10^{-4}} \approx 1015\ \text{kWh/kg TOC removed}$$

From the mineralization current efficiency, it was observed that a significant portion of the applied current was effectively utilized for organic mineralization, along with some side reactions such as oxygen evolution. Operational cost was calculated based on Manitoba Hydro industrial rates, which are 9.864 ¢/kWh. The estimated operational cost per cubic meter of treated wastewater and cost per kg of TOC removed were found to be 6.51 CAD/m^3 and 1001 CAD/kg TOC removed.

Cost per $m^3 = 66 \times 0.09864 = 6.51\ CAD/m3$

Cost per kg TOC $= 1015 \times 0.09864 = \sim 100.15\ CAD/kg$ TOC removed

The mineralization efficiency and an estimated operational cost of 6.51 CAD/m^3 indicate that Nb/BDD electrooxidation is better suited as an advanced polishing step for antibiotic-containing wastewater.

5.7 Conclusion and future recommendations

The RSM model based on a central composite design successfully optimized H_2O_2-supplemented Nb/BDD electrooxidation for the simultaneous treatment of SN, TC-HCl, and SMZ in biologically treated synthetic wastewater. For sulfanilamide, the linear H_2O_2 term was not statistically significant within the investigated concentration range which indicates that variations in H_2O_2 concentration did not produce a measurable independent effect on sulfanilamide removal after accounting for the other model factors. Therefore, the sulfanilamide response is not interpreted as

evidence of H_2O_2-enhanced oxidation. Its removal was more strongly influenced by current density, pH, initial concentration, and the interaction between current density and pH.

In contrast, H_2O_2-related model terms influenced the responses of the other target compounds and contributed to the simultaneous optimization of the three removal efficiencies. This result indicates that H_2O_2 supplementation may affect individual antibiotics differently because of differences in molecular structure, reaction kinetics, electrode interactions, and susceptibility to the oxidizing species present in the system. Also, the added H_2O_2 may undergo electrode-mediated oxidation or reduction reactions and may contribute to the reactive-oxygen-species pool. Nevertheless, the specific activation pathway and the relative contribution of H_2O_2-derived species were not directly determined. Accordingly, the process is described as BDD-based electrochemical oxidation with H_2O_2 supplementation, and the close agreement between predicted and experimental removal efficiencies confirmed the reliability of the developed model and showed that the selected design space adequately represented the process behavior. Among the operating variables, current density provided the major electrochemical driving force for the selected antibiotic degradation, while pH, H_2O_2 dose, and initial concentration modified the response through changes in antibiotic speciation, radical availability, and oxidant demand.

The optimized conditions of 30 mA/cm^2, pH 4.95, 2.5 mM H_2O_2, and 6000 µg/L initial concentration resulted in experimental removals of 97%, 95.50%, and 88% for SN, TC-HCl, and SMZ, respectively. The corresponding TOC reduction of 76.47% confirmed that the process achieved substantial mineralization rather than only parent-compound removal. Energy analysis showed a specific energy consumption of 66 kWh/m^3 and an estimated electrical cost of 6.51 CAD/m^3, indicating that the process is technically promising and could be used as a targeted advanced treatment or polishing step.

Future recommendations

- Future development and research could extend the optimization framework by incorporating TOC removal, toxicity reduction, and energy consumption as additional response variables. This would allow the process to be optimized not only for parent-antibiotic removal but also for mineralization efficiency and operational feasibility.
- Further analysis of transformation products using LC-MS/MS or high-resolution mass spectrometry is recommended to clarify degradation pathways and assess the potential persistence and toxicity of intermediate compounds.
- The optimized process also needs to be tested with real wastewater matrices because chloride, sulfate, bicarbonate, ammonia, and natural organic matter may influence radical chemistry, by-product formation, and current efficiency. Further mechanistic studies using scavenger experiments and carefully controlled EPR measurements are required to determine the relative contribution of individual reactive species.
- Although the RSM validation confirmed satisfactory short-term reproducibility, further continuous flow and long-term cycling experiments, along with surface characterization, are required to evaluate electrode stability, fouling, voltage behavior, treatment cost, and overall practical applicability under realistic operating conditions. These measurements could be complemented by electrochemical and surface analyses, such as cyclic voltammetry, electrochemical impedance spectroscopy, scanning electron microscopy, Raman spectroscopy, or X-ray photoelectron spectroscopy.
- For future application to real municipal or hospital wastewater, suspended solids production, cathodic scaling, electrode wear, and dissolved metals needs to be monitored before estimating sludge handling costs and total cost estimations.

- Future studies could evaluate the operation of the Nb/BDD electrooxidation system using photovoltaic electricity. Because the process is operated under galvanostatic conditions, solar integration may include suitable power conditioning and, where required, energy storage to maintain the selected current density during variations in solar irradiance. The assessment should consider electrical energy consumption, H_2O_2 demand, electrode stability, and total treatment cost. Solar-powered electrocoagulation has shown potential for reducing grid-energy demand in combined wastewater-treatment systems (Al-Qodah, Al-Shannag, et al., 2024).
- For scale up operation, electrocoagulation could be selected as a pretreatment option for wastewaters containing organic and inorganic pollutants (Al-Qodah, AL-Rajabi, Al Amayreh, et al., 2025; Al-Qodah, AL-Rajabi, Da'na, et al., 2025). Accordingly, a combined continuous system consisting of electrocoagulation pretreatment followed by Nb/BDD electrooxidation may be investigated. The electrocoagulation stage could reduce suspended, colloidal, and bulk organic matter, while the Nb/BDD stage could provide oxidative removal of residual pharmaceutical compounds. This type of treatment would require separate optimization of pharmaceutical removal, mineralization, sludge production, transformation products, toxicity, and operating cost.

Chapter 6: Conclusion

6.1 Integrated conclusion

The findings of this thesis showed that BDD electrooxidation is a highly effective treatment technology for the removal of organic matter, color, and nutrients from landfill leachate, as well as for the degradation of selected antibiotics in wastewater. These outcomes are achieved when the operating conditions are properly optimized. In Chapter 3, BDD electrooxidation was applied to landfill leachate for the removal of COD, color, ammonium, and phosphate. The results showed that current density and pH were important operating variables controlling the treatment performance. The use of factorial design, RSM, ANOVA, and desirability profiling provided a systematic basis for identifying suitable operating conditions. This chapter confirmed that BDD electrooxidation can improve the quality of landfill leachate treatment by targeting pollutants that are often difficult to remove using biological treatment alone. In Chapter 4, the study was extended to the removal of a ternary antibiotic mixture containing sulfanilamide, tetracycline hydrochloride, and sulfamethazine. The results demonstrated that antibiotic removal was strongly influenced by current density, pH, treatment time, and initial concentration. Current density increased the formation of oxidizing species at the BDD surface, while pH affected antibiotic speciation and oxidant activity. Treatment time improved removal by increasing oxidant exposure, where a higher initial concentration increased oxidant demand and reduced removal efficiency under limited operating conditions. These findings showed that mixed pharmaceutical removal cannot be fully understood from single-factor or single-compound behaviour. In Chapter 5, RSM was used to optimize H_2O_2-supplemented Nb/BDD electrooxidation for simultaneous removal of SN, TC-HCl, and SMZ. The optimum condition was identified at 30 mA/ cm^2, pH 4.95, 2.5 mM H_2O_2, and 6000 µg/ L initial antibiotic concentration at 90 min. Under this condition, the model predicted removals

of 95.32%, 92.35%, and 86.16% for SN, TC-HCl, and SMZ, respectively, with an overall desirability of 0.817. Experimental validation confirmed close agreement with the predicted values, achieving 97%, 95.50%, and 88% removal, respectively. These results confirmed the suitability of the RSM model and the reliability of the selected design space. The TOC analysis provided further evidence that the optimized process achieved more than parent-compound removal. TOC removal was achieved to 76.47% mineralization. This result indicates significant oxidation of organic carbon and transformation products during treatment. The energy input under the optimized condition was 0.198 kWh for a 3.0 L batch, equal to 66 kWh/m³. The estimated electrical cost was 6.51 CAD/ m^3. These values show that Nb/BDD electrooxidation is technically effective but energy intensive. Overall, the thesis confirmed that BDD electrooxidation could be used as an advanced polishing treatment option for refractory compounds removal in wastewater under optimized conditions.

6.2 Engineering significance

This thesis has practical significance for advanced wastewater treatment because it evaluates BDD electrooxidation across two important environmental applications; landfill leachate treatment and antibiotic-contaminated wastewater. These two types of wastewater contain contaminants that are difficult to remove by conventional biological treatment. Landfill leachate may contain refractory organic matter, ammonium, phosphate, color, and inorganic constituents. Pharmaceutical wastewater may contain persistent antibiotics and biologically active transformation products. The results show that BDD electrooxidation can be used as a flexible treatment platform for both types of contamination.

The work is significant because it links pollutant removal with process optimization. In engineering practice, treatment efficiency alone is not sufficient as it also requires assessing the

operating conditions, energy demand, treatment time, and process reliability. This thesis used RSM, factorial design, ANOVA, and desirability functions to identify suitable operating regions rather than relying on one factor at a time testing. This approach provides stronger decision support for process design and scale-up.

For landfill leachate, the findings support the use of Nb/BDD electrooxidation as a polishing step after biological or physical and chemical treatment processes. The process successfully removed COD, color, ammonium, and phosphate. This is important for mature landfill leachate, where biodegradability is often low and conventional treatment may not meet discharge limits. The ability to generate oxidants in situ also reduces the need for continuous chemical dosing.

For antibiotic-bearing wastewater, the study demonstrates that BDD electrooxidation can remove multiple antibiotics at the same time. This is important because real wastewater does not contain a single contaminant. The simultaneous removal of SN, TC-HCl, and SMZ shows that the process can treat structurally different pharmaceutical compounds under one optimized condition. The validation results also show that RSM can provide a reliable prediction of multi-response treatment performance.

The inclusion of H_2O_2-supplemented electrooxidation adds further engineering value. Moderate H_2O_2 addition improved oxidant availability and supported antibiotic degradation. However, the results also show that oxidant dose needs to be balanced because excessive oxidant addition may increase chemical cost and may reduce efficiency through radical scavenging. Therefore, optimized dosing is necessary for practical application. The TOC results are also important from an engineering perspective. Parent-compound removal does not always confirm treatment completeness. Antibiotics may transform into intermediate products that still contain organic carbon and toxicity. The observed TOC reduction of 76.47% under the optimized condition

confirms that the process achieved large mineralization. This strengthens the case for BDD electrooxidation as a polishing technology for persistent organic contaminants removal.

The energy and cost analysis provides a realistic boundary for process application. The estimated specific energy consumption of 66 kWh/ m^3 and electrical cost of 6.51 CAD/m^3 indicate that the process is effective but slightly energy demanding. For this reason, full-scale applications should focus on high-strength wastewater streams, concentrated side-streams, hospital effluents, pharmaceutical wastewater, landfill leachate concentrates, or final polishing after bulk organic load removal. The process may not be economical as a primary treatment step for large volume, low-strength wastewater.

The thesis also contributes to reactor operation understanding. Current density was confirmed as a major driver of oxidation performance. However, higher current density is not always the best option. Excessive current can increase oxygen evolution, radical recombination, electrode heating, and energy loss. This finding is directly relevant to engineering design because it shows the need to balance removal efficiency with current efficiency and power consumption.

The findings can also support future hybrid treatment systems. BDD electrooxidation may be integrated with biological treatment, membrane filtration, adsorption, coagulation, or ion exchange. In such systems, conventional treatment can remove bulk contaminants, while BDD electrooxidation can target residual refractory organics and micropollutants. This approach may reduce energy consumption and improve treatment reliability.

In summary, the engineering significance of this thesis lies in its combined evaluation of treatment efficiency, optimization, validation, mineralization, and energy demand. The results provide a practical basis for considering BDD electrooxidation as an advanced treatment and polishing process for landfill leachate and antibiotic-contaminated wastewater.

6.3 Future work

- Future studies need to evaluate BDD electrooxidation in real wastewater matrices for the removal of pharmaceutical compounds under longer operating periods. The antibiotic experiments in this thesis used biologically treated synthetic wastewater. Real municipal, hospital, livestock, and pharmaceutical wastewaters may contain chloride, sulfate, bicarbonate, ammonia, natural organic matter, suspended solids, and competing micropollutants. These matrix constituents can change oxidant chemistry, radical availability, by-product formation, and current efficiency. Testing real wastewater will improve the practical relevance of the optimized conditions.
- A detailed identification of transformation products is also required. HPLC analysis confirmed parent-compound removal, while TOC analysis confirmed mineralization. However, intermediate products were not fully identified without the literature support. LC-MS/MS or high-resolution mass spectrometry could be used to determine degradation pathways for SN, TC-HCl, and SMZ. This analysis would clarify hydroxylation, bond cleavage, ring opening, desulfonation, demethylation, and mineralization pathways. It would also help identify whether any persistent or toxic intermediates remain after treatment.
- Toxicity assessment should also be included in future studies. Some transformation products may show higher toxicity than the original compound. Acute toxicity, chronic toxicity, antimicrobial activity, and bacterial inhibition tests could be used before and after treatment. This would provide a stronger environmental assessment of the treated effluent.
- For future optimization studies, TOC removal, toxicity reduction, energy consumption, and treatment cost should also be included as response variables. In this thesis, RSM focused mainly on parent antibiotic removal, with TOC and energy assessed under the optimized condition. A

broader multi-response optimization would identify conditions that balance antibiotic degradation, mineralization, detoxification, and energy efficiency. This would provide a more complete basis for engineering design.

- Long-term electrode performance needs to be investigated. BDD electrodes are chemically stable, but full-scale operation requires evaluation of electrode lifetime, surface fouling, passivation, coating durability, and cleaning requirements. Future studies should monitor voltage behaviour, electrode surface condition, and treatment performance over continuous operation.
- Continuous-flow reactor studies are needed for scale-up. Batch experiments provide useful mechanistic and optimization information, but real wastewater treatment facilities usually require continuous operation. Future research should evaluate hydraulic retention time, flow regime, electrode spacing, mass transfer, mixing intensity, current distribution, and scale-up energy demand. Continuous flow testing would help translate laboratory findings into a pilot-scale design.
- Future studies should examine pulsed current operation, intermittent electrolysis, optimized electrode spacing, improved hydrodynamics, higher mass-transfer rates, and staged treatment. These strategies may reduce oxygen evolution and improve current efficiency.
- The role of H_2O_2 could be examined in more detail. Moderate H_2O_2 addition supported antibiotic degradation, but excessive doses may scavenge hydroxyl radicals and reduce efficiency. Future work should quantify H_2O_2 residuals, utilization efficiency, radical formation, and scavenging effects. The timing of H_2O_2 addition could also be tested, including single dose, stepwise dose, and continuous dose strategies.

- Chloride-containing matrices need to be evaluated more carefully. Chloride can promote the formation of active chlorine species, which may improve contaminant degradation but may also form chlorinated byproducts, which are mainly important for landfill leachate and real wastewater. Future studies should measure chlorate, perchlorate, adsorbable organic halides, and selected disinfection byproducts where chloride is present.
- In addition to this, landfill leachate studies may be extended to different leachate ages and strengths. Young, intermediate, and mature leachates have different COD, BOD/COD ratio, ammonium, color, conductivity, and humic substance content. Testing different leachate types would help define where BDD electrooxidation is most suitable.
- Future studies should compare BDD electrooxidation with other advanced treatment technologies. Useful comparisons may include ozonation, UV/H_2O_2, Fenton and photo-Fenton processes, adsorption, ion exchange, membrane filtration, and electro-Fenton systems. These comparisons may use common performance indicators such as removal efficiency, TOC reduction, toxicity reduction, sludge production, chemical use, energy demand, and cost.
- In addition, a more complete cost assessment is also required. The present energy-cost calculation considered only electricity. A full techno-economic analysis should include electrode depreciation, reactor capital cost, power supply, chemical consumption, pH adjustment, H_2O_2 cost, labour, maintenance, cleaning, sludge or concentrate handling, and electrode replacement. Life cycle assessment may also be useful to evaluate environmental trade-offs.
- Pilot-scale testing is recommended as the next major step. Pilot studies may use realistic wastewater volumes, site-specific water quality, continuous operation, and practical monitoring parameters. The pilot system should measure pollutant removal, TOC, toxicity, voltage, energy

consumption, electrode stability, and operational cost. This would provide the strongest basis for assessing field-scale application.

- Overall, future research may move from removal-focused laboratory optimization toward integrated performance evaluation. The next stage may combine real wastewater testing, transformation product analysis, toxicity assessment, continuous flow operation, energy reduction, and techno-economic evaluation. This approach is important to clarify the practical role of BDD electrooxidation as an advanced treatment and polishing technology for landfill leachate and antibiotic-contaminated wastewater.

References

Abbas, A. A., Jingsong, G., Ping, L. Z., Ya, P. Y., & Al-Rekabi, W. S. (2009). Review on landfill leachate treatments. *American Journal of Applied Sciences*, *6*(4). https://doi.org/10.3844/ajas.2009.672.684

Abdel-Shafy, H. I., Ibrahim, A. M., Al-Sulaiman, A. M., & Okasha, R. A. (2024). Landfill leachate: Sources, nature, organic composition, and treatment: An environmental overview. In *Ain Shams Engineering Journal* (Vol. 15, Issue 1). https://doi.org/10.1016/j.asej.2023.102293

Abdelhameed, R. M., & El-Shahat, M. (2024). Efficient removal of sulfamethazine and sulphanilamide using modified amberlite with metal organic framework based copper and cobalt. *Environmental Nanotechnology, Monitoring & Management*, *22*, 100987. https://doi.org/10.1016/J.ENMM.2024.100987

Adeoye, J. B., Tan, Y. H., Lau, S. Y., Tan, Y. Y., Chiong, T., Mubarak, N. M., & Khalid, M. (2024). Advanced oxidation and biological integrated processes for pharmaceutical wastewater treatment: A review. *Journal of Environmental Management*, *353*, 120170. https://doi.org/10.1016/J.JENVMAN.2024.120170

Agustina, F., Bagastyo, A. Y., & Nurhayati, E. (2019). Electro-oxidation of landfill leachate using boron-doped diamond: Role of current density, pH and ions. *Water Science and Technology*, *79*(5), 921–928. https://doi.org/10.2166/wst.2019.040

Ahmed, H. R., Ealias, A. M., & George, G. (2025). Advanced oxidation processes for the removal of antidepressants from wastewater: a comprehensive review. In *RSC Advances* (Vol. 15, Issue 56). https://doi.org/10.1039/d5ra07764h

Akbari, M. Z., Xu, Y., Lu, Z., & Peng, L. (2021). Review of antibiotics treatment by advance

oxidation processes. In *Environmental Advances* (Vol. 5). https://doi.org/10.1016/j.envadv.2021.100111

Akhtar, N. A., Iskurt, C., Gengec, E., Khataee, A., & Kobya, M. (2025a). Development of an advanced electrooxidation reactor with gas recycling for efficient treatment of pretreated landfill leachate nanofiltration concentrates. *Journal of Water Process Engineering*, *77*, 108502. https://doi.org/10.1016/J.JWPE.2025.108502

Akhtar, N. A., Iskurt, C., Gengec, E., Khataee, A., & Kobya, M. (2025b). Development of an advanced electrooxidation reactor with gas recycling for efficient treatment of pretreated landfill leachate nanofiltration concentrates. *Journal of Water Process Engineering*, *77*, 108502. https://doi.org/10.1016/J.JWPE.2025.108502

Alfaro, M. A. Q., Ferro, S., Martínez-Huitle, C. A., & Vong, Y. M. (2006). Boron doped diamond electrode for the wastewater treatment. *Journal of the Brazilian Chemical Society*, *17*(2), 227–236. https://doi.org/10.1590/S0103-50532006000200003

Ali, I., Barros de Souza, A., Liu, Z., Cabooter, D., Katsaounis, A., De Laet, S., Van Eyck, K., & Dewil, R. (2023). Improving the removal of losartan, irbesartan and their transformation products through in situ produced hydrogen peroxide in electrochemical oxidation processes. *Journal of Water Process Engineering*, *55*. https://doi.org/10.1016/j.jwpe.2023.104133

Amor, C., Torres-Socías, E. De, Peres, J. A., Maldonado, M. I., Oller, I., Malato, S., & Lucas, M. S. (2015). Mature landfill leachate treatment by coagulation/flocculation combined with Fenton and solar photo-Fenton processes. *Journal of Hazardous Materials*, *286*. https://doi.org/10.1016/j.jhazmat.2014.12.036

Anglada, Á., Urtiaga, A., Ortiz, I., Mantzavinos, D., & Diamadopoulos, E. (2011). Boron-doped

diamond anodic treatment of landfill leachate: Evaluation of operating variables and formation of oxidation by-products. *Water Research*, *45*(2), 828–838. https://doi.org/10.1016/j.watres.2010.09.017

Asadollahzadeh, M., Tavakoli, H., Torab-Mostaedi, M., Hosseini, G., & Hemmati, A. (2014). Response surface methodology based on central composite design as a chemometric tool for optimization of dispersive-solidification liquid-liquid microextraction for speciation of inorganic arsenic in environmental water samples. *Talanta*, *123*. https://doi.org/10.1016/j.talanta.2013.11.071

Autoridad Nacional del Servicio Civil. (2021). Standard Method for the Examination of Water and Wastewater. *Angewandte Chemie International Edition, 6(11), 951–952.*, *20th edn*, 2013–2015.

Balseviciute, A., Patiño-Cantero, I., Carrillo-Abad, J., Giner-Sanz, J. J., García-Gabaldón, M., Pérez-Herranz, V., & Martí-Calatayud, M. C. (2025). Degradation of multicomponent pharmaceutical mixtures by electrochemical oxidation: Insights about the process evolution at varying applied currents and concentrations of organics and supporting electrolyte. *Separation and Purification Technology*, *362*, 131697. https://doi.org/10.1016/J.SEPPUR.2025.131697

Barhoumi, N., Oturan, N., Olvera-Vargas, H., Brillas, E., Gadri, A., Ammar, S., & Oturan, M. A. (2016). Pyrite as a sustainable catalyst in electro-Fenton process for improving oxidation of sulfamethazine. Kinetics, mechanism and toxicity assessment. *Water Research*, *94*. https://doi.org/10.1016/j.watres.2016.02.042

Bari, A., Alam, R., Aqeel, M. A., Faisal, M., & Khan, S. U. (2025). An overview of electrochemical advanced oxidation assisted processes for the treatment of pharmaceutical

wastewater. In *Advanced Oxidation Process-Based Integrated and Hybrid Technologies for Degradation of Pharmaceuticals and Personal Care Products*. https://doi.org/10.1016/B978-0-443-21887-3.00022-5

Barroso-Martínez, J. S., Romo, A. I. B., Pudar, S., Putnam, S. T., Bustos, E., & Rodríguez-López, J. (2022). Real-Time Detection of Hydroxyl Radical Generated at Operating Electrodes via Redox-Active Adduct Formation Using Scanning Electrochemical Microscopy. *Journal of the American Chemical Society*, *144*(41). https://doi.org/10.1021/jacs.2c06278

Bashir, M. J. K., Isa, M. H., Kutty, S. R. M., Awang, Z. Bin, Aziz, H. A., Mohajeri, S., & Farooqi, I. H. (2009). Landfill leachate treatment by electrochemical oxidation. *Waste Management*, *29*(9), 2534–2541. https://doi.org/10.1016/j.wasman.2009.05.004

Bayabil, H. K., Teshome, F. T., & Li, Y. C. (2022). Emerging Contaminants in Soil and Water. In *Frontiers in Environmental Science* (Vol. 10). https://doi.org/10.3389/fenvs.2022.873499

Bello, M. M., Abdul Raman, A. A., & Purushothaman, M. (2017). Applications of fluidized bed reactors in wastewater treatment – A review of the major design and operational parameters. In *Journal of Cleaner Production* (Vol. 141). https://doi.org/10.1016/j.jclepro.2016.09.148

Bezerra, M. A., Santelli, R. E., Oliveira, E. P., Villar, L. S., & Escaleira, L. A. (2008). Response surface methodology (RSM) as a tool for optimization in analytical chemistry. In *Talanta* (Vol. 76, Issue 5). https://doi.org/10.1016/j.talanta.2008.05.019

Bikash Adhikari, & Sanjay Nath Khanal. (2015). Qualitative Study of Landfill Leachate from Different Ages of Landfill Sites of Various Countries Including Nepal\n. *IOSR Journal of Environmental Science, Toxicology and Food Technology (IOSR-JESTFT)*, *9*(1).

Bosio, M., de Souza-Chaves, B. M., Saggioro, E. M., Bassin, J. P., Dezotti, M. W. C., Quinta-Ferreira, M. E., & Quinta-Ferreira, R. M. (2021). Electrochemical degradation of psychotropic pharmaceutical compounds from municipal wastewater and neurotoxicity evaluations. *Environmental Science and Pollution Research*, *28*(19). https://doi.org/10.1007/s11356-020-12133-9

Brillas, E., & Garcia-Segura, S. (2025). Electrochemical Advanced Oxidation Processes for Real Wastewater Remediation: Systems, Performance, and Generated Oxidants. *ACS Electrochemistry*, *1*(11). https://doi.org/10.1021/acselectrochem.5c00311

Brillas, E., Sirés, I., & Oturan, M. A. (2009). Electro-fenton process and related electrochemical technologies based on fenton's reaction chemistry. *Chemical Reviews*, *109*(12). https://doi.org/10.1021/cr900136g

Brinzila, C. I., Monteiro, N., Pacheco, M. J., Ciríaco, L., Siminiceanu, I., & Lopes, A. (2014). Degradation of tetracycline at a boron-doped diamond anode: Influence of initial pH, applied current intensity and electrolyte. *Environmental Science and Pollution Research*, *21*(14). https://doi.org/10.1007/s11356-014-2778-y

Brinzila, C. I., Pacheco, M. J., Ciríaco, L., Ciobanu, R. C., & Lopes, A. (2012). Electrodegradation of tetracycline on BDD anode. *Chemical Engineering Journal*, *209*. https://doi.org/10.1016/j.cej.2012.07.112

Brito, N. N., Paterniani, J. E. S., Brota, G. A., & Pelegrini, R. T. (2010). Ammonia removal from leachate by photochemical process using H2O2. *Ambiente e Agua - An Interdisciplinary Journal of Applied Science*, *5*(2). https://doi.org/10.4136/ambi-agua.136

Brouwir, L., KleinJan, H., Balent, C., Quabron, G., Salmerón, I., Venditti, S., & Gritten, F. (2025). Fate and Removal of Antibiotics and Antibiotic Resistance Genes in a Rural

Wastewater Treatment Plant: A Microbial Perspective of Nature-Based Versus Advanced Technologies. *Microorganisms*, *13*(12). https://doi.org/10.3390/microorganisms13122663

Cabeza, A., Primo, Ó., Urtiaga, A. M., & Ortiz, I. (2007). Definition of a clean process for the treatment of landfill leachates integration of electrooxidation and ion exchange technologies. *Separation Science and Technology*, *42*(7). https://doi.org/10.1080/01496390701290383

Cabeza, A., Urtiaga, A. M., & Ortiz, I. (2007). Electrochemical treatment of landfill leachates using a boron-doped diamond anode. *Industrial and Engineering Chemistry Research*, *46*(5). https://doi.org/10.1021/ie061373x

Cabeza, A., Urtiaga, A., Rivero, M. J., & Ortiz, I. (2007). Ammonium removal from landfill leachate by anodic oxidation. *Journal of Hazardous Materials*, *144*(3). https://doi.org/10.1016/j.jhazmat.2007.01.106

Całus-Makowska, K., Dziubińska, J., Grosser, A., & Grobelak, A. (2025). Application of the Fenton and photo-Fenton processes in pharmaceutical removal: New perspectives in environmental protection. *Desalination and Water Treatment*, *321*. https://doi.org/10.1016/j.dwt.2024.100949

Calzadilla, W., Espinoza, L. C., Diaz-Cruz, M. S., Sunyer, A., Aranda, M., Peña-Farfal, C., & Salazar, R. (2021). Simultaneous degradation of 30 pharmaceuticals by anodic oxidation: Main intermediaries and by-products. *Chemosphere*, *269*. https://doi.org/10.1016/j.chemosphere.2020.128753

Canabarro, M. I., Fuhr, A. C. F. P., Bertizzolo, E. G., Carissimi, E., & Leichtweis, J. (2026). From generation to treatment: A comprehensive and critical review of landfill leachate. In *Environmental Science and Policy* (Vol. 176). https://doi.org/10.1016/j.envsci.2026.104308

Carvalho, I. T., & Santos, L. (2016). Antibiotics in the aquatic environments: A review of the European scenario. In *Environment International* (Vol. 94). https://doi.org/10.1016/j.envint.2016.06.025

Castillo-Cabrera, G. X., Pliego-Cerdán, C. I., Méndez, E., & Espinoza-Montero, P. J. (2023). Step-by-step guide for electrochemical generation of highly oxidizing reactive species on BDD for beginners. *Frontiers in Chemistry*, *11*. https://doi.org/10.3389/fchem.2023.1298630

Chang, H., Hu, J. Y., Wang, L. Z., & Shao, B. (2008). Occurrence of sulfonamide antibiotics in sewage treatment plants. *Chinese Science Bulletin*, *53*(4). https://doi.org/10.1007/s11434-008-0123-x

Chen, H., Xu, H., Zhong, C., Liu, M., Yang, L., He, J., Sun, Y., Zhao, C., & Wang, D. (2024). Treatment of landfill leachate by coagulation: A review. In *Science of the Total Environment* (Vol. 912). https://doi.org/10.1016/j.scitotenv.2023.169294

Chen, L., Fu, H., Ren, X., Chen, Y., Song, K., Cheng, X., & Liu, Y. (2025). Electrochemical advanced oxidation processes for treating wastewater containing tetracycline antibiotics: Methods, mechanisms, and perspectives. *Journal of Environmental Chemical Engineering*, *13*(6). https://doi.org/10.1016/j.jece.2025.119963

Chen, T. S., Tsai, R. W., Chen, Y. S., & Huang, K. L. (2014). Electrochemical degradation of tetracycline on BDD in aqueous solutions. *International Journal of Electrochemical Science*, *9*(12). https://doi.org/10.1016/s1452-3981(23)11057-1

Chen, Yexiang, Xu, H., Khan, M. S., Han, S., & Zhu, S. (2025). Recent advances in layered double hydroxides for pharmaceutical wastewater treatment: A critical review. *Critical Reviews in Environmental Science and Technology*, *55*(14), 1097–1123.

https://doi.org/10.1080/10643389.2025.2488808

Chen, Yufan, Zuo, W., Sun, H., Liu, Y., Hou, J., Xie, H., & Wang, L. (2024). Electrochemical oxidation of low concentrated tetracycline (TC) in aqueous solution: Operation optimization, degradation mechanisms, and detoxification efficiency. *Journal of Environmental Chemical Engineering*, *12*(3), 112604. https://doi.org/10.1016/J.JECE.2024.112604

Comninellis, C. (1994). Electrocatalysis in the electrochemical conversion/combustion of organic pollutants for waste water treatment. *Electrochimica Acta*, *39*(11–12). https://doi.org/10.1016/0013-4686(94)85175-1

Contreras, D., Moreno, Y., Salgado, Y., Cárdenas, G., Baggio, R., Peña, O., & Pivan, J. Y. (2007). Synthesis and optimization of experimental variables of a hybrid organic–inorganic compound. *New Journal of Chemistry*, *31*(10), 1751–1754. https://doi.org/10.1039/B703592F

Córdova, R. N., Nagel-Hassemer, M. E., Matias, W. G., Muller, J. M., & de Castilhos Junior, A. B. (2019). Removal of organic matter and ammoniacal nitrogen from landfill leachate using the UV/H2O2 photochemical process. *Environmental Technology (United Kingdom)*, *40*(6). https://doi.org/10.1080/09593330.2017.1408692

Costa, A. M., Alfaia, R. G. de S. M., & Campos, J. C. (2019). Landfill leachate treatment in Brazil – An overview. In *Journal of Environmental Management* (Vol. 232, pp. 110–116). https://doi.org/10.1016/j.jenvman.2018.11.006

Costa, C. R., Montilla, F., Morallón, E., & Olivi, P. (2009). Electrochemical oxidation of acid black 210 dye on the boron-doped diamond electrode in the presence of phosphate ions: Effect of current density, pH, and chloride ions. *Electrochimica Acta*, *54*(27), 7048–7055.

https://doi.org/10.1016/j.electacta.2009.07.027

da Silva, S. W., Navarro, E. M. O., Rodrigues, M. A. S., Bernardes, A. M., & Pérez-Herranz, V. (2019). Using p-Si/BDD anode for the electrochemical oxidation of norfloxacin. *Journal of Electroanalytical Chemistry*, *832*. https://doi.org/10.1016/j.jelechem.2018.10.049

Dargahi, A., Moradi, M., Hasani, K., & Vosoughi, M. (2023). Improved degradation of tetracycline antibiotic in electrochemical advanced oxidation processes (EAOPs): Bioassay using bacteria and identification of intermediate compounds. *International Journal of Chemical Reactor Engineering*, *21*(2). https://doi.org/10.1515/ijcre-2022-0041

Das, S., Parida, V. K., Tiwary, C. S., Gupta, A. K., & Chowdhury, S. (2024). Emerging Contaminants in the Aquatic Environment: Fate, Occurrence, Impacts, and Toxicity. In *Bioremediation of Emerging Contaminants in Water. Volume 1* (Vol. 1475, p. 1). American Chemical Society. https://doi.org/doi:10.1021/bk-2024-1475.ch001

de Souza, A. B., Gadi, N., van de Goor, T., Boelee, N. C., Dewil, R., & Cabooter, D. (2024). Occurrence and elimination of pharmaceutical residues in municipal wastewater effluent by electrochemical anodic oxidation. *Journal of Water Process Engineering*, *66*, 105899. https://doi.org/10.1016/J.JWPE.2024.105899

Deng, Y., & Englehardt, J. D. (2007). Electrochemical oxidation for landfill leachate treatment. *Waste Management*, *27*(3), 380–388. https://doi.org/10.1016/j.wasman.2006.02.004

Dereli, R. K., Grelot, A., Heffernan, B., van der Zee, F. P., & van Lier, J. B. (2014). Implications of changes in solids retention time on long term evolution of sludge filterability in anaerobic membrane bioreactors treating high strength industrial wastewater. *Water Research*, *59*. https://doi.org/10.1016/j.watres.2014.03.073

Derringer, G., & Suich, R. (1980). Simultaneous Optimization of Several Response Variables.

Journal of Quality Technology, *12*(4). https://doi.org/10.1080/00224065.1980.11980968

Deshpande, A. M., Ramakant, & Satyanarayan, S. (2012). Treatment of Pharmaceutical Wastewater by Electrochemical Method: Optimization of Operating Parameters by Response Surface Methodology. *Journal of Hazardous, Toxic, and Radioactive Waste*, *16*(4). https://doi.org/10.1061/(asce)hz.2153-5515.0000133

Divyapriya, G., & Nidheesh, P. V. (2021). Electrochemically generated sulfate radicals by boron doped diamond and its environmental applications. *Current Opinion in Solid State and Materials Science*, *25*(3). https://doi.org/10.1016/j.cossms.2021.100921

Dong, H., Chi, W., Gao, A., Xie, T., & Gao, B. (2021). Electrochemical Degradation of Tetracycline Using a Ti/Ta(2)O(5)-IrO(2) Anode: Performance, Kinetics, and Degradation Mechanism. *Materials (Basel, Switzerland)*, *14*(15). https://doi.org/10.3390/ma14154325

Eapen, J. V., Thomas, S., Antony, S., George, P., & Antony, J. (2024). A review of the effects of pharmaceutical pollutants on humans and aquatic ecosystem. *Exploration of Drug Science*, *2*(5), 484–507. https://doi.org/10.37349/eds.2024.00058

El-Ghenymy, A., Cabot, P. L., Centellas, F., Garrido, J. A., Rodríguez, R. M., Arias, C., & Brillas, E. (2013). Electrochemical incineration of the antimicrobial sulfamethazine at a boron-doped diamond anode. *Electrochimica Acta*, *90*, 254–264. https://doi.org/10.1016/J.ELECTACTA.2012.11.125

El-Ghenymy, A., Garrido, J. A., Rodríguez, R. M., Cabot, P. L., Centellas, F., Arias, C., & Brillas, E. (2013). Degradation of sulfanilamide in acidic medium by anodic oxidation with a boron-doped diamond anode. *Journal of Electroanalytical Chemistry*, *689*. https://doi.org/10.1016/j.jelechem.2012.11.013

El Kateb, M., Trellu, C., Darwich, A., Rivallin, M., Bechelany, M., Nagarajan, S., Lacour, S.,

Bellakhal, N., Lesage, G., Héran, M., & Cretin, M. (2019). Electrochemical advanced oxidation processes using novel electrode materials for mineralization and biodegradability enhancement of nanofiltration concentrate of landfill leachates. *Water Research*, *162*. https://doi.org/10.1016/j.watres.2019.07.005

ELECTRICITY RATES EFFECTIVE APPROVED IN. (2026).

Enache, T. A., Chiorcea-Paquim, A. M., Fatibello-Filho, O., & Oliveira-Brett, A. M. (2009). Hydroxyl radicals electrochemically generated in situ on a boron-doped diamond electrode. *Electrochemistry Communications*, *11*(7). https://doi.org/10.1016/j.elecom.2009.04.017

Espinoza-Montero, P. J., Alulema-Pullupaxi, P., Frontana-Uribe, B. A., & Barrera-Diaz, C. E. (2022). Electrochemical production of hydrogen peroxide on Boron-Doped diamond (BDD) electrode. In *Current Opinion in Solid State and Materials Science* (Vol. 26, Issue 3). https://doi.org/10.1016/j.cossms.2022.100988

Espinoza, L. C., Henríquez, A., Contreras, D., & Salazar, R. (2018). Evidence for the production of hydroxyl radicals at boron-doped diamond electrodes with different sp3/sp2 ratios and its relationship with the anodic oxidation of aniline. *Electrochemistry Communications*, *90*. https://doi.org/10.1016/j.elecom.2018.03.007

Fabiańska, A., Białk-Bielińska, A., Stepnowski, P., Stolte, S., & Siedlecka, E. M. (2014). Electrochemical degradation of sulfonamides at BDD electrode: Kinetics, reaction pathway and eco-toxicity evaluation. *Journal of Hazardous Materials*, *280*. https://doi.org/10.1016/j.jhazmat.2014.08.050

Fan, H. jung, Shu, H. Y., Yang, H. S., & Chen, W. C. (2006). Characteristics of landfill leachates in central Taiwan. *Science of the Total Environment*, *361*(1–3), 25–37. https://doi.org/10.1016/j.scitotenv.2005.09.033

Feki, F., Aloui, F., Feki, M., & Sayadi, S. (2009). Electrochemical oxidation post-treatment of landfill leachates treated with membrane bioreactor. *Chemosphere*, *75*(2), 256–260. https://doi.org/10.1016/j.chemosphere.2008.12.013

Fernandes, A., Pacheco, M. J., Ciríaco, L., & Lopes, A. (2015). Review on the electrochemical processes for the treatment of sanitary landfill leachates: Present and future. In *Applied Catalysis B: Environmental* (Vols. 176–177, pp. 183–200). https://doi.org/10.1016/j.apcatb.2015.03.052

Ferreira, S. L. C., Bruns, R. E., Ferreira, H. S., Matos, G. D., David, J. M., Brandão, G. C., da Silva, E. G. P., Portugal, L. A., dos Reis, P. S., Souza, A. S., & dos Santos, W. N. L. (2007). Box-Behnken design: An alternative for the optimization of analytical methods. In *Analytica Chimica Acta* (Vol. 597, Issue 2). https://doi.org/10.1016/j.aca.2007.07.011

Field, A. (2017). Discovering Statistic Using IBM SPSS Statistic 5th. *Sage Publication*, *53*(9).

Gaetan, A. A., Bi Gouessé Henri, B., Veronique junior, N. T., Benjamin, Y. K., & Patrick, D. (2025). Electrochemical oxidation of four pharmaceutical pollutants using Ti/IrO2 and Nb/BDD anodes: Application of factorial design methodology. *International Journal of Electrochemical Science* , *20*(12). https://doi.org/10.1016/j.ijoes.2025.101211

Ganiyu, S. O., Oturan, N., Raffy, S., Cretin, M., Causserand, C., & Oturan, M. A. (2019). Efficiency of plasma elaborated sub-stoichiometric titanium oxide (Ti4O7) ceramic electrode for advanced electrochemical degradation of paracetamol in different electrolyte media. *Separation and Purification Technology*, *208*. https://doi.org/10.1016/j.seppur.2018.03.076

Gao, L., Shi, Y., Li, W., Niu, H., Liu, J., & Cai, Y. (2012). Occurrence of antibiotics in eight sewage treatment plants in Beijing, China. *Chemosphere*, *86*(6).

https://doi.org/10.1016/j.chemosphere.2011.11.019

Gao, X., Li, W., Mei, R., Zhu, C., Zhou, B., Ma, L., Wei, Q., & Liu, T. (2019). Effect of the B2H6/CH4/H2 ratios on the structure and electrochemical properties of boron-doped diamond electrode in the electrochemical oxidation process of azo dye. *Journal of Electroanalytical Chemistry*, *832*, 247–253. https://doi.org/10.1016/j.jelechem.2018.11.009

García-Espinoza, J. D., & Nacheva, P. M. (2019). Degradation of pharmaceutical compounds in water by oxygenated electrochemical oxidation: Parametric optimization, kinetic studies and toxicity assessment. *Science of the Total Environment*, *691*. https://doi.org/10.1016/j.scitotenv.2019.07.118

García-Montoya, M. F., Gutiérrez-Granados, S., Alatorre-Ordaz, A., Galindo, R., Ornelas, R., & Peralta-Hernández, J. M. (2015). Application of electrochemical/BDD process for the treatment wastewater effluents containing pharmaceutical compounds. *Journal of Industrial and Engineering Chemistry*, *31*. https://doi.org/10.1016/j.jiec.2015.06.030

Gaur, V. K., Gautam, K., Vishvakarma, R., Sharma, P., Pandey, U., Srivastava, J. K., Varjani, S., Chang, J. S., Ngo, H. H., & Wong, J. W. C. (2024). Integrating advanced techniques and machine learning for landfill leachate treatment: Addressing limitations and environmental concerns. *Environmental Pollution*, *354*, 124134. https://doi.org/10.1016/J.ENVPOL.2024.124134

Ghanbari, F., Wang, Q., Hassani, A., Wacławek, S., Rodríguez-Chueca, J., & Lin, K. Y. A. (2021). Electrochemical activation of peroxides for treatment of contaminated water with landfill leachate: Efficacy, toxicity and biodegradability evaluation. *Chemosphere*, *279*. https://doi.org/10.1016/j.chemosphere.2021.130610

Gokgoz, M., Zhang, W., Manage, N., Mbengue, M., Bolyard, S., & Chen, J. (2023). Survey on

the current leachate treatments of public municipal solid waste landfills and the potential impact of per- and polyfluorinatedalkyl substances in the Eastern and Northwestern United States. *Journal of the Air & Waste Management Association*, *73*(8), 638–648. https://doi.org/10.1080/10962247.2023.2235313

Gonzaga, I. M. D., Moratalla, A., Eguiluz, K. I. B., Salazar-Banda, G. R., Cañizares, P., Rodrigo, M. A., & Saez, C. (2020). Influence of the doping level of boron-doped diamond anodes on the removal of penicillin G from urine matrixes. *Science of the Total Environment*, *736*. https://doi.org/10.1016/j.scitotenv.2020.139536

Goukeh, M. N., Ssekimpi, D., Asefaw, B. K., & Zhang, Z. (2025). Occurrence of per- and polyfluorinated substances, microplastics, pharmaceuticals and personal care products as emerging contaminants in landfill leachate: A review. *Total Environment Engineering*, *3*, 100019. https://doi.org/10.1016/J.TEENGI.2025.100019

Grebel, J. E., Pignatello, J. J., & Mitch, W. A. (2010). Effect of halide ions and carbonates on organic contaminant degradation by hydroxyl radical-based advanced oxidation processes in saline waters. *Environmental Science and Technology*, *44*(17). https://doi.org/10.1021/es1010225

Hai, H., Xing, X., Li, S., Xia, S., & Xia, J. (2020). Electrochemical oxidation of sulfamethoxazole in BDD anode system: Degradation kinetics, mechanisms and toxicity evaluation. *Science of the Total Environment*, *738*. https://doi.org/10.1016/j.scitotenv.2020.139909

Hama Aziz, K. H., Mustafa, F. S., Karim, M. A. H., & Hama, S. (2025). Pharmaceutical pollution in the aquatic environment: advanced oxidation processes as efficient treatment approaches: a review. *Materials Advances*, *6*(11), 3433–3454.

https://doi.org/10.1039/D4MA01122H

Hasan Anik, A., Hossain, S., Alam, M., Binte Sultan, M., Hasnine, M. T., & Rahman, M. M. (2021). Microplastics pollution: A comprehensive review on the sources, fates, effects, and potential remediation. In *Environmental Nanotechnology, Monitoring and Management* (Vol. 16). https://doi.org/10.1016/j.enmm.2021.100530

Hasnine, M. D. T., Anand, N., Zoungrana, A., Palani, S. G., & Yuan, Q. (2022). *An Overview of Physicochemical and Biological Treatment of Landfill Leachate BT - Circular Economy in Municipal Solid Waste Landfilling: Biomining & Leachate Treatment : Sustainable Solid Waste Management: Waste to Wealth* (P. Pathak & S. G. Palani (Eds.); pp. 115–152). Springer International Publishing. https://doi.org/10.1007/978-3-031-07785-2_6

Hasnine, M. T., Rout, P. R., & Yuan, Q. (2025). Forever chemicals (PFAS) in landfill leachate: Insights into fate, transport, and treatment strategies. *Desalination and Water Treatment*, *324*. https://doi.org/10.1016/j.dwt.2025.101565

Hasnine, T., Lumbaque, E. C., & Yuan, Q. (2023). Optimisation of electrochemical oxidation process with boron doped diamond (BDD) for removing COD, colour, ammonium, and phosphate in landfill leachate. *Environmental Technology (United Kingdom)*. https://doi.org/10.1080/09593330.2023.2210769

He, Y., Lin, H., Guo, Z., Zhang, W., Li, H., & Huang, W. (2019). Recent developments and advances in boron-doped diamond electrodes for electrochemical oxidation of organic pollutants. In *Separation and Purification Technology* (Vol. 212, pp. 802–821). https://doi.org/10.1016/j.seppur.2018.11.056

Henke, A. H., Saunders, T. P., Pedersen, J. A., & Hamers, R. J. (2019). Enhancing Electrochemical Efficiency of Hydroxyl Radical Formation on Diamond Electrodes by

Functionalization with Hydrophobic Monolayers. *Langmuir*, *35*(6). https://doi.org/10.1021/acs.langmuir.8b04030

Hu, J., Bian, X., Xia, Y., Weng, M., Zhou, W., & Dai, Q. (2020). Application of response surface methodology in electrochemical degradation of amoxicillin with Cu-PbO2 electrode: Optimization and mechanism. *Separation and Purification Technology*, *250*, 117109. https://doi.org/10.1016/J.SEPPUR.2020.117109

Hu, S., Lv, Y., Hou, X., Li, J., Hou, Y., Fu, X., & Xu, T. (2025a). BDD electrode pulsed alternating electrochemical oxidation of sulfamethazine in antibiotic wastewater: Process optimization and degradation mechanism. *Environmental Research*, *275*, 121375. https://doi.org/10.1016/J.ENVRES.2025.121375

Hu, S., Lv, Y., Hou, X., Li, J., Hou, Y., Fu, X., & Xu, T. (2025b). BDD electrode pulsed alternating electrochemical oxidation of sulfamethazine in antibiotic wastewater: Process optimization and degradation mechanism. *Environmental Research*, *275*, 121375. https://doi.org/10.1016/J.ENVRES.2025.121375

Hussain, S., Steter, J. R., Gul, S., & Motheo, A. J. (2017). Photo-assisted electrochemical degradation of sulfamethoxazole using a Ti/Ru0.3Ti0.7O2 anode: Mechanistic and kinetic features of the process. *Journal of Environmental Management*, *201*. https://doi.org/10.1016/j.jenvman.2017.06.043

Iakovides, I. C., Michael-Kordatou, I., Moreira, N. F. F., Ribeiro, A. R., Fernandes, T., Pereira, M. F. R., Nunes, O. C., Manaia, C. M., Silva, A. M. T., & Fatta-Kassinos, D. (2019). Continuous ozonation of urban wastewater: Removal of antibiotics, antibiotic-resistant Escherichia coli and antibiotic resistance genes and phytotoxicity. *Water Research*, *159*. https://doi.org/10.1016/j.watres.2019.05.025

Iglesias, A., Nebot, C., Miranda, J. M., Vázquez, B. I., Franco Abuín, C. M., & Cepeda, A. (2013). Determination of the presence of three antimicrobials in surface water collected from urban and rural areas. *Antibiotics*, *2*(1). https://doi.org/10.3390/antibiotics2010046

Igwegbe, C. A., López-Maldonado, E. A., Landázuri, A. C., Ovuoraye, P. E., Ogbu, A. I., Vela-García, N., & Białowiec, A. (2024). Sustainable municipal landfill leachate management: Current practices, challenges, and future directions. *Desalination and Water Treatment*, *320*, 100709. https://doi.org/10.1016/J.DWT.2024.100709

Islam, M., Xu, Q., & Yuan, Q. (2020). Advanced biological sequential treatment of mature landfill leachate using aerobic activated sludge SBR and fungal bioreactor. *Journal of Environmental Health Science and Engineering*, *18*(1), 285–295. https://doi.org/10.1007/s40201-020-00466-z

Ivantsova, N. A., Kuzin, E. N., Kuznetsov, V. V., Filatova, E. A., Pirogov, A. V., Timchenko, Y. V., Poineau, F., German, K. E., Averina, Y. M., & Kolesnikov, A. V. (2025). Advanced electrochemical treatment of tetracycline-contaminated water using Pt/Ti electrodes. *RSC Advances*, *15*(27), 21785–21793. https://doi.org/10.1039/d5ra02632f

Jagaba, A. H., Kutty, S. R. M., Lawal, I. M., Abubakar, S., Hassan, I., Zubairu, I., Umaru, I., Abdurrasheed, A. S., Adam, A. A., Ghaleb, A. A. S., Almahbashi, N. M. Y., Al-dhawi, B. N. S., & Noor, A. (2021). Sequencing batch reactor technology for landfill leachate treatment: A state-of-the-art review. In *Journal of Environmental Management* (Vol. 282). https://doi.org/10.1016/j.jenvman.2021.111946

Jaiswal, N., Khan, H., John, S., Singh, S., Tricoli, A., Liu, B., & Ramanujam, K. (2025). Advances in boron-doped diamond electrodes: Fabrication, electrochemical properties, and applications. In *Journal of Alloys and Compounds* (Vol. 1036).

https://doi.org/10.1016/j.jallcom.2025.181723

Jiang, T., Wu, W., Ma, M., Hu, Y., & Li, R. (2024). Occurrence and distribution of emerging contaminants in wastewater treatment plants: A globally review over the past two decades. *Science of The Total Environment*, *951*, 175664. https://doi.org/10.1016/J.SCITOTENV.2024.175664

Jiang, Y., Zhao, H., Liang, J., Yue, L., Li, T., Luo, Y., Liu, Q., Lu, S., Asiri, A. M., Gong, Z., & Sun, X. (2021). Anodic oxidation for the degradation of organic pollutants: Anode materials, operating conditions and mechanisms. A mini review. In *Electrochemistry Communications* (Vol. 123). https://doi.org/10.1016/j.elecom.2020.106912

Jones, E. R., Bierkens, M. F. P., Wanders, N., Sutanudjaja, E. H., van Beek, L. P. H., & van Vliet, M. T. H. (2022). Current wastewater treatment targets are insufficient to protect surface water quality. *Communications Earth & Environment*, *3*(1), 221. https://doi.org/10.1038/s43247-022-00554-y

Kanakaraju, D., Glass, B. D., & Goh, P. S. (2025). Advanced oxidation process-mediated removal of pharmaceuticals from water: a review of recent advances. *Environmental Science and Pollution Research*, *32*(24), 14316–14350. https://doi.org/10.1007/s11356-025-36547-5

Kapałka, A., Joss, L., Anglada, Á., Comninellis, C., & Udert, K. M. (2010). Direct and mediated electrochemical oxidation of ammonia on boron-doped diamond electrode. *Electrochemistry Communications*, *12*(12), 1714–1717. https://doi.org/10.1016/j.elecom.2010.10.004

Kaplan, E., Ofek, M., Jurkevitch, E., & Cytryn, E. (2013). Characterization of fluoroquinolone resistance and qnr diversity in Enterobacteriaceae from municipal biosolids. *Frontiers in*

Microbiology, *4*(JUN). https://doi.org/10.3389/fmicb.2013.00144

Karim, A. V., Nidheesh, P. V., & Oturan, M. A. (2021). Boron-doped diamond electrodes for the mineralization of organic pollutants in the real wastewater. *Current Opinion in Electrochemistry*, *30*. https://doi.org/10.1016/j.coelec.2021.100855

Kaur, R., Kushwaha, J. P., & Singh, N. (2018). Electro-oxidation of Ofloxacin antibiotic by dimensionally stable Ti/RuO2 anode: Evaluation and mechanistic approach. *Chemosphere*, *193*. https://doi.org/10.1016/j.chemosphere.2017.11.065

Kaza, S., Yao, L., Bhada-Tata, P., & Woerden, F. Van. (2018). What a waste 2.0: a global review of solid waste management. *World Bank*, *15*(November), 1–100. https://openknowledge.worldbank.org/handle/10986/17388

Khamis, D., Mahé, E., Dardoize, F., & Devilliers, D. (2010). Peroxodisulfate generation on boron-doped diamond microelectrodes array and detection by scanning electrochemical microscopy. *Journal of Applied Electrochemistry*, *40*(10). https://doi.org/10.1007/s10800-010-0114-x

Khodadoost, S., Hadi, A., Karimi-Sabet, J., Mehdipourghazi, M., & Golzary, A. (2017). Optimization of hydrothermal synthesis of Bismuth titanate nanoparticles and application for photocatalytic degradation of Tetracycline. *Journal of Environmental Chemical Engineering*, *5*(6). https://doi.org/10.1016/j.jece.2017.10.006

Khorram, A. G., & Fallah, N. (2018). Treatment of textile dyeing factory wastewater by electrocoagulation with low sludge settling time: Optimization of operating parameters by RSM. *Journal of Environmental Chemical Engineering*, *6*(1). https://doi.org/10.1016/j.jece.2017.12.054

Kim, J. G., Ehsan, M. F., Alshawabkeh, A. N., & Baek, K. (2025). Simultaneous removal of

Cr(VI), As(III), and sulfanilamide via an e-barrier electrochemical system: A pilot study. *Journal of Hazardous Materials*, *490*, 137735. https://doi.org/10.1016/J.JHAZMAT.2025.137735

Kim, J. G., Kim, H. Bin, Jeong, W. G., Lee, K. H., & Baek, K. (2024). Electrochemical oxidation and mechanism of sulfanilamide from groundwater in a flow-through system using carbon fiber (CF) anode. *Chemosphere*, *349*. https://doi.org/10.1016/j.chemosphere.2023.140817

Kjeldsen, P., Barlaz, M. A., Rooker, A. P., Baun, A., Ledin, A., & Christensen, T. H. (2002). Present and long-term composition of MSW landfill leachate: A review. In *Critical Reviews in Environmental Science and Technology* (Vol. 32, Issue 4, pp. 297–336). https://doi.org/10.1080/10643380290813462

Kokoszka, K., Wilk, J., Felis, E., & Bajkacz, S. (2021). Application of UHPLC-MS/MS method to study occurrence and fate of sulfonamide antibiotics and their transformation products in surface water in highly urbanized areas. *Chemosphere*, *283*. https://doi.org/10.1016/j.chemosphere.2021.131189

Körbahti, B. K., & Alaca, S. (2021). Electrochemical degradation of tetracycline antibiotic with boron-doped diamond electrodes and effect of parameters on removal of reaction intermediates. *Desalination and Water Treatment*, *236*. https://doi.org/10.5004/dwt.2021.27716

Körbahti, B. K., & Taşyürek, S. (2015). Electrochemical oxidation of ampicillin antibiotic at boron-doped diamond electrodes and process optimization using response surface methodology. *Environmental Science and Pollution Research*, *22*(5). https://doi.org/10.1007/s11356-014-3101-7

Körbahti, B. K., & Taşyürek, S. (2016). Electrochemical oxidation of sulfadiazine antibiotic using boron-doped diamond anode: application of response surface methodology for process optimization. *Desalination and Water Treatment*, *57*(6). https://doi.org/10.1080/19443994.2015.1043590

Kulikowska, D., & Klimiuk, E. (2008). The effect of landfill age on municipal leachate composition. *Bioresource Technology*, *99*(13), 5981–5985. https://doi.org/10.1016/j.biortech.2007.10.015

Kumari, P., & Kumar, A. (2023). ADVANCED OXIDATION PROCESS: A remediation technique for organic and non-biodegradable pollutant. In *Results in Surfaces and Interfaces* (Vol. 11). https://doi.org/10.1016/j.rsurfi.2023.100122

Kurniawan, T. A., Lo, W. H., & Chan, G. Y. S. (2006). Physico-chemical treatments for removal of recalcitrant contaminants from landfill leachate. *Journal of Hazardous Materials*, *129*(1–3), 80–100. https://doi.org/10.1016/j.jhazmat.2005.08.010

Leili, M., Fazlzadeh, M., & Bhatnagar, A. (2018). Green synthesis of nano-zero-valent iron from Nettle and Thyme leaf extracts and their application for the removal of cephalexin antibiotic from aqueous solutions. *Environmental Technology (United Kingdom)*, *39*(9). https://doi.org/10.1080/09593330.2017.1323956

Leili, M., Shirmohammadi Khorram, N., Godini, K., Azarian, G., Moussavi, R., & Peykhoshian, A. (2020). Application of central composite design (CCD) for optimization of cephalexin antibiotic removal using electro-oxidation process. *Journal of Molecular Liquids*, *313*, 113556. https://doi.org/10.1016/j.molliq.2020.113556

Lenth, R. V. (2010). Response-Surface Methods in R, Using rsm. *Journal of Statistical Software*, *32*(7), 1–17. https://doi.org/10.18637/JSS.V032.I07

Li, D., Guo, X., Shao, X., Zhou, A., Zhu, L., Zhang, Y., Li, B., Du, Y., Cao, L., & Yang, J. (2024). Stabilized Hf-doped Ti/Sb-SnO2 electrode for efficient degradation of tetracycline. *Environmental Science and Pollution Research*, *31*(35), 47960–47973. https://doi.org/10.1007/s11356-024-34354-y

Li, H., Jiang, H., Liu, C., Zhu, C., & Zhu, X. P. (2019). Electrochemical Oxidation of Sulfonamides with Boron-Doped Diamond and Pt Anodes. *ChemistryOpen*, *8*(12). https://doi.org/10.1002/open.201900250

Li, Jiale, Li, P., Jin, C., Zhao, Y., Guo, L., & Ji, J. (2019). Treatment of Municipal Landfill Leachate by Electrochemical Oxidation: Assessing Operating Variables and Oxidation Products. *Environmental Engineering Science*, *36*(12). https://doi.org/10.1089/ees.2019.0186

Li, Juan, Yang, Z. H., Xu, H. Y., Song, P. P., Huang, J., Xu, R., Zhang, Y. J., & Zhou, Y. (2016). Electrochemical treatment of mature landfill leachate using Ti/RuO2-IrO2 and Al electrode: Optimization and mechanism. *RSC Advances*, *6*(53). https://doi.org/10.1039/c6ra05080h

Li, Q., Cui, H., Li, Y., Song, X., Liu, W., Wang, Y., Hou, H., Zhang, H., Li, Y., Wang, F., Song, J., Ye, H., Song, S., Che, T., Shao, S., Kong, D., & Liang, B. (2023). Challenges and engineering application of landfill leachate concentrate treatment. In *Environmental Research* (Vol. 231). https://doi.org/10.1016/j.envres.2023.116028

Li, S., Lin, Y., Zhu, S., & Liu, G. (2022). Electrocatalytic degradation of sulfamethylthiadiazole by GAC@Ni/Fe three-dimensional particle electrode. *Environmental Science and Pollution Research*, *29*(38). https://doi.org/10.1007/s11356-022-19021-4

Li, Xiaobao, Fan, S., Jin, C., Gao, M., Zhao, Y., Guo, L., Ji, J., & She, Z. (2022). Electrochemical degradation of tetracycline hydrochloride in sulfate solutions on boron-

doped diamond electrode: The accumulation and transformation of persulfate. *Chemosphere*, *305*. https://doi.org/10.1016/j.chemosphere.2022.135448

Li, Xingyu, Shen, X., Jiang, W., Xi, Y., & Li, S. (2024). Comprehensive review of emerging contaminants: Detection technologies, environmental impact, and management strategies. *Ecotoxicology and Environmental Safety*, *278*, 116420. https://doi.org/10.1016/J.ECOENV.2024.116420

Liu, G., Zhang, C., Zhou, Y., & Yan, Q. (2021). Insight into the overpotential and thermodynamic mechanism of hydroxyl radical formation on diamond anode. *Applied Surface Science*, *565*. https://doi.org/10.1016/j.apsusc.2021.150559

Liu, M., Lü, Z., Chen, Z., Yu, S., & Gao, C. (2011). Comparison of reverse osmosis and nanofiltration membranes in the treatment of biologically treated textile effluent for water reuse. *Desalination*, *281*(1), 372–378. https://doi.org/10.1016/j.desal.2011.08.023

Liu, X., Zhou, Y., Zhang, J., Luo, L., Yang, Y., Huang, H., Peng, H., Tang, L., & Mu, Y. (2018). Insight into electro-Fenton and photo-Fenton for the degradation of antibiotics: Mechanism study and research gaps. In *Chemical Engineering Journal* (Vol. 347). https://doi.org/10.1016/j.cej.2018.04.142

Long, X., Li, D., Huang, R., Huang, S., & Zhang, S. (2024). Insights of Electrocatalytic Oxidation Mechanisms Utilizing Different Oxidants for Degradation of Organic Pollutants: Option for Sustainability. *ACS Sustainable Chemistry and Engineering*, *12*(12). https://doi.org/10.1021/acssuschemeng.4c00277

Loos, G., Scheers, T., Van Eyck, K., Van Schepdael, A., Adams, E., Van der Bruggen, B., Cabooter, D., & Dewil, R. (2018). Electrochemical oxidation of key pharmaceuticals using a boron doped diamond electrode. *Separation and Purification Technology*, *195*.

https://doi.org/10.1016/j.seppur.2017.12.009

Lu, J., Lu, H., Liang, D., Feng, S., Li, Y., & Li, J. (2023). A review of the occurrence, monitoring, and removal technologies for the remediation of per- and polyfluoroalkyl substances (PFAS) from landfill leachate. *Chemosphere*, *332*, 138824. https://doi.org/10.1016/j.chemosphere.2023.138824

Luu, T. Le. (2020). Post treatment of ICEAS-biologically landfill leachate using electrochemical oxidation with Ti/BDD and Ti/RuO2 anodes. *Environmental Technology and Innovation*, *20*. https://doi.org/10.1016/j.eti.2020.101099

Ma, G., Li, X., Long, Y., Huang, J., Zhang, Z., Liu, F., Han, P., & He, B. (2024). Nanostructured boron-doped diamond electrodes for two-electron water oxidation to produce hydrogen peroxide. *Diamond and Related Materials*, *145*, 111125. https://doi.org/10.1016/J.DIAMOND.2024.111125

Mahvi, A. H., Ebrahimi, S. J. A. din, Mesdaghinia, A., Gharibi, H., & Sowlat, M. H. (2011). Performance evaluation of a continuous bipolar electrocoagulation/electrooxidation-electroflotation (ECEO-EF) reactor designed for simultaneous removal of ammonia and phosphate from wastewater effluent. *Journal of Hazardous Materials*, *192*(3), 1267–1274. https://doi.org/10.1016/j.jhazmat.2011.06.041

Mandal, P., Dubey, B. K., & Gupta, A. K. (2017). Review on landfill leachate treatment by electrochemical oxidation: Drawbacks, challenges and future scope. In *Waste Management* (Vol. 69, pp. 250–273). https://doi.org/10.1016/j.wasman.2017.08.034

Mariano, S. M. F., Angeles, L. F., Aga, D. S., Villanoy, C. L., & Jaraula, C. M. B. (2023). Emerging pharmaceutical contaminants in key aquatic environments of the Philippines. *Frontiers in Earth Science*, *Volume 11*. https://doi.org/10.3389/feart.2023.1124313

Martínez-Huitle, Carlos A., Rodrigo, M. A., Sirés, I., & Scialdone, O. (2015). Single and Coupled Electrochemical Processes and Reactors for the Abatement of Organic Water Pollutants: A Critical Review. In *Chemical Reviews* (Vol. 115, Issue 24). https://doi.org/10.1021/acs.chemrev.5b00361

Martínez-Huitle, Carlos Alberto, & Panizza, M. (2018). Electrochemical oxidation of organic pollutants for wastewater treatment. In *Current Opinion in Electrochemistry* (Vol. 11, pp. 62–71). https://doi.org/10.1016/j.coelec.2018.07.010

Matejczyk, M., Płaza, G. A., Nałcz-Jawecki, G., Ulfig, K., & Markowska-Szczupak, A. (2011). Estimation of the environmental risk posed by landfills using chemical, microbiological and ecotoxicological testing of leachates. *Chemosphere*, *82*(7), 1017–1023. https://doi.org/10.1016/j.chemosphere.2010.10.066

Mavrikis, S., Göltz, M., Perry, S. C., Bogdan, F., Leung, P. K., Rosiwal, S., Wang, L., & Ponce de León, C. (2021). Effective Hydrogen Peroxide Production from Electrochemical Water Oxidation. *ACS Energy Letters*, *6*(7). https://doi.org/10.1021/acsenergylett.1c00904

McBeath, S. T., Wilkinson, D. P., & Graham, N. J. D. (2019). Application of boron-doped diamond electrodes for the anodic oxidation of pesticide micropollutants in a water treatment process: A critical review. In *Environmental Science: Water Research and Technology* (Vol. 5, Issue 12, pp. 2090–2107). https://doi.org/10.1039/c9ew00589g

Meena, V., Swami, D., Chandel, A., Joshi, N., & Prasher, S. O. (2025). Selected emerging contaminants in water: Global occurrence, existing treatment technologies, regulations and associated risk. *Journal of Hazardous Materials*, *483*, 136541. https://doi.org/10.1016/J.JHAZMAT.2024.136541

Mehrkhah, R., Hadavifar, M., Mehrkhah, M., Baghayeri, M., & Lee, B. H. (2025). Recent

advances in titanium-based boron-doped diamond electrodes for enhanced electrochemical oxidation in industrial wastewater treatment: A review. In *Separation and Purification Technology* (Vol. 358). https://doi.org/10.1016/j.seppur.2024.130218

Mongomery, D. C. (2017). Montgomery: Design and Analysis of Experiments. In *John Willy & Sons*.

Monje-Ramirez, I., & Velásquez, M. T. O. De. (2004). Removal and transformation of recalcitrant organic matter from stabilized saline landfill leachates by coagulation-ozonation coupling processes. *Water Research*, *38*(9). https://doi.org/10.1016/j.watres.2004.02.011

Moraes, P. B., & Bertazzoli, R. (2005). Electrodegradation of landfill leachate in a flow electrochemical reactor. *Chemosphere*, *58*(1), 41–46. https://doi.org/10.1016/j.chemosphere.2004.09.026

Moreira, F. C., Boaventura, R. A. R., Brillas, E., & Vilar, V. J. P. (2017). Electrochemical advanced oxidation processes: A review on their application to synthetic and real wastewaters. In *Applied Catalysis B: Environmental* (Vol. 202, pp. 217–261). https://doi.org/10.1016/j.apcatb.2016.08.037

Moreira, F. C., Garcia-Segura, S., Vilar, V. J. P., Boaventura, R. A. R., & Brillas, E. (2013). Decolorization and mineralization of Sunset Yellow FCF azo dye by anodic oxidation, electro-Fenton, UVA photoelectro-Fenton and solar photoelectro-Fenton processes. *Applied Catalysis B: Environmental*, *142–143*, 877–890. https://doi.org/10.1016/j.apcatb.2013.03.023

Morker, H. K., & Saini, B. (2024). A study of advanced oxidation processes for the removal of refractory pollutants from pharmaceutical wastewater. *Development in Wastewater Treatment Research and Processes: Innovative Trends in Removal of Refractory Pollutants*

from Pharmaceutical Wastewater, 271–287. https://doi.org/10.1016/B978-0-323-99278-7.00006-7

Mostafa, E., Reinsberg, P., Garcia-Segura, S., & Baltruschat, H. (2018). Chlorine species evolution during electrochlorination on boron-doped diamond anodes: In-situ electrogeneration of Cl2, Cl2O and ClO2. *Electrochimica Acta*, *281*, 831–840. https://doi.org/10.1016/J.ELECTACTA.2018.05.099

Najafinejad, M. S., Chianese, S., Fenti, A., Iovino, P., & Musmarra, D. (2023). Application of Electrochemical Oxidation for Water and Wastewater Treatment: An Overview. In *Molecules* (Vol. 28, Issue 10). https://doi.org/10.3390/molecules28104208

Nashat, M., Mossad, M., El-Etriby, H. K., & Gar Alalm, M. (2022). Optimization of electrochemical activation of persulfate by BDD electrodes for rapid removal of sulfamethazine. *Chemosphere*, *286*. https://doi.org/10.1016/j.chemosphere.2021.131579

Nekouei, F., & Nekouei, S. (2017). Comparative study of photocatalytic activities of Zn5(OH)8Cl2·H2O and ZnO nanostructures in ciprofloxacin degradation: Response surface methodology and kinetic studies. *Science of the Total Environment*, *601–602*. https://doi.org/10.1016/j.scitotenv.2017.05.117

Nguyen, V. T., Duy Dat, N., Duong, T. G. H., Dinh, V. C., & Vo, T. D. H. (2025). Degradation of tetracycline in water using hydrogen peroxide activated by soybean residue-derived magnetic biochar. *Water Science and Engineering*, *18*(2). https://doi.org/10.1016/j.wse.2024.10.001

Nidheesh, P. V., Ganiyu, S. O., Martínez-Huitle, C. A., Mousset, E., Olvera-Vargas, H., Trellu, C., Zhou, M., & Oturan, M. A. (2023). Recent advances in electro-Fenton process and its emerging applications. In *Critical Reviews in Environmental Science and Technology* (Vol.

53, Issue 8). https://doi.org/10.1080/10643389.2022.2093074

Nidheesh, P. V., Divyapriya, G., Oturan, N., Trellu, C., & Oturan, M. A. (2019). Environmental Applications of Boron-Doped Diamond Electrodes: 1. Applications in Water and Wastewater Treatment. In *ChemElectroChem* (Vol. 6, Issue 8, pp. 2124–2142). https://doi.org/10.1002/celc.201801876

Nishmitha, P. S., Akhilghosh, K. A., Aiswriya, V. P., Ramesh, A., Muthuchamy, M., & Muthukumar, A. (2025). Understanding emerging contaminants in water and wastewater: A comprehensive review on detection, impacts, and solutions. *Journal of Hazardous Materials Advances*, *18*, 100755. https://doi.org/10.1016/J.HAZADV.2025.100755

Oturan, M. A. (2021). Outstanding performances of the BDD film anode in electro-Fenton process: Applications and comparative performance. *Current Opinion in Solid State and Materials Science*, *25*(3). https://doi.org/10.1016/j.cossms.2021.100925

Oturan, M. A., & Aaron, J. J. (2014). Advanced oxidation processes in water/wastewater treatment: Principles and applications. A review. In *Critical Reviews in Environmental Science and Technology* (Vol. 44, Issue 23). https://doi.org/10.1080/10643389.2013.829765

Oturan, N., Wu, J., Zhang, H., Sharma, V. K., & Oturan, M. A. (2013). Electrocatalytic destruction of the antibiotic tetracycline in aqueous medium by electrochemical advanced oxidation processes: Effect of electrode materials. *Applied Catalysis B: Environmental*, *140–141*. https://doi.org/10.1016/j.apcatb.2013.03.035

Ou, D., Chen, B., Bai, R., Song, P., & Lin, H. (2015). Contamination of sulfonamide antibiotics and sulfamethazine-resistant bacteria in the downstream and estuarine areas of Jiulong River in Southeast China. *Environmental Science and Pollution Research*, *22*(16). https://doi.org/10.1007/s11356-015-4473-z

Panakoulias, T., Kalatzis, P., Kalderis, D., & Katsaounis, A. (2010). Electrochemical degradation of Reactive Red 120 using DSA and BDD anodes. *Journal of Applied Electrochemistry*, *40*(10). https://doi.org/10.1007/s10800-010-0138-2

Panizza, M., & Cerisola, G. (2008). Removal of colour and COD from wastewater containing acid blue 22 by electrochemical oxidation. *Journal of Hazardous Materials*, *153*(1–2), 83–88. https://doi.org/10.1016/j.jhazmat.2007.08.023

Panizza, M., & Cerisola, G. (2009). Direct and mediated anodic oxidation of organic pollutants. *Chemical Reviews*, *109*(12). https://doi.org/10.1021/cr9001319

Panizza, M., & Martinez-Huitle, C. A. (2013). Role of electrode materials for the anodic oxidation of a real landfill leachate – Comparison between Ti–Ru–Sn ternary oxide, PbO2 and boron-doped diamond anode. *Chemosphere*, *90*(4), 1455–1460. https://doi.org/10.1016/J.CHEMOSPHERE.2012.09.006

Pei, S., Shen, C., Zhang, C., Ren, N., & You, S. (2019). Characterization of the Interfacial Joule Heating Effect in the Electrochemical Advanced Oxidation Process. *Environmental Science and Technology*, *53*(8). https://doi.org/10.1021/acs.est.8b06773

Pérez, G., Saiz, J., Ibañez, R., Urtiaga, A. M., & Ortiz, I. (2012). Assessment of the formation of inorganic oxidation by-products during the electrocatalytic treatment of ammonium from landfill leachates. *Water Research*, *46*(8), 2579–2590. https://doi.org/10.1016/j.watres.2012.02.015

Podder, S., & Mukherjee, S. (2024). Response Surface Methodology (Rsm) As a Tool in Pharmaceutical Formulation Development. In *Asian Journal of Pharmaceutical and Clinical Research* (Vol. 17, Issue 11, pp. 18–25). https://doi.org/10.22159/ajpcr.2024v17i11.52149

Postacchini, L., Ciarapica, F. E., & Bevilacqua, M. (2018). Environmental assessment of a landfill leachate treatment plant: Impacts and research for more sustainable chemical alternatives. *Journal of Cleaner Production*, *183*, 1021–1033. https://doi.org/10.1016/j.jclepro.2018.02.219

Puri, M., Gandhi, K., & Kumar, M. S. (2023). Emerging environmental contaminants: A global perspective on policies and regulations. *Journal of Environmental Management*, *332*, 117344. https://doi.org/10.1016/j.jenvman.2023.117344

Qi, C., Huang, J., Wang, B., Deng, S., Wang, Y., & Yu, G. (2018). Contaminants of emerging concern in landfill leachate in China: A review. In *Emerging Contaminants* (Vol. 4, Issue 1, pp. 1–10). https://doi.org/10.1016/j.emcon.2018.06.001

Qi, C., Liu, X., Lin, C., Zhang, H., Li, X., & Ma, J. (2017). Activation of peroxymonosulfate by microwave irradiation for degradation of organic contaminants. *Chemical Engineering Journal*, *315*, 201–209. https://doi.org/10.1016/j.cej.2017.01.012

Qi, C., Liu, X., Lin, C., Zhang, X., Ma, J., Tan, H., & Ye, W. (2014). Degradation of sulfamethoxazole by microwave-activated persulfate: Kinetics, mechanism and acute toxicity. *Chemical Engineering Journal*, *249*, 6–14. https://doi.org/10.1016/j.cej.2014.03.086

Qi, H., Shi, X., Liu, Z., Yan, Z., & Sun, Z. (2023). In situ etched graphite felt modified with CuFe2O4/Cu2O/Cu catalyst derived from CuFe PBA for the efficient removal of sulfamethoxazole through a heterogeneous electro-Fenton process. *Applied Catalysis B: Environmental*, *331*. https://doi.org/10.1016/j.apcatb.2023.122722

Qiao, L., Zhang, H., Zhao, J., Cen, Z., & Yu, T. (2024). Mechanism and Process Optimization in the Electrooxidation of Oxalic Acid Using BDD Electrode under Nitric Acid Environment.

ACS Omega, *9*(50), 49839–49848. https://doi.org/10.1021/acsomega.4c08628

Quan, X., Cheng, Z., Chen, B., & Zhu, X. (2013). Electrochemical oxidation of recalcitrant organic compounds in biologically treated municipal solid waste leachate in a flow reactor. *Journal of Environmental Sciences (China)*, *25*(10), 2023–2030. https://doi.org/10.1016/S1001-0742(12)60253-8

Radjenovic, J., & Sedlak, D. L. (2015). Challenges and Opportunities for Electrochemical Processes as Next-Generation Technologies for the Treatment of Contaminated Water. In *Environmental Science and Technology* (Vol. 49, Issue 19). https://doi.org/10.1021/acs.est.5b02414

Rahmani, A. R., Azarian, G., & Nematollahi, D. (2018). New insights into electrocatalytic ozone generation using Pt/Ni-Sb-SnO2 and GC/Ni-Sb-SnO2 electrodes. *Journal of Electroanalytical Chemistry*, *824*, 216–225. https://doi.org/10.1016/j.jelechem.2018.07.050

Rahmani, A. R., Nematollahi, D., Samarghandi, M. R., Samadi, M. T., & Azarian, G. (2018). A Central Composite Design to Optimize In-Situ Electrochemically Produced Ozone for Removal of Reactive Red 198. *Journal of The Electrochemical Society*, *165*(3), E121–E128. https://doi.org/10.1149/2.0201803jes

Ren, Q., Zhang, W., Yan, W., & Wang, Z. (2025). Highly stable and efficient Sb doped Ti/RuO2-IrO2-SnO2 electrode toward organic pollutants degradation by in situ generated oxidizing species. *Separation and Purification Technology*, *354*, 129345. https://doi.org/10.1016/J.SEPPUR.2024.129345

Renou, S., Givaudan, J. G., Poulain, S., Dirassouyan, F., & Moulin, P. (2008). Landfill leachate treatment: Review and opportunity. In *Journal of Hazardous Materials* (Vol. 150, Issue 3, pp. 468–493). https://doi.org/10.1016/j.jhazmat.2007.09.077

Rice, D., Westerhoff, P., Perreault, F., & Garcia-Segura, S. (2018). Electrochemical self-cleaning anodic surfaces for biofouling control during water treatment. *Electrochemistry Communications*, *96*. https://doi.org/10.1016/j.elecom.2018.10.002

Robinson, A. A., Belden, J. B., & Lydy, M. J. (2005). Toxicity of fluoroquinolone antibiotics to aquatic organisms. *Environmental Toxicology and Chemistry*, *24*(2). https://doi.org/10.1897/04-210R.1

Rocha, J. H. B., Gomes, M. M. S., Fernandes, N. S., Da Silva, D. R., & Martínez-Huitle, C. A. (2012). Application of electrochemical oxidation as alternative treatment of produced water generated by Brazilian petrochemical industry. *Fuel Processing Technology*, *96*, 80–87. https://doi.org/10.1016/j.fuproc.2011.12.011

Sabba, F., Kassar, C., Zeng, T., Mallick, S. P., Downing, L., & McNamara, P. (2025). PFAS in landfill leachate: Practical considerations for treatment and characterization. *Journal of Hazardous Materials*, *481*, 136685. https://doi.org/10.1016/J.JHAZMAT.2024.136685

Sakkas, V. A., Calza, P., Islam, M. A., Medana, C., Baiocchi, C., Panagiotou, K., & Albanis, T. (2009). TiO2/H2O2 mediated photocatalytic transformation of UV filter 4-methylbenzylidene camphor (4-MBC) in aqueous phase: Statistical optimization and photoproduct analysis. *Applied Catalysis B: Environmental*, *90*(3–4), 526–534. https://doi.org/10.1016/j.apcatb.2009.04.013

Saleh, M., Yildirim, R., Isik, Z., Karagunduz, A., Keskinler, B., & Dizge, N. (2021). Optimization of the electrochemical oxidation of textile wastewater by graphite electrodes by response surface methodology and artificial neural network. *Water Science and Technology*, *84*(5). https://doi.org/10.2166/wst.2021.240

Sambaza, S. S., & Naicker, N. (2023). Contribution of wastewater to antimicrobial resistance: A

review article. In *Journal of Global Antimicrobial Resistance* (Vol. 34). https://doi.org/10.1016/j.jgar.2023.05.010

Sanchez-Castrillon, S., Benítez, L. N., Vazquez-Arenas, J., Ferraro, F., & Palma-Goyes, R. E. (2024). Reaction Mechanism of Oxytetracycline Degradation by Electrogenerated Reactive Chlorine: The Influence of Current Density and pH. *ACS Omega*, *9*(46), 46302–46311. https://doi.org/10.1021/acsomega.4c07234

Sánchez-Sánchez, C. M., Expósito, E., Casado, J., & Montiel, V. (2007). Goethite as a more effective iron dosage source for mineralization of organic pollutants by electro-Fenton process. *Electrochemistry Communications*, *9*(1). https://doi.org/10.1016/j.elecom.2006.08.023

Santos, J. P. T. da S., Tonholo, J., de Andrade, A. R., Del Colle, V., & Zanta, C. L. de P. e. S. (2021). The electro-oxidation of tetracycline hydrochloride in commercial DSA® modified by electrodeposited platinum. *Environmental Science and Pollution Research*, *28*(19). https://doi.org/10.1007/s11356-020-09919-2

Schranck, A., & Doudrick, K. (2020). Effect of reactor configuration on the kinetics and nitrogen byproduct selectivity of urea electrolysis using a boron doped diamond electrode. *Water Research*, *168*. https://doi.org/10.1016/j.watres.2019.115130

Senthil Rathi, B., Senthil Kumar, P., Parthasarathy, V., Gokul, R., Dharani, R., Lavanya, R., & Rangasamy, G. (2024). Current research progress in the biological removal of emerging contaminants from the water environment. *Water Practice and Technology*, *19*(8), 3154–3181. https://doi.org/10.2166/wpt.2024.189

Simonetti, F., Brillarelli, S., Agostini, M., Mancini, M., Gioia, V., Murtas, S., & Migliorati, V. (2025). A review on the latest frontiers in water quality in the era of emerging

contaminants: A focus on perfluoroalkyl compounds. *Environmental Pollution*, *381*, 126402. https://doi.org/10.1016/J.ENVPOL.2025.126402

Singh, A., Lalung, J., Ivshina, I., & Kostova, I. (2024). Editorial: Pharmaceutically active micropollutants - how serious is the problem and is there a microbial way out? In *Frontiers in microbiology* (Vol. 15, p. 1466334). https://doi.org/10.3389/fmicb.2024.1466334

Sirés, I., & Brillas, E. (2012). Remediation of water pollution caused by pharmaceutical residues based on electrochemical separation and degradation technologies: A review. In *Environment International* (Vol. 40, Issue 1). https://doi.org/10.1016/j.envint.2011.07.012

Sirés, I., Brillas, E., Oturan, M. A., Rodrigo, M. A., & Panizza, M. (2014a). Electrochemical advanced oxidation processes: Today and tomorrow. A review. *Environmental Science and Pollution Research*, *21*(14). https://doi.org/10.1007/s11356-014-2783-1

Sirés, I., Brillas, E., Oturan, M. A., Rodrigo, M. A., & Panizza, M. (2014b). Electrochemical advanced oxidation processes: Today and tomorrow. A review. *Environmental Science and Pollution Research*, *21*(14), 8336–8367. https://doi.org/10.1007/s11356-014-2783-1

Song, Y., Xiao, M., Li, Z., Luo, Y., Zhang, K., Du, X., Zhang, T., Wang, Z., & Liang, H. (2022). Degradation of antibiotics, organic matters and ammonia during secondary wastewater treatment using boron-doped diamond electro-oxidation combined with ceramic ultrafiltration. *Chemosphere*, *286*. https://doi.org/10.1016/j.chemosphere.2021.131680

Sopaj, F., Rodrigo, M. A., Oturan, N., Podvorica, F. I., Pinson, J., & Oturan, M. A. (2015). Influence of the anode materials on the electrochemical oxidation efficiency. Application to oxidative degradation of the pharmaceutical amoxicillin. *Chemical Engineering Journal*, *262*. https://doi.org/10.1016/j.cej.2014.09.100

Sun, M., Wang, X., Winter, L. R., Zhao, Y., Ma, W., Hedtke, T., Kim, J.-H., & Elimelech, M.

(2021). Electrified Membranes for Water Treatment Applications. *ACS ES&T Engineering*, *1*(4), 725–752. https://doi.org/10.1021/acsestengg.1c00015

Sundararaman, S., Aravind Kumar, J., Deivasigamani, P., & Devarajan, Y. (2022). Emerging pharma residue contaminants: Occurrence, monitoring, risk and fate assessment – A challenge to water resource management. *Science of the Total Environment*, *825*. https://doi.org/10.1016/j.scitotenv.2022.153897

Tang, J., Yao, S., Xiao, F., Xia, J., & Xing, X. (2022). Electrochemical Oxidation of Landfill Leachate after Biological Treatment by Electro-Fenton System with Corroding Electrode of Iron. *International Journal of Environmental Research and Public Health*, *19*(13). https://doi.org/10.3390/ijerph19137745

Teng, C., Zhou, K., Peng, C., & Chen, W. (2021). Characterization and treatment of landfill leachate: A review. In *Water Research* (Vol. 203). https://doi.org/10.1016/j.watres.2021.117525

Teng, J., Liu, G., Liang, J., & You, S. (2020). Electrochemical oxidation of sulfadiazine with titanium suboxide mesh anode. *Electrochimica Acta*, *331*. https://doi.org/10.1016/j.electacta.2019.135441

Teófilo, R. F., & Ferreira, M. M. C. (2006). Chemometrics II: Spreadsheets for experimental design calculations, A tutorial. *Quimica Nova*, *29*(2), 338–350. https://doi.org/10.1590/s0100-40422006000200026

Tian, X., Liu, J., Wang, Y., Shi, F., Shan, Z., Zhou, J., & Liu, J. (2019). Adsorption of antibiotics from aqueous solution by different aerogels. *Journal of Non-Crystalline Solids*, *505*. https://doi.org/10.1016/j.jnoncrysol.2018.10.033

Ting, W. P., Lu, M. C., & Huang, Y. H. (2008). The reactor design and comparison of Fenton,

electro-Fenton and photoelectro-Fenton processes for mineralization of benzene sulfonic acid (BSA). *Journal of Hazardous Materials*, *156*(1–3). https://doi.org/10.1016/j.jhazmat.2007.12.031

Tisler, S., Kilpinen, K., Devers, J., Castro, M., Jørgensen, M. B., Mandava, G., Lundqvist, J., Cedergreen, N., & Christensen, J. H. (2025). Mapping Emerging Contaminants in Wastewater Effluents through Multichromatographic Platform Analysis and Source Correlations. *Environmental Science & Technology*, *59*(11), 5766–5774. https://doi.org/10.1021/acs.est.5c01139

Turan, A., Keyikoglu, R., Kobya, M., & Khataee, A. (2020). Degradation of thiocyanate by electrochemical oxidation process in coke oven wastewater: Role of operative parameters and mechanistic study. *Chemosphere*, *255*, 127014. https://doi.org/10.1016/J.CHEMOSPHERE.2020.127014

Turro, E., Giannis, A., Cossu, R., Gidarakos, E., Mantzavinos, D., & Katsaounis, A. (2012). Reprint of: Electrochemical oxidation of stabilized landfill leachate on DSA electrodes. *Journal of Hazardous Materials*, *207–208*, 73–78. https://doi.org/10.1016/j.jhazmat.2012.01.083

Urtiaga, A., Gómez-Lavín, S., & Soriano, A. (2022). Electrochemical treatment of municipal landfill leachates and implications for poly- and perfluoroalkyl substances (PFAS) removal. *Journal of Environmental Chemical Engineering*, *10*(3). https://doi.org/10.1016/j.jece.2022.107900

Urtiaga, A., Ortiz, I., Anglada, A., Mantzavinos, D., & Diamadopoulos, E. (2012). Kinetic modeling of the electrochemical removal of ammonium and COD from landfill leachates. *Journal of Applied Electrochemistry*, *42*(9). https://doi.org/10.1007/s10800-012-0458-5

Vanlangendonck, Y., Corbisier, D., & Van Lierde, A. (2005). Influence of operating conditions on the ammonia electro-oxidation rate in wastewaters from power plants (ELONITA^{TM} technique). *Water Research*, *39*(13), 3028–3034. https://doi.org/10.1016/j.watres.2005.05.013

Vasilie, S., Manea, F., Baciu, A., & Pop, A. (2018). Dual use of boron-doped diamond electrode in antibiotics-containing water treatment and process control. *Process Safety and Environmental Protection*, *117*. https://doi.org/10.1016/j.psep.2018.05.024

Veli, S., Arslan, A., Isgoren, M., Bingol, D., & Demiral, D. (2021). Experimental design approach to COD and color removal of landfill leachate by the electrooxidation process. *Environmental Challenges*, *5*. https://doi.org/10.1016/j.envc.2021.100369

Vinayagam, V., Palani, K. N., Ganesh, S., Rajesh, S., Akula, V. V., Avoodaiappan, R., Kushwaha, O. S., & Pugazhendhi, A. (2024). Recent developments on advanced oxidation processes for degradation of pollutants from wastewater with focus on antibiotics and organic dyes. *Environmental Research*, *240*, 117500. https://doi.org/10.1016/J.ENVRES.2023.117500

Wachter, N., Aquino, J. M., Denadai, M., Barreiro, J. C., Silva, A. J., Cass, Q. B., Bocchi, N., & Rocha-Filho, R. C. (2019). Electrochemical degradation of the antibiotic ciprofloxacin in a flow reactor using distinct BDD anodes: Reaction kinetics, identification and toxicity of the degradation products. *Chemosphere*, *234*. https://doi.org/10.1016/j.chemosphere.2019.06.053

Wada, O. Z., & Olawade, D. B. (2025). Recent occurrence of pharmaceuticals in freshwater, emerging treatment technologies, and future considerations: A review. *Chemosphere*, *374*, 144153. https://doi.org/10.1016/J.CHEMOSPHERE.2025.144153

Wainaina, S., Awasthi, M. K., Sarsaiya, S., Chen, H., Singh, E., Kumar, A., Ravindran, B., Awasthi, S. K., Liu, T., Duan, Y., Kumar, S., Zhang, Z., & Taherzadeh, M. J. (2020). Resource recovery and circular economy from organic solid waste using aerobic and anaerobic digestion technologies. In *Bioresource Technology* (Vol. 301). https://doi.org/10.1016/j.biortech.2020.122778

Wakejo, W. K., Meshesha, B. T., Kang, J. W., Dessalegn, E. E., & Demesa, A. G. (2024). Integrated electrochemical-adsorption for simultaneous removal of pharmaceuticals from water: Process optimization and synergistic insights. *Chemosphere*, *365*, 143402. https://doi.org/10.1016/J.CHEMOSPHERE.2024.143402

Wang, Jiachen, & Qiao, Z. (2024). A comprehensive review of landfill leachate treatment technologies. *Frontiers in Environmental Science*, *12*(September). https://doi.org/10.3389/fenvs.2024.1439128

Wang, Jianbing, Zhi, D., Zhou, H., He, X., & Zhang, D. (2018a). Evaluating tetracycline degradation pathway and intermediate toxicity during the electrochemical oxidation over a Ti/Ti4O7 anode. *Water Research*, *137*. https://doi.org/10.1016/j.watres.2018.03.030

Wang, Jianbing, Zhi, D., Zhou, H., He, X., & Zhang, D. (2018b). Evaluating tetracycline degradation pathway and intermediate toxicity during the electrochemical oxidation over a Ti/Ti(4)O(7) anode. *Water Research*, *137*, 324–334. https://doi.org/10.1016/j.watres.2018.03.030

Wang, W., Li, Y., Li, Y., Zhou, M., & Arotiba, O. A. (2020). Electro-Fenton and photoelectro-Fenton degradation of sulfamethazine using an active gas diffusion electrode without aeration. *Chemosphere*, *250*. https://doi.org/10.1016/j.chemosphere.2020.126177

Wang, Xinyu, Li, X., Li, S., Du, W., Yan, W., & Xu, H. (2025). Degradation of antibiotics by

electrochemical oxidation: Current issues, environmental risks, and future strategies. In *Chemical Engineering Journal* (Vol. 516). https://doi.org/10.1016/j.cej.2025.163941

Wang, Xuechun, Jing, J., Zhou, M., & Dewil, R. (2023). Recent advances in H2O2-based advanced oxidation processes for removal of antibiotics from wastewater. *Chinese Chemical Letters*, *34*(3). https://doi.org/10.1016/j.cclet.2022.06.044

Wroński, M., Trawiński, J., & Skibiński, R. (2025). Environmental remediation of anti-infective drugs using boron-doped diamond electrodes: Opportunities and challenges. In *Desalination and Water Treatment* (Vol. 323). https://doi.org/10.1016/j.dwt.2025.101332

Wu, L., Yang, Y., Wang, Y., Wang, C., Zhang, Y., Xu, J., Jiao, Z., & Peng, Y. (2025). Electrochemical treatment of bio-treated landfill leachate: Influence of electrode materials, current density, and sodium chloride concentration. *Frontiers of Environmental Science & Engineering*, *19*(6), 76. https://doi.org/10.1007/s11783-025-1996-5

Xiang, R., Wei, W., Mei, T., Wei, Z., Yang, X., Liang, J., & Zhu, J. (2025). A Review on Landfill Leachate Treatment Technologies: Comparative Analysis of Methods and Process Innovation. In *Applied Sciences* (Vol. 15, Issue 7). https://doi.org/10.3390/app15073878

xiangyu, B., Chao, L., Shilong, H., jiping, Z., & Hu, J. (2025). Combining advanced oxidation processes with biological processes in organic wastewater treatment: Recent developments, trends, and advances. *Desalination and Water Treatment*, *323*, 101263. https://doi.org/10.1016/J.DWT.2025.101263

Xu, T., Tang, X., Qiu, M., Lv, X., Shi, Y., Zhou, Y., Xie, Y., Naushad, M., Lam, S. S., Ng, H. S., Sonne, C., & Ge, S. (2023). Degradation of levofloxacin from antibiotic wastewater by pulse electrochemical oxidation with BDD electrode. *Journal of Environmental Management*, *344*. https://doi.org/10.1016/j.jenvman.2023.118718

Xu, W., Zhang, G., Li, X., Zou, S., Li, P., Hu, Z., & Li, J. (2007). Occurrence and elimination of antibiotics at four sewage treatment plants in the Pearl River Delta (PRD), South China. *Water Research*, *41*(19). https://doi.org/10.1016/j.watres.2007.06.023

Yaşar Çırak, S., Öztürk, D., & Akyol, A. (2025). Electrocatalytic Oxidation of Toxic Wastewater using Electrodes based on Transition d-metal Oxides. *Water, Air, & Soil Pollution*, *236*(2), 91. https://doi.org/10.1007/s11270-024-07727-9

Yin, J., Zhang, H., Luo, M., Zhao, J., Zhou, X., Wang, F., Zhou, H., Yuan, Y., Liu, Y., Shi, Y., Xiong, Z., & Lai, B. (2025). Electro-Fenton process for wastewater treatment: From selective H2O2 generation to efficient •OH conversion. *Chemical Engineering Journal*, *507*, 160709. https://doi.org/10.1016/J.CEJ.2025.160709

Yu, Xia, Tang, L., Yan, R., Wang, J., Zhao, W., Lyu, S., & Sui, Q. (2025). Quantifying PFAS contamination and environmental risk in municipal solid waste landfill refuse: Implications for landfill reuse. *Water Research*, *283*, 123881. https://doi.org/10.1016/J.WATRES.2025.123881

Yu, Xinmin, Zhou, M., Hu, Y., Groenen Serrano, K., & Yu, F. (2014). Recent updates on electrochemical degradation of bio-refractory organic pollutants using BDD anode: A mini review. *Environmental Science and Pollution Research*, *21*(14). https://doi.org/10.1007/s11356-014-2820-0

Yuan, Q., Qu, S., Li, R., Huo, Z. Y., Gao, Y., & Luo, Y. (2023). Degradation of antibiotics by electrochemical advanced oxidation processes (EAOPs): Performance, mechanisms, and perspectives. In *Science of the Total Environment* (Vol. 856). https://doi.org/10.1016/j.scitotenv.2022.159092

Yuan, S. fen, Liu, Z. hua, Yin, H., Dang, Z., Wu, P. xiao, Zhu, N. wu, & Lin, Z. (2019). Trace

determination of sulfonamide antibiotics and their acetylated metabolites via SPE-LC-MS/MS in wastewater and insights from their occurrence in a municipal wastewater treatment plant. *Science of the Total Environment*, *653*. https://doi.org/10.1016/j.scitotenv.2018.10.417

Zambrano, J., & Min, B. (2020). Electrochemical treatment of leachate containing highly concentrated phenol and ammonia using a Pt/Ti anode at different current densities. *Environmental Technology and Innovation*, *18*. https://doi.org/10.1016/j.eti.2020.100632

Zha, F., Zhang, M., & Xu, G. (2015). Treatment of landfill leachate by sonolysis followed by Fenton process. *New Pub: Balaban*, *53*(2), 360–366. https://doi.org/10.1080/19443994.2013.839398

Zhang, Haiya, Mu, Y., Li, S., Wang, Y., Ya, T., Chen, C., & Duan, L. (2025). Challenges and Future Directions of Neglected Emerging Contaminants in Wastewater Treatment Plants. *ACS ES&T Water*, *5*(5), 2005–2008. https://doi.org/10.1021/acsestwater.5c00394

Zhang, Hui, Ran, X., Wu, X., & Zhang, D. (2011). Evaluation of electro-oxidation of biologically treated landfill leachate using response surface methodology. *Journal of Hazardous Materials*, *188*(1–3). https://doi.org/10.1016/j.jhazmat.2011.01.097

Zhang, J., Yang, T., Wang, H., Yang, K., Fang, C., Lv, B., & Yang, X. (2015). Study on treating old landfill leachate by Ultrasound–Fenton oxidation combined with MAP chemical precipitation. *Chemical Speciation and Bioavailability*, *27*(4), 175–182. https://doi.org/10.1080/09542299.2015.1118360

Zhao, R., Zhang, X., Chen, F., Man, X., & Jiang, W. (2019). Study on Electrochemical Degradation of Nicosulfuron by IrO2-Based DSA Electrodes: Performance, Kinetics, and Degradation Mechanism. In *International Journal of Environmental Research and Public*

Health (Vol. 16, Issue 3). https://doi.org/10.3390/ijerph16030343

Zhou, B., Yu, Z., Wei, Q., Long, H. Y., Xie, Y., & Wang, Y. (2016). Electrochemical oxidation of biological pretreated and membrane separated landfill leachate concentrates on boron doped diamond anode. *Applied Surface Science*, *377*. https://doi.org/10.1016/j.apsusc.2016.03.045

Zhou, L. J., Ying, G. G., Zhao, J. L., Yang, J. F., Wang, L., Yang, B., & Liu, S. (2011). Trends in the occurrence of human and veterinary antibiotics in the sediments of the Yellow River, Hai River and Liao River in northern China. *Environmental Pollution*, *159*(7). https://doi.org/10.1016/j.envpol.2011.03.034

Zolfaghari, M., Jardak, K., Drogui, P., Brar, S. K., Buelna, G., & Dubé, R. (2016). Landfill leachate treatment by sequential membrane bioreactor and electro-oxidation processes. *Journal of Environmental Management*, *184*, 318–326. https://doi.org/10.1016/j.jenvman.2016.10.010

Zoungrana, A., Hasnine, M. D. T., & Yuan, Q. (2022). *Landfill Mining: Significance, Operation and Global Perspectives BT - Circular Economy in Municipal Solid Waste Landfilling: Biomining & Leachate Treatment : Sustainable Solid Waste Management: Waste to Wealth* (P. Pathak & S. G. Palani (Eds.); pp. 25–45). Springer International Publishing. https://doi.org/10.1007/978-3-031-07785-2_2

Appendix-A

Supporting information for Chapter 3 titled "Optimization of electrochemical oxidation process with Boron-doped diamond (BDD) electrodes for the removal of COD, color, ammonium, and phosphate in mature landfill leachate"

Table S1: Analysis of variance for linear models (ANOVA)

COD removal					
VS	**QS**	**DF**	**QA**	**F test**	***p***
Regression	682	2	341	28.471392*	0.004308
Residuals	47.9	4	12		
Lack off it	19.4	2	9.69	0.6791725	0.5955314
Pure error	28.5	2	14.3		
Total	730	6			
% variance explained				93.436467	
% maximum variance explainable				96.09121	
Color removal					
VS	**QS**	**DF**	**QA**	**F test**	***p***
Regression	84	2	42	11.678434*	0.021379
Residuals	14.4	4	3.6		
Lack off it	11.9	2	5.91	4.8857081	0.1699031
Pure error	2.44	2	1.22		
Total	98.4	6			
% variance explained				85.378443	
% maximum variance explainable				97.515752	
NH_4^+ removal					
VS	**QS**	**DF**	**QA**	**F test**	***p***
Regression	2076	2	1038	5.22226	0.1054057

Residuals	795	4	199		
Lack off it	775	2	387	37.792732	0.1142686
Pure error	20.5	2	10.2		
Total	2871	6			
% variance explained				72.307837	
% maximum variance explainable				99.286151	

PO_4^{3-} removal					
VS	**QS**	**DF**	**QA**	**F test**	***p***
Regression	1196	2	598	8.5140846*	0.036184
Residuals	281	4	70.2		
Lack off it	203	2	101	2.5857963	0.2788003
Pure error	78.3	2	39.2		
Total	1477	6			
% variance explained				80.977897	
% maximum variance explainable				94.696631	

* Significant values

VS: variance source, **QS**: quadratic sums, **DF**: degrees of freedom, **QA**: quadratic mean, **F test**: calculated value of measured test F, **p**: statistical parameter p.

Table S2: Chloride (Cl^-) concentration

Experiment	**Variable**		
	Current densities (mA/cm^2)	**pH**	**Chloride (Cl^-) mg/L**
1	64	3	773
2	125	3	339
3	64	8	790
4	125	8	748
5	95	5.5	840
6	95	5.5	812
7	95	5.5	826
Raw leachate			1248

Appendix- B

Supplementary information for Chapter 4 titled "Influence of operational parameters on mixed pharmaceutical antibiotics removal from wastewater using Boron-doped diamond (BDD) electrooxidation".

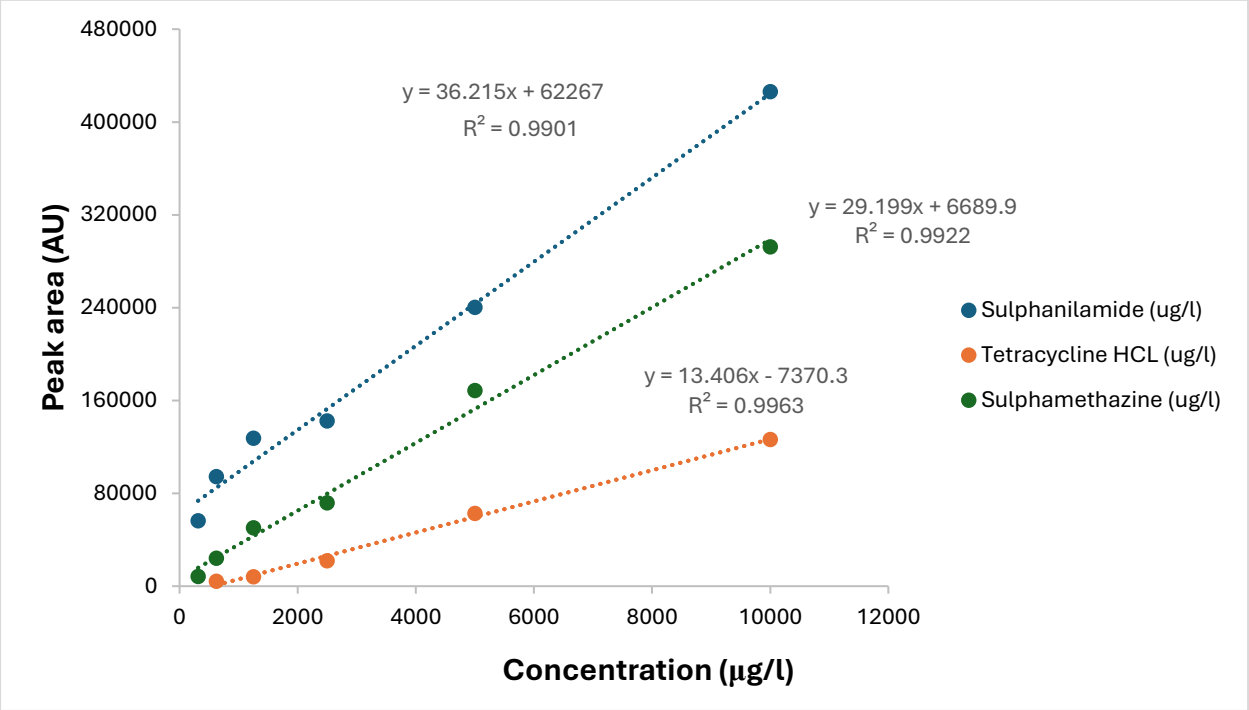

Figure S1: Standard calibration curve for mixed pharmaceuticals in HPLC

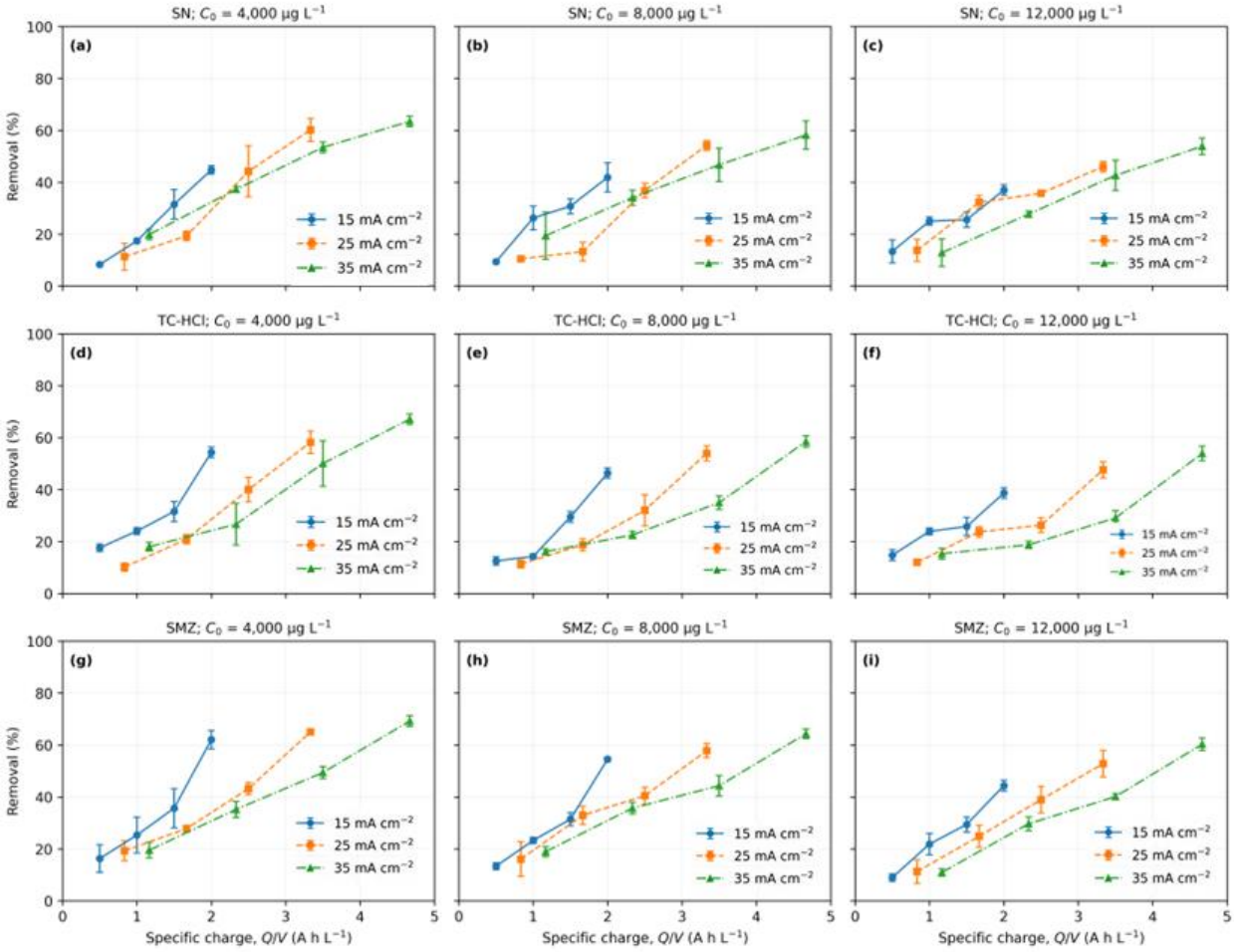

Figure S2: Removal of sulfanilamide (SN), tetracycline hydrochloride (TC-HCl), and sulfamethazine (SMZ) as a function of volumetric specific charge at pH 7.0 and initial concentrations of 4000, 8000, and 12000 µg/L. Symbols and error bars represent mean ± standard deviation of triplicate measurements. Current density series correspond to 15, 25, and 35 mA/cm^2.

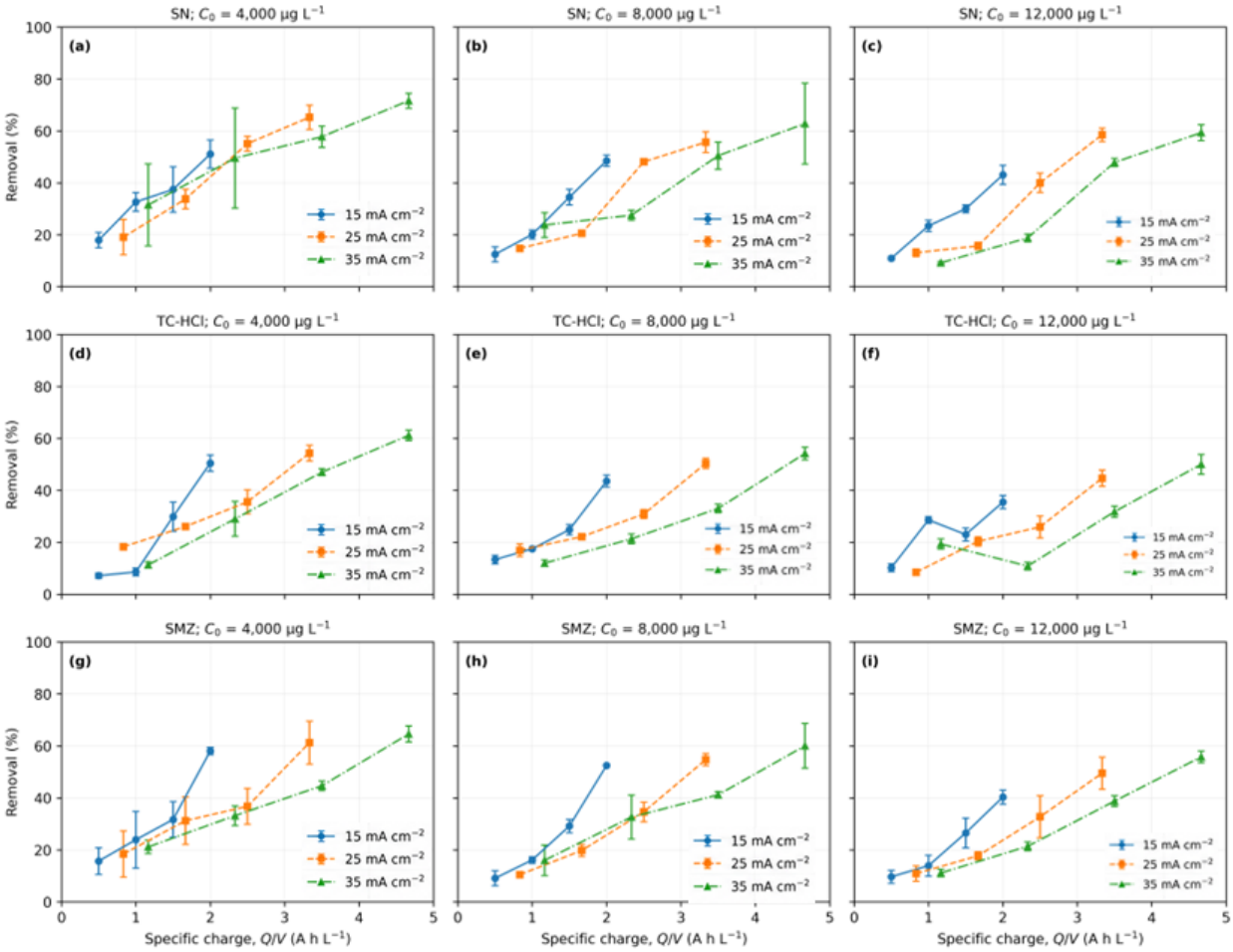

Figure S3: Removal of sulfanilamide (SN), tetracycline hydrochloride (TC-HCl), and sulfamethazine (SMZ) as a function of volumetric specific charge at pH 9.0 and initial concentrations of 4000, 8000, and 12000 µg/L. Symbols and error bars represent mean ± standard deviation of triplicate measurements. Current density series correspond to 15, 25, and 35 mA/cm^2.

Table S1: Calibration parameters of the standard curve

Analyte	No. of calibration point	Concentration range µg/L	Regression equation	R^2	Mean RT ± SD (min.)	RT-RSD (%)
Sulfanilamide	6	312.5–10,000	(y = 36.2155x + 62,266.8)	0.9901	2.162 ± 0.006	0.28
Tetracycline-HCl	5	625–10,000	(y = 13.4059x - 7,370.3)	0.9963	4.201 ± 0.007	0.18
Sulfamethazine	6	312.5–10,000	(y = 29.1986x + 6,689.9)	0.9922	4.860 ± 0.008	0.17

Table S2: Regression-derived LOD/LOQ estimates

Analyte	LOD signal threshold in area	LOQ signal threshold in area	Conservative regression LOD (3.3× (σ/S) (µg/L)	Conservative regression LOQ (10× (σ/S) (µg/L)	Intercept-based LOD (µg/L)	Intercept-based LOQ (µg/L)
Sulfanilamide	111,905.50	212,687.00	1,370.60	4,153.50	779.4	2,362.00
Tetracycline-HCl	4,479.90	28,539.40	884	2,678.60	598.4	1,813.50
Sulfamethazine	42,197.80	114,289.40	1,216.10	3,685.10	691.5	2,095.60

where (σ) is the standard deviation of the response and (S) is the slope of the regression line.

Table S3: Electrical dose delivered after 60 min

Current density (mA/cm^2)	Current (A)	Time (min)	Q/V ($A\ h\ L^{-1}$)	Q/V ($C\ L^{-1}$)
15	6	60	2.0	7200
25	10	60	3.33	12000
35	14	60	4.66	16800

Table S4: Average removal at an equal specific charge of 2.0 A h L^{-}

Antibiotic	15 mA/cm^2	25 mA/cm^2	35 mA/cm^2
SN	46.97%	31.42%	27.95%
TC-HCl	47.20%	27.83%	23.80%
SMZ	55.03%	33.06%	29.17%

Table S5: Tukey HSD Table (Significant-Only)

Group1	Group2	meandiff	*p*-adj	lower	upper	reject	compound	pH	time	stars
15	35	6.7971	0.0009	2.7515	10.8428	True	Sulfanilamide	3.5	15.0	***
25	35	5.4286	0.0072	1.3829	9.4742	True	Sulfanilamide	3.5	15.0	**
15	35	13.0758	0.0045	3.8785	22.273	True	Sulfanilamide	3.5	30.0	**
15	25	13.5344	0.0035	4.2853	22.7835	True	Sulfanilamide	3.5	45.0	**
15	35	19.6795	0.0001	10.4304	28.9286	True	Sulfanilamide	3.5	45.0	***
15	25	10.2339	0.003	3.3609	17.107	True	Sulfanilamide	3.5	60.0	**
15	35	18.0907	0.0	11.2176	24.9638	True	Sulfanilamide	3.5	60.0	***
25	35	7.8568	0.0229	0.9837	14.7298	True	Sulfanilamide	3.5	60.0	*
15	35	7.015	0.0099	1.5685	12.4615	True	Sulfanilamide	7.0	15.0	**
25	35	5.5207	0.0465	0.0742	10.9672	True	Sulfanilamide	7.0	15.0	*
15	35	10.1258	0.0066	2.6674	17.5843	True	Sulfanilamide	7.0	30.0	**

25	35	11.3783	0.0024	3.9199	18.8368	True	Sulfanilamide	7.0	30.0	**
15	25	9.6316	0.0055	2.6874	16.5759	True	Sulfanilamide	7.0	45.0	**
15	35	18.3154	0.0	11.3711	25.2597	True	Sulfanilamide	7.0	45.0	***
25	35	8.6838	0.0124	1.7395	15.628	True	Sulfanilamide	7.0	45.0	*
15	25	12.2268	0.0003	5.6353	18.8183	True	Sulfanilamide	7.0	60.0	***
15	35	17.2694	0.0	10.6779	23.8609	True	Sulfanilamide	7.0	60.0	***
15	25	13.7498	0.0002	6.5463	20.9534	True	Sulfanilamide	9.0	45.0	***
15	35	18.0476	0.0	10.844	25.2512	True	Sulfanilamide	9.0	45.0	***
15	25	12.2541	0.0032	3.9587	20.5495	True	Sulfanilamide	9.0	60.0	**
15	35	17.0213	0.0001	8.7259	25.3167	True	Sulfanilamide	9.0	60.0	***
15	35	8.4551	0.0038	2.615	14.2952	True	Tetracycline-HCL	3.5	15.0	**
25	35	11.2118	0.0002	5.3717	17.0518	True	Tetracycline-HCL	3.5	15.0	***
15	35	11.6168	0.005	3.3442	19.8893	True	Tetracycline-HCL	3.5	30.0	**
25	35	8.3473	0.0477	0.0748	16.6198	True	Tetracycline-HCL	3.5	30.0	*
15	35	23.2877	0.0	14.1255	32.4499	True	Tetracycline-HCL	3.5	45.0	***
25	35	14.92	0.0012	5.7578	24.0822	True	Tetracycline-HCL	3.5	45.0	**
15	25	8.9787	0.0357	0.5318	17.4256	True	Tetracycline-HCL	3.5	60.0	*
15	35	15.7638	0.0003	7.3169	24.2107	True	Tetracycline-HCL	3.5	60.0	***
15	25	-3.7854	0.0018	-6.2024	-1.3684	True	Tetracycline-HCL	7.0	15.0	**
25	35	5.2998	0.0	2.8828	7.7168	True	Tetracycline-HCL	7.0	15.0	***
15	35	9.0955	0.0485	0.0524	18.1385	True	Tetracycline-HCL	7.0	45.0	*
15	35	13.3905	0.0004	6.0245	20.7564	True	Tetracycline-HCL	7.0	60.0	***
15	35	11.3707	0.0011	4.454	18.2873	True	Tetracycline-HCL	9.0	45.0	**
15	35	11.9488	0.0006	5.1212	18.7764	True	Tetracycline-HCL	9.0	60.0	***
15	35	5.804	0.0214	0.7794	10.8287	True	Sulfamethazine	3.5	15.0	*
15	35	11.0867	0.0028	3.6795	18.4939	True	Sulfamethazine	3.5	30.0	**
15	25	8.3115	0.0108	1.7836	14.8394	True	Sulfamethazine	3.5	45.0	*
15	35	15.9988	0.0	9.4709	22.5267	True	Sulfamethazine	3.5	45.0	***
25	35	7.6873	0.0189	1.1594	14.2152	True	Sulfamethazine	3.5	45.0	*
15	35	11.2085	0.0008	4.5971	17.82	True	Sulfamethazine	3.5	60.0	***
25	35	6.8506	0.0413	0.2392	13.462	True	Sulfamethazine	3.5	60.0	*
15	25	5.0485	0.0457	0.0851	10.0118	True	Sulfamethazine	7.0	30.0	*

15	35	10.045	0.0001	5.0817	15.0084	True	Sulfamethazine	7.0	30.0	***
25	35	4.9966	0.0483	0.0332	9.9599	True	Sulfamethazine	7.0	30.0	*
15	25	8.7122	0.0012	3.3808	14.0437	True	Sulfamethazine	7.0	45.0	**
15	35	12.4653	0.0	7.1339	17.7968	True	Sulfamethazine	7.0	45.0	***
15	35	10.979	0.0031	3.5677	18.3353	True	Sulfamethazine	7.0	60.0	**
15	35	11.084	0.0132	2.1151	20.0279	True	Sulfamethazine	9.0	30.0	*
15	35	12.4164	0.0	6.7047	18.128	True	Sulfamethazine	9.0	45.0	***
25	35	6.8533	0.0166	1.1417	12.565	True	Sulfamethazine	9.0	45.0	*
15	35	9.8608	0.02	1.4121	18.3094	True	Sulfamethazine	9.0	60.0	*

Statistical differences among current densities were evaluated using one-way ANOVA followed by Tukey HSD at each compound × pH × time condition. Tukey annotations are shown relative to 15 mA/cm² (reference): *$p < 0.05$; **$p < 0.01$; ***$p < 0.001$; ns = $p \geq 0.05$ (Tukey-adjusted).

Table S6: Two-way ANOVA results for Sulfanilamide removal efficiency (35 mA/cm^2)

pH	Factor	F (df1, df2)	p-value
3.5	Initial concentration	F(2,24) = 59.81	<0.001***
3.5	time	F(3,24) = 416.23	<0.001***
3.5	Initial concentration × time	F(6,24) = 4.25	0.005**
7.0	Initial concentration	F(2,24) = 12.40	<0.001***
7.0	time	F(3,24) = 138.13	<0.001***
7.0	Initial concentration × time	F(6,24) = 0.28	0.942 (ns)
9.0	Initial concentration	F(2,24) = 13.54	<0.001***
9.0	time	F(3,24) = 42.57	<0.001***
9.0	Initial concentration × time	F(6,24) = 1.08	0.402 (ns)

Factors: initial concentration and time) at pH 3.5, 7.0, and 9.0. Each F-value is given with degrees of freedom in parentheses, and *p*-values indicate significance (**$p < 0.001$; *$p < 0.01$; ns: not significant). The error degrees of freedom for all analyses = 24.

Two-way ANOVA tables (per compound × concentration, **EC**-35 mA/cm^2**).** Each table reports SS, df, MS, F, p, partial η² (effect size).

A) Sulfanilamide

Table S7: Sulfanilamide — 4000 µg/L

Source	SS	df	MS	F	p	partial η²
pH	633.469	2	316.735	5.720	0.0093	0.323
Time	10648.050	3	3549.350	64.098	1.33e-11	0.889
Time: pH	287.511	6	47.918	0.865	0.5342	0.178
Residual	1328.964	24	55.373			

Table S8 Sulfanilamide — 8000 µg/L

Source	SS	df	MS	F	p	partial η²
pH	36.618	2	18.309	0.279	0.7594	0.023
Time	7450.590	3	2483.530	37.828	2.52e-09	0.825
Time: pH	556.922	6	92.820	1.414	0.1176	0.261
Residual	1575.729	24	65.655			

Table S9: Sulfanilamide — 12000 µg/L

Source	SS	df	MS	F	p	partial η²
pH	238.877	2	119.438	2.649	0.0889	0.181
Time	8277.891	3	2759.297	61.192	2.68e-11	0.884
Time: pH	884.892	6	147.482	3.269	0.0048	0.449
Residual	1082.471	24	45.103			

Post-hoc (Time, Tukey HSD):

- For concentration 4000 µg/l: All time pairs significant.
- For concentration 8000 µg/l: 15 vs 30 not significant (*p*_adj=0.1179); all other pairs significant.
- For concentration 12000 µg/l: All time pairs significant.

Post-hoc (pH, Tukey within each timepoint):

Table S10: Sulfanilamide — 4000 µg/L (significant pH contrasts)

Time	Contrast	Δ mean	*p*_adj
45	3.5 vs 7.0	-10.77	0.0078
60	3.5 vs 7.0	-13.93	0.0005
60	3.5 vs 9.0	-5.74	0.0352
60	7.0 vs 9.0	8.19	0.0073

Table S11: Sulfanilamide — 8000 µg/L (significant pH contrasts)

Time	Contrast	Δ mean	*p*_adj
45	3.5 vs 7.0	-10.36	0.0089
60	3.5 vs 7.0	-11.90	0.0043

Table S12: Sulfanilamide — 12000 µg/L (significant pH contrasts)

Time	Contrast	Δ mean	*p*_adj
45	3.5 vs 7.0	-9.39	0.0128
60	3.5 vs 7.0	-10.16	0.0092
60	7.0 vs 9.0	5.46	0.1096

Here the interaction is significant for time-specific pH.

B) Tetracycline-HCl

Table S13: Tetracycline-HCl — 4000 µg/L

Source	SS	df	MS	F	*p*	partial η²
pH	2130.214	2	1065.107	43.321	5.15e-09	0.783
Time	14252.802	3	4750.934	193.213	1.11e-16	0.960
Time: pH	354.227	6	59.038	2.401	0.1656	0.375
Residual	590.653	24	24.610			

Table S14: Tetracycline-HCl — 8000 µg/L

Source	SS	df	MS	F	*p*	partial η²
pH	2676.984	2	1338.492	177.036	3.11e-15	0.937

Source	SS	df	MS	F	*p*	partial η²
Time	7643.255	3	2547.752	336.825	2.10e-18	0.977
Time: pH	114.020	6	19.003	2.511	0.2287	0.386
Residual	181.535	24	7.564			

Table S15: Tetracycline-HCl — 12000 µg/L

Source	SS	df	MS	F	*p*	partial η²
pH	1719.926	2	859.963	64.977	1.68e-09	0.844
Time	6805.971	3	2268.657	171.462	2.57e-16	0.956
Time: pH	530.598	6	88.433	6.682	3.57e-06	0.625
Residual	317.607	24	13.234			

Post-hoc (Time, Tukey HSD):

- For the concentration of 4000 µg/l: All time pairs significant.
- For the concentration of 8000 µg/l: 15 vs 30 not significant (*p*_adj=0.0678); all other pairs significant.
- For the concentration of 12000 µg/l: 15 vs 30 not significant *(p*_adj=0.9961); all other pairs significant.

Post-hoc (pH within each timepoint):

Table S16: Tetracycline-HCl — 12000 µg/l (key significant pH contrasts; interaction significant)

Time	Contrast	Δ mean	*p*_adj
45	3.5 vs 7.0	-18.30	0.0003
45	3.5 vs 9.0	-15.59	0.0007
60	3.5 vs 9.0	-10.50	0.0148

For 4000 and 8000 µg/l, significant pH differences occur at multiple timepoints; the dominant pattern is pH 3.5 > pH 7 > pH 9 at mid/late reaction times.

C) Sulfamethazine

Table S17: Sulfamethazine — 4000 µg/L

Source	SS	df	MS	F	*p*	partial η²
pH	845.089	2	422.545	32.814	2.69e-08	0.732
Time	11368.847	3	3789.616	294.323	1.01e-18	0.974
Time: pH	226.661	6	37.777	2.933	0.0189	0.423
Residual	309.145	24	12.881			

Table S18 : Sulfamethazine — 8000 µg/L

Source	SS	df	MS	F	*p*	partial η²
pH	289.538	2	144.769	6.487	0.0043	0.351
Time	7050.494	3	2350.165	105.351	2.44e-13	0.929
Time: pH	164.096	6	27.349	1.226	0.2527	0.235
Residual	535.394	24	22.308			

Table S19: Sulfamethazine — 12000 µg/L

Source	SS	df	MS	F	p	partial η²
pH	1307.552	2	653.776	35.693	1.18e-09	0.748
Time	8978.456	3	2992.819	163.352	3.42e-16	0.953
Time: pH	135.994	6	22.666	1.237	0.5066	0.236
Residual	439.616	24	18.317			

Post-hoc (Time, Tukey HSD): all time pairs significant for 4000, 8000, 12000 µg/l

Post-hoc (pH within each timepoint):

Table S20: Sulfamethazine — 4000 µg/L (interaction significant; key late-time differences)

Time	Contrast	Δ mean	*p*_adj
60	3.5 vs 7.0	-10.11	0.0119
60	3.5 vs 9.0	-14.75	0.0018

Combined analysis (3-way ANOVA per compound)

Model: **Removal ~ pH × Time × Concentration** (EC-35 mA/cm^2, triplicates)

Table S21: Sulfanilamide (3-way ANOVA)

Source	SS	df	MS	F	p-value	partial η²
Time	33338.952	3	11112.984	296.074	2.076e-40	0.925
pH	386.518	2	193.259	5.149	8.129e-03	0.125
Conc	3791.308	2	1895.654	50.504	1.966e-14	0.584
Time × pH	707.059	6	117.843	3.140	8.627e-03	0.207
Time × Conc	452.827	6	75.471	2.011	7.524e-02	0.144
pH × Conc	342.128	4	85.532	2.279	6.906e-02	0.112
Time × pH × Conc	409.634	12	34.136	0.909	5.420e-01	0.132
Residual	2702.478	72	37.534			

Sulfanilamide: Time is dominant (very large effect), concentration is strongly significant, and Time × pH is significant, consistent with pH effects becoming more pronounced at later times in some panels.

Table S22: TC-HCl (3-way ANOVA)

Source	SS	df	MS	F	p-value	partial η²
Time	28973.270	3	9657.757	888.493	8.888e-57	0.974
pH	3858.458	2	1929.229	177.485	1.478e-28	0.831
Conc	3033.439	2	1516.719	139.535	1.697e-25	0.795
Time × pH	237.741	6	39.623	3.645	3.245e-03	0.233
Time × Conc	1038.484	6	173.081	15.923	1.488e-11	0.570
pH × Conc	260.678	4	65.169	5.995	3.199e-04	0.250
Time × pH × Conc	341.124	12	28.427	2.615	5.968e-03	0.304
Residual	782.627	72	10.870			

TC-HCl): Very strong main effects for Time, pH, and Conc, plus significant 2-way and 3-way interactions, indicating that time-dependent pH behavior changes with concentration (consistent with the strong divergence seen in the 12000 µg/L panel).

Table S23: Sulfamethazine (3-way ANOVA)

Source	SS	df	MS	F	*p*-value	partial η^2
Time	33600.182	3	11200.061	694.729	4.777e-53	0.967
pH	1845.236	2	922.618	57.229	1.328e-15	0.614
Conc	1298.157	2	649.078	40.262	1.836e-12	0.528
Time × pH	248.485	6	41.414	2.569	2.601e-02	0.176
Time × Conc	61.423	6	10.237	0.635	7.018e-01	0.050
pH × Conc	28.110	4	7.028	0.436	7.822e-01	0.024
Time × pH × Conc	108.803	12	9.067	0.562	8.649e-01	0.086
Residual	1160.747	72	16.121			

Sulfamethazine: Strong main effects of Time, pH, Conc; interaction structure is comparatively weaker (only Time×pH significant), aligning with panels where it is pH dependent but less concentration-dependent than tetracycline-HCL.

Assumption checks for

- Shapiro–Wilk on ANOVA residuals (normality)
- Levene's test across Time×pH (variance homogeneity)

With replicated experimental data (n=36 per panel), Shapiro can be very sensitive; mild non-normality is common. ANOVA is generally robust when design is balanced and group sizes are equal (Field, 2017; Mongomery, 2017).

Table S24: Diagnostics summary (per compound × concentration)

Compound	Conc (µg/L)	Shapiro p	Levene p	Interaction p
Sulfanilamide	4000	3.34e-06	0.6152	0.5342
Sulfanilamide	8000	0.0026	0.7155	0.1176
Sulfanilamide	12000	4.24e-06	0.2133	0.0048
Tetracycline-HCL	4000	1.45e-07	0.0830	0.1656
Tetracycline-HCL	8000	5.65e-08	0.2160	0.2287
Tetracycline-HCL	12000	1.64e-06	0.1136	3.57e-06

Compound	Conc (µg/L)	Shapiro p	Levene p	Interaction p
Sulfamethazine	4000	1.50e-08	0.0515	0.0189
Sulfamethazine	8000	2.31e-10	0.1087	0.2527
Sulfamethazine	12000	2.66e-09	0.6810	0.5066

`

`

Appendix- C

Supporting information for chapter 5 titled "Application of response surface methodology for optimization and electrochemical oxidation of three mixed antibiotics at boron-doped diamond electrodes".

Table S1: ANOVA for response surface quadratic model based on CCD for Sulfanilamide (SN)

Y_1=SN removal (%)						
Source	**Sum of Squares**	**df**	**Mean Square**	**F Value**	***p*-Value Prob > F**	
Model	5729.05	14	409.22	71.58	< 0.0001	**significant**
X_1-Current densities	192.67	1	192.67	33.7	< 0.0001	
X_2-pH	416.67	1	416.67	72.89	< 0.0001	
X_3-H_2O_2	2.67	1	2.67	0.47	0.505	
X_4-Concentration	4648.17	1	4648.17	813.09	< 0.0001	
X_1X_2	169	1	169	29.56	< 0.0001	
X_1X_3	36	1	36	6.3	0.0241	
X_1X_4	56.25	1	56.25	9.84	0.0068	
X_2X_3	30.25	1	30.25	5.29	0.0362	
X_2X_4	25	1	25	4.37	0.0539	
X_3X_4	25	1	25	4.37	0.0539	
$X1^2$	114.33	1	114.33	20	0.0004	
$X2^2$	0.19	1	0.19	0.033	0.8576	
$X3^2$	0.19	1	0.19	0.033	0.8576	
X_4^2	12.19	1	12.19	2.13	0.1648	
Residual	85.75	15	5.72			

Lack of Fit	70.92	10	7.09	2.39	0.1741	**not significant**
Pure Error	14.83	5	2.97			
Cor Total	5814.8	29				

Table S2: ANOVA for response surface quadratic model based on CCD for TC-HCL

Y_2= TC-HCl removal (%)						
Source	**Sum of Squares**	**df**	**Mean Square**	**F Value**	***P*- value Prob > F**	
Model	538.2	14	38.44	12.3	< 0.0001	**significant**
X_1-Current densities	13.5	1	13.5	4.31	0.0555	
X_2-pH	24	1	24	7.66	0.0144	
X_3-H_2O_2	24	1	24	7.66	0.0144	
X_4-Concentration	88.17	1	88.17	28.1	< 0.0001	
X_1X_2	56.25	1	56.25	18	0.0007	
X_1X_3	42.25	1	42.25	13.5	0.0023	
X_1X_4	121	1	121	38.6	< 0.0001	
X_2X_3	2.25	1	2.25	0.72	0.4101	
X_2X_4	4	1	4	1.28	0.2763	
X_3X_4	16	1	16	5.11	0.0391	
X_1^2	100.76	1	100.8	32.2	< 0.0001	
X_2^2	8.05	1	8.05	2.57	0.1299	
X_3^2	65.19	1	65.19	20.8	0.0004	

X_4^2	2.33	1	2.33	0.74	0.4018	
Residual	47	15	3.13			
Lack of Fit	32.17	10	3.22	1.08	0.4949	**not significant**
Pure Error	14.83	5	2.97			
Cor Total	585.2	29				

Table S3: ANOVA for response surface quadratic model based on CCD for sulfamethazine (SMZ)

Y_3= SMZ removal (%)						
Source	**Sum of Squares**	**df**	**Mean Square**	**F Value**	***P* value- Prob > F**	
Model	2451.12	14	175.08	67.77	< 0.0001	**significant**
X_1-Current densities	1134.38	1	1134.4	439.1	< 0.0001	
X_2-pH	0.042	1	0.042	0.016	0.9006	
X_3-H_2O_2	84.38	1	84.38	32.66	< 0.0001	
X_4-Concentration	425.04	1	425.04	164.5	< 0.0001	
X_1X_2	45.56	1	45.56	17.64	0.0008	
X_1X_3	5.06	1	5.06	1.96	0.1819	
X_1X_4	95.06	1	95.06	36.8	< 0.0001	
X_2X_3	126.56	1	126.56	48.99	< 0.0001	
X_2X_4	33.06	1	33.06	12.8	0.0027	
X_3X_4	22.56	1	22.56	8.73	0.0098	
X_1^2	0.5	1	0.5	0.19	0.6653	
X_2^2	7.15	1	7.15	2.77	0.117	
X_3^2	469.07	1	469.07	181.6	< 0.0001	

X_4^2	0.5	1	0.5	0.19	0.6653	
Residual	38.75	15	2.58			
Lack of Fit	27.42	10	2.74	1.21	0.4415	**not significant**
Pure Error	11.33	5	2.27			
Cor Total	2489.87	29				

Table S4: Optimum operating conditions (X_1–X_4) and corresponding removal efficiencies (Y_1–Y_3) with overall desirability

Current densities (X_1)	**pH (X_2)**	**H_2O_2 (X_3)**	**Concentration (X_4)**	**SN removal (%) (Y_1)**	**TC-HCl removal (%) (Y_2)**	**SMZ removal (%) (Y_3)**	**Desirability**
30	4.95	2.5	6000	95.32	92.35	86.16	**0.817**
29.99	4.98	2.5	6001	95.06	92.31	86.50	0.816
30	5.03	2.5	6000	94.66	92.27	86.46	0.814
30	4.95	2.44	6001	95.08	92.70	85.59	0.812
30	5.07	2.5	6001	94.37	92.24	86.42	0.811
29.98	4.95	2.42	6000	95.04	92.78	85.35	0.81
30	4.95	2.4	6000	94.97	92.89	85.10	0.807
29.94	4.95	1.5	6000	92.35	92.29	87.02	0.801
30	4.95	1.5	6069	92.01	92.25	86.90	0.797
30	5.01	1.5	6000	92.03	92.25	86.84	0.797
29.26	5.08	2.5	6000	94.55	92.24	84.81	0.796
30	4.95	1.61	6000	92.67	92.96	85.42	0.793

30	4.95	1.64	6000	92.75	93.08	85.07	0.791
29.92	4.95	2.25	6000	94.52	93.47	83.44	0.79
30	5.02	2.3	6008	94.10	93.25	83.85	0.79
30	4.95	1.67	6000	92.82	93.20	84.73	0.789
30	4.95	1.66	6009	92.74	93.15	84.82	0.789
30	4.95	1.71	6000	92.94	93.37	84.25	0.786
28.53	4.95	2.49	6000	95.46	92.22	83.13	0.784
30	4.95	2.04	6000	93.87	93.86	82.72	0.78
30	4.95	1.98	6001	93.69	93.87	82.73	0.779
30	4.95	2.49	6337	93.03	91.59	84.85	0.779
29.69	4.95	2.14	6000	94.17	93.68	82.24	0.775
30	4.95	2.46	6394	92.55	91.69	84.04	0.767
30	5.7	2.5	6000	89.68	91.66	85.98	0.763
30	5.86	2.5	6000	88.46	91.47	85.90	0.751
30	4.95	1.5	7239	85.49	90.62	82.78	0.687
24.97	4.95	2.5	6000	94.50	90.32	75.49	0.666
28.22	7.45	2.5	6000	79.15	89.84	83.11	0.622

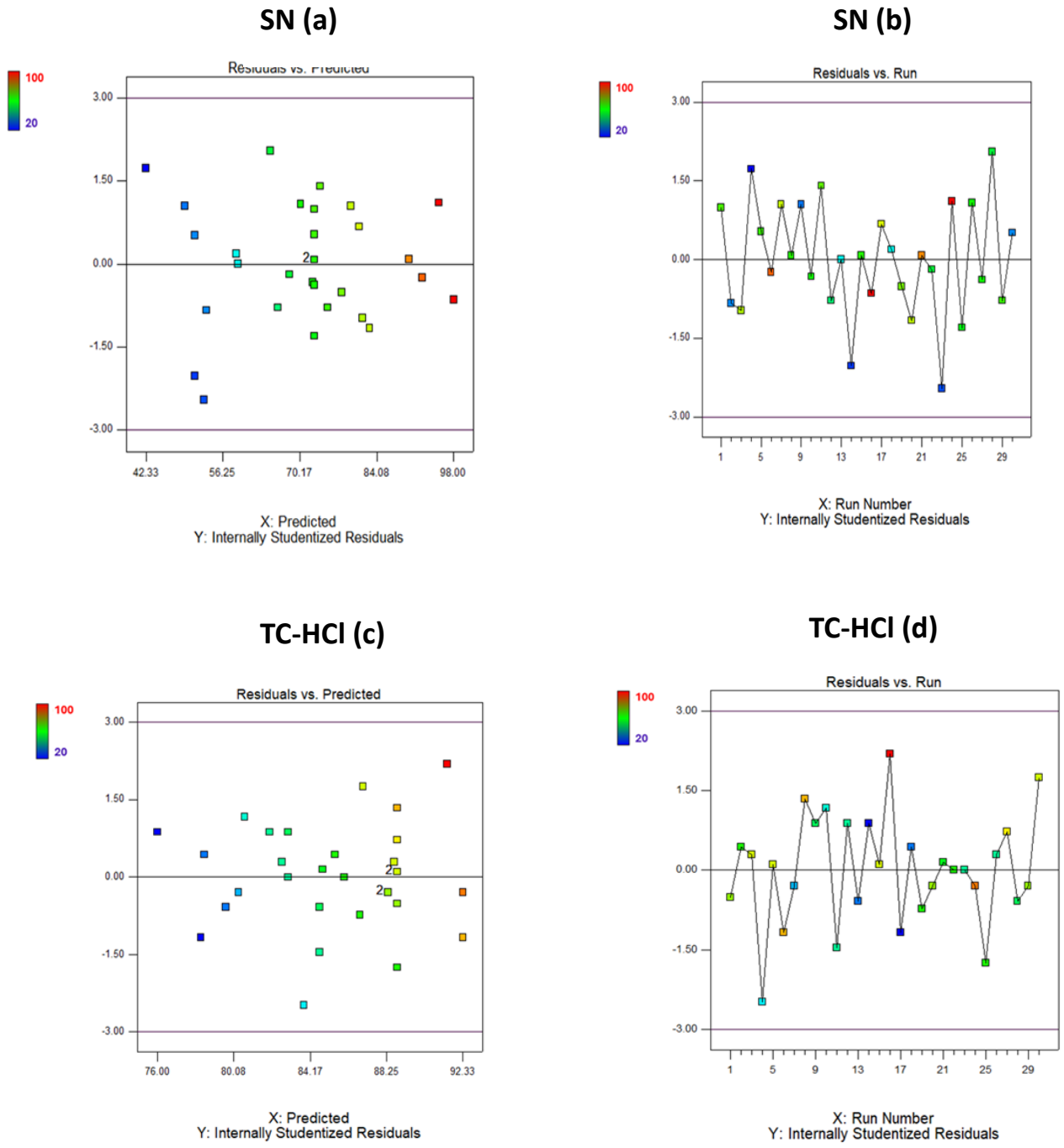

Figure S1: Diagnostic residual plots for the CCD based response surface models of sulfanilamide and tetracycline hydrochloride removal: residuals versus predicted values for SN **(a)** and TC-HCl **(b)**; residuals versus run order for SN **(c)** and TC-HCl **(d)**.

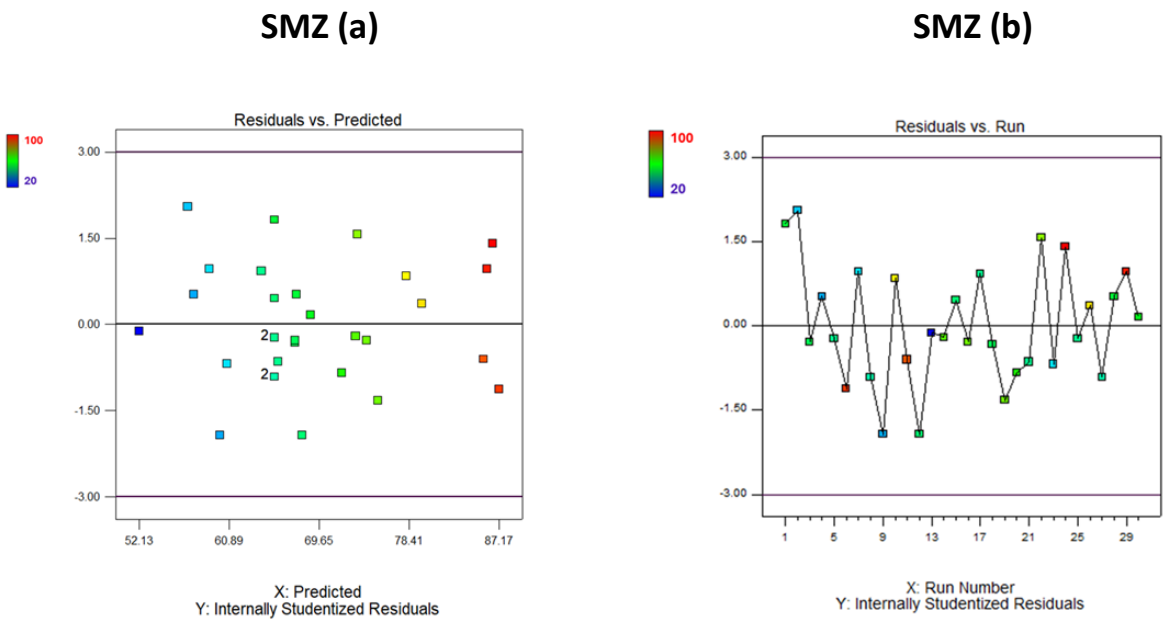

Figure S2: Diagnostic residual plots for the CCD based response surface model of sulfamethazine removal: **(a)** residuals versus predicted values and **(b)** residuals versus run order.